Modelling of Coupled Vessel-Ampelmann Systems for Workability Studies

J.J. Wiegerink

Master of Science Thesis

TU Delft Delft University of Technology

Offshore and Dredging Engineering

Modelling of Coupled Vessel-Ampelmann Systems for Workability Studies

Master of Science Thesis

For the degree of Master of Science in Offshore and Dredging Engineering at Delft University of Technology

J.J. Wiegerink

May 29, 2015

Faculty of Mechanical, Maritime and Materials Engineering (3mE) · Delft University of Technology

The work in this thesis is supported by Ampelmann Operations B.V. Their cooperation is hereby gratefully acknowledged.

Delft University of Technology
Department of

The undersigned hereby certify that they have read and recommend to the Faculty of Mechanical, Maritime and Materials Engineering (3mE) for acceptance a thesis entitled

Modelling of Coupled Vessel-Ampelmann Systems for Workability Studies

by

J.J. Wiegerink

in partial fulfillment of the requirements for the degree of

Master of Science Offshore and Dredging Engineering

Dated: May 29, 2015

Supervisor(s):

Prof.dr.ir. R.H.M. Huijsmans

Ir. A. van Leer

Dr.ir. M.A. Gutiérrez

Reader(s):

Ir. J. den Haan

Dr.ir. S.A. Miedema

Abstract

Workability studies are performed that determine the workability of the Ampelmann system on a vessel. Due to the dynamic interaction between the vessel and the Ampelmann system in certain cases the dynamic behaviour of the vessel changes, vessel motions amplify and the natural frequencies of the vessel shift. The workability studies are based on the frequency characteristics of the vessel. However, the dynamic interaction between the vessel and the Ampelmann is not incorporated into the calculated workability. As a results the calculated workability overestimates the practical workability.

A frequency domain model of the coupled vessel-Ampelmann system is made to calculate vessel frequency characteristics that takes into account the dynamic interaction of the coupled vessel-Ampelmann system. The model input variables are the hydromechanic properties of the vessel, the mass properties of the Ampelmann system and the vessel and the location of the Ampelmann system on the vessel. The coupled frequency characteristics are applied to the workability study. This gives a better estimation of the practical workability.

The control system of the Ampelmann determines how the transfer deck moves with respect to the vessel. Three control systems are applied to the model and the results are compared. Insight is gained into the dynamic interaction between the vessel and the Ampelmann system. Vessel surge, sway and roll motions amplify when the Ampelmann is activated and the roll natural frequency shifts to a higher frequency. A new compensation method is proposed, which does not amplify vessel motions and significantly increases the workability. This method shall be optimized to the capabilities of the Ampelmann system.

Table of Contents

Acknowledgements

For the completion of this thesis I would like to thank, first of all my supervisors Prof.dr.ir. René Huijsmans from Delft University of Technology, Ir. Arnoud van Leer and Dr.ir. Miguel Gutiérrez both from Ampelmann Operation B.V. for their guidance, feedback and support throughout this research.

I would like to thank Dr.ir David Cerda Salzmann, Ir. Joost den Haan and Dr.ir. Pepijn de Jong for their support and feedback during my research phase.

This project has been made possible by the company Ampelmann Operation B.V. Hereby, I would like to thank all people from Ampelmann and my colleague graduates, Gerrit and Gilles who helped me during my work.

I wish to thanks my friends and family for there love and support throughout my entire study.

Finally, thanks to my girlfriend Rosa for her love and trust.

Delft, University of Technology J.J. Wiegerink
May 29, 2015

Chapter 1

Introduction

1-1 The Ampelmann on a vessel

The Ampelmann system is a ship-based self-stabilizing platform that actively compensates all vessel motions using a Stewart platform to make access to offshore structures safe, easy and fast. This is done by continuously measuring the motions of the host vessel. Then, the required lengths of the six cylinders are calculated to keep the Transfer deck completely motionless. Finally each hydraulic actuator is controlled separately.

Figure 1-1: The Ampelmann system during operation

Many Ampelmann systems are installed on large vessels. However, the demand for an Ampelmann system on small ships is growing. Based on the sea state and the frequency characteristics of the host vessel a workability study is performed. This is performed to check the

operability of the Ampelmann system. Due to the changing dynamic behaviour of the host vessel under influence of the Ampelmann system, the calculated workability is higher than the practical workability.

1-2 Problem description

In the early days of Ampelmann operations B.V. changing dynamic vessel behaviour was witnessed during model tests. Now more systems are operating throughout the world on all sorts of vessels. In certain cases the vessel behaviour changes directly when the Ampelmann is activated. In general vessel motion amplitudes increase and/or the natural frequencies of the vessel motions are affected. Figure 1-2 shows four cases where an active Ampelmann causes a changing dynamic vessel behaviour. These are briefly discussed below.

Figure 1-2: Four cases where the Ampelmann system influences the dynamic behaviour of the host vessel

1. *Model testing*: Model tests with a small vessel and the P-type Ampelemann system, a small electrical Stewart platform, are performed. During these tests a roll resonance phenomena was encountered. The coupling between the vessel and the Ampelmann system resulted in self excitation of the vessel's roll motion in still water, Figure 1-2, top left.

2. Full scale testing, *Smit Bronco*: The Smit Bronco, a tug, performed the first full scale tests with a full size Ampelmann A-type system on deck. When the Ampelmann system was activated the vessel motions are observed to increase. Figure 1-2, top right.

3. *SKANDI FJORD*: The CTS2 (Cargo transfer system version 2), Ampelmann's fully compensated crane was tested on the SKANDI FJORD, a platform support vessel. When the Ampelmann system was elevated from a passive settled position to the passive neutral position the roll frequency of the vessel noticeably changed to a lower frequency. Figure 1-2, bottom left.
4. *DP Galyna* and *DP Gezina*: Both walk to work vessels experience an increasing roll motion when the Ampelmann system is activated. Figure 1-2, bottom right.

Changing vessel behaviour does not necessarily affect the motions of the transfer deck, the part of the Ampelmann that is kept motionless. It is capable to compensate for the induced vessel motions. The major problem arises to the workability of the Ampelmann on the vessel. Larger vessel motions require a larger cylinder stroke length, assuming that the TD is kept motionless and vessel motions increase. The maximum stroke length of the hydraulic cylinders supporting the transfer deck is reached earlier. This directly causes a reduced practical workability. Workability calculations are based on vessel frequency characteristics, these characteristics do not take into account the dynamic interaction with the Ampelmann system. Therefore the calculated workability overestimates the practical workability.

1-3 Research objective

The main objective of this research is to develop a calculation method to recalculate vessel frequency characteristics. This method shall take into account the dynamic interaction between the vessel and the Ampelmann system. The recalculated frequency characteristics apply to the workability study. A better estimation of the practical workability is obtained. The research objective is defined as follows:

"Application of the dynamic behaviour of coupled vessel-Ampelmann systems to workability studies"

1-4 Thesis approach

The main thesis objective is split into a series of sub-objectives. These are illustrated in Figure 1-3 on page 4. The figure should be read from left to right.

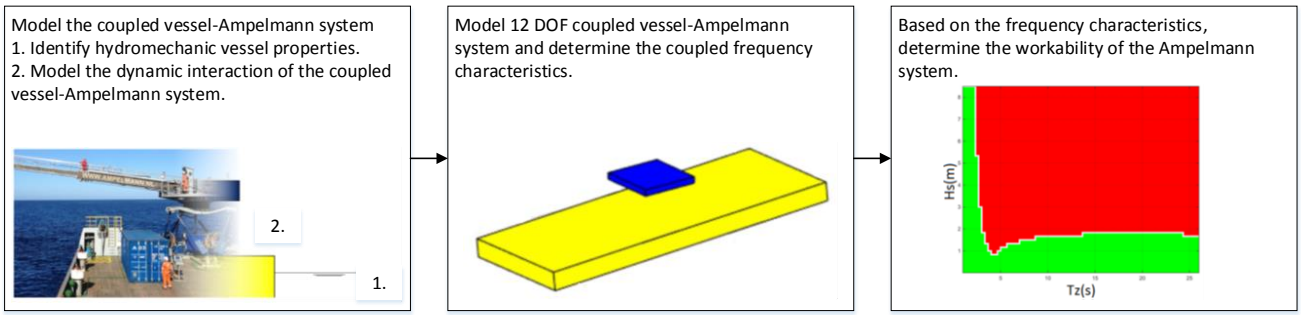

Figure 1-3: General approach for the application of the dynamic interaction of the coupled vessel-Ampelmann system to workability studies

The coupled vessel-Ampelmann system consists of two major components. The vessel and the Ampelmann system. To calculate vessel frequency characteristics the hydromechanic properties of the host vessel are determined. Then a set of simplified frequency domain models is made that model the dynamic interaction of the coupled vessel-Ampelmann system. This gives a fundamental understanding of the coupling mechanism. Next, indicated in the center of Figure 1-3: based on the simplified models a model of the coupled vessel-Ampelmann system is made that includes all DOF (Degree of freedom). The vessel frequency characteristics are calculated and are input to the workability analysis. These frequency characteristics take into account the dynamic interaction between the vessel and the Ampelmann system. A workability assessment is performed that takes into account the dynamic interaction between the vessel and the Ampelmann system, the right side of Figure 1-3.

The detailed approach is illustrated in Figure 1-4, it shows the structure of the remainder of this thesis. In chapter 2 the starting point for this research is discussed. A literature review on related topics and previous research is discussed. Chapter 3 elaborates on the determination of hydromechanic vessel properties. In chapter 4 the coupled vessel-Ampelmann model is introduced. Then in chapter 5 simplified models are made where selectively the number of DOF of the model is increased. Chapter 6 discusses the coupled vessel-Ampelmann model that includes all DOF for the vessel and the Ampelmann system. This model allows to vary the location of the Ampelmann system on the vessel. The results of this chapter form input to the workability analysis in chapter 7. Each chapter has a similar structure, first it starts with an introduction followed by the content of that chapter and it finalizes with a conclusion. In the final chapter of this thesis, chapter 8, the conclusions and recommendations are stated.

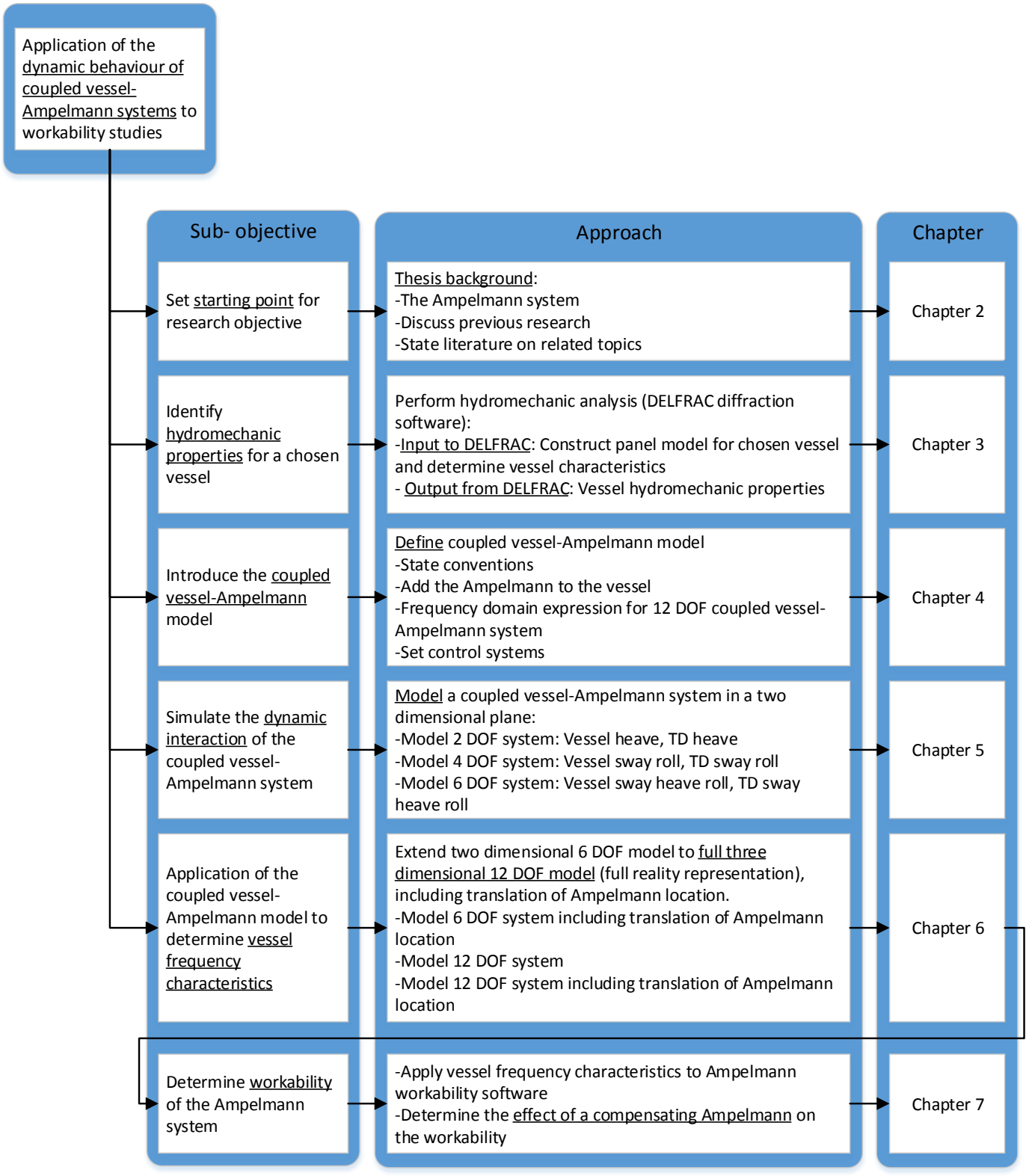

Figure 1-4: Flow chart for the research objective, the approach and the report structure. (TD: Transfer deck)

Chapter 2

Background

2-1 Introduction

Figure 2-1: Flow chart of the objective and approach of this chapter

This chapters objective is to set the starting point for this research. First the Ampelmann system is discussed in section 2-2. Next previous research on the dynamic interaction between the Ampelmann system and the vessel is discussed. Then a literature overview is given on relevant topics: ship stability, determination of vessel frequency characteristics and Ampelmann workability software.

2-2 The Ampelmann system

The Ampelmann system consists of multiple components. Figure 2-2 shows the most important components in order to understand the capabilities of the system.

The main objective of the Ampelmann system is to make offshore access as easy as crossing the street. This is achieved by perfectly compensating vessel motions. Vessel motions are measured and are processed in the *control cabinet*. The control cabinet actively controls the *hydraulic cylinders*, 6 in total. The hydraulic cylinders connect the *bottom frame* to the *Mercedes frame*. The *gimbals* allow the hydraulic cylinders to pivot. The Mercedes frame connects to the *transfer deck*. The transfer deck may rotate, slew, relative to the Mercedes frame via the *slewing ring*. The transfer deck is the waiting area for transferring crew and is kept motionless by the 6 hydraulic cylinders. The *gangway* connects the transfer deck to

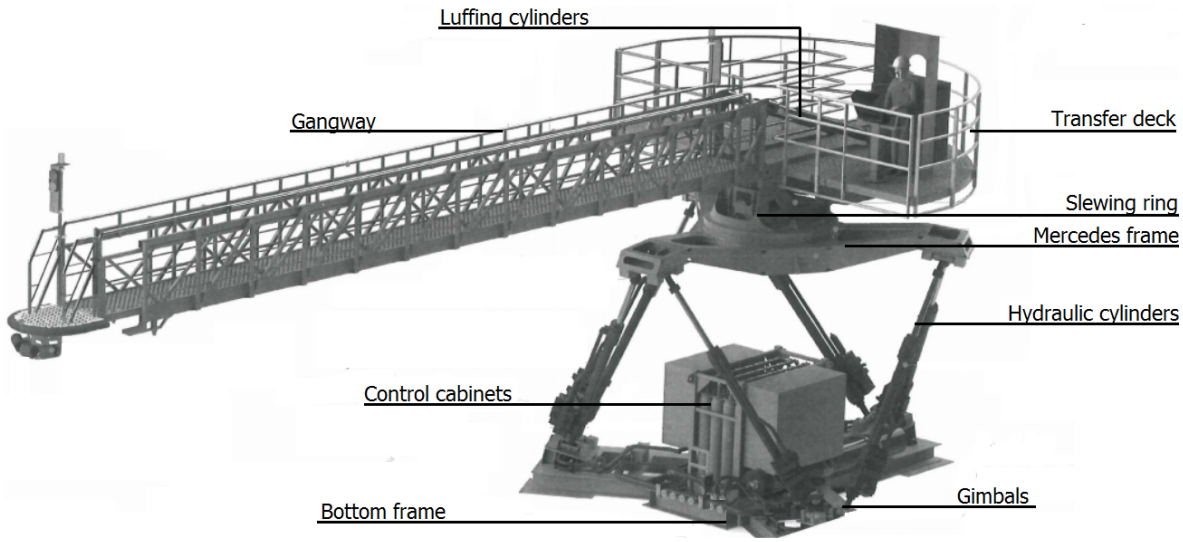

Figure 2-2: Components of the Ampelmann system

the target platform by actively pushing with the tip of the gangway. The gangway elongates where required: telescoping. Depending on the elevation of the target platform, the gangway can luff by controlling the *luffing cylinders*. The compensation philosophy of the Ampelmann system is to keep the transfer deck motionless, undesired residual motions are absorbed by slewing, luffing and telescoping. For more conventions, see Appendix A.

The bottom frame, the hydraulic cylinders and the Mercedes frame together are a Stewart platform. The Stewart platform allows to move the transfer deck relative to the bottom frame. The bottom frame is fixed to the vessel. In case of a passive system the Mercedes frame moves with the bottom frame and all cylinders have a fixed length. An active system compensated all bottom frame motions, the cylinders have a controllable length depending on the vessel motions.

2-3 Previous research

In the early days of Ampelmann Operations B.V. changing dynamic vessel behaviour was observed during model testing: observation 1 from Figure 1-2. Research was done to get preliminary insight into the roll resonance phenomenon. A model of a ship was made, which was given an initial displacement. Based on a computational Simulink model to simulated roll resonance, illustrated in Figure 2-3, the following conclusions are drawn: The resonance effect is caused by the shift of the top plate's center of gravity (CoG) in combination with the horizontal acceleration of the top plate's mass; both phenomena will increase the roll motion when the system's damping is insufficient. In practice residual motions of the transfer deck exist causing reaction forces to the vessel.

Also the effect of parameter variation was studied. First, the time lag of the control system was varied. It was found that for an increasing time lag, the roll amplitude increases faster. Secondly, the mass of the top plate was varied: an increasing top plate mass significantly

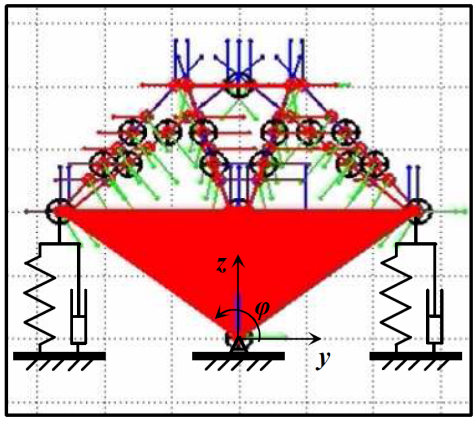

Figure 2-3: Computational model to simulate roll resonance [1]

increases the resonant behaviour. Finally the damping was increased. At a certain value, the damping is large enough to stop the model resonance. This was already proven during model testing: applying bilge keels as roll dampers solved the resonance problem [1].

2-4 Literature review

In this section three topics are discussed. First: ship stability. Second: the determination of vessel frequency characteristics and finally Ampelmann workability software.

2-4-1 Ship stability

The buoyancy force required to keep the vessel floating is defined by the Archimedes law.

$$F_{buoyancy} = \rho_w g \nabla \tag{2-1}$$

The buoyancy force $F_{buoyancy}$ is a function of the water density ρ_w the gravity constant g and the vessels submerged volume ∇. In hydrostatic ship stability, the buoyancy force equals the total weight of the vessel. When the vessel has a static vertical displacement the buoyancy increases, the water works as a spring forcing the vessel back to its equilibrium position. For a stable upright floating vessel the resultant of the buoyancy force and the gravity force are vertically aligned. See Figure 2-4. A stable vessel with a roll angle has a righting moment. Due to a roll angle the buoyancy point shifts more than the gravity, causing a non alignment of the two forces forcing the vessel to its stable upright position.

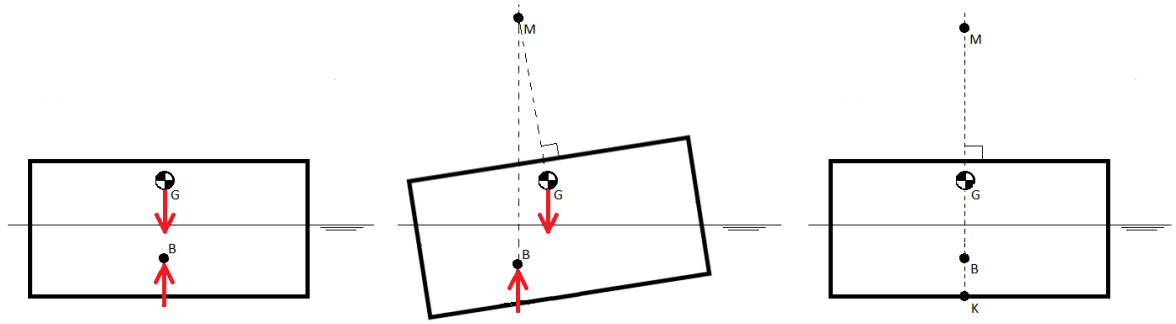

Figure 2-4: Hydrostatic ship stability

In terms of vessel stability, four virtual points on the vessel are defined. The keel, K, the buoyancy point, B, the CoG, G, and the metacenter, M. For a stable upright floating vessel the metacentric heigh shall be above the CoG of the vessel [2]. Length $\overline{GM}$ is defined as:

$$\overline{GM} = \overline{KB} + \overline{BM} - \overline{KG} \tag{2-2}$$

Where $\overline{KB}$, $\overline{BM}$ and $\overline{KG}$ are the lengths between the defined points. $\overline{KB}$ and $\overline{KG}$ follow from the hull and vessel geometry. $\overline{BM}$ is defined as:

$$\overline{BM} = \frac{I_t}{\nabla} \tag{2-3}$$

I_t is the area moment of inertia of the water plane area and ∇ the submerged volume of the vessel. A stable upright floating vessel fulfils the condition:

$$\overline{GM} > 0[m] \tag{2-4}$$

The metacenter is a fixed point in space relative to the vessel, independent of the roll angle the resultant of the buoyancy works through this virtual point. As long as $\overline{GM} > 0[m]$, then for an initial roll angle the buoyancy force causes a counteracting moment forcing the vessel to a stable upright position.

2-4-2 Determination of vessel frequency characteristics

The vessel frequency characteristics form input for the workability analysis. This section discusses what conventions are made and how vessel frequency characteristics are obtained[2]. Vessel frequency characteristics are determined for a statically stable upright floating vessel.

Axis conventions

The motions of a vessel can be split up into three mutually perpendicular translations of the CoG and three rotations around the CoG. Three right handed orthogonal coordinate systems are used to define the vessel motions, see Figure 2-5.

- *Earth-bound coordinate system,* $S(x_0, y_0, z_0)$: the (x_0, y_0)-plane lies on the still water level, positive z_0 is pointing upwards. The positive x_0-axis is defined relative to the steadily translating coordinate system by wave incident angle μ.

- *Body-bound coordinate system, $G(x_b, y_b, z_b)$*: The origin of this coordinate system lies at the CoG of the ship. x_b directs to the bow of the ship, y_b to port side and z_0 upwards. When the ship is located in still water the (x_b, y_b)-plane is parallel to the (x_0, y_0)-plane.

- *Steadily translating coordinate system $O(x, y, z)$*: This system is moving forward with a constant speed V, when the Ampelmann system is operational $V = 0[m/s^2]$. If the ship is stationary, the direction of the $O(x, y, z)$ axes are the same as those of the $G(x_b, y_b, z_b)$ axes. The (x, y)-plane lies on the still water surface with the origin O, above or below the time-averaged position of the CoG. The ship is supposed to carry out oscillations around coordinate system $O(x, y, z)$ [2].

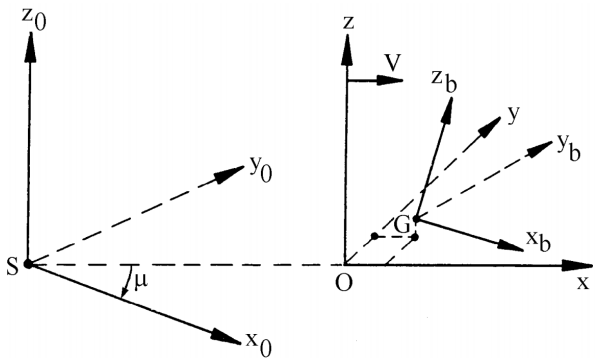

Figure 2-5: Coordinate systems [2]

Vessel frequency characteristics are described in the steadily translating coordinate system. For the analysis in this thesis the vessel has zero forward speed.

Vessel motions and harmonic wave forces

Vessel amplitude frequency characteristics, known as the response amplitude operators (RAO) are defined as the ratio between the vessel motion amplitudes and the wave amplitude. Frequency characteristics include the phase angles of the motions with respect to the wave elevation. Both RAO and phases depend on the wave frequency and the wave direction. When analysing first order linear vessel motions, the input frequency and the output frequency are always the same. In case of analysing ship motions, the input frequency is a harmonic wave and the output frequency are the vessel motions. The motions in the steadily translating coordinate system of and about the vessel's CoG are described as: Three translational motions, 1, 2 and 3 and three rotational motions, 4, 5 and 6. See Figure 2-6 and Equation 2-5.

$$\begin{array}{lcl} \text{Surge(1)} & : & x = X_a \cos(\omega t + \epsilon_{x\zeta}) \\ \text{Sway(2)} & : & y = Y_a \cos(\omega t + \epsilon_{y\zeta}) \\ \text{Heave(3)} & : & z = Z_a \cos(\omega t + \epsilon_{z\zeta}) \\ \text{Roll(4)} & : & \phi = \Phi_a \cos(\omega t + \epsilon_{\phi\zeta}) \\ \text{Pitch(5)} & : & \theta = \Theta_a \cos(\omega t + \epsilon_{\theta\zeta}) \\ \text{Yaw(6)} & : & \psi = \Psi_a \cos(\omega t + \epsilon_{\psi\zeta}) \end{array} \tag{2-5}$$

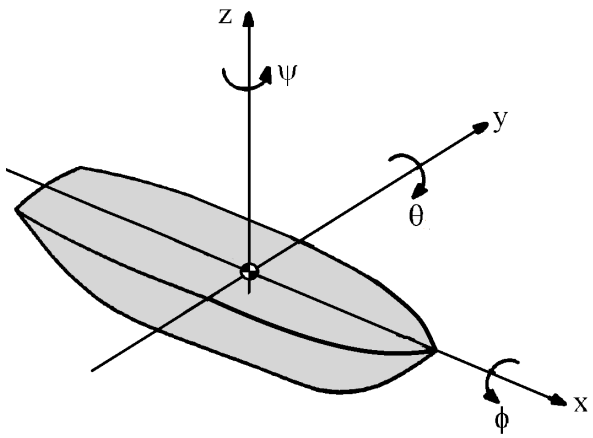

Figure 2-6: Vessel coordinate system for determination of frequency characteristics

In a frequency domain analysis, the motion of each DOF is written as a harmonic motion: x, y, z, ϕ, θ and ψ. All motions are defined by an oscillation amplitude: X_a, Y_a, Z_a, Φ_a, Θ_a, Ψ_a. The excitation frequency: ω and a phase angle with respect to the wave elevation: $\epsilon_{x\zeta}$, $\epsilon_{y\zeta}$, $\epsilon_{z\zeta}$, $\epsilon_{\phi\zeta}$, $\epsilon_{\theta\zeta}$, $\epsilon_{\psi\zeta}$. The motion frequency has the same frequency as the wave. The wave elevation is defined by the wave amplitude: ζ_a the wave amplitude and the wave frequency ω:

$$\zeta = \zeta_a \cos(\omega t) \tag{2-6}$$

When a wave interacts with the hull surface, wave forces and moments result due to pressure fluctuations. Waves have a wave incident angle with respect to the vessel orientation. The wave forces and moments depend on the wave incident angle and act in each DOF:

$$\begin{aligned} F_x &= F_1 \cos(\omega t + \epsilon_{F_x\zeta}) \\ F_y &= F_2 \cos(\omega t + \epsilon_{F_y\zeta}) \\ F_z &= F_3 \cos(\omega t + \epsilon_{F_z\zeta}) \\ M_\phi &= M_4 \cos(\omega t + \epsilon_{M_\phi\zeta}) \\ M_\theta &= M_5 \cos(\omega t + \epsilon_{M_\theta\zeta}) \\ M_\psi &= M_6 \cos(\omega t + \epsilon_{M_\psi\zeta}) \end{aligned} \tag{2-7}$$

As with the vessel motions, the wave forces and moments are defined by an amplitude, the excitation frequency and a phase angle with respect to the wave elevation.

Mathematical vessel model

To obtain frequency characteristics of a vessel a set of equations is defined. The results, of solving this set of equations, are the vessel frequency characteristics. The vessel is modelled as a coupled mass spring damper system with 6 DOF. For a harmonic wave loading the equation of motion (EOM) has the following form.

$$[\mathbf{M} + \mathbf{A}(\omega)] \begin{bmatrix} \ddot{x} \\ \ddot{y} \\ \ddot{z} \\ \ddot{\phi} \\ \ddot{\theta} \\ \ddot{\psi} \end{bmatrix} + [\mathbf{B}(\omega)] \begin{bmatrix} \dot{x} \\ \dot{y} \\ \dot{z} \\ \dot{\phi} \\ \dot{\theta} \\ \dot{\psi} \end{bmatrix} + [\mathbf{C}] \begin{bmatrix} x \\ y \\ z \\ \phi \\ \theta \\ \psi \end{bmatrix} = \begin{bmatrix} F_x \\ F_y \\ F_z \\ M_\phi \\ M_\theta \\ M_\psi \end{bmatrix} \tag{2-8}$$

$[\mathbf{M}]$ is the mass matrix of the vessel. $[\mathbf{A}(\omega)]$, $[\mathbf{B}(\omega)]$ and $[\mathbf{C}]$ together with the wave forces and moments are all hydromechanic properties of the vessel. $[\mathbf{A}(\omega)]$ is the added mass matrix of the vessel. This matrix values depend on the hull shape and on the excitation frequency. The added mass is defined as the water surrounding the vessel that moves with the vessel. Then the damping matrix $[\mathbf{B}(\omega)]$ contains all damping terms that also depend on the excitation frequency. $[\mathbf{C}]$ is the static restoring matrix, which is independent of the excitation frequency. Each matrix contains all coupling terms: vessel motions in 1 DOF may be affected by vessel motions in other DOF: a more elaborate expression of the EOM is given below.

$$\begin{bmatrix} M_v+a_{11} & a_{12} & a_{13} & a_{14} & a_{15} & a_{16} \\ a_{21} & M_v+a_{22} & a_{23} & a_{24} & a_{25} & a_{26} \\ a_{31} & a_{32} & M_v+a_{33} & a_{34} & a_{35} & a_{36} \\ a_{41} & a_{42} & a_{43} & I_{xx1}+a_{44} & a_{45} & a_{46} \\ a_{51} & a_{52} & a_{53} & a_{54} & I_{yy1}+a_{55} & a_{56} \\ a_{61} & a_{62} & a_{63} & a_{64} & a_{65} & I_{zz1}+a_{66} \end{bmatrix} \begin{bmatrix} \ddot{x} \\ \ddot{y} \\ \ddot{z} \\ \ddot{\phi} \\ \ddot{\theta} \\ \ddot{\psi} \end{bmatrix} + \begin{bmatrix} b_{11} & b_{12} & b_{13} & b_{14} & b_{15} & b_{16} \\ b_{21} & b_{22} & b_{23} & b_{24} & b_{25} & b_{26} \\ b_{31} & b_{32} & b_{33} & b_{34} & b_{35} & b_{36} \\ b_{41} & b_{42} & b_{43} & b_{44} & b_{45} & b_{46} \\ b_{51} & b_{52} & b_{53} & b_{54} & b_{55} & b_{56} \\ b_{61} & b_{62} & b_{63} & b_{64} & b_{65} & b_{66} \end{bmatrix} \begin{bmatrix} \dot{x} \\ \dot{y} \\ \dot{z} \\ \dot{\phi} \\ \dot{\theta} \\ \dot{\psi} \end{bmatrix} + \begin{bmatrix} c_{11} & c_{12} & c_{13} & c_{14} & c_{15} & c_{16} \\ c_{21} & c_{22} & c_{23} & c_{24} & c_{25} & c_{26} \\ c_{31} & c_{32} & c_{33} & c_{34} & c_{35} & c_{36} \\ c_{41} & c_{42} & c_{43} & c_{44} & c_{45} & c_{46} \\ c_{51} & c_{52} & c_{53} & c_{54} & c_{55} & c_{56} \\ c_{61} & c_{62} & c_{63} & c_{64} & c_{65} & c_{66} \end{bmatrix} \begin{bmatrix} x \\ y \\ z \\ \phi \\ \theta \\ \psi \end{bmatrix} = \begin{bmatrix} F_x \\ F_y \\ F_z \\ M_x \\ M_y \\ M_z \end{bmatrix} \tag{2-9}$$

M_v, I_{xx1}, I_{yy1}, I_{zz1} are all mass and mass moment of inertia terms corresponding to the vessel. All terms on the diagonal of each matrix are reaction forces and moments in the direction of the motion due to that motion. All non diagonal terms are coupling terms: reaction forces and moments in 1 DOF due to motions in another DOF. Each term with a double subscript shall be read as, a_{23}: added mass in sway(2) due to heave(3). b_{54}: damping in pitch(5) due to roll(4). c_{16}: restoring term in surge(1) due to yaw(6).

Prior to solving the EOM for the motions, all hydromechanic properties shall be determined. This is either performed experimentally or by special software. At the TU-delft DELFRAC diffraction software is available, which calculates all hydromechanic terms based on potential theory. Assuming that all terms in the EOM are known it is solved. The unknown motions, the acceleration, the velocity and the displacement and the known wave forces and moments are substituted in complex notation:

$$\begin{aligned} \text{Displacement} &: x = X_a \cos(\omega t + \epsilon_{x\zeta}) \rightarrow \mathfrak{Re}\{X_a e^{i(\omega t+\epsilon_{x\zeta})}\} = \mathfrak{Re}\{\hat{X}_a e^{i\omega t}\} \\ \text{Velocity} &: \dot{x} = -\omega X_a \sin(\omega t + \epsilon_{x\zeta}) \rightarrow \mathfrak{Re}\{i\omega X_a e^{i(\omega t+\epsilon_{x\zeta})}\} = \mathfrak{Re}\{i\omega \hat{X}_a e^{i\omega t}\} \\ \text{Acceleration} &: \ddot{x} = -\omega^2 X_a \cos(\omega t + \epsilon_{x\zeta}) \rightarrow \mathfrak{Re}\{-\omega^2 X_a e^{i(\omega t+\epsilon_{x\zeta})}\} = \mathfrak{Re}\{-\omega^2 \hat{X}_a e^{i\omega t}\} \\ \text{Wave force} &: F_x = F_1 \cos(\omega t + \epsilon_{F_x\zeta}) \rightarrow \mathfrak{Re}\{F_1 e^{i(\omega t+\epsilon_{F_x\zeta})}\} = \mathfrak{Re}\{\hat{F}_1 e^{i\omega t}\} \end{aligned} \tag{2-10}$$

Each motion and force is written as a multiplication of a complex amplitude, $\hat{X}_a$, with a harmonic part $e^{i\omega t}$. The complex amplitude contains amplitude information and phase information. After substitution to the EOM, $e^{i\omega t}$ is excluded. The frequency domain expression for the EOM is obtained.

$$\left(-\omega^2 \begin{bmatrix} M_v+a_{11} & a_{12} & a_{13} & a_{14} & a_{15} & a_{16} \\ a_{21} & M_v+a_{22} & a_{23} & a_{24} & a_{25} & a_{26} \\ a_{31} & a_{32} & M_v+a_{33} & a_{34} & a_{35} & a_{36} \\ a_{41} & a_{42} & a_{43} & I_{xx1}+a_{44} & a_{45} & a_{46} \\ a_{51} & a_{52} & a_{53} & a_{54} & I_{yy1}+a_{55} & a_{56} \\ a_{61} & a_{62} & a_{63} & a_{64} & a_{65} & I_{zz1}+a_{66} \end{bmatrix} + i\omega \begin{bmatrix} b_{11} & b_{12} & b_{13} & b_{14} & b_{15} & b_{16} \\ b_{21} & b_{22} & b_{23} & b_{24} & b_{25} & b_{26} \\ b_{31} & b_{32} & b_{33} & b_{34} & b_{35} & b_{36} \\ b_{41} & b_{42} & b_{43} & b_{44} & b_{45} & b_{46} \\ b_{51} & b_{52} & b_{53} & b_{54} & b_{55} & b_{56} \\ b_{61} & b_{62} & b_{63} & b_{64} & b_{65} & b_{66} \end{bmatrix} + \begin{bmatrix} c_{11} & c_{12} & c_{13} & c_{14} & c_{15} & c_{16} \\ c_{21} & c_{22} & c_{23} & c_{24} & c_{25} & c_{26} \\ c_{31} & c_{32} & c_{33} & c_{34} & c_{35} & c_{36} \\ c_{41} & c_{42} & c_{43} & c_{44} & c_{45} & c_{46} \\ c_{51} & c_{52} & c_{53} & c_{54} & c_{55} & c_{56} \\ c_{61} & c_{62} & c_{63} & c_{64} & c_{65} & c_{66} \end{bmatrix} \right) \begin{bmatrix} \hat{X}_a \\ \hat{Y}_a \\ \hat{Z}_a \\ \hat{\Phi}_a \\ \hat{\Theta}_a \\ \hat{\Psi}_a \end{bmatrix} = \begin{bmatrix} \hat{F}_1 \\ \hat{F}_2 \\ \hat{F}_3 \\ \hat{M}_4 \\ \hat{M}_5 \\ \hat{M}_6 \end{bmatrix} \tag{2-11}$$

Wave forces and moments are linearly related to the wave elevation. RAO are obtained by dividing the motion amplitude by the wave elevation.

$$RAO_x = \frac{X_a}{\zeta_a} \tag{2-12}$$

For a range of wave frequencies the EOM is solved. The RAO and phase graphs are obtained: the frequency characteristics of the vessel. This forms input for the workability analysis.

Motion superposition

The vessel motions of and about the CoG are known. The Ampelmann system is translated relative to the CoG of the vessel this point is indicated as point B. Because the vessel motions are known also the local vessel motions of point B are known [3], the linearised expression is shown below as a frequency domain expression:

$$\begin{bmatrix} \hat{X}_B \\ \hat{Y}_B \\ \hat{Z}_B \\ \hat{\Phi}_B \\ \hat{\Theta}_B \\ \hat{\Psi}_B \end{bmatrix} = \begin{bmatrix} 1 & 0 & 0 & 0 & L_z & -L_y \\ 0 & 1 & 0 & -L_z & 0 & L_x \\ 0 & 0 & 1 & L_y & -L_x & 0 \\ 0 & 0 & 0 & 1 & 0 & 0 \\ 0 & 0 & 0 & 0 & 1 & 0 \\ 0 & 0 & 0 & 0 & 0 & 1 \end{bmatrix} \begin{bmatrix} \hat{X}_1 \\ \hat{Y}_1 \\ \hat{Z}_1 \\ \hat{\Phi}_1 \\ \hat{\Theta}_1 \\ \hat{\Psi}_1 \end{bmatrix} \tag{2-13}$$

All indices B refer to local vessel motions of point B. L_x, L_y and L_z define to location of point B relative to the vessel's CoG.

2-4-3 Workability study

An Ampelmann project starts with a theoretical workability study. The client delivers vessel frequency characteristics of the host vessel. Then based on these frequency characteristics a workability study is performed. Ampelmann workability software AWESOME (Ampelmann Workability Evaluation Ship Orientated Motions and cylinder Excitations) calculates the workability of the Ampelmann system on the vessel. Based on the vessel frequency characteristics a time trace is made of the vessel motions. In most cases the Ampelmann system is positioned at a point B relative to the CoG of the vessel, for this point the local vessel motions are determined. These motions shall be compensated by the Ampelmann system. For the workability analysis it is assumed that the transfer deck is motionless. A time trace is made of the ship motions, see Appendix G. When the maximum cylinder length is exceeded for more than 3% of the time, the situation is marked as not workable.

2-5 Conclusion

The Ampelmann system compensates all 6 DOF vessel motions by use of the 6 hydraulic cylinders of the Stewart platform. Residual motions are compensated by three additional functionalities of the Ampelmann system: gangway telescoping, gangway luffing and transfer deck slewing.

In previous research a computational model is built to simulate the roll resonance of the coupled vessel-Ampelmann system. Three factors are identified that affect the roll resonance behaviour: the ship's damping, the time lag in the control system and the mass of the transfer

deck.

The dynamic behaviour of a vessel is described by its frequency characteristics, which are determined by a frequency domain analysis. Hydromechanic vessel properties are required to perform the frequency domain analysis and are vessel specific. The workability analysis requires vessel frequency characteristics as input.

Chapter 3

Hydromechanic vessel properties

3-1 Introduction

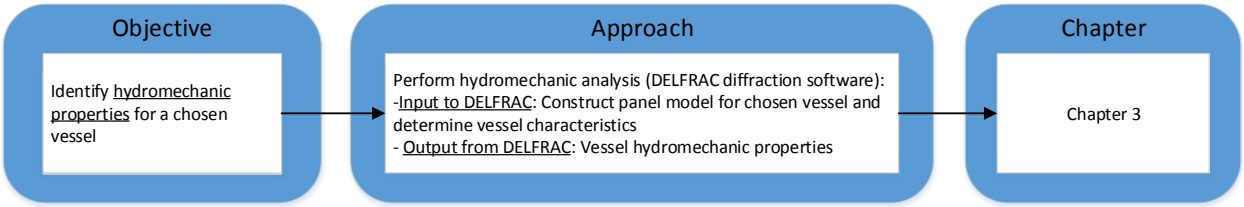

Figure 3-1: Flow chart of the objective and approach of this chapter

This chapter's objective is to identify the hydromechanic properties of a vessel. Hydromechanic vessel properties are required to calculated the vessel frequency characteristics, which are input for the workability analysis. The hydromechanic properties of a vessel depend on the hull shape, the mass of the vessel, the mass moment of inertia of the vessel and the location of the CoG of the vessel. DELFRAC diffraction software calculates the hydromechanic properties of a chosen vessel. This chapter elaborates on the DELFRAC software and how the hydromechanic properties are determined by DELFRAC.

DELFRAC is based on potential theory. The hydromechanic vessel properties or vessel parameters are determined from the potentials, which are calculated by DELFRAC [3]. The vessel parameters include: the frequency dependent added mass and damping, the restoring terms and the frequency dependent wave forces with wave phases. DELFRAC requires an input, calculates the potentials and gives an output. This is illustrated in Figure 3-2 on page 18. First a vessel is chosen, for this vessel a panel model is made. The panel model is substituted to DELFRAC. DELFRAC calculates the vessel parameters with the corresponding frequency characteristics.

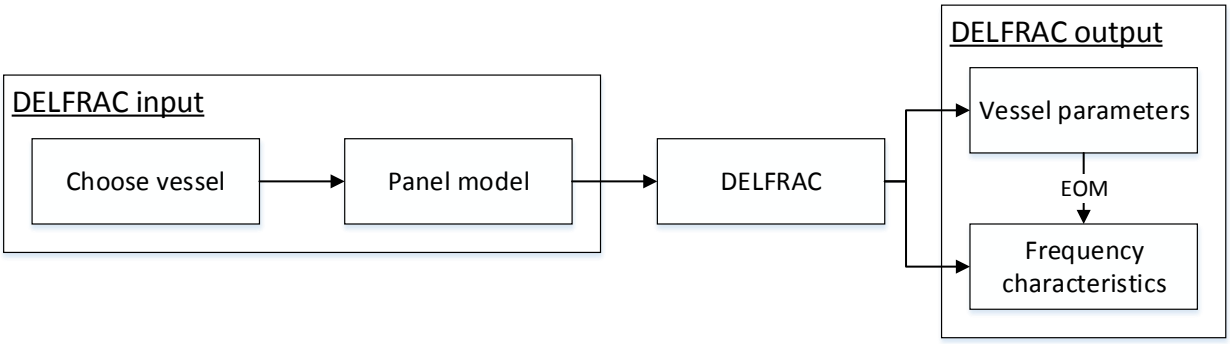

Figure 3-2: DELFRAC input and DELFRAC output

Section 3-2 briefly describes the working principle of DELFRAC. The input for DELFRAC comprises two steps, first a hull shape is chosen and secondly for this hull shape a panel model is made. This is discussed in section 3-3. Section 3-4 discusses the DELFRAC output: the vessel parameters and the frequency characteristics. The frequency characteristics are calculated by substituting the vessel parameters to the EOM. The results in this thesis are based on a case study, for this case study the vessel parameters are determined.

3-2 DELFRAC diffraction software

DELFRAC uses 3D (3 dimensional) potential theory. It computes frequency dependent wave loads on free-floating or fixed bodies and frequency dependent motions of floating bodies. DELFRAC is restricted to arbitrary shaped bodies with zero mean forward speed. It solves the wave potential on the wetted hull surface defined as: the surface separating the body and the water while free floating in still water. To solve the potentials the following boundary conditions shall be met:

- *The continuity condition* or Laplace equation.
- *The seabed boundary condition*: The seabed is watertight.
- *The free surface boundary condition*: The surface pressure equals the atmospheric pressure and the water particles cannot leave the free surface.
- *The boundary condition at the ship's hull surface*: The ship shall be watertight. The normal velocity of the water particles at the hull surface equals the normal velocity of the hull surface itself.
- *Radiation condition*: at a great distance from the body the potentials disappear.

In order to create the potential flows, the wetted hull surface is represented as a source sheet. This can be imagined as if the vessel is wrapped into a blanket of panels, with each panel defining an in strength varying sink or source enabling to meet the *boundary condition at the hull surface*. Furthermore the sink/source distribution satisfies the *radiation potential* where the effect of the sink/source vanishes at large distance from the source. The source sheet distribution is visualized in Figure 3-3.

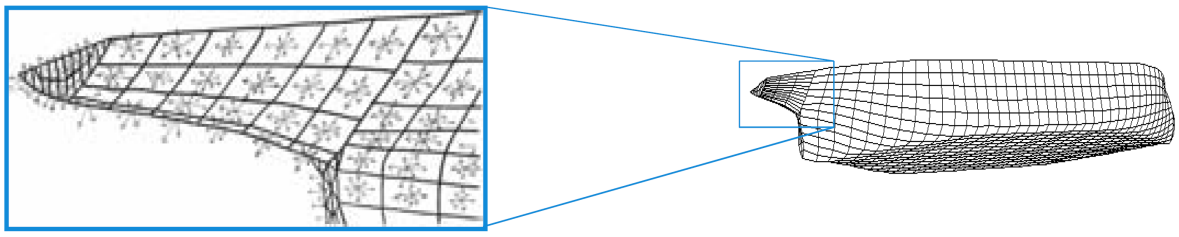

Figure 3-3: The hull surface as a source sheet [3]

The potentials are determined by use of the Green's function. This is part of the diffraction software. It satisfies the *free surface boundary condition* and the *seabed boundary condition*. The Green's function relates the source strengths to the potentials. Potential theory only includes potential damping: wave generation. In practice this is the major part of the damping. Viscous effects, including skin fiction and vortices are not taken into account. Especially for rolling vessel motions viscous effects can be significant [2].

3-3 DELFRAC input

The DELFRAC input comprises two steps. First, a hull shape is chosen. Second, for this hull shape a panel model is made. A barge is chosen as shown in Figure 3-4.

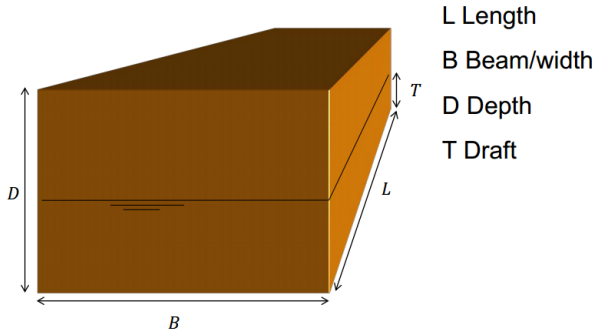

Figure 3-4: Conventions for the chosen hull shape [4]

With $L = 34[m]$, $B = 12[m]$, $D = 6[m]$ and $T = 3[m]$, these dimensions are based on the walk to work vessels DP Galyna and DP Gezina from the introduction of this thesis. These vessels have a draft of approximately $3[m]$, a width of $12[m]$ and a displacement of $1224[m^3]$. The corresponding length for this barge shape to match the displacement is $34[m]$. The mass properties are determined as if it is a homogeneous solid body with the CoG centered, the CoG coincides with the still water level since $D = 2T$. For this barge shaped vessel a panel model of the wetted surface is made. A panel model is build up of vertex points. A set of four vertex points defines a panel. The size of each panel must be chosen small enough to assume constant pressure on the panel [5], which depends on the frequency range for which the analysis is performed. For a frequency range from $\omega = 0[rad/s]$ to $\omega = 3[rad/s]$ a panel size of $1[m] \times 1[m]$ is sufficient [5]. DELFRAC requires a list of vertices with a corresponding

list of vertices that define the panels. Figure 3-6 shows the 3D scatter plot of all vertex points. All blue points show the bottom plate of the barge and all red points show all side plates. Figure 3-5 shows a 2D (2 dimensional) representation of the scatter plot: Top view (left), right side view (center) and front view (right). Appendix B, section B-1 shows the detailed DELFRAC input file and elaborates on the barge mass properties.

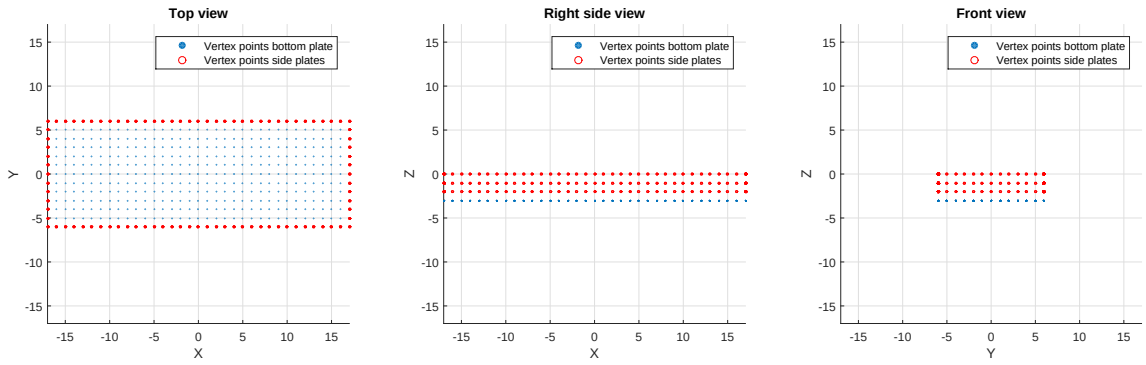

Figure 3-5: Barge, 2D scatter plots of the vertices defining the wetted surface. $Z = 0[m]$: Still water level.

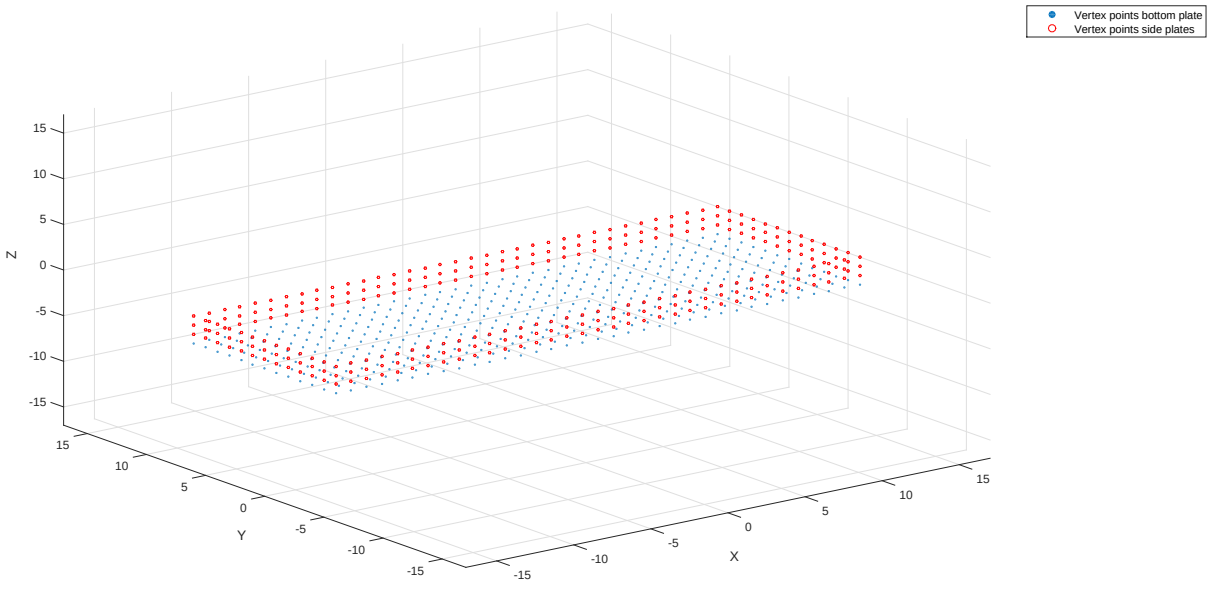

Figure 3-6: Barge, 3D scatter plot of all vertices defining the wetted surface. $Z = 0[m]$: Still water level.

3-4 DELFRAC output

DELFRAC gives two outputs. First all vessel parameters are given, these contain the frequency dependent added mass and damping, the restoring terms and the frequency dependent wave forces with wave phases. Second, DELFRAC calculates the frequency characteristics of the vessel. These include the RAO and the phases. The frequency characteristics are calculated by substituting the vessel parameters to the EOM:

$$\{-\omega^2[\underbrace{\mathbf{M}}_{1}+\underbrace{\mathbf{A}(\omega)}_{2}]+i\omega[\underbrace{\mathbf{B}(\omega)}_{3}]+[\underbrace{\mathbf{C}}_{4}]\}\underbrace{\begin{bmatrix}\hat{X}_a\\ \hat{Y}_a\\ \hat{Z}_a\\ \hat{\Phi}_a\\ \hat{\Theta}_a\\ \hat{\Psi}_a\end{bmatrix}}_{5}=\underbrace{\begin{bmatrix}\hat{F}_1\\ \hat{F}_2\\ \hat{F}_3\\ \hat{M}_4\\ \hat{M}_5\\ \hat{M}_6\end{bmatrix}}_{6} \tag{3-1}$$

1. The mass matrix. Input to DELFRAC and is known.
2. The frequency dependent added mass matrix. From DELFRAC
3. The frequency dependent damping matrix. From DELFRAC.
4. The restoring matrix, independent of frequency. From DELFRAC.
5. The complex motion amplitude vector. To be determined.
6. The complex wave force and moment amplitudes. From DELFRAC.

The wave forces and moments in DELFRAC are computed for a wave amplitude of $1[m]$. Solving the EOM directly gives the complex motion amplitudes. By taking the absolute value the RAO is obtained and by taking the angle the phase is obtained.

The frequency characteristics are computed for all 6 DOF vessel motions and for a chosen wave incident angle. This calculation method used throughout this thesis, to get from vessel parameters to frequency characteristics is validated in Appendix B section B-2.

3-5 Conclusion

A hull shape is derived based on the hull shape of an existing vessel. For this hull shape the hydromechanic properties are determined by DELFRAC. DELFRAC is based on 3D potential theory, for the hull shape a panel model is made. This is input for DELFRAC. Then DELFRAC calculates the hydromechanic properties of the vessel for a range of frequencies.

Chapter 4

Modelling coupled vessel-Ampelmann systems

4-1 Introduction

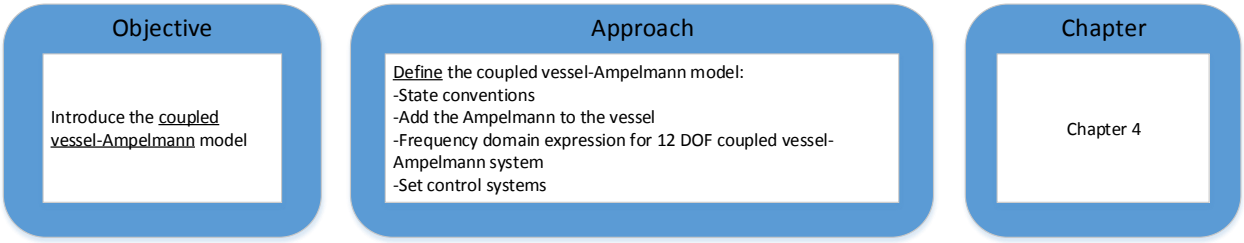

Figure 4-1: Flow chart of the objective and approach of this chapter

This chapters objective is to introduce the coupled vessel-Ampelmann model. The conventions for the two body system are stated in section 4-2. Then a general description is given of the coupled vessel-Ampelmann system in section 4-3, followed by the mathematical representation of the coupled vessel-Ampelmann model in section 4-4. The control system of the Ampelmann determines how the transfer deck moves with respect to the vessel. Three control systems are defined in section 4-5.

4-2 Conventions

The Ampelmann system is a multibody system with its bottom frame fixed to the vessel. The 6 hydraulic cylinders connect the bottom frame to the Mercedes frame. All components that are suspended by the hydraulic cylinders: the Mercedes frame, the slewing ring, the transfer deck, the luffing cylinders and the gangway are named as the TD (transfer deck). For the models discussed in this thesis it is assumed that in static equilibrium the TD mass

is vertically aligned with its position on the vessel.

A vessel has 6 DOF and the TD has 6 DOF. The combination of the vessel and the TD has 12 DOF. Both the vessel and the TD may move in: surge, sway, heave, roll, pitch and yaw. See Figure 4-2, all vessel DOF are subscripted with 1 and all TD DOF with 2. Both the vessel and the TD are defined in a steadily translating coordinate/reference system with zero forward speed. Both the vessel and the TD have their own reference system. In the frequency domain analysis vessel and TD oscillations are all described with respect to their reference system.

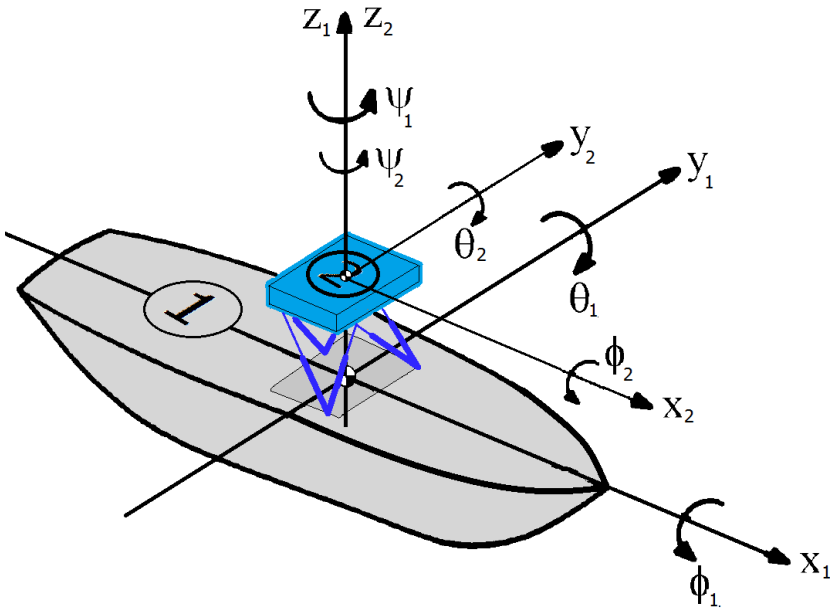

Figure 4-2: Conventions for 6 DOF vessel motions and 6 DOF Ampelmann motions

4-3 Adding the Ampelmann to the vessel

Figure 4-3 on page 25 shows how the TD is added to the vessel. On the left hand side the vessel is shown. The vessel is only hydromechanically coupled. In the center figure the Ampelmann is added to the vessel. The vessel is hydromechanically coupled with the surrounding water and mechanically coupled with the Ampelmann system. On the right hand side the coupled vessel-Ampelmann model is shown. The vessel (1) is connected to the TD (2) via the hydraulic cylinders. The hydraulic cylinders are modelled as a rigid massless clamped beam with a controllable length and inclination angle. Forces and moments due to the TD work directly through this beam on the vessel and visa versa. The offset between the vessel and the TD is indicated with length L_a.

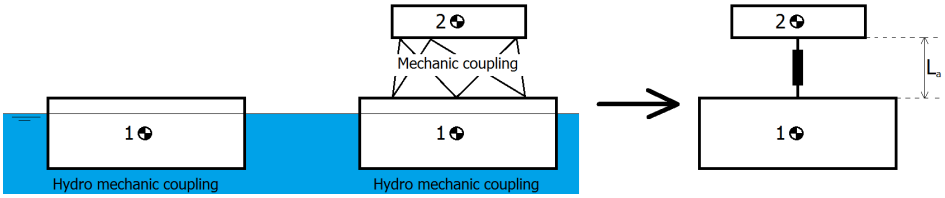

Figure 4-3: The vessel is hydromechanically coupled with the water and mechanically coupled with the TD

A schematic representation of the coupled vessel-Ampelmann system is shown in Figure 4-4. On the left and right side the vessel and the TD are indicated with 6 DOF each. From practice it is known that when activating the Ampelmann system the dynamic behaviour of the vessel changes, indicated with: motion coupling. The behaviour of the TD is determined by the control system, the center block. For a passive system the TD has a fixed position with respect to the vessel, it moves with the vessel. For an active system the TD is compensated and is motionless. In the transition from a passive to an active system the dynamic vessel behaviour changes. The control system applicable for the coupled vessel-Ampelmann models are discussed in section 4-5.

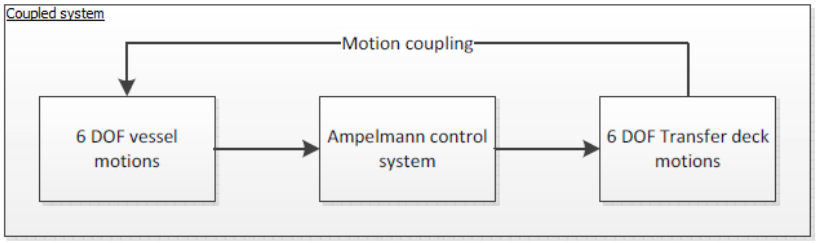

Figure 4-4: The control system determines how the TD moves with respect to the vessel

4-4 Mathematical coupled vessel-Ampelmann model

The coupled vessel-Ampelmann system has 12 DOF. The 6 DOF vessel frequency domain expression, Equation 2-11, is extended with the 6 DOF TD motions in an identical format. Note that vessel motions are now subscripted with: 1, in each DOF instead of: a. TD motions are subscripted with: 2. On the right hand side of the EOM the external forces working on the system are stated. Only the vessel is excited by waves.

$$\left(-\omega^2[\mathbf{M}+\mathbf{A}(\omega)]+i\omega[\mathbf{B}(\omega)]+[\mathbf{C}]\right)\begin{bmatrix}\hat{X}_1\\ \hat{Y}_1\\ \hat{Z}_1\\ \hat{\Phi}_1\\ \hat{\Theta}_1\\ \hat{\Psi}_1\\ \hat{X}_2\\ \hat{Y}_2\\ \hat{Z}_2\\ \hat{\Phi}_2\\ \hat{\Theta}_2\\ \hat{\Psi}_2\end{bmatrix} = \begin{bmatrix}\hat{F}_1\\ \hat{F}_2\\ \hat{F}_3\\ \hat{M}_4\\ \hat{M}_5\\ \hat{M}_6\\ 0\\ 0\\ 0\\ 0\\ 0\\ 0\end{bmatrix} \tag{4-1}$$

The complex vessel and TD motions: $\hat{X}_1$, $\hat{Y}_1$, $\hat{Z}_1$, $\hat{\Phi}_1$, $\hat{\Theta}_1$, $\hat{\Psi}_1$, $\hat{X}_2$, $\hat{Y}_2$, $\hat{Z}_2$, $\hat{\Phi}_2$, $\hat{\Theta}_2$ and $\hat{\Psi}_2$ are obtained by solving the 12 DOF coupled system. The goal is to find expressions for the 12×12 matrices $[\mathbf{M} + \mathbf{A}(\omega)]$, $[\mathbf{B}(\omega)]$ and $[\mathbf{C}]$. Then this system of equations is solved, the vessel frequency characteristics are obtained and form input to the workability analysis. These frequency characteristics take into account the dynamic interaction between the vessel and the TD. The input variables to this coupled vessel-Ampelmann model are:

- The mass and mass moment of inertia of the vessel and the TD: m_1, I_{xx1}, I_{yy1}, I_{zz1}, m_2, I_{xx2}, I_{yy2} and I_{zz2}.
- Hydromechanic vessel properties. $[\mathbf{A}(\omega)]$, $[\mathbf{B}(\omega)]$, $[\mathbf{C}]$, $\hat{F}_{1,2,3}$ and $\hat{M}_{4,5,6}$.
- The location of the Ampelmann on the vessel. Defined by point B: L_x, L_y and L_z with respect to the CoG of the vessel. The TD mass has a vertical offset L_a with respect to point B.
- The control system of the Ampelmann.

Equation 4-1 describes the total coupled system. This expression with a large number of variables gives no fundamental understanding of the coupling mechanisms involved between the vessel and the Ampelmann system. Therefore to get a fundamental understanding of all mechanisms involved multiple steps are taken. First simplified models are made starting with only 2 DOF in a 2D plane. Gradually the number of DOF is increased until the complete 3D 12 DOF coupled vessel-Ampelmann model is obtained, which contains all input variables. In chapter 5 the coupled system is modelled in a 2D plane and gives a fundamental understanding of the coupling mechanisms involved. Chapter 6 derives and determines the 12 DOF coupled system including all input variables stated above.

The hydromechanic properties are substituted to the coupled 12 DOF EOM. Each top left quadrant of the $[\mathbf{M} + \mathbf{A}(\omega)]$ matrix, $[\mathbf{B}(\omega)]$ matrix and $[\mathbf{C}]$ matrix contain all the hydromechanic coupling terms and the vessel mass terms.

$$[\mathbf{M}+\mathbf{A}(\omega)] = \begin{bmatrix} m_1+a_{11}(\omega) & a_{12}(\omega) & a_{13}(\omega) & a_{14}(\omega) & a_{15}(\omega) & a_{16}(\omega) & \cdots & \cdots & \cdots & \cdots & \cdots & \cdots \\ a_{21}(\omega) & m_1+a_{22}(\omega) & a_{23}(\omega) & a_{24}(\omega) & a_{25}(\omega) & a_{26}(\omega) & \cdots & \cdots & \cdots & \cdots & \cdots & \cdots \\ a_{31}(\omega) & a_{32}(\omega) & m_1+a_{33}(\omega) & a_{34}(\omega) & a_{35}(\omega) & a_{36}(\omega) & \cdots & \cdots & \cdots & \cdots & \cdots & \cdots \\ a_{41}(\omega) & a_{42}(\omega) & a_{43}(\omega) & I_{xx1}+a_{44}(\omega) & a_{45}(\omega) & a_{46}(\omega) & \cdots & \cdots & \cdots & \cdots & \cdots & \cdots \\ a_{51}(\omega) & a_{52}(\omega) & a_{53}(\omega) & a_{54}(\omega) & I_{yy1}+a_{55}(\omega) & a_{56}(\omega) & \cdots & \cdots & \cdots & \cdots & \cdots & \cdots \\ a_{61}(\omega) & a_{62}(\omega) & a_{63}(\omega) & a_{64}(\omega) & a_{65}(\omega) & I_{zz1}+a_{66}(\omega) & \cdots & \cdots & \cdots & \cdots & \cdots & \cdots \\ \cdots & \cdots & \cdots & \cdots & \cdots & \cdots & \cdots & \cdots & \cdots & \cdots & \cdots & \cdots \\ \cdots & \cdots & \cdots & \cdots & \cdots & \cdots & \cdots & \cdots & \cdots & \cdots & \cdots & \cdots \\ \cdots & \cdots & \cdots & \cdots & \cdots & \cdots & \cdots & \cdots & \cdots & \cdots & \cdots & \cdots \\ \cdots & \cdots & \cdots & \cdots & \cdots & \cdots & \cdots & \cdots & \cdots & \cdots & \cdots & \cdots \\ \cdots & \cdots & \cdots & \cdots & \cdots & \cdots & \cdots & \cdots & \cdots & \cdots & \cdots & \cdots \\ \cdots & \cdots & \cdots & \cdots & \cdots & \cdots & \cdots & \cdots & \cdots & \cdots & \cdots & \cdots \end{bmatrix} \tag{4-2}$$

$$[\mathbf{B}(\omega)] = \begin{bmatrix} b_{11}(\omega) & b_{12}(\omega) & b_{13}(\omega) & b_{14}(\omega) & b_{15}(\omega) & b_{16}(\omega) & \cdots & \cdots & \cdots & \cdots & \cdots & \cdots \\ b_{21}(\omega) & b_{22}(\omega) & b_{23}(\omega) & b_{24}(\omega) & b_{25}(\omega) & b_{26}(\omega) & \cdots & \cdots & \cdots & \cdots & \cdots & \cdots \\ b_{31}(\omega) & b_{32}(\omega) & b_{33}(\omega) & b_{34}(\omega) & b_{35}(\omega) & b_{36}(\omega) & \cdots & \cdots & \cdots & \cdots & \cdots & \cdots \\ b_{41}(\omega) & b_{42}(\omega) & b_{43}(\omega) & b_{44}(\omega) & b_{45}(\omega) & b_{46}(\omega) & \cdots & \cdots & \cdots & \cdots & \cdots & \cdots \\ b_{51}(\omega) & b_{52}(\omega) & b_{53}(\omega) & b_{54}(\omega) & b_{55}(\omega) & b_{56}(\omega) & \cdots & \cdots & \cdots & \cdots & \cdots & \cdots \\ b_{61}(\omega) & b_{62}(\omega) & b_{63}(\omega) & b_{64}(\omega) & b_{65}(\omega) & b_{66}(\omega) & \cdots & \cdots & \cdots & \cdots & \cdots & \cdots \\ \cdots & \cdots & \cdots & \cdots & \cdots & \cdots & \cdots & \cdots & \cdots & \cdots & \cdots & \cdots \\ \cdots & \cdots & \cdots & \cdots & \cdots & \cdots & \cdots & \cdots & \cdots & \cdots & \cdots & \cdots \\ \cdots & \cdots & \cdots & \cdots & \cdots & \cdots & \cdots & \cdots & \cdots & \cdots & \cdots & \cdots \\ \cdots & \cdots & \cdots & \cdots & \cdots & \cdots & \cdots & \cdots & \cdots & \cdots & \cdots & \cdots \\ \cdots & \cdots & \cdots & \cdots & \cdots & \cdots & \cdots & \cdots & \cdots & \cdots & \cdots & \cdots \\ \cdots & \cdots & \cdots & \cdots & \cdots & \cdots & \cdots & \cdots & \cdots & \cdots & \cdots & \cdots \end{bmatrix} \tag{4-3}$$

$$[\mathbf{C}] = \begin{bmatrix} c_{11} & c_{12} & c_{13} & c_{14} & c_{15} & c_{16} & \cdots & \cdots & \cdots & \cdots & \cdots & \cdots \\ c_{21} & c_{22} & c_{23} & c_{24} & c_{25} & c_{26} & \cdots & \cdots & \cdots & \cdots & \cdots & \cdots \\ c_{31} & c_{32} & c_{33} & c_{34} & c_{35} & c_{36} & \cdots & \cdots & \cdots & \cdots & \cdots & \cdots \\ c_{41} & c_{42} & c_{43} & c_{44} & c_{45} & c_{46} & \cdots & \cdots & \cdots & \cdots & \cdots & \cdots \\ c_{51} & c_{52} & c_{53} & c_{54} & c_{55} & c_{56} & \cdots & \cdots & \cdots & \cdots & \cdots & \cdots \\ c_{61} & c_{62} & c_{63} & c_{64} & c_{65} & c_{66} & \cdots & \cdots & \cdots & \cdots & \cdots & \cdots \\ \cdots & \cdots & \cdots & \cdots & \cdots & \cdots & \cdots & \cdots & \cdots & \cdots & \cdots & \cdots \\ \cdots & \cdots & \cdots & \cdots & \cdots & \cdots & \cdots & \cdots & \cdots & \cdots & \cdots & \cdots \\ \cdots & \cdots & \cdots & \cdots & \cdots & \cdots & \cdots & \cdots & \cdots & \cdots & \cdots & \cdots \\ \cdots & \cdots & \cdots & \cdots & \cdots & \cdots & \cdots & \cdots & \cdots & \cdots & \cdots & \cdots \\ \cdots & \cdots & \cdots & \cdots & \cdots & \cdots & \cdots & \cdots & \cdots & \cdots & \cdots & \cdots \\ \cdots & \cdots & \cdots & \cdots & \cdots & \cdots & \cdots & \cdots & \cdots & \cdots & \cdots & \cdots \end{bmatrix} \tag{4-4}$$

All other matrix positions are to be filled in. Later in this thesis the top left quadrants together with the top right quadrants give the force and moment relations between the vessel and the Ampelmann system. In the lower half of each matrix the implicit mathematical relations are substituted relating vessel and TD motions, which depend on the control system see section 4-5.

4-4-1 Application of DELFRAC output

DELFRAC performs a hydromechanic analysis for a vessel with a certain underwater hull geometry. To keep the hydromechanic data valid when applying the Ampelmann to the vessel, the underwater hull geometry may not change. The vessel's draft and the static trim angle shall remain unchanged.

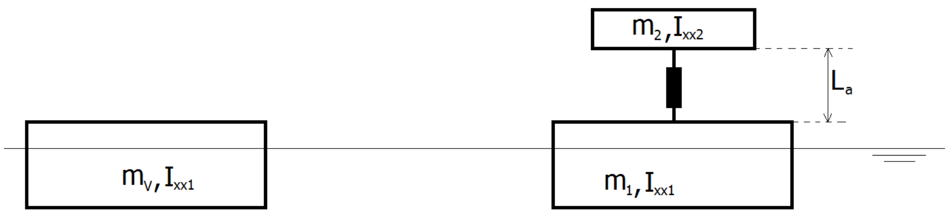

Figure 4-5: Difference between DELFRAC input and coupled vessel-Ampelmann model

The DELFRAC analysis is performed for a vessel with a mass m_v and a mass moment of inertia I_{xx1}, Figure F-1 left side. The right figure shows the application of the Ampelmann on the vessel. In order to keep the draft constant, the vessel mass m_v (left figure) reduces to a vessel mass of m_1 (right figure) with the application of m_2.

$$m_v = m_1 + m_2 \tag{4-5}$$

On application of the Ampelmann, the vessel's mass moment of inertia stays I_{xx1}. The mass moment of inertia of the combined system increases with the TD mass moment of inertia to: $I_{xx2} + m_2 L_a^2$ with respect to the CoG of the vessel.

$$I_{xx1} \rightarrow I_{xx1} + I_{xx2} + m_2 L_a^2 \tag{4-6}$$

Changing the draft of the combined system or the vessels static trim angle causes invalid hydromechanic data. Before performing a DELFRAC analysis, the application of the Ampelmann shall be taken into account first.

4-5 Set control systems

Four vessel configurations are distinguished during the entire operational cycle on application of the Ampelmann system. These are illustrated in Figure 4-6.

1. The vessel only: the dynamic behaviour of the vessel is only determined by the hydromechanic properties of the vessel. No Ampelmann is present.
2. The vessel with a passive Ampelmann in settled state: The Ampelmann is mounted to the deck of the vessel. The Ampelmann acts as a static payload to the vessel and moves with the vessel, the hydraulic cylinders have a fixed length and are fully retracted. By motion superposition the motions of the TD are derived. The Ampelmann and the TD form one rigid body.
3. The vessel with a passive Ampelmann in neutral state: Prior to the operation the TD is elevated from a settled to a neutral state. The hydraulic cylinders have a fixed length: half extended. The TD moves with the vessel as a static payload.
4. The vessel with a compensating Ampelmann: An active Ampelmann system. The vessel motions are measured and the hydraulic cylinders are controlled to keep the TD fixed in space. The hydraulic cylinders have a variable length depending on the vessel motions. The vessel and the TD move with respect to each other.

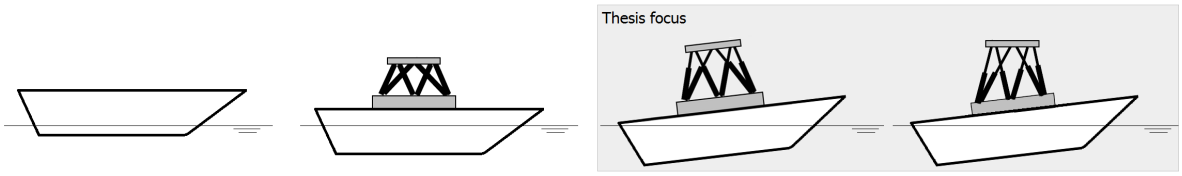

Figure 4-6: Four vessel configurations during the operational cycle

Based on observations for each configuration the dynamic behaviour of the vessel differs. Changing from configuration 1 to 2: Payload is added to the vessel, the draft of the vessel increases and the CoG of the combination shifts. Changing from configuration 2 to 3: The TD is elevated, the draft of the vessel remains but the CoG of the total system is elevated and the mass moment of inertia increases. Changing from configuration 3 to 4 is the focus of this thesis. The Ampelmann is activated from a passive state where it changes to a compensating state. From observations the dynamic behaviour changes.

A linear first order frequency domain analysis is performed. This requires a continuous EOM. In reality there are multiple discontinuities, these are mainly caused by mechanical limitations: a cylinder has a maximum stroke length and a maximum cylinder velocity. In the Ampelmann control system, asymptote functions are used to ensure the cylinder does not makes an abrupt stop when it reaches a minimum or maximum stroke length. It smoothens the TD motions. These discontinuities can not be taken into account in a frequency domain analysis. It is assumed that there are no limitations to the cylinder length. When the dynamic behaviour of a vessel is studied and these discontinuities should be taken into account,

a time domain analysis shall be performed. This is beyond the scope of this thesis.

The control system determines how the TD moves with respect to the vessel. In Appendix C the Ampelmann control system is studied. Three control systems are identified that apply to the coupled vessel-Ampelmann models discussed throughout this thesis. See Figure 4-7.

1. No compensation: A passive Ampelmann system. The TD moves with the vessel, all hydraulic cylinders have a fixed length. The TD acts as a static weight to the vessel. TD motions are determined by motion superposition.
2. Perfect compensation: An active Ampelmann system. The TD is motionless. In absence of mechanical limitations of the Ampelmann system the control system is capable to perfectly compensate vessel motions.
3. Filter compensation: An active Ampelmann system. Residual motions are caused due to mechanical limitations of the Ampelmann system. These limitations can not be taken into account in a frequency domain analysis. The same second order low pass filter as used in the Ampelmann control system is applied to induce residual TD motions to the coupled vessel-Ampelmann model. Filters introduce a time lag and gain to the control signal. It allows to study the effect of residual TD motions on the dynamic behaviour of the coupled system.

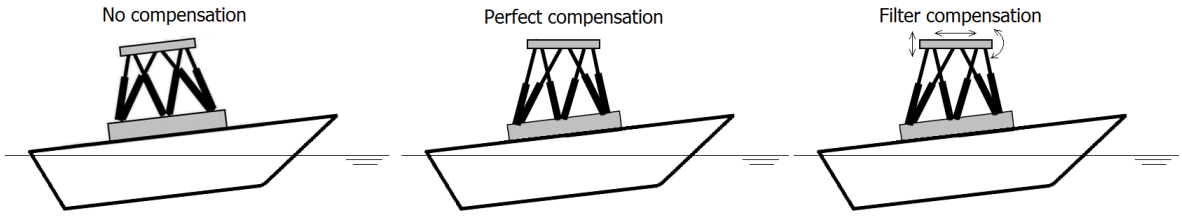

Figure 4-7: Identification of control systems

Three control systems are identified: No compensation, Perfect compensation and Filter compensation. When comparing No compensation with Perfect compensation it is shown how the dynamic behaviour of the vessel changes when the Ampelmann is activated. From the comparison between Perfect compensation and Filter compensation the effect of residual TD motions on the dynamic behaviour of the coupled system is analysed.

In the next three sections each control system: No compensation, Perfect compensation and Filter compensation are discussed in detail. Mathematical expressions are derived relating complex TD motions to complex vessel motions. These are implicit relations for the forces and moments working between the vessel and the TD. The expressions are finally substituted to the EOM.

4-5-1 No compensation

A passive Ampelmann has a fixed positions relative to the vessel, all hydraulic cylinders have a fixed length. The TD moves with the vessel and has a constant offset L_a with respect to

point B. TD motions are described in the frequency domain in complex format.

$$\begin{bmatrix} \hat{X}_2 \\ \hat{Y}_2 \\ \hat{Z}_2 \\ \hat{\Phi}_2 \\ \hat{\Theta}_2 \\ \hat{\Psi}_2 \end{bmatrix} = \begin{bmatrix} \hat{X}_B \\ \hat{Y}_B \\ \hat{Z}_B \\ \hat{\Phi}_B \\ \hat{\Theta}_B \\ \hat{\Psi}_B \end{bmatrix} + \begin{bmatrix} 0 & 0 & 0 & 0 & L_a & 0 \\ 0 & 0 & 0 & -L_a & 0 & 0 \\ 0 & 0 & 0 & 0 & 0 & 0 \\ 0 & 0 & 0 & 0 & 0 & 0 \\ 0 & 0 & 0 & 0 & 0 & 0 \\ 0 & 0 & 0 & 0 & 0 & 0 \end{bmatrix} \begin{bmatrix} \hat{X}_1 \\ \hat{Y}_1 \\ \hat{Z}_1 \\ \hat{\Phi}_1 \\ \hat{\Theta}_1 \\ \hat{\Psi}_1 \end{bmatrix} \tag{4-7}$$

By substitution of Equation 2-13, the TD motions are written in terms of vessel motions.

$$\begin{bmatrix} \hat{X}_2 \\ \hat{Y}_2 \\ \hat{Z}_2 \\ \hat{\Phi}_2 \\ \hat{\Theta}_2 \\ \hat{\Psi}_2 \end{bmatrix} = \begin{bmatrix} 1 & 0 & 0 & 0 & L_z + L_a & -L_y \\ 0 & 1 & 0 & -(L_z + L_a) & 0 & L_x \\ 0 & 0 & 1 & L_y & -L_x & 0 \\ 0 & 0 & 0 & 1 & 0 & 0 \\ 0 & 0 & 0 & 0 & 1 & 0 \\ 0 & 0 & 0 & 0 & 0 & 1 \end{bmatrix} \begin{bmatrix} \hat{X}_1 \\ \hat{Y}_1 \\ \hat{Z}_1 \\ \hat{\Phi}_1 \\ \hat{\Theta}_1 \\ \hat{\Psi}_1 \end{bmatrix} \tag{4-8}$$

4-5-2 Perfect compensation

The TD is motionless. No residual motions occur, the TD is fixed in space. All motions are perfectly compensated.

$$\begin{bmatrix} \hat{X}_2 & \hat{Y}_2 & \hat{Z}_2 & \hat{\Phi}_2 & \hat{\Theta}_2 & \hat{\Psi}_2 \end{bmatrix}^T = \begin{bmatrix} 0 & 0 & 0 & 0 & 0 & 0 \end{bmatrix}^T \tag{4-9}$$

4-5-3 Filter compensation

The Ampelmann control system measures the vessel motions at the bottom frame, processes the signals and controls the hydraulic cylinders with the control signals. A filter introduces a time lag and a gain to the signal. A second order low pass filter with a cut off frequency of $2[Hz]$ is applied to the Filter compensation model. As a result residual motions are introduced to the TD.

In the vessel reference system the TD motions are a result of vessel motions and the cylinder motions. Suppose the bottom frame has a regular heave motion $\hat{Z}_1$. In No compensation the TD moves at a fixed distance L_a with respect to $\hat{Z}_1$.

$$\hat{Z}_2 = \hat{Z}_1 \tag{4-10}$$

In case of Perfect compensation or Filter compensation, a TD motion is a result of a vessel motion and a changing cylinder length.

$$\hat{Z}_2 = \hat{Z}_1 + L_a \tag{4-11}$$

In Perfect compensation the cylinder length is controlled such that it matches the negative of $\hat{Z}_1 \rightarrow L_a = -\hat{Z}_1$. Substitution of L_a to Equation 4-11 yields the equation for Perfect compensation.

$$\hat{Z}_2 = 0 \tag{4-12}$$

For Filter compensation the second order low pass filter is expressed by the following frequency domain expression.

$$H(\omega) = \frac{\omega_c^2}{-\omega^2 + 2i\omega_c\omega + \omega_c^2} \tag{4-13}$$

With $\omega_c = 2\pi f_c$. In Perfect compensation $L_a = -\hat{Z}_1$ for Filter compensation the actuator length is a result of the filtered vessel motion. Therefore the TD motion is a result of the vessel motion and the negative of the filtered vessel motion. The frequency domain expression becomes, $L_a = -H(\omega)\hat{Z}_1$. Substitution to Equation 4-11 yields:

$$\hat{Z}_2 = \hat{Z}_1 - H(\omega)\hat{Z}_1 \tag{4-14}$$

The following relations, relating the vessel and the TD motions are obtained.

$$\left(-\omega^2[\mathbf{M}_{filt}] + i\omega[\mathbf{B}_{filt}] + [\mathbf{C}_{filt}]\right) \begin{bmatrix} \hat{X}_1 \\ \hat{Y}_1 \\ \hat{Z}_1 \\ \hat{\Phi}_1 \\ \hat{\Theta}_1 \\ \hat{\Psi}_1 \\ \hat{X}_2 \\ \hat{Y}_2 \\ \hat{Z}_2 \\ \hat{\Phi}_2 \\ \hat{\Theta}_2 \\ \hat{\Psi}_2 \end{bmatrix} = \begin{bmatrix} 0 \\ 0 \\ 0 \\ 0 \\ 0 \\ 0 \end{bmatrix} \tag{4-15}$$

$$[\mathbf{M}_{filt}] = \begin{bmatrix} 1 & 0 & 0 & 0 & (L_z+L_a) & -L_y & -1 & 0 & 0 & 0 & 0 & 0 \\ 0 & 1 & 0 & -(L_z+L_a) & 0 & L_x & 0 & -1 & 0 & 0 & 0 & 0 \\ 0 & 0 & 1 & L_y & -L_x & 0 & 0 & 0 & -1 & 0 & 0 & 0 \\ 0 & 0 & 0 & 1 & 0 & 0 & 0 & 0 & 0 & -1 & 0 & 0 \\ 0 & 0 & 0 & 0 & 1 & 0 & 0 & 0 & 0 & 0 & -1 & 0 \\ 0 & 0 & 0 & 0 & 0 & 1 & 0 & 0 & 0 & 0 & 0 & -1 \end{bmatrix} \tag{4-16}$$

$$[\mathbf{B}_{filt}] = \begin{bmatrix} 2\omega_c & 0 & 0 & 0 & 2\omega_c(L_z+L_a) & -2\omega_c L_y & -2\omega_c & 0 & 0 & 0 & 0 & 0 \\ 0 & 2\omega_c & 0 & -2\omega_c(L_z+L_a) & 0 & 2\omega_c L_x & 0 & -2\omega_c & 0 & 0 & 0 & 0 \\ 0 & 0 & 2\omega_c & 2\omega_c L_y & -2\omega_c L_x & 0 & 0 & 0 & -2\omega_c & 0 & 0 & 0 \\ 0 & 0 & 0 & 2\omega_c & 0 & 0 & 0 & 0 & 0 & -2\omega_c & 0 & 0 \\ 0 & 0 & 0 & 0 & 2\omega_c & 0 & 0 & 0 & 0 & 0 & -2\omega_c & 0 \\ 0 & 0 & 0 & 0 & 0 & 2\omega_c & 0 & 0 & 0 & 0 & 0 & -2\omega_c \end{bmatrix} \tag{4-17}$$

$$[\mathbf{C}_{filt}] = \begin{bmatrix} 0 & 0 & 0 & 0 & 0 & 0 & -\omega_c^2 & 0 & 0 & 0 & 0 & 0 \\ 0 & 0 & 0 & 0 & 0 & 0 & 0 & -\omega_c^2 & 0 & 0 & 0 & 0 \\ 0 & 0 & 0 & 0 & 0 & 0 & 0 & 0 & -\omega_c^2 & 0 & 0 & 0 \\ 0 & 0 & 0 & 0 & 0 & 0 & 0 & 0 & 0 & -\omega_c^2 & 0 & 0 \\ 0 & 0 & 0 & 0 & 0 & 0 & 0 & 0 & 0 & 0 & -\omega_c^2 & 0 \\ 0 & 0 & 0 & 0 & 0 & 0 & 0 & 0 & 0 & 0 & 0 & -\omega_c^2 \end{bmatrix} \tag{4-18}$$

4-6 Conclusion

The coupled vessel-Ampelmann system is a 12 DOF system. Both the vessel and Ampelmann have 6 DOF. From practice it is known that transfer deck motions affect the vessel motions. The transfer deck motions are determined by the control system. Depending on how the transfer deck is controlled the vessel experiences a changing dynamic behaviour. The focus of this thesis is to show how the dynamic behaviour of the vessel changes when the Ampelmann is activated. Three control system are examined: 1) No compensation, the transfer deck has a fixed position with respect to the vessel. 2) Perfect compensation, the transfer deck is fixed in space, no residual motions exist. 3) Filter compensation, residual transfer deck motions are a result of at time lag and gain in the control signal. For each control system, the coupled vessel-Ampelmann model is defined by a set of linear mathematical relations that allow the following variables: The hydromechanic vessel properties, the mass and mass moment of inertia of the vessel and transfer deck and the location of the Ampelmann on the vessel. By comparing the results for each control system the changing dynamic vessel behaviour is examined.

Chapter 5

Modelling the coupled vessel-Ampelmann system

5-1 Introduction

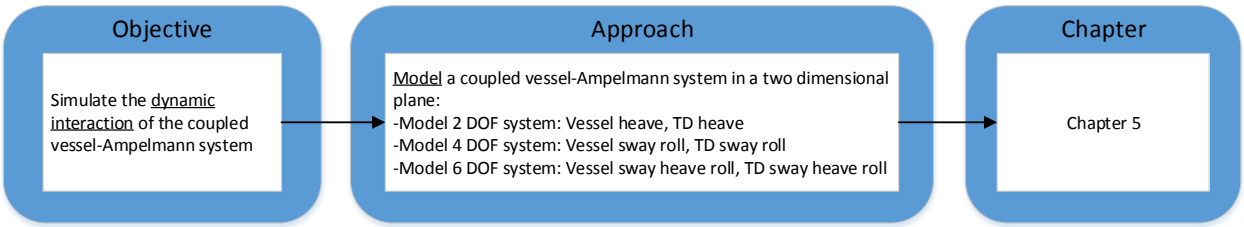

Figure 5-1: Flow chart of the objective and approach of this chapter

This chapters objective is to model the coupled vessel-Ampelmann system. From practice it is shown that a compensating Ampelmann changes the dynamic behaviour of the vessel. The behaviour of the coupled system is determined by the control system of the Ampelmann. For each model in this chapter three control systems apply: No compensation, Perfect compensation and Filter compensation. Three models are made where gradually the number of DOF is increased. Each model adds a fundamental understanding to the dynamic interaction of the coupled vessel-Ampelmann system. Figure 5-2 shows each model, the lower block of each figure represents the vessel, the upper block the TD and the center piece connects both.

- 2 DOF heave model: Both the vessel and TD are constrained to move in heave, Figure 5-2 left. Both bodies move in line. It is shown how the vessels natural frequency is affected, what happens to the vertical cylinder force and how the TD moves due to each control system. Section 5-2.
- 4 DOF sway and roll model: The vessel and the TD are both constrained to move in sway and roll, Figure 5-2 center. For each control system the differences in dynamic behaviour are shown. The important factors affecting the changing dynamic behaviour are discussed. Section 5-3.

- 6 DOF sway, heave and roll model: The vessel and the TD are both constrained to move in sway, heave and roll, Figure 5-2 right. This 6 DOF model gives a complete two dimensional representation of the coupled vessel-Ampelmann system. Section5-4.

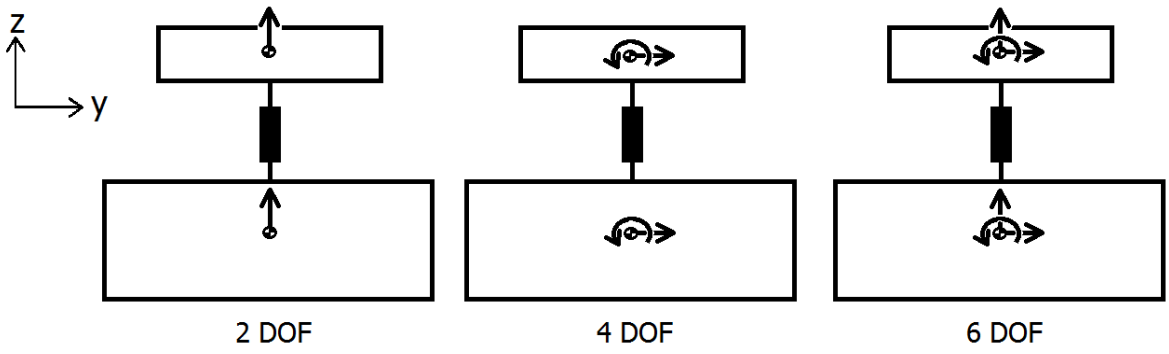

Figure 5-2: Models to simulated the dynamic interaction between the vessel and the Ampelmann system

Each model is simplified such that the CoG of the vessel and the TD are vertically aligned in neutral state, the Ampelmann system is positioned at the CoG of the vessel, $L_x = L_y = L_z = 0[m]$. The Stewart platform is modelled as a rigid clamped beam and depending on the control system it may have a controllable length and inclination angle. It connects the vessel with the TD.

5-2 2 DOF heave model

The vessel and TD are constrained to move in heave only. TD motions are in line with the vessel motions. The distance between the vessel and the TD system is controlled by the hydraulic cylinders. The frequency domain expression for the vessel, z_1, and TD, z_2, are derived from Figure 5-3. This expression is only valid for harmonic loading.

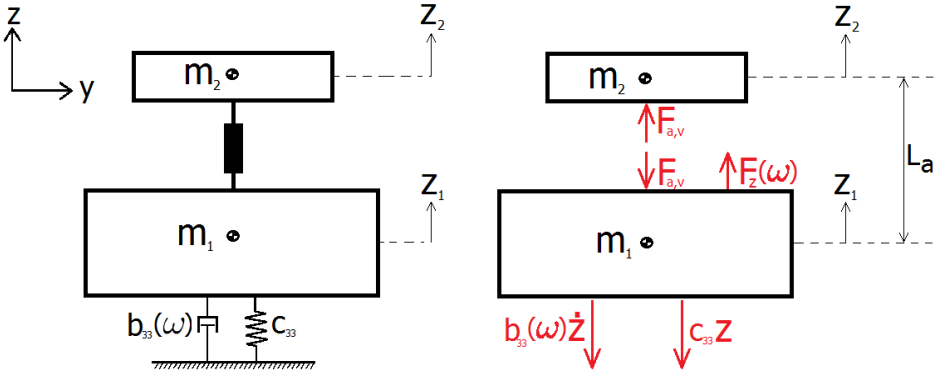

Figure 5-3: Free body diagram heave, frequency domain only harmonic loading

L_a states the offset of the reference axis z_2 relative to z_1. Furthermore, the hydromechanic terms b_{33} and c_{33} are the vessel damping and restoring terms in heave due to heave, these

yield from DELFRAC. Equation 5-1 gives the equations of motion for the vessel and the TD. Both are related via the vertical actuator force $F_{a,v}$. $F_z(\omega)$ is the complex wave load in heave direction acting on the vessel.

$$\begin{bmatrix} m_1 + a_{33}(\omega) & 0 \\ 0 & m_2 \end{bmatrix} \begin{bmatrix} \ddot{z}_1 \\ \ddot{z}_2 \end{bmatrix} + \begin{bmatrix} b_{33}(\omega) & 0 \\ 0 & 0 \end{bmatrix} \begin{bmatrix} \dot{z}_1 \\ \dot{z}_2 \end{bmatrix} + \begin{bmatrix} c_{33} & 0 \\ 0 & 0 \end{bmatrix} \begin{bmatrix} z_1 \\ z_2 \end{bmatrix} + \begin{bmatrix} F_{a,v} \\ -F_{a,v} \end{bmatrix} = \begin{bmatrix} F_z(\omega) \\ 0 \end{bmatrix} \quad (5\text{-}1)$$

The frequency domain expression contains 2 equation and 3 unknowns, $\hat{Z}_1$, $\hat{Z}_2$ and $F_{a,v}$:

$$\left(-\omega^2 \begin{bmatrix} m_1 + a_{33}(\omega) & m_2 \\ 0 & m_2 \end{bmatrix} + i\omega \begin{bmatrix} b_{33}(\omega) & 0 \\ 0 & 0 \end{bmatrix} + \begin{bmatrix} c_{33} & 0 \\ 0 & 0 \end{bmatrix} \right) \begin{bmatrix} \hat{Z}_1 \\ \hat{Z}_2 \end{bmatrix} + \begin{bmatrix} 0 \\ -F_{a,v} \end{bmatrix} = \begin{bmatrix} \hat{F}_3 \\ 0 \end{bmatrix} \quad (5\text{-}2)$$

In order to solve, an additional equation shall be found that describes the cylinder force $F_{a,v}$. An implicit relation is found relating $\hat{Z}_1$ and $\hat{Z}_2$ these depend on the control system, No compensation, Perfect compensation or Filter compensation. Expressions in the following form are obtained where on the second row of each matrix the implicit relation for $F_{a,v}$ is substituted.

$$\left(-\omega^2 \begin{bmatrix} m_1 + a_{33}(\omega) & m_2 \\ \dots & \dots \end{bmatrix} + i\omega \begin{bmatrix} b_{33}(\omega) & 0 \\ \dots & \dots \end{bmatrix} + \begin{bmatrix} c_{33} & 0 \\ \dots & \dots \end{bmatrix} \right) \begin{bmatrix} \hat{Z}_1 \\ \hat{Z}_2 \end{bmatrix} = \begin{bmatrix} \hat{F}_3 \\ 0 \end{bmatrix} \quad (5\text{-}3)$$

5-2-1 No compensation

A passive Ampelmann system has a fixed cylinder length. $\hat{Z}_1$ and $\hat{Z}_2$ are related by Equation 4-8. Substitution to Equation 5-3 yields.

$$\left(-\omega^2 \begin{bmatrix} m_1 + a_{33}(\omega) & m_2 \\ 0 & 0 \end{bmatrix} + i\omega \begin{bmatrix} b_{33}(\omega) & 0 \\ 0 & 0 \end{bmatrix} + \begin{bmatrix} c_{33} & 0 \\ -1 & 1 \end{bmatrix} \right) \begin{bmatrix} \hat{Z}_1 \\ \hat{Z}_2 \end{bmatrix} = \begin{bmatrix} \hat{F}_3 \\ 0 \end{bmatrix} \quad (5\text{-}4)$$

5-2-2 Perfect compensation

The TD is motionless. $\hat{Z}_2$ is described by Equation 4-9, substitution to Equation 5-3 yields.

$$\left(-\omega^2 \begin{bmatrix} m_1 + a_{33}(\omega) & m_2 \\ 0 & 0 \end{bmatrix} + i\omega \begin{bmatrix} b_{33}(\omega) & 0 \\ 0 & 0 \end{bmatrix} + \begin{bmatrix} c_{33} & 0 \\ 0 & 1 \end{bmatrix} \right) \begin{bmatrix} \hat{Z}_1 \\ \hat{Z}_2 \end{bmatrix} = \begin{bmatrix} \hat{F}_3 \\ 0 \end{bmatrix} \quad (5\text{-}5)$$

5-2-3 Filter compensation

In Filter compensation the TD motions are a result of the vessel motions and the negative of the filtered vessel motions. $\hat{Z}_1$ and $\hat{Z}_2$ are related by Equation 4-15. Substitution to Equation 5-3 yields.

$$\left(-\omega^2 \begin{bmatrix} m_1 + a_{33}(\omega) & m_2 \\ 1 & -1 \end{bmatrix} + i\omega \begin{bmatrix} b_{33}(\omega) & 0 \\ -2\omega_c & 2\omega_c \end{bmatrix} + \begin{bmatrix} c_{33} & 0 \\ 0 & \omega_c^2 \end{bmatrix} \right) \begin{bmatrix} \hat{Z}_1 \\ \hat{Z}_2 \end{bmatrix} = \begin{bmatrix} \hat{F}_3 \\ 0 \end{bmatrix} \quad (5\text{-}6)$$

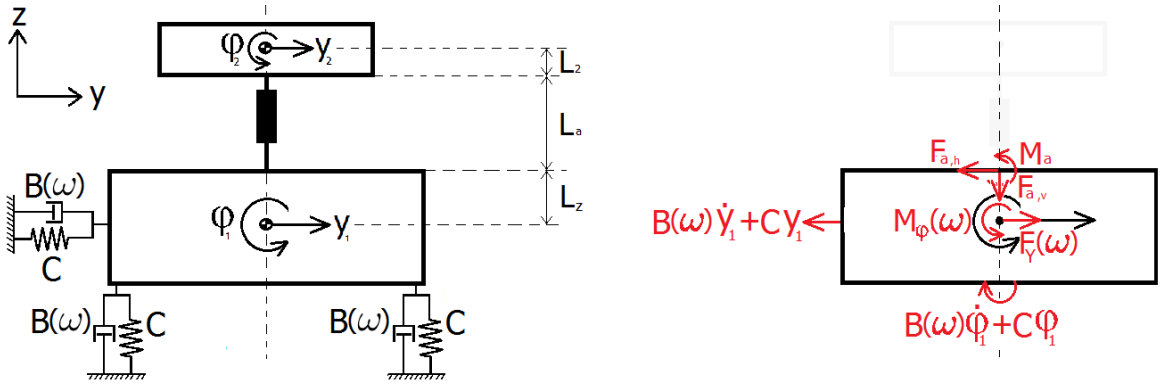

Figure 5-4: Free body diagram roll and sway, frequency domain only harmonic loading

5-3 4 DOF sway and roll model

The EOM for the coupled sway and roll motion of the coupled vessel-Ampelmann system is derived using Figure 5-4.

Both the TD and the vessel have two DOF, roll and sway. The TD is supported by the hydraulic cylinders, the spacing between the vessel and the TD is indicated by the length L_a. The Ampelmann is positioned at the CoG of the vessel, therefore $L_z = 0$. Length L_2 is assumed to be zero. Furthermore the vessel is horizontally and vertically supported by springs and dampers, the hydrostatic an hydrodynamic terms. The vessel is excited by harmonic wave loads F_y and M_ϕ. These are all known from DELFRAC. The forces $F_{a,h}$, $F_{a,v}$ and M_a are forces and moments due to the TD, these are derived from Figure 5-5.

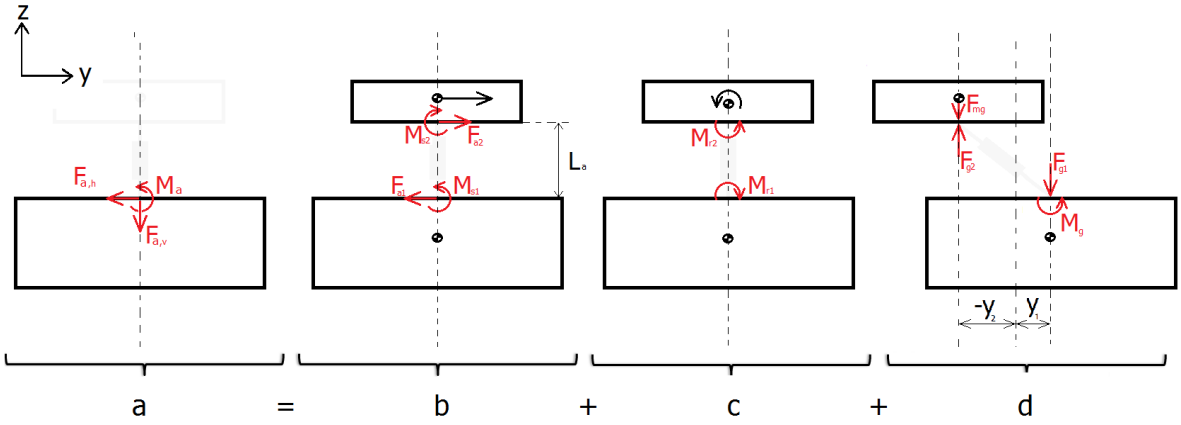

Figure 5-5: Derivation of forces resulting from the Ampelmann system

Figure 5-5 is subdivided into four figures, a, b, c and d. a is a the summation of b, c, and d:

- b: Reaction force and moment due to TD sway acceleration.
- c: Reaction moment due to TD angular roll acceleration.

- d: Reaction moment due to a relative horizontal displacement between the TD and the vessel. Both the vessel and the TD oscillated with respect to their reference position, in case both are not vertically aligned the weight of the Ampelman causes a reaction moment to the vessel.

The relations between $\hat{Y}_1$, $\hat{\Phi}_1$, $\hat{Y}_2$, $\hat{\Phi}_2$, $F_{a,h}$ and M_a are given below. The static weight of the TD $F_{a,v}$ has been taken into account in the hydromechanic analysis and is therefore excluded.

$$\begin{bmatrix} m_1+a_{22}(\omega) & a_{24}(\omega) & 0 & 0 \\ a_{42}(\omega) & I_{xx1}+a_{44}(\omega) & 0 & 0 \\ 0 & 0 & m_2 & 0 \\ 0 & 0 & -L_a m_2 & I_{xx2} \end{bmatrix} \begin{bmatrix} \ddot{y}_1 \\ \ddot{\phi}_1 \\ \ddot{y}_2 \\ \ddot{\phi}_2 \end{bmatrix} + \begin{bmatrix} b_{22}(\omega) & b_{24}(\omega) & 0 & 0 \\ b_{42}(\omega) & b_{44}(\omega) & 0 & 0 \\ 0 & 0 & 0 & 0 \\ 0 & 0 & 0 & 0 \end{bmatrix} \begin{bmatrix} \dot{y}_1 \\ \dot{\phi}_1 \\ \dot{y}_2 \\ \dot{\phi}_2 \end{bmatrix} + \begin{bmatrix} c_{22} & c_{24} & 0 & 0 \\ c_{42} & c_{44} & 0 & 0 \\ 0 & 0 & 0 & 0 \\ -m_2 g & 0 & m_2 g & 0 \end{bmatrix} \begin{bmatrix} y_1 \\ \phi_1 \\ y_2 \\ \phi_2 \end{bmatrix} + \begin{bmatrix} F_{a,h} \\ -M_a \\ -F_{a,h} \\ M_a \end{bmatrix} = \begin{bmatrix} F_y(\omega) \\ M_\phi(\omega) \\ 0 \\ 0 \end{bmatrix} \tag{5-7}$$

This expression contains 4 equations and 6 unknowns: $\hat{Y}_1$, $\hat{\Phi}_1$, $\hat{Y}_2$, $\hat{\Phi}_2$, $F_{a,h}$ and M_a. In order to solve, two additional equations shall be found that describes the cylinder force $F_{a,v}$ and M_a. Implicit relations are found that relate $\hat{Y}_1$, $\hat{\Phi}_1$, $\hat{Y}_2$ and $\hat{\Phi}_2$. These depend on the control system, No compensation, Perfect compensation or Filter compensation. Expressions in the following form are obtained where on the third and fourth row of each matrix the implicit relations for $F_{a,v}$ and M_a are substituted.

$$\left(-\omega^2 \begin{bmatrix} m_1+a_{22}(\omega) & a_{24}(\omega) & m_2 & 0 \\ a_{42}(\omega) & I_{xx1}+a_{44}(\omega) & -L_a m_2 & I_{xx2} \\ \dots & \dots & \dots & \dots \\ \dots & \dots & \dots & \dots \end{bmatrix} + i\omega \begin{bmatrix} b_{22}(\omega) & b_{24}(\omega) & 0 & 0 \\ b_{42}(\omega) & b_{44}(\omega) & 0 & 0 \\ \dots & \dots & \dots & \dots \\ \dots & \dots & \dots & \dots \end{bmatrix} + \begin{bmatrix} c_{22} & c_{24} & 0 & 0 \\ -m_2 g + c_{42} & c_{44} & m_2 g & 0 \\ \dots & \dots & \dots & \dots \\ \dots & \dots & \dots & \dots \end{bmatrix} \right) \begin{bmatrix} \hat{Y}_1 \\ \hat{\Phi}_1 \\ \hat{Y}_2 \\ \hat{\Phi}_2 \end{bmatrix} = \begin{bmatrix} \hat{F}_2 \\ \hat{M}_4 \\ 0 \\ 0 \end{bmatrix} \tag{5-8}$$

5-3-1 No compensation

A passive Ampelmann system has a fixed cylinder length. $\hat{Z}_1$, $\hat{\Phi}_1$, $\hat{Z}_2$ and $\hat{\Phi}_2$ are related by Equation 4-8. Substitution to Equation 5-8 yields.

$$\left(-\omega^2 \begin{bmatrix} m_1+a_{22}(\omega) & a_{24}(\omega) & m_2 & 0 \\ a_{42}(\omega) & I_{xx1}+a_{44}(\omega) & -L_a m_2 & I_{xx2} \\ 0 & 0 & 0 & 0 \\ 0 & 0 & 0 & 0 \end{bmatrix} + i\omega \begin{bmatrix} b_{22}(\omega) & b_{24}(\omega) & 0 & 0 \\ b_{42}(\omega) & b_{44}(\omega) & 0 & 0 \\ 0 & 0 & 0 & 0 \\ 0 & 0 & 0 & 0 \end{bmatrix} + \begin{bmatrix} c_{22} & c_{24} & 0 & 0 \\ -m_2 g + c_{42} & c_{44} & m_2 g & 0 \\ 1 & -L_a & -1 & 0 \\ 0 & 1 & 0 & -1 \end{bmatrix} \right) \begin{bmatrix} \hat{Y}_1 \\ \hat{\Phi}_1 \\ \hat{Y}_2 \\ \hat{\Phi}_2 \end{bmatrix} = \begin{bmatrix} \hat{F}_2 \\ \hat{M}_4 \\ 0 \\ 0 \end{bmatrix} \tag{5-9}$$

This expression is written in a reduced form where only the vessel motions $\hat{Y}_1$ and $\hat{\Phi}_1$ are unknown.

$$\left(-\omega^2 \begin{bmatrix} m_1+m_2+a_{22}(\omega) & -L_a m_2 + a_{24}(\omega) \\ -L_a m_2 + a_{42}(\omega) & I_{xx1}+I_{xx2}+L_a^2 m_2 + a_{44}(\omega) \end{bmatrix} + i\omega \begin{bmatrix} b_{22}(\omega) & b_{24}(\omega) \\ b_{42}(\omega) & b_{44}(\omega) \end{bmatrix} + \begin{bmatrix} c_{22} & c_{24} \\ c_{42} & c_{44} - L_a m_2 g \end{bmatrix} \right) \begin{bmatrix} \hat{Y}_1 \\ \hat{\Phi}_1 \end{bmatrix} = \begin{bmatrix} \hat{F}_2 \\ \hat{M}_4 \end{bmatrix} \tag{5-10}$$

5-3-2 Perfect compensation

The TD is motionless. $\hat{Y}_2$ and $\hat{\Phi}_2$ are described by Equation 4-9. Substitution to Equation 5-8 yields.

$$\left(-\omega^2 \begin{bmatrix} m_1+a_{22}(\omega) & a_{24}(\omega) & m_2 & 0 \\ a_{42}(\omega) & I_{xx1}+a_{44}(\omega) & -L_a m_2 & I_{xx2} \\ 0 & 0 & 0 & 0 \\ 0 & 0 & 0 & 0 \end{bmatrix} + i\omega \begin{bmatrix} b_{22}(\omega) & b_{24}(\omega) & 0 & 0 \\ b_{42}(\omega) & b_{44}(\omega) & 0 & 0 \\ 0 & 0 & 0 & 0 \\ 0 & 0 & 0 & 0 \end{bmatrix} + \begin{bmatrix} c_{22} & c_{24} & 0 & 0 \\ -m_2 g + c_{42} & c_{44} & m_2 g & 0 \\ 0 & 0 & 1 & 0 \\ 0 & 0 & 0 & 1 \end{bmatrix} \right) \begin{bmatrix} \hat{Y}_1 \\ \hat{\Phi}_1 \\ \hat{Y}_2 \\ \hat{\Phi}_2 \end{bmatrix} = \begin{bmatrix} \hat{F}_2 \\ \hat{M}_4 \\ 0 \\ 0 \end{bmatrix} \tag{5-11}$$

This expression is written in a reduced form where only the complex vessel motions, $\hat{Y}_1$ and $\hat{\Phi}_1$ are unknown.

$$\left(-\omega^2 \begin{bmatrix} m_1 + a_{22}(\omega) & a_{24}(\omega) \\ a_{42}(\omega) & I_{xx1} + a_{44}(\omega) \end{bmatrix} + i\omega \begin{bmatrix} b_{22}(\omega) & b_{24}(\omega) \\ b_{42}(\omega) & b_{44}(\omega) \end{bmatrix} + \begin{bmatrix} c_{22} & c_{24} \\ -m_2 g + c_{42} & c_{44} \end{bmatrix}\right) \begin{bmatrix} \hat{Y}_1 \\ \hat{\Phi}_1 \end{bmatrix} = \begin{bmatrix} \hat{F}_2 \\ \hat{M}_4 \end{bmatrix} \tag{5-12}$$

5-3-3 Filter compensation

In Filter compensation the TD motions are a result of the vessel motions and the negative of the filtered vessel motions. $\hat{Y}_1$, $\hat{\Phi}_1$, $\hat{Y}_2$ and $\hat{\Phi}_2$ are related by Equation 4-15. Substitution to Equation 5-8 yields.

$$\left(-\omega^2 \begin{bmatrix} m_1 + a_{22}(\omega) & a_{24}(\omega) & m_2 & 0 \\ a_{42}(\omega) & I_{xx1} + a_{44}(\omega) & -L_a m_2 & I_{xx2} \\ -1 & L_a & 1 & 0 \\ 0 & -1 & 0 & 1 \end{bmatrix} + i\omega \begin{bmatrix} b_{22}(\omega) & b_{24}(\omega) & 0 & 0 \\ b_{42}(\omega) & b_{44}(\omega) & 0 & 0 \\ -2\omega_c & 2\omega_c L_a & 2\omega_c & 0 \\ 0 & -2\omega_c & 0 & 2\omega_c \end{bmatrix} + \begin{bmatrix} c_{22} & c_{24} & 0 & 0 \\ -m_2 g + c_{42} & c_{44} & m_2 g & 0 \\ 0 & 0 & w_c^2 & 0 \\ 0 & 0 & 0 & w_c^2 \end{bmatrix}\right) \begin{bmatrix} \hat{Y}_1 \\ \hat{\Phi}_1 \\ \hat{Y}_2 \\ \hat{\Phi}_2 \end{bmatrix} = \begin{bmatrix} \hat{F}_2(\omega) \\ \hat{M}_4(\omega) \\ 0 \\ 0 \end{bmatrix} \tag{5-13}$$

5-4 6 DOF sway, heave and roll model

This section determines the EOM for the 6 DOF sway, heave and roll model. The combination of the 2 DOF model and the 4 DOF model form the 6 DOF model. The models describe only first order motions. For this reason, in terms of mechanical coupling, no additional coupling mechanisms are present and the 2 DOF model can directly be added to the 4 DOF model resulting in the 6 DOF model. The 6 DOF model has the following format.

$$\Big(-\omega^2[\mathbf{M} + \mathbf{A}(\omega)] + i\omega[\mathbf{B}(\omega)] + [\mathbf{C}]\Big) \begin{bmatrix} \hat{Y}_1 \\ \hat{Z}_1 \\ \hat{\Phi}_1 \\ \hat{Y}_2 \\ \hat{Z}_2 \\ \hat{\Phi}_2 \end{bmatrix} = \begin{bmatrix} \hat{F}_2 \\ \hat{F}_3 \\ \hat{M}_4 \\ 0 \\ 0 \\ 0 \end{bmatrix} \tag{5-14}$$

With $[\mathbf{M} + \mathbf{A}(\omega)]$, $[\mathbf{B}(\omega)]$ and $[\mathbf{C}]$ defined as.

$$[\mathbf{M} + \mathbf{A}(\omega)] = \begin{bmatrix} m_1 + a_{22}(\omega) & a_{23}(\omega) & a_{24}(\omega) & m_2 & 0 & 0 \\ a_{32}(\omega) & m_1 + a_{33}(\omega) & a_{34}(\omega) & 0 & m_2 & 0 \\ a_{42}(\omega) & a_{43}(\omega) & I_{xx1} + a_{44}(\omega) & -L_a m_2 & 0 & I_{xx2} \\ \dots & \dots & \dots & \dots & \dots & \dots \\ \dots & \dots & \dots & \dots & \dots & \dots \\ \dots & \dots & \dots & \dots & \dots & \dots \end{bmatrix} \tag{5-15}$$

$$[\mathbf{B}(\omega)] = \begin{bmatrix} b_{22}(\omega) & b_{23}(\omega) & b_{24}(\omega) & 0 & 0 & 0 \\ b_{32}(\omega) & b_{33}(\omega) & b_{34}(\omega) & 0 & 0 & 0 \\ b_{42}(\omega) & b_{43}(\omega) & b_{44}(\omega) & 0 & 0 & 0 \\ \dots & \dots & \dots & \dots & \dots & \dots \\ \dots & \dots & \dots & \dots & \dots & \dots \\ \dots & \dots & \dots & \dots & \dots & \dots \end{bmatrix} \tag{5-16}$$

$$[\mathbf{C}] = \begin{bmatrix} c_{22} & c_{23} & c_{24} & 0 & 0 & 0 \\ c_{32} & c_{33} & c_{34} & 0 & 0 & 0 \\ -m_2 g + c_{42} & c_{43} & c_{44} & m_2 g & 0 & 0 \\ ... & ... & ... & ... & ... & ... \\ ... & ... & ... & ... & ... & ... \\ ... & ... & ... & ... & ... & ... \end{bmatrix} \tag{5-17}$$

From Equation 4-8, 4-9 and 4-15 three relations yield depending on the control system, No compensation, Perfect compensation and Filter compensation. The results are shown in Appendix E, section E-1.

5-5 Results

The set of equations for each model is solved by MATLAB. Depending on the input variables different results are obtained. For the case study discussed in section 3-3, the hydromechanic properties are determined by DELFRAC. Hydromechanic properties may be scaled, which allows to analyse a vessel of geometric similitude of a different size. The main advantage of scaling is that when the hydromechanic properties of a vessel are known, the hydromechanic properties of a scaled version of the vessel with geometric similitude are also known. This scaling tool is build into the model with geometric scaling factor λ, for the determined DELFRAC data $\lambda = 1[-]$. Scaling of vessel parameters is discussed and validated in Appendix B. For larger vessels the effect of an active Ampelmann on the vessel dynamics becomes insignificant, for smaller vessels the effect may become significant. The results in this section are given for two cases $\lambda = 1[-]$ and $\lambda = 0.65[-]$. Note however that the TD mass is kept constant, the Ampelmann does not scale. Because the model is build such that:

$$m_v = m_1 + m_2 \tag{5-18}$$

Both cases for $\lambda = 1[-]$ and $\lambda = 0.65[-]$ do not have vessels with geometric similitude because the vessel mass does not scale according to the scaling laws but the scaled hydromechanic properties remain valid. For the purpose of the results this is not important and only the case study changes.

The results presented in this section are computed for a wave incident angle of $90[deg]$. Other input variables are listed in Table 5-1 on page 40. L_a is taken from Appendix A for the Ampelmann A-type+Gangway XL. The TD mass and mass moment of inertia are estimated from the basis of design of the Ampelmann A-Type [6].

Table 5-1: Input values for couple vessel-Ampelmann model

Input variable	Input value, $\lambda = 1[-]$	Input value, $\lambda = 0.65[-]$
m_1	$12.34 \cdot 10^5[kg]$	$3.197 \cdot 10^5[kg]$
I_{xx1}	$18.82 \cdot 10^6[kgm^2]$	$2.135 \cdot 10^6[kgm^2]$
m_2	$2 \cdot 10^4[kg]$	$2 \cdot 10^4[kg]$
I_{xx2}	$1 \cdot 10^5[kgm^2]$	$1 \cdot 10^5[kgm^2]$
L_a	$3.8[m]$	$3.8[m]$

5-5-1 Results 2 DOF model

Both the vessel and TD frequency characteristics in heave are plotted in Figure 5-6. Perfect compensation and Filter compensation are slightly shifted to the right with respect to No compensation. The TD frequency characteristics match with the vessel frequency characteristics for No compensation. The TD moves with the vessel. A perfectly compensated TD is motionless, the frequency characteristics are all zero. Filter compensation shows residual motions and a phase shift with respect the vessel. The TD is slightly moving with the vessel.

At a frequency of approximately $2.5[rad/s]$ the results show a small peak. This is a result of the hydromechanic properties calculated by DELFRAC not due to the presence of the Ampelmann.

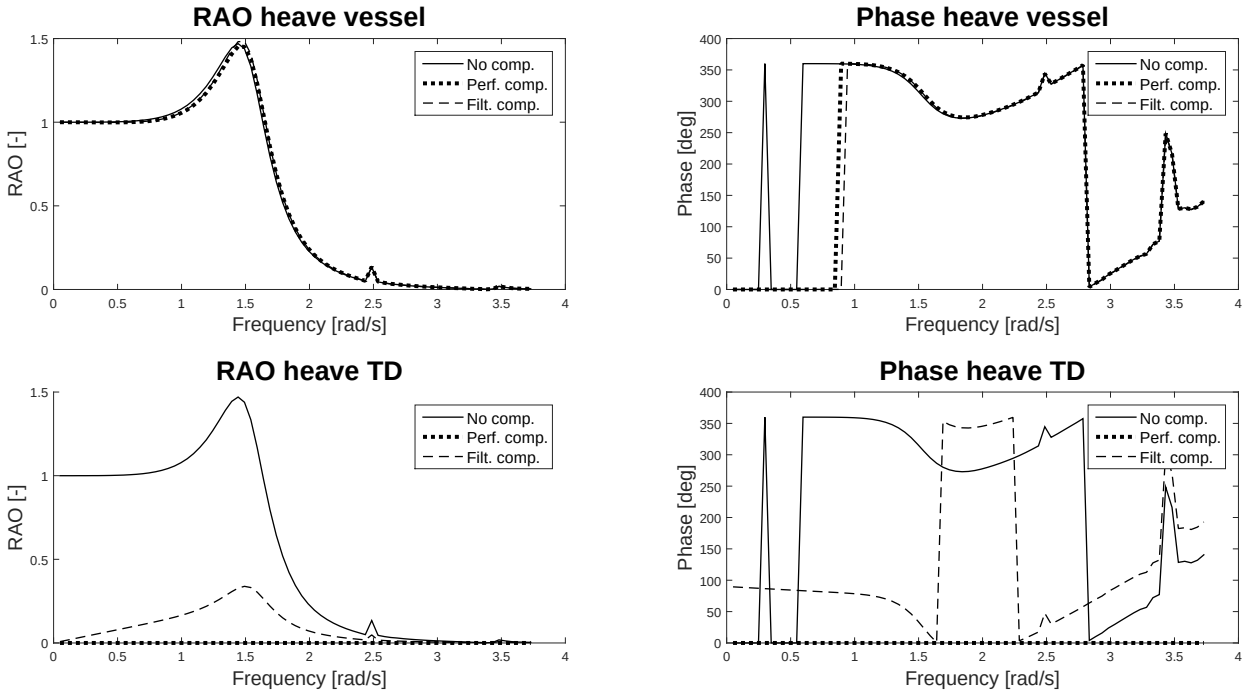

Figure 5-6: Vessel and TD frequency characteristics in heave, $\lambda = 0.65[-]$

5-5-2 Results 4 DOF model

The vessel frequency characteristics are plotted in Figure 5-7, for $\lambda = 0.65[-]$. Both Perfect compensation and Filter compensation show similar results.

For the entire frequency range the vessel RAO in sway increases for a compensating Ampelmann, for both Perfect compensation and Filter compensation. At the roll natural frequency the sway RAO shows an impulsive change. This is due to the coupling between sway and roll. For each control system the sway phase shows similar results.

The roll RAO is affected in two ways: a compensating Ampelmann causes the natural frequency to shift to a higher frequency and for the full range of frequencies the RAO increases. The frequency shift is also witnessed in the roll phase graph, the $90[deg]$ phase shift shifts with the roll natural frequency peak. The increased roll RAO is shown in Figure5-8.

The EOM for No compensation, Equation 5-10, shows that the roll restoring term: c_{33} is reduced with $L_a m_2 g$. For an increasing L_a the roll restoring term of the vessel decreases. Equation 5-10 also shows that in the $[\mathbf{M} + \mathbf{A}(\omega)]$ matrix the term $-L_a m_2$ appears in the top right and bottom left corner. This is because the CoG of the combined system does not coincide with the CoG of the vessel. In the EOM for Perfect compensation, Equation 5-12, the term $-m_2 g$ appears. The TD is fixed in space, a sway displacement of the vessel causes a resulting moment to the vessel due to the static weight of the TD.

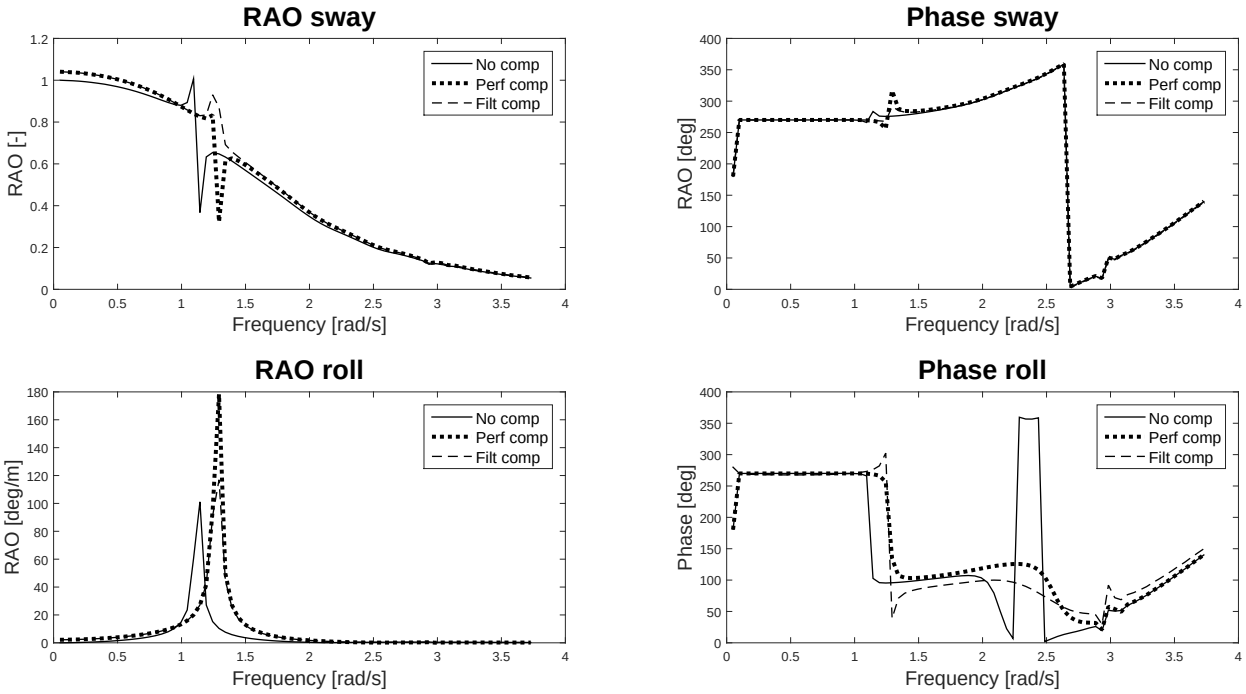

Figure 5-7: Vessel frequency characteristics for 4 DOF sway roll model, $\lambda = 0.65[-]$

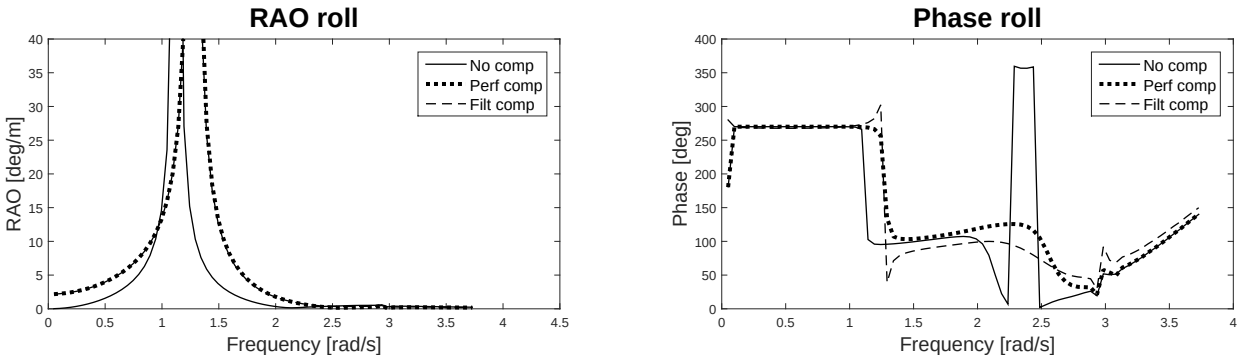

Figure 5-8: Vessel roll frequency characteristics for 4 DOF sway roll model zoomed in, $\lambda = 0.65[-]$

5-5-3 Results 6 DOF model

The 6 DOF model results are a combination of the two previous discussed models combined. See Figure 5-9. All plots are identical and show identical results. The TD frequency characteristics are given in Figure 5-10. During No compensation the TD moves with the vessel, due to coupling the TD sway RAO increases at the roll natural frequency. In roll the vessel and TD frequency characteristics are identical. The TD frequency characteristics for Perfect compensation are zero, the TD is perfectly compensated. In Filter compensation residual motions exist in all three DOF. At the natural heave and roll frequency the TD RAO increase due to increasing vessel motions.

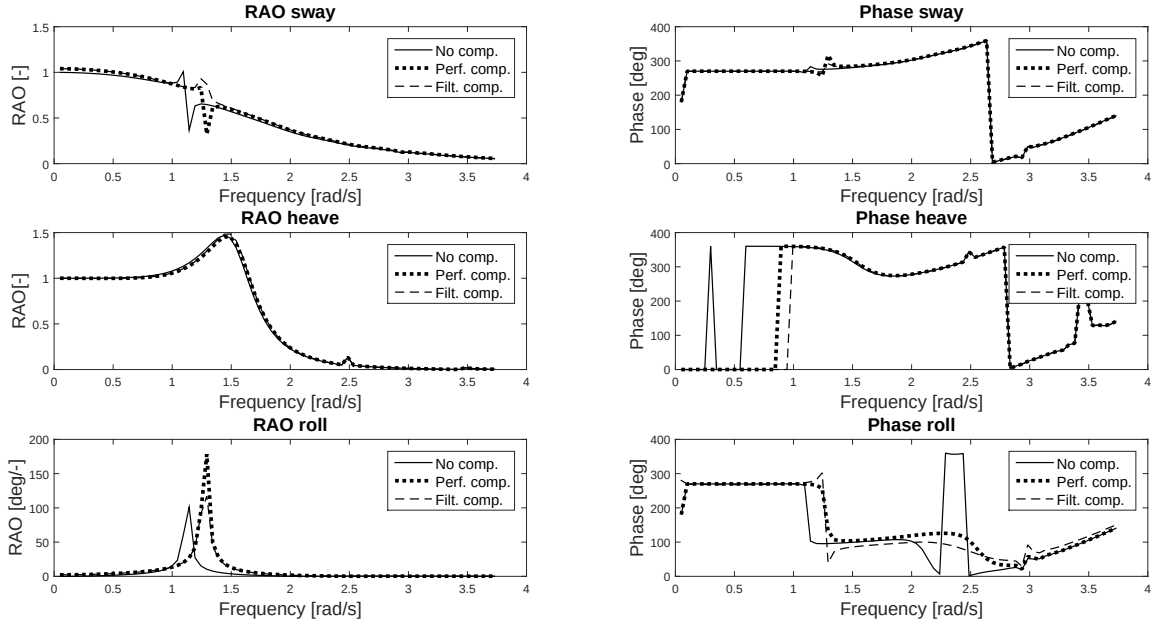

Figure 5-9: Vessel frequency characteristics for 6 DOF model sway, heave, roll. $\lambda = 0.65[-]$

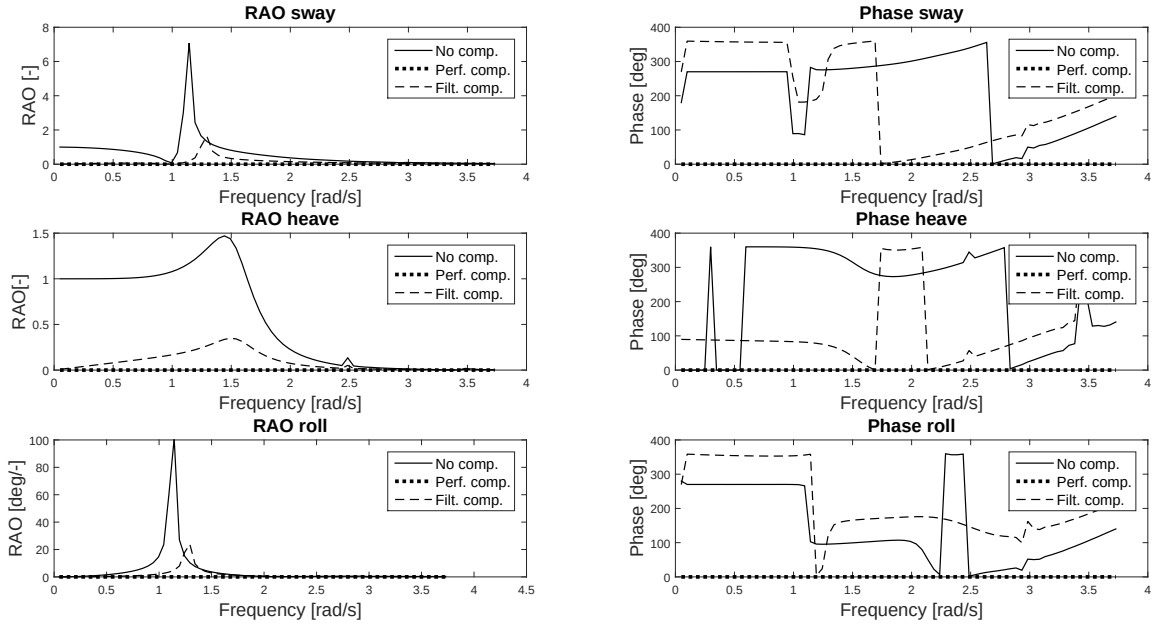

Figure 5-10: TD frequency characteristics for 6 DOF model sway, heave, roll. $\lambda = 0.65[-]$

5-6 Model validation and verification

This research is based on observations, changing vessel behaviour is witnessed during operation when the Ampelmann is activated. It is observed that in certain cases vessel motions amplify and vessel motion frequencies change. No logged data is available. Comparing the model results to practical data is beyond the scope of this thesis. The results do confirm the observations but this is not a qualitative validation that confirms the validity of the model. Two validation steps are performed in section 5-6-1. The results of the No compensation model are compared to the DELFRAC results. Then the TD motions for Perfect compensation are compared to a time trance of the TD motions based on the modelled Ampelmann control system [7]. It is assumed that the DELFRAC results and the time trace of the TD motions are a representation of reality. The differences between the results are explained. Ultimately to confirm the validity of the models practical tests shall be performed. In section 5-6-2 models results are verified. The differences between the results for the No compensation model and the compensating models are explained.

5-6-1 Validation of No compensation and Perfect compensation

Validation of the No compensation model is performed by comparing the results to the DELFRAC results. This comparison is only valid for a wave incident angle of $90[deg]$. Then due to hull symmetry surge, pitch and yaw RAO are all zero. See Appendix F, Figure F-1. Figure 5-11 shows the results for No compensation and the DELFRAC results.

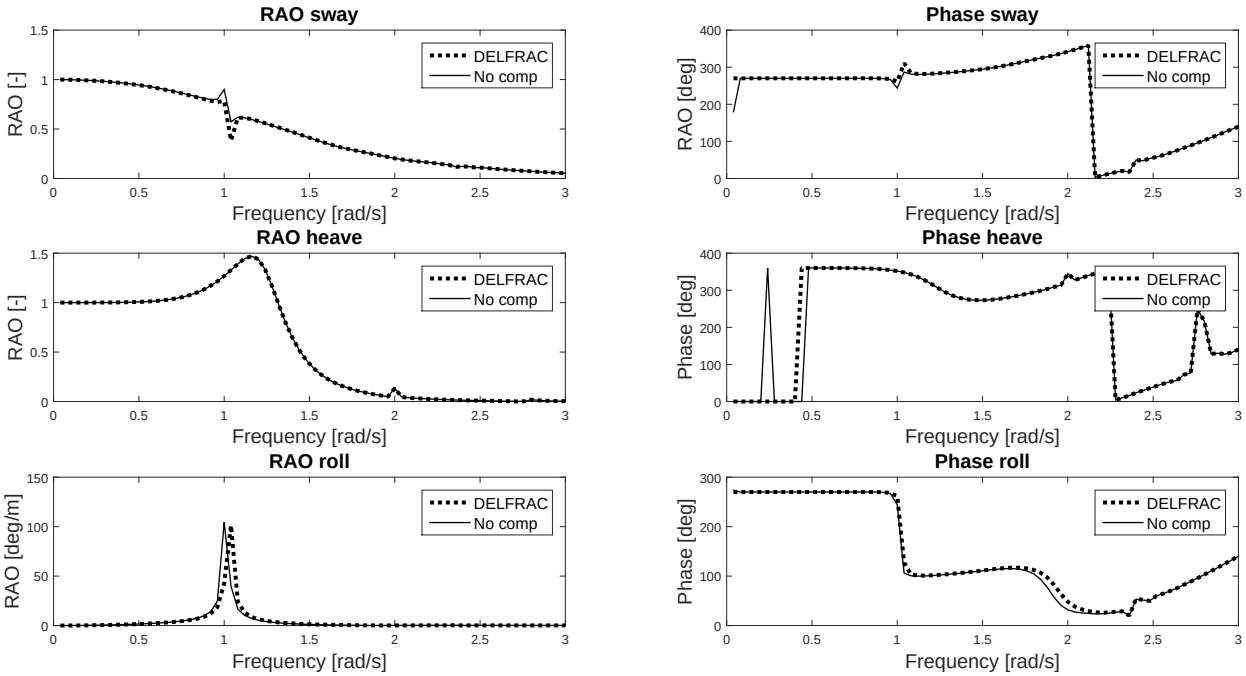

Figure 5-11: Frequency characteristics No compensation and DELFRAC results. $\lambda = 1[-]$

The results are not identical. The difference is explained, it is expected that the natural roll frequency for No compensation shifts to a lower frequency because the mass moment of inertia has increased to:

$$I_{xx1} \rightarrow I_{xx1} + I_{xx2} + m_2 L_a^2 \tag{5-19}$$

Sway and heave are unaffected because the total mass $m_1 + m_2 = m_v$ does not change. Furthermore the calculated TD frequency characteristics are compared to a time trance of the TD motions. This time trace is shown in Figure C-5 in Appendix C: The TD of a compensating Ampelmann system is kept motionless, here it does not reach it's mechanical limitations. The TD frequency characteristics for Perfect compensation are shown in Figure 5-10, all RAO are zero. In absence of mechanical limitations of the Ampelmann system the results coincide confirming the validity of the Perfect compensation model.

5-6-2 Model verification

To confirm the correctness of the models first the model input parameters are changed and compared to the DELFRAC results. Then the differences between the results for No compensation, Perfect compensation and Filter compensation are discussed.

By changing model input variables for each control system the correctness of each model is verified with respect to the DELFRAC results. By setting the model input to $m_2 = 0[kg]$ and $I_{xx2} = 0[kgm^2]$ causes $m_1 = m_v$. With this input the No compensation, Perfect compensation and Filter compensation results are compared to the DELFRAC results. As expected

all results coincide, see Appendix F, Figure F-3, F-4 and F-5. This confirms that all models calculate the correct results for a massless TD.

The results for Perfect compensation and Filter compensation are compared to the results for No compensation, the change in dynamic behaviour is verified and explained.

Increased amplitude sway: The TD of a compensating Ampelmann is motionless. The resultant of the vertical cylinder forces are constant in time and equal the mass of the TD. The resultant horizontal cylinder forces are zero, no TD acceleration are present. When the Ampelmann system is compensating the TD mass in sway is excluded from the vessel motions, this is confirmed by the EOM for perfect compensation where m_2 is excluded from the mass matrix, see Equation 5-12. When compensating, the wave force is working on a smaller mass: only the mass of the vessel m_1 moves. Increased sway is explained as follows: In sway the vessel does not have any restoring force, it is represented as a mass, m. On this mass a sinusoidal force is working with an amplitude F and an excitation frequency ω:

$$m\ddot{y} = Fsin(\omega t) \tag{5-20}$$

Note that damping is not taken into account. $y = Ysin(\omega t)$ is substituted and the motion amplitude Y is calculated as.

$$Y = \frac{F}{-\omega^2 m} \tag{5-21}$$

For a decreasing m the motion amplitude Y increases. The mass of a compensated TD is excluded from the mass matrix causing the vessel motion to increase. When the relative mass of the TD increases this effect increases. The vessel mass of a compensating system corresponds to m_1 and the vessel mass of a non compensating system to $m_1 + m_2$. For both cases the motion amplitude is described:

$$Y_{nocomp} = \frac{F}{-\omega^2(m_1 + m_2)} \tag{5-22}$$

$$Y_{comp} = \frac{F}{-\omega^2 m_1} \tag{5-23}$$

The following relative mass ratio, μ_m, is made:

$$\mu_m = \frac{Y_{comp}}{Y_{nocomp}} = \frac{m_1 + m_2}{m_1} \tag{5-24}$$

For the results shown in Figure 5-9 this ratio is $1.063[-]$ ($m_1 = 3.197 \cdot 10^5, m_2 = 2 \cdot 10^4$). $1.063[-]$ is approximately the increase in sway motion when compensating when compared to No compensation. The relation between the vessel sway RAO for compensation and no compensation yields.

$$Y_{comp} \approx \mu_m \cdot Y_{nocomp} \tag{5-25}$$

Unchanged natural frequency heave: From Figure 5-9 the heave results show a minor differences. In heave the vessel is modelled as a mass spring system. The natural frequency of a mass spring system changes when the mass of the excited body changes. The stiffness remains unchanged. Below the mathematical representation is given for a mass spring system with an

harmonic excitation with the corresponding natural frequency ω_n. Note that the frequency dependent added mass terms and damping are not taken into account.

$$m\ddot{z} + c_{33}z = Fsin(\omega t) \tag{5-26}$$

$$\omega_{n3} = \sqrt{\frac{c_{33}}{m}} \tag{5-27}$$

During compensation a reduction of the excited mass causes the natural frequency of the body to increase.

$$\omega_{n3,nocomp} = \sqrt{\frac{c_{33}}{m_1 + m_2}} \tag{5-28}$$

$$\omega_{n3,comp} = \sqrt{\frac{c_{33}}{m_1}} \tag{5-29}$$

The ratio is taken by dividing the natural frequency for No compensation by the natural frequency for compensation.

$$\frac{\omega_{n3,comp}}{\omega_{n3,nocomp}} = \sqrt{\frac{m_1 + m_2}{m_1}} = \sqrt{\mu_m} \tag{5-30}$$

The change in natural frequency goes with the square root of the relative mass ratio, μ_m. For the results from Figure 5-9 the natural frequency shift is hardly noticeable, $\sqrt{\mu_m} = 1.031[-]$.

Natural frequency shift roll: The natural roll frequency depends on the roll stiffness c_{44} and the mass moment of inertia of the system. In roll the vessel is described as a mass spring system excited by a harmonic load. Damping and the frequency dependent added mass are neglected.

$$I_{xx}\ddot{\phi} + c_{44}\phi = Msin(\omega t) \tag{5-31}$$

The natural frequency for No compensation and compensation are described as:

$$\omega_{n4,nocomp} = \sqrt{\frac{c_{44} - L_a m_2 g}{I_{xx1} + I_{xx2} + L_a^2 m_2}} \tag{5-32}$$

$$\omega_{n4,comp} = \sqrt{\frac{c_{44}}{I_{xx1}}} \tag{5-33}$$

The natural shift between No compensation and compensation is related by the ratio $\sqrt{\mu_I \mu_c}$:

$$\sqrt{\mu_I \mu_c} = \frac{\omega_{n4,comp}}{\omega_{n4,nocomp}} = \sqrt{\frac{I_{xx1} + I_{xx2} + L_a^2 m_2}{I_{xx1}} \cdot \frac{c_{44}}{c_{44} - L_a m_2 g}} \tag{5-34}$$

Hence $\sqrt{\mu_I \mu_c} = 1.17[-]$ for $\lambda = 0.65[-]$: $I_{xx1} = 2.135 \cdot 10^6[kgm^2]$, $I_{xx2} = 1 \cdot 10^5[kgm^2]$, $L_a = 3.8[m]$, $m_2 = 2 \cdot 10^4[kg]$ and $c_{44} = 5.4 \cdot 10^6[Nm]$. The natural frequency shift is significantly higher than for heave. This is caused by the increased stiffness ratio μ_c and the mass moment of inertia ratio μ_I. By multiplying the frequency range of the No compensation frequency characteristics with $\sqrt{\mu_I \mu_c}$ and plotting the results in one graph, the natural frequencies for both No compensation and compensation show similar results. This is confirmed by the phase graph where the $90[deg]$ phase shift for each control system matches. See Figure 5-12. It is

confirmed that the natural frequency shift mainly depends on the changing stiffness and mass moment of inertia.

$$\omega_{n,comp} \approx \sqrt{\mu_I \mu_c} \cdot \omega_{n,nocomp} \tag{5-35}$$

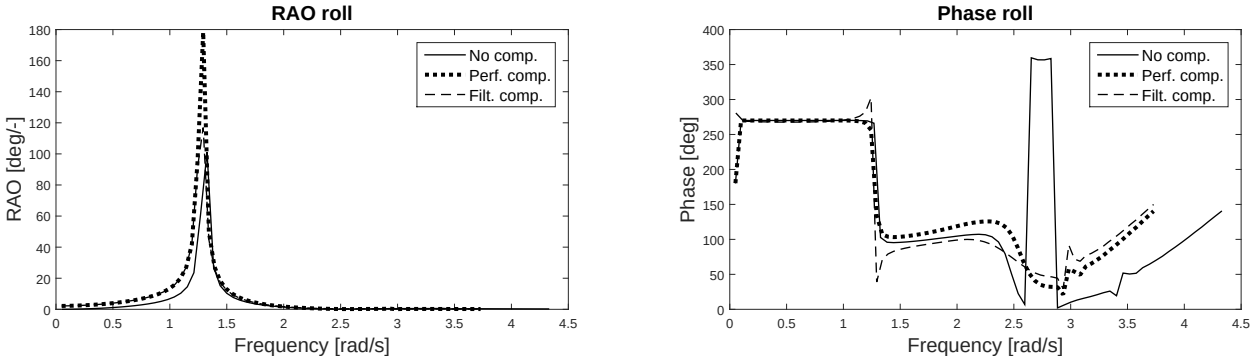

Figure 5-12: The frequency characteristics, multiply the frequency for No compensation with $\sqrt{\mu_I \mu_c} = 1.17[-]$. $\lambda = 0.65[-]$

Increased amplitude roll: The term gm_2 from Equation 5-12 where a relative TD sway couples to vessel roll causes the roll amplitude of the vessel to increase. This is verified by setting the gravity constant to zero: $g = 0[m/s^2]$, this excludes the term $-m_2 g$ from the EOM. Then for the entire frequency range the roll RAO drops to the original level of No compensation, see Figure 5-13. Note that by setting $g = 0[m/s^2]$ the natural frequency of No compensation shows a minor shift to a higher frequency, this follows from Equation 5-34 because μ_c is a function of g. By setting $g = 0[m/s^2]$ the natural frequency shift decreases. Perfect compensation and Filter compensation show identical results.

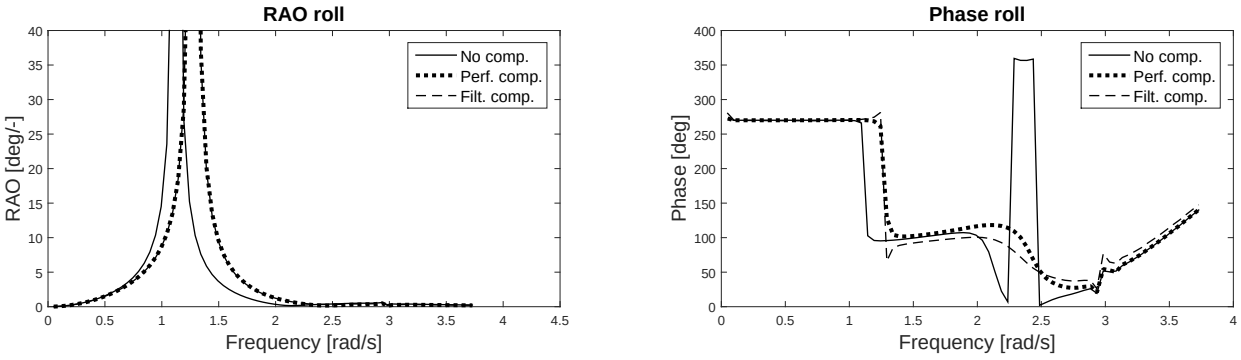

Figure 5-13: Roll frequency characteristics, set $g = 0[m/s^2]$. $\lambda = 0.65[-]$

5-7 Evaluation of results

The results presented previously are computed for a specific vessel. Each vessel has its own characteristics and will respond different. Based on specific terms appearing in the EOM for

each control system the changing dynamic behaviour is explained. This is independent of the hydromechanic properties. The principles that cause the changing dynamic vessel behaviour are combined and applied in the proposition to an alternative compensation method.

5-7-1 Insight to increased roll amplitudes

The vessel roll amplitude for the entire frequency range is higher when compensating. This results from a relative sway motion of the vessel relative to the TD. A compensated TD is fixed in space, when the vessel experiences a sway motion a lever arm with respect to the static weight component of the TD is created. This results in a roll moment working on the vessel. See Figure 5-14.

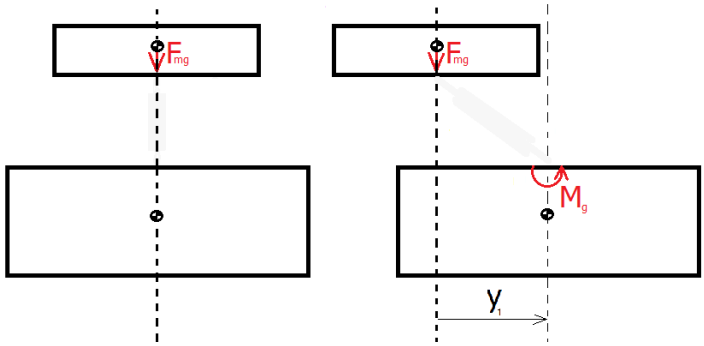

Figure 5-14: The source for amplified roll amplitudes when compensating

This also results from Equation 5-12. The term $-m_2 g$ in the restoring matrix is the major factor causing amplified roll motions. Furthermore in the validation of the results in Figure 5-13, it is shown that: when setting $g = 0[m/s^2]$, for the whole frequency range the roll RAO is reduced to the original level of No compensation. This also confirms that when compensating, the static weight of the TD has a major effect on the vessel roll amplitude.

5-7-2 An alternative compensation method

The knowledge obtained previous is used to make a proposition for an alternative compensation method. The TD is supported by 6 hydraulic cylinder that allow 6 DOF TD motions, 3 translation and 3 rotations. In addition the Ampelmann system has 3 more functionalities: telescoping, slewing and luffing. These functionalities compensate for the residual motions of the TD. In this philosophy the TD is kept motionless and residual motions are taken care of by the 3 additional functionalities. From the analysis it is shown that the static weight of the Ampelmann causes a roll moment to the vessel due to a relative sway motion of the vessel. This contribution is excluded by allowing TD motions and not compensating for sway. This way the TD mass in sway moves with the vessel. It stays vertically aligned with its reference position on the vessel eliminating the occurrence of a lever arm due to the static weight of the TD relative to the vessel. No external roll moment will result reducing the vessel roll motions. The vessel sway amplitude is reduced back to its original amplitude value. The mass of the TD moves with the vessel in sway, $\hat{Y}_2 = \hat{Y}_1$. This compensation method is named

as: No Sway Compensation (NSC). The introduced TD motions shall be compensated by, telescoping slewing and luffing. For the 4 DOF model the implicit relations relating $\hat{Y}_1$, $\hat{\Phi}_1$, $\hat{Y}_2$ and $\hat{\Phi}_2$ for NSC are.

$$\begin{bmatrix} \hat{Y}_2 \\ \hat{\Phi}_2 \end{bmatrix} = \begin{bmatrix} \hat{Y}_1 \\ 0 \end{bmatrix} \tag{5-36}$$

Substitution to Equation 5-8 yields the following system of equations.

$$\left(-\omega^2 \begin{bmatrix} m_1 + a_{22}(\omega) & a_{24}(\omega) & m_2 & 0 \\ a_{42}(\omega) & I_{xx1} + a_{44}(\omega) & -L_a m_2 & I_{xx2} \\ 0 & 0 & 0 & 0 \\ 0 & 0 & 0 & 0 \end{bmatrix} + i\omega \begin{bmatrix} b_{22}(\omega) & b_{24}(\omega) & 0 & 0 \\ b_{42}(\omega) & b_{44}(\omega) & 0 & 0 \\ 0 & 0 & 0 & 0 \\ 0 & 0 & 0 & 0 \end{bmatrix} + \begin{bmatrix} c_{22} & c_{24} & 0 & 0 \\ -m_2 g + c_{42} & c_{44} & m_2 g & 0 \\ -1 & 0 & 1 & 0 \\ 0 & 0 & 0 & 1 \end{bmatrix} \right) \begin{bmatrix} \hat{Y}_1 \\ \hat{\Phi}_1 \\ \hat{Y}_2 \\ \hat{\Phi}_2 \end{bmatrix} = \begin{bmatrix} \hat{F}_2 \\ \hat{M}_4 \\ 0 \\ 0 \end{bmatrix} \tag{5-37}$$

The expression is derived that only describes the vessel motions for the condition of NSC.

$$\left(-\omega^2 \begin{bmatrix} m_1 + m_2 + a_{33}(\omega) & a_{24}(\omega) \\ a_{42}(\omega) - L_a m_2 & I_{xx1} + a_{44}(\omega) \end{bmatrix} + i\omega \begin{bmatrix} b_{22}(\omega) & b_{24}(\omega) \\ b_{42}(\omega) & b_{44}(\omega) \end{bmatrix} + \begin{bmatrix} c_{22} & c_{24} \\ c_{42} & c_{44} \end{bmatrix} \right) = \begin{bmatrix} \hat{Y}_1 \\ \hat{\Phi}_1 \end{bmatrix} = \begin{bmatrix} \hat{F}_2 \\ \hat{M}_4 \end{bmatrix} \tag{5-38}$$

This expression shows that the excited mass in sway-direction equals the combined mass of the vessel and the TD, $m_1 + m_2$. It is expected that the vessel sway RAO for NSC reduces to the level of No compensation. Furthermore the term $-m_2 g$ is excluded from the stiffness matrix. It is expected that the vessel roll RAO atleast drops back to their original level of No compensation. Furthermore the natural frequency shift remains because the TD does not add tot he roll mass moment of inertia.

Equation 5-37 is solved. The vessel frequency characteristics are plotted in Figure 5-15. In Figure 5-16 the roll RAO is zoomed in. From the plots it is observed that compensating with NSC the sway and roll RAO are reduced to their original level of No compensation. There is one discrepancy, both No compensation and NSC experiences a phase shift at their roll natural frequency. The NSC natural frequency in roll matches the natural frequency for a full compensated Ampelmann system. Compared to No compensation the natural frequency peak is shifted to the right. The sway phase remains unaffected, the roll RAO drops back to the level of No compensation.

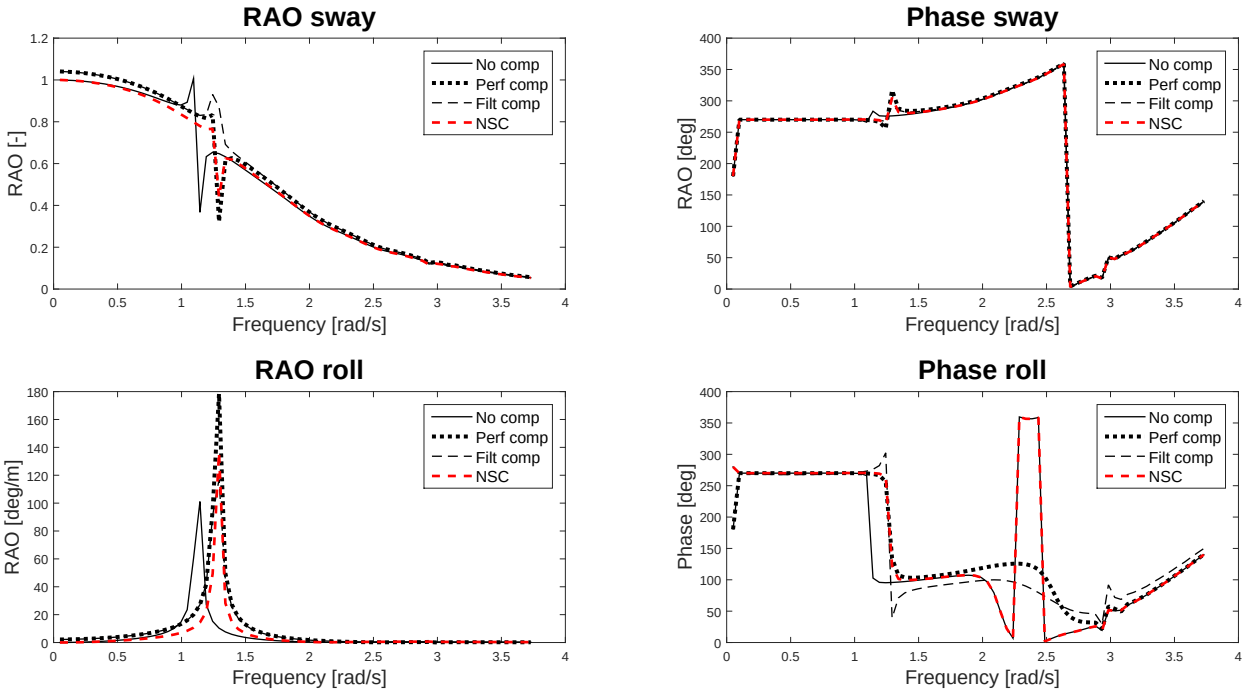

Figure 5-15: Frequency characteristics for 4 DOF sway roll model including NSC, $\lambda = 0.65[-]$

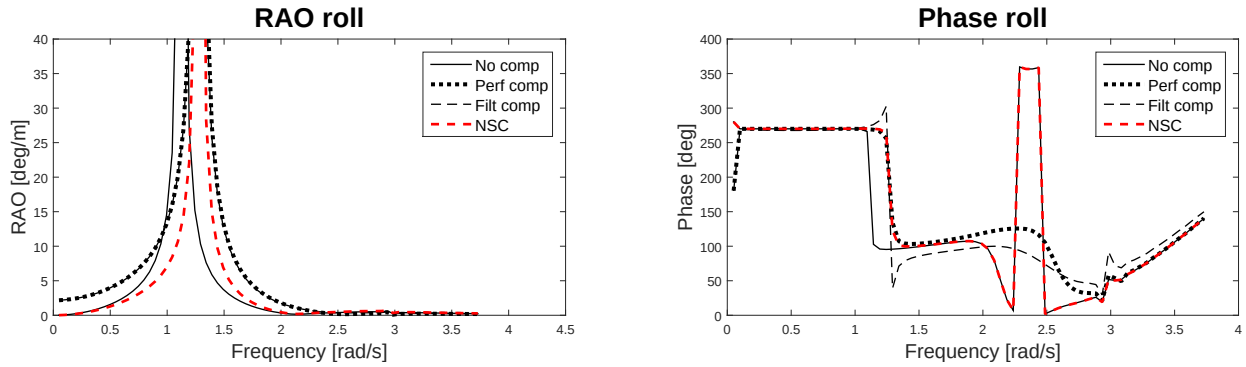

Figure 5-16: 4 DOF sway roll model, roll frequency characteristics including NSC, $\lambda = 0.65[-]$

By NSC vessel RAO are reduced to their original level of No compensation. Vessel motions are not amplified and the roll natural frequency is shifted to a higher frequency. In chapter 7 it is shown that the workability is significantly increased by applying NSC.

5-7-3 Feasibility of the No sway compensation method

Initially the Ampelmann system is a 6 DOF compensated platform. Previous research shows that the workability of the Ampelmann on a vessel is increased by selectively allowing heave motions to the TD [7]. Within Ampelmann Operations B.V. this is named as the hyper ellipsoid. When a hydraulic cylinders tends to reach its maximum stroke length residual TD

heave motions are introduced, extending its working range and workability. The residual TD motions are compensated by, slewing, luffing and telescoping. Guidelines are set to maximum transfer deck velocities and accelerations based on maximum cylinder velocities and maximum allowable accelerations for crew safety. See Table 5-2.

Table 5-2: Maximum TD velocities and acceleration [8]

DOF	Max. TD velocities	Max. TD accelerations
x,y	$0.5[m/s]$	$0.5[m/s^2]$
z	$0.5[m/s]$	$1[m/s^2]$
ϕ, θ, ψ	Not defined	Not defined

These guidelines together with the maximum allowable slew, pitch and telescope velocities and accelerations form the design criteria for implementation of NSC in practice. The results shown in Figure 5-15 and 5-16 are for a full NSC, $\hat{Y}_2 = \hat{Y}_1$. When exceeding the design criteria also partial NSC is possible, for example $\hat{Y}_2 = \alpha \hat{Y}_1$ with $0 < \alpha < 1$ ($\alpha = 0$: Perfect compensation). Then by Equation 5-39 vessel amplitudes are partially reduced. See Figure 5-17.

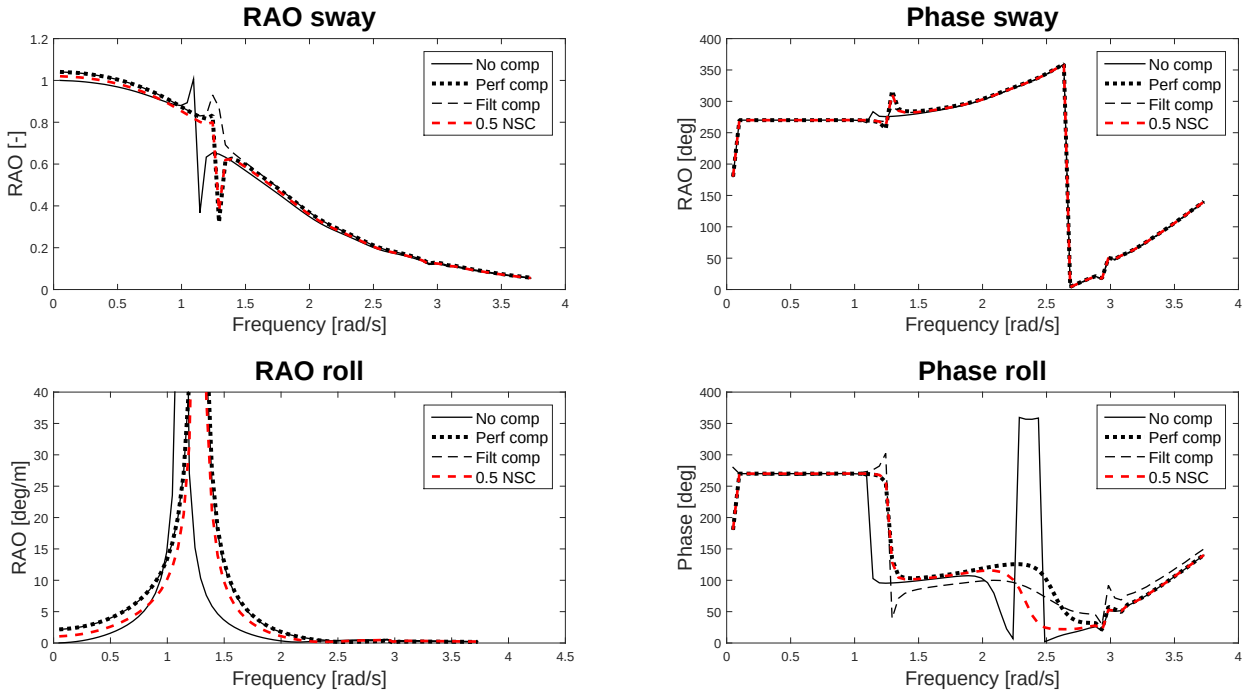

Figure 5-17: Vessel frequency characteristics for 4 DOF sway roll model with partial NSC, $\alpha = 0.5[-]$. $\lambda = 0.65[-]$

$$\left(-\omega^2 \begin{bmatrix} m_1 + \alpha m_2 + a_{33}(\omega) & a_{24}(\omega) \\ a_{42}(\omega) - \alpha L_a m_2 & I_{xx1} + a_{44}(\omega) \end{bmatrix} + i\omega \begin{bmatrix} b_{22}(\omega) & b_{24}(\omega) \\ b_{42}(\omega) & b_{44}(\omega) \end{bmatrix} + \begin{bmatrix} c_{22} & c_{24} \\ (\alpha - 1)m_2 g + c_{42} & c_{44} \end{bmatrix}\right) = \begin{bmatrix} \hat{Y}_1 \\ \hat{\Phi}_1 \end{bmatrix} = \begin{bmatrix} \hat{F}_2 \\ \hat{M}_4 \end{bmatrix} \tag{5-39}$$

In proposing this new compensation methodology it is assumed that all residual motions are compensated by slewing, telescoping and luffing and that this does not affect the external forces and moments working on the vessel. Chapter 7 elaborates further on the concept of NSC.

5-8 Conclusion

Three coupled vessel-Ampelmann models are made in a 2D plane where the Ampelmann is positioned at the CoG of the vessel. For each model three control systems are applied: No compensation, Perfect compensation and Filter compensation. The first model has 2 DOF, vessel heave and TD heave. This gives a basic understanding of how the models are build. The second model has 4 DOF and includes sway and roll motions for both the vessel and the TD. It gives a basic understanding of the coupling mechanisms between the vessel and the Ampelmann system. The combination of the 2 DOF model 4 DOF model results in the 6 DOF model. Because only first order motions are taken into account, the results of the 2 DOF and 4 DOF model combined are identical to the results for the 6 DOF model.

The models confirm a changing vessel behaviour when the Ampelmann is compensating. Also the transfer deck frequency characteristics for each control system confirm their intention: No compensation, the transfer deck moves with the vessel. Perfect compensation, all frequency characteristics are zero. Filter compensation, the transfer deck has residual motions, these are small compared to the vessel motions.

Perfect compensation and Filter compensation show similar results, residual transfer deck motions due to the application of a second order low pass filter are not the major source for changing vessel behaviour. The results of both compensation models are compared to the No compensation results. All differences are verified and explained. An active Ampelmann system causes the vessel sway and roll RAO to increase, it also causes the vessel's roll natural frequency to shift to a higher frequency. The factor causing the vessel roll motions to amplify is due to the relative displacement of the vessel with respect to the TD. Then the static weight of the transfer deck causes a roll moment to the vessel. A new compensation philosophy is proposed that does not amplify vessel motions and increases the working range of the Ampelmann system. This compensation method is named as No sway compensation.

Chapter 6

Determine coupled frequency characteristics

6-1 Introduction

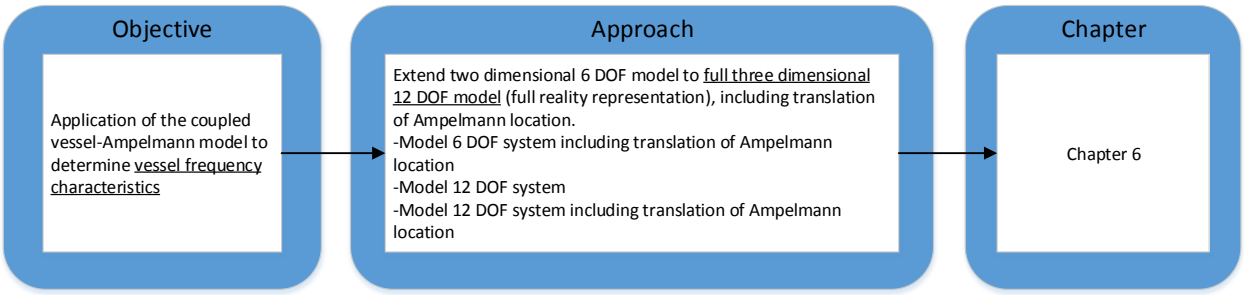

Figure 6-1: Flow chart of the objective and approach of this chapter

This chapters objective is to determine the vessel frequency characteristics for the coupled vessel-Ampelmann system, the calculated frequency characteristics are input to the workability analysis. The 3D representation of the system is made including all 12 DOF. For each control system the model variables are the hydromechanic properties of the vessel for a chosen wave incident angle, the mass and mass moment of inertia of the vessel and the TD and the location of the Ampelmann system on the vessel. The 12 DOF model is derived or determined in three steps based on the 6 DOF model from the previous chapter. See Figure 6-2.

1. The 6 DOF model from chapter 5 is extended to a model in the 2D plane where the location of point B is defined relative to the CoG of the vessel. This model is named as: 6 DOF model including translation of the Ampelmann location. The TD moves with respect to point B.

2. The 6 DOF model from chapter 5 is extended to a 3D model with 12 DOF. The Ampelmann system is positioned at point the CoG of the vessel. This model is named as: 12 DOF model.

3. The results from step 1 and 2 are combined to obtain a 3D 12 DOF model with point B located relative to the CoG of the vessel. This model is named as: 12 DOF model including translation of the Ampelmann location. This model includes all 12 DOF and allows all model variables stated above.

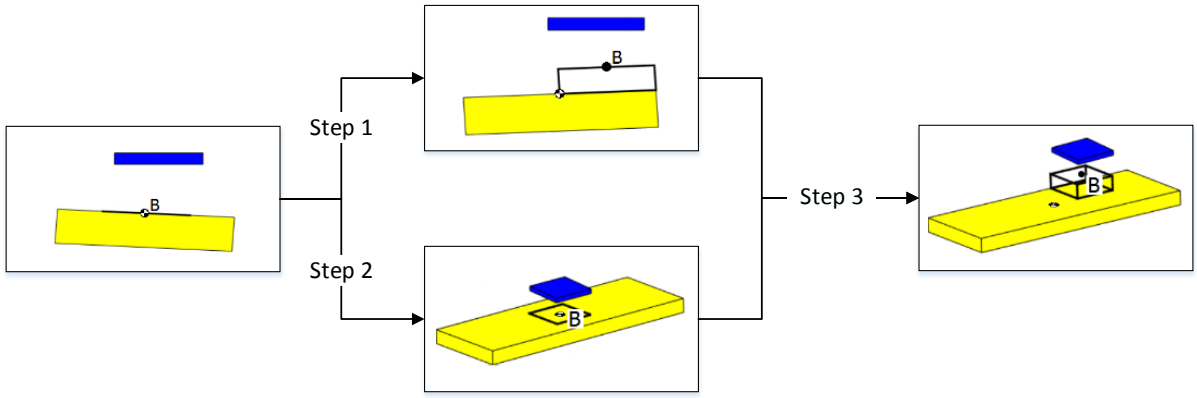

Figure 6-2: Steps taken to derive of determine 12 DOF model including the translation of point B with respect to the vessels CoG

In section 6-2 first the limitations and conditions for translating the Ampelmann system are discussed. Then the two modelsthat yield from step 1 and 2 are discussed in section 6-3 and 6-4. Finally the 12 DOF model including the translation of the Ampelmann location is discussed in section 6-5. The obtained vessel frequency characteristics are input for the workability analysis and include the dynamic interaction of the coupled vessel-Ampelmann system.

6-2 Translation of the Ampelmann location

The Ampelmann system may be translated vertically in z direction by L_z and in horizontal direction in x and y by L_x and L_y. All translations are relative to the CoG of the vessel. Translating the Ampelmann may go beyond the hydrostatic stability limits of the vessel. Furthermore a translated Ampelmann may result in a static trim angle of the vessel, which causes invalid hydromechanic data. This section discuses the limitations and conditions for the translation of the Ampelmann location.

6-2-1 Limitation for vertical translations

Computing the frequency characteristics is based on linear theory. The response frequency of the excited body equals the frequency of the force. Independent of whether the vessel is hydrostatically stable, the frequency characteristics are computed. A vessel is hydrostatically stable when the stability moment is positive $\overline{GM} > 0[m]$. The stability criteria presented in this section are for a passive Ampelmann system on a vessel. Theory on hydrostatic stability is stated in section 2-4-1. From figure 6-3, the length $\overline{GM}$ is calculated as.

$$\overline{GM} = \overline{KB} + \overline{BM} - \overline{KG} = \overline{KB} + \frac{I_t}{\nabla} - \overline{KG} \tag{6-1}$$

Where $\overline{BM}$ is written in terms of I_t the area moment of inertia and ∇ the submerged volume of the vessel. The lengths $\overline{GM}$, $\overline{KB}$, $\overline{BM}$ and $\overline{KG}$ are repeated in Figure 6-3. The points G, B, K and M are the CoG of the combined vessel and the Ampelmann, the buoyancy point, the keel and the metacenter.

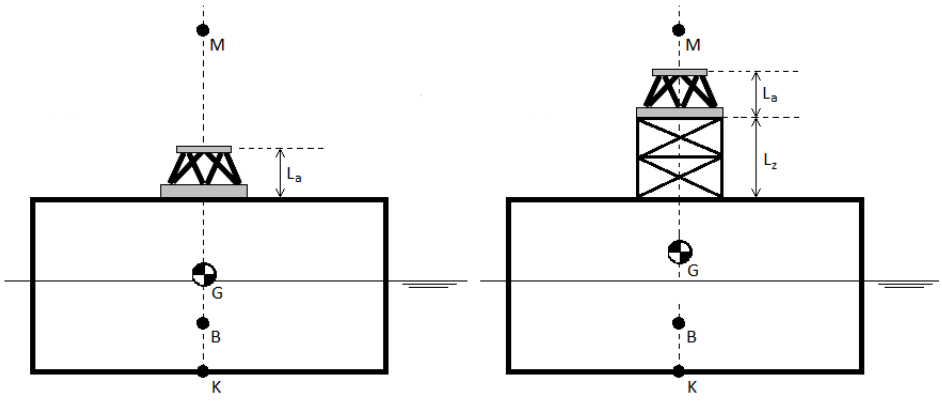

Figure 6-3: Hydrostatic stability criteria vessel

Elevating the Ampelmann system on the vessel causes $\overline{KG}$ to increase. This causes $\overline{GM}$ to decrease. $\overline{KB}$ and $\overline{BM}$ remain constant. The Ampelmann may be elevated till $\overline{GM} = 0[m]$.

$$\overline{KB} + \overline{BM} - \overline{KG} > 0 \tag{6-2}$$

$\overline{KG}$ the length from the keel to the CoG of the combined vessel-Ampelmann system. $\overline{KG}_1$ is the length from the keel to the CoG of the vessel. $\overline{KG}$ can then be written in terms of $\overline{KG}_1$, the vessel m_1, the TD mass m_2 and the TD elevation L_a and L_z with respect to the CoG of the vessel.

$$\overline{KG} = \frac{m_1\overline{KG}_1 + m_2(\overline{KG}_1 + L_z + L_a)}{m_1 + m_2} \tag{6-3}$$

The maximum value for L_z for $\overline{GM} > 0[m]$ is determined by rewriting L_z in terms of $\overline{KG}_1$, m_1, m_2, L_a, $\overline{KB}$ and $\overline{BM}$. This is the maximum allowable vertical translation, for which the vessel is hydrostatically stable.

$$\frac{m_1 + m_2}{m_2}\left(\overline{KB} + \overline{BM} - \overline{KG}_1\right) - L_a > L_z \tag{6-4}$$

6-2-2 Conditions for horizontal translations

A horizontal Ampelmann translation causes a static roll moment to the vessel resulting in a trim angle. This is shown in Figure 6-4. The right figure shows the Ampelmann system centred on the vessel. The middle figure shows the horizontally translated Ampelmann, this causes the CoG of the vessel-Ampelmann combination to shift in direction of the translation L_y. The resulting heel angle causes the hydromechanic vessel properties to change. For this reason to keep the hydromechanic properties valid for the model it is assumed that when translating the Ampelmann horizontally the vessel does not experience a static heel angle.

The hydromechanic properties are unaffected and the location of the CoG remains centred. See Figure 6-4 right side. Half of the static weight of the Ampelmann is removed from the left side of the vessel and is added at the right side. The vertical force equilibrium is maintained and the static heel moment $M_a = 0[Nm]$. As a result the vessel's mass moment of inertia may change, this effect is assumed to be negligible.

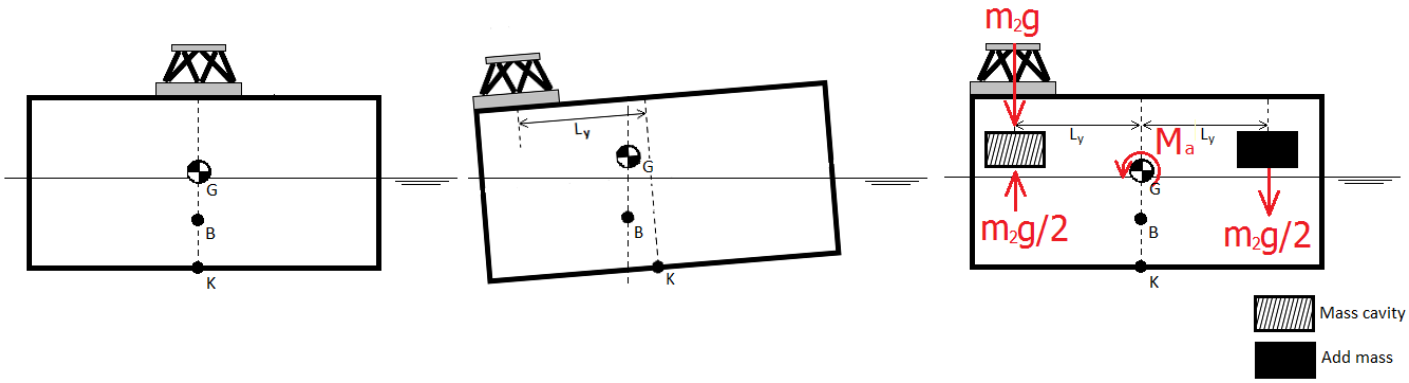

Figure 6-4: Hydrostatic roll moment causing a heel angle

6-3 6 DOF model include translation of Ampelmann location

Figure 6-5 shows the free body diagram for the derivation of the 6 DOF model including the translation of the Ampelmann location. Both the vessel and the TD are constrained to move in 3 DOF: sway, heave and roll. The Ampelmann is positioned at a location L_y and L_z relative to the CoG of the vessel. This point is indicated with B. The reaction forces and moments of the Ampelmann system working on the vessel are indicated with, $F_{a,h}$, $F_{a,v}$ and M_a.These result from figure 6-6 on page 57. All other forces and moments are hydromechanic terms.

The general frequency domain expression for a 6 DOF model is written below where the three top rows of $[\mathbf{M} + \mathbf{A}(\omega)]$, $[\mathbf{B}(\omega)]$ and $[\mathbf{C}]$ are to be determined from Figure 6-5 and 6-6. First the force relations between the vessel and the TD are derived, then implicit relations relating the forces and moments between the TD and the vessel are substituted. These depend on the control system. The EOM has the following form, with on the left hand side all mass, damping and stiffness terms and on the right hand side the external loading to the coupled system.

$$\left(-\omega^2[\mathbf{M} + \mathbf{A}(\omega)] + i\omega[\mathbf{B}(\omega)] + [\mathbf{C}]\right) \begin{bmatrix} \hat{Y}_1 \\ \hat{Z}_1 \\ \hat{\Phi}_1 \\ \hat{Y}_2 \\ \hat{Z}_2 \\ \hat{\Phi}_2 \end{bmatrix} = \begin{bmatrix} \hat{F}_2 \\ \hat{F}_3 \\ \hat{M}_4 \\ 0 \\ 0 \\ 0 \end{bmatrix} \tag{6-5}$$

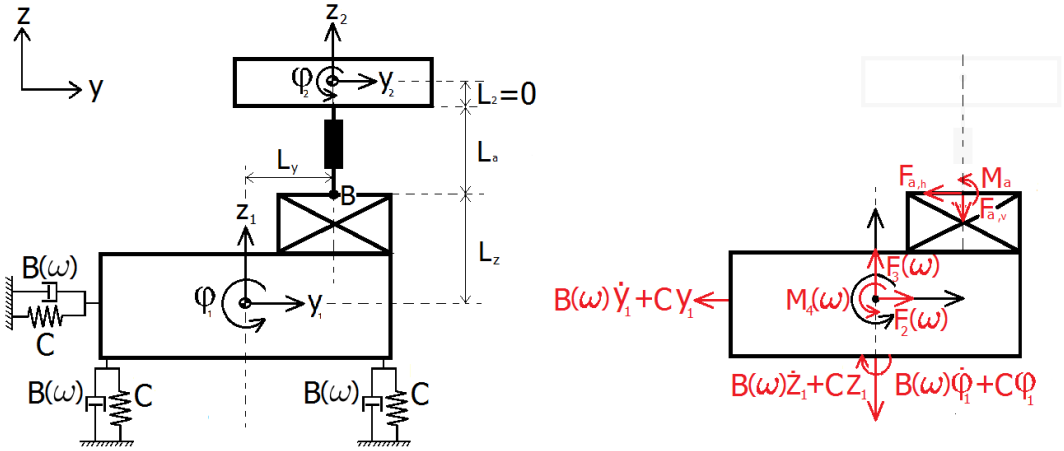

Figure 6-5: Free body diagram 6 DOF model including translation of Ampelmann location

Only linear first order motions are taken into account. Figure 6-6 shows 5 subfigures indicated with a, b, c, d and e. These are explained below.

- a: Total reaction forces and moments due to the Ampelmann system on the vessel.
- b: Reaction force and moment due to TD sway acceleration.
- c: Reaction moment due to TD angular roll acceleration.
- d: Reaction force due to a TD heave acceleration.
- e: Reaction moment due to the static weight of the Ampelmann caused by a relative horizontal displacement of the TD's CoG and the vessel's CoG. For illustrative purposes item e shows only a vertically translated Ampelmann system and no horizontal translation, this remains valid because only first order motions are taken into account.

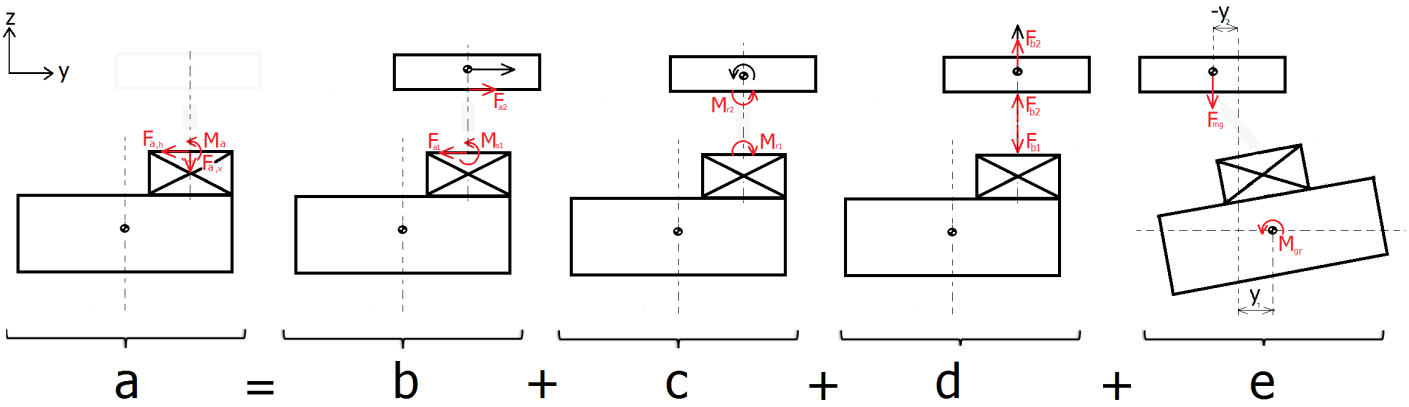

Figure 6-6: Reaction forces due to the Ampelmann, the TD is modelled as a point mass with inertia

The following expression yields with $[\mathbf{M}+\mathbf{A}(\omega)]$, $[\mathbf{B}(\omega)]$ and $[\mathbf{C}]$

$$\left(-\omega^2[\mathbf{M}+\mathbf{A}(\omega)]+i\omega[\mathbf{B}(\omega)]+[\mathbf{C}]\right)\begin{bmatrix}\hat{Y}_1\\ \hat{Z}_1\\ \hat{\Phi}_1\\ \hat{Y}_2\\ \hat{Z}_2\\ \hat{\Phi}_2\end{bmatrix}+\begin{bmatrix}F_{a,h}\\ F_{a,v}\\ M_a\\ -F_{a,h}\\ -F_{a,v}\\ -M_a\end{bmatrix}=\begin{bmatrix}\hat{F}_2\\ \hat{F}_3\\ \hat{M}_4\\ 0\\ 0\\ 0\end{bmatrix} \tag{6-6}$$

$$[\mathbf{M}+\mathbf{A}(\omega)]=\begin{bmatrix}m_1+a_{22}(\omega) & a_{23}(\omega) & a_{24}(\omega) & 0 & 0 & 0\\ a_{32}(\omega) & m_1+a_{33}(\omega) & a_{34}(\omega) & 0 & 0 & 0\\ a_{42}(\omega) & a_{43}(\omega) & I_{xx1}+a_{44}(\omega) & 0 & 0 & 0\\ 0 & 0 & 0 & m_2 & 0 & 0\\ 0 & 0 & 0 & 0 & m_2 & 0\\ 0 & 0 & 0 & -(L_a+L_z)m_2 & L_y m_2 & I_{xx2}\end{bmatrix} \tag{6-7}$$

$$[\mathbf{B}(\omega)]=\begin{bmatrix}b_{22}(\omega) & b_{23}(\omega) & b_{24}(\omega) & 0 & 0 & 0\\ b_{32}(\omega) & b_{33}(\omega) & b_{34}(\omega) & 0 & 0 & 0\\ b_{42}(\omega) & b_{43}(\omega) & b_{44}(\omega) & 0 & 0 & 0\\ 0 & 0 & 0 & 0 & 0 & 0\\ 0 & 0 & 0 & 0 & 0 & 0\\ 0 & 0 & 0 & 0 & 0 & 0\end{bmatrix} \tag{6-8}$$

$$[\mathbf{C}]=\begin{bmatrix}c_{22} & c_{23} & c_{24} & 0 & 0 & 0\\ c_{32} & c_{33} & c_{34} & 0 & 0 & 0\\ c_{42} & c_{43} & c_{44} & 0 & 0 & 0\\ 0 & 0 & 0 & 0 & 0 & 0\\ 0 & 0 & 0 & 0 & 0 & 0\\ -m_2 g & 0 & 0 & m_2 g & 0 & 0\end{bmatrix} \tag{6-9}$$

This frequency domain expression contains 9 unknowns $\hat{Y}_1$, $\hat{Z}_1$, $\hat{\Phi}_1$, $\hat{Y}_2$, $\hat{Z}_2$, $\hat{\Phi}_2$, $F_{a,h}$, $F_{a,v}$ and M_a. In order to solve implicit relations are found relating vessel and TD motions. These depend on the control system. Expressions in the form of Equation 6-5 are obtained with $[\mathbf{M}+\mathbf{A}(\omega)]$, $[\mathbf{B}(\omega)]$ and $[\mathbf{C}]$ written below. The implicit expressions are substituted to the empty matrix entries.

$$[\mathbf{M}+\mathbf{A}(\omega)]=\begin{bmatrix}m_1+a_{22}(\omega) & a_{23}(\omega) & a_{24}(\omega) & m_2 & 0 & 0\\ a_{32}(\omega) & m_1+a_{33}(\omega) & a_{34}(\omega) & 0 & m2 & 0\\ a_{42}(\omega) & a_{43}(\omega) & I_{xx1}+a_{44}(\omega) & -(L_a+L_z)m_2 & L_y m_2 & I_{xx2}\\ \dots & \dots & \dots & \dots & \dots & \dots\\ \dots & \dots & \dots & \dots & \dots & \dots\\ \dots & \dots & \dots & \dots & \dots & \dots\end{bmatrix} \tag{6-10}$$

$$[\mathbf{B}(\omega)] = \begin{bmatrix} b_{22}(\omega) & b_{23}(\omega) & b_{24}(\omega) & 0 & 0 & 0 \\ b_{32}(\omega) & b_{33}(\omega) & b_{34}(\omega) & 0 & 0 & 0 \\ b_{42}(\omega) & b_{43}(\omega) & b_{44}(\omega) & 0 & 0 & 0 \\ ... & ... & ... & ... & ... & ... \\ ... & ... & ... & ... & ... & ... \\ ... & ... & ... & ... & ... & ... \end{bmatrix} \tag{6-11}$$

$$[\mathbf{C}] = \begin{bmatrix} c_{22} & c_{23} & c_{24} & 0 & 0 & 0 \\ c_{32} & c_{33} & c_{34} & 0 & 0 & 0 \\ -m_2 g + c_{42} & c_{43} & c_{44} & m_2 g & 0 & 0 \\ ... & ... & ... & ... & ... & ... \\ ... & ... & ... & ... & ... & ... \\ ... & ... & ... & ... & ... & ... \end{bmatrix} \tag{6-12}$$

For this model three control system are applicable, No compensation, Perfect compensation and Filter compensation. The final expressions for each control system are obtained by substitution of Equation 4-8, 4-9 and 4-15. The results are shown in Appendix E, section E-2.

Two 6 DOF models are determined. First the 6 DOF model from chapter 5, there the Ampelmann system is positioned at the CoG of the vessel: $L_y = L_z = 0[m]$. L_y, L_z are omitted from the equation. In the 6 DOF model in this section the Ampelmann system may be located at a chosen positions defined by L_y and L_z. These two terms add to the mass and added mass matrix $[\mathbf{M} + \mathbf{A}(\omega)]$, see Equation 6-10. Vessel roll motions (third row) are coupled by TD sway and heave motions (fourth and fifth entry of the third row). Here L_z adds to L_a and L_y causes a TD heave to coupled to a vessel roll motion.

6-4 12 DOF model

The 12 DOF model includes all vessel and TD DOF, $\hat{X}_1$, $\hat{Y}_1$, $\hat{Z}_1$, $\hat{\Phi}_1$, $\hat{\Theta}_1$, $\hat{\Psi}_1$, $\hat{X}_2$, $\hat{Y}_2$, $\hat{Z}_2$, $\hat{\Phi}_2$, $\hat{\Theta}_2$ and $\hat{\Psi}_2$. This section determines the EOM for the 12 DOF coupled vessel-Ampelmann system where the Ampelmann is positioned at the CoG of the vessel, hence $L_x = L_y = L_z = 0$.

For the determination of the 12 DOF model see Figure 6-7. Until now only 6 DOF coupled vessel-Ampelmann systems are analysed in the 2D y-z plane. In a similar fashion 6 DOF models in the 2D x-z plane may be analysed. Then $\hat{X}_1$, $\hat{Z}_1$, $\hat{\Theta}_1$, $\hat{X}_2$, $\hat{Z}_2$ and $\hat{\Theta}_2$ are included. The same principles holds. Because only first order motions are taken into account no additional mechanical coupling mechanisms appear between the y-z plane model and x-z plane model. Both models are directly combined in one model. The same reasoning applies for adding the y-z plane model to the rest.

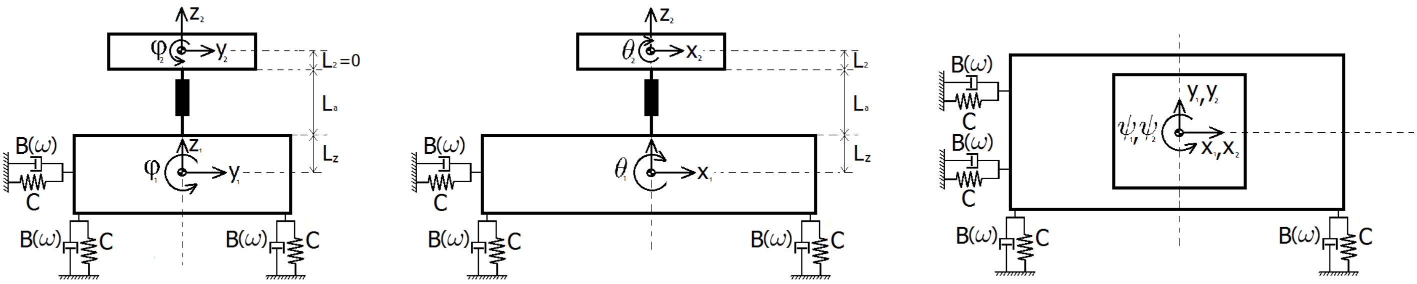

Figure 6-7: x-y, x-z and y-z plane representation for coupled vessel-Ampelmann system. Ampelmann positioned at CoG of vessel

The EOM has the following format with $[\mathbf{M}+\mathbf{A}(\omega)]$, $[\mathbf{B}(\omega)]$ and $[\mathbf{C}]$. The lower six rows are to be filled by the implicit expressions relating the vessel and TD motions. These depend on the control system.

$$\left(-\omega^2[\mathbf{M}+\mathbf{A}(\omega)]+i\omega[\mathbf{B}(\omega)]+[\mathbf{C}]\right)\begin{bmatrix}\hat{X}_1\\ \hat{Y}_1\\ \hat{Z}_1\\ \hat{\Phi}_1\\ \hat{\Theta}_1\\ \hat{\Psi}_1\\ \hat{X}_2\\ \hat{Y}_2\\ \hat{Z}_2\\ \hat{\Phi}_2\\ \hat{\Theta}_2\\ \hat{\Psi}_2\end{bmatrix}=\begin{bmatrix}\hat{F}_1\\ \hat{F}_2\\ \hat{F}_3\\ \hat{M}_4\\ \hat{M}_5\\ \hat{M}_6\\ 0\\ 0\\ 0\\ 0\\ 0\\ 0\end{bmatrix} \tag{6-13}$$

$$[\mathbf{M}+\mathbf{A}(\omega)]=$$
$$\begin{bmatrix}
m_1+a_{11}(\omega) & a_{12}(\omega) & a_{13}(\omega) & a_{14}(\omega) & a_{15}(\omega) & a_{16}(\omega) & m_2 & 0 & 0 & 0 & 0 & 0\\
a_{21}(\omega) & m_1+a_{22}(\omega) & a_{23}(\omega) & a_{24}(\omega) & a_{25}(\omega) & a_{26}(\omega) & 0 & m_2 & 0 & 0 & 0 & 0\\
a_{31}(\omega) & a_{32}(\omega) & m_1+a_{33}(\omega) & a_{34}(\omega) & a_{35}(\omega) & a_{36}(\omega) & 0 & 0 & m_2 & 0 & 0 & 0\\
a_{41}(\omega) & a_{42}(\omega) & a_{43}(\omega) & I_{xx1}+a_{44}(\omega) & a_{45}(\omega) & a_{46}(\omega) & 0 & -L_a m_2 & 0 & I_{xx2} & 0 & 0\\
a_{51}(\omega) & a_{52}(\omega) & a_{53}(\omega) & a_{54}(\omega) & I_{yy1}+a_{55}(\omega) & a_{56}(\omega) & L_a m_2 & 0 & 0 & 0 & I_{yy2} & 0\\
a_{61}(\omega) & a_{62}(\omega) & a_{63}(\omega) & a_{64}(\omega) & a_{65}(\omega) & I_{zz1}+a_{66}(\omega) & 0 & 0 & 0 & 0 & 0 & I_{zz2}\\
\cdots & \cdots & \cdots & \cdots & \cdots & \cdots & \cdots & \cdots & \cdots & \cdots & \cdots & \cdots\\
\cdots & \cdots & \cdots & \cdots & \cdots & \cdots & \cdots & \cdots & \cdots & \cdots & \cdots & \cdots\\
\cdots & \cdots & \cdots & \cdots & \cdots & \cdots & \cdots & \cdots & \cdots & \cdots & \cdots & \cdots\\
\cdots & \cdots & \cdots & \cdots & \cdots & \cdots & \cdots & \cdots & \cdots & \cdots & \cdots & \cdots\\
\cdots & \cdots & \cdots & \cdots & \cdots & \cdots & \cdots & \cdots & \cdots & \cdots & \cdots & \cdots\\
\cdots & \cdots & \cdots & \cdots & \cdots & \cdots & \cdots & \cdots & \cdots & \cdots & \cdots & \cdots
\end{bmatrix} \tag{6-14}$$

$$[\mathbf{B}(\omega)]=\begin{bmatrix}
b_{11}(\omega) & b_{12}(\omega) & b_{13}(\omega) & b_{14}(\omega) & b_{15}(\omega) & b_{16}(\omega) & 0 & 0 & 0 & 0 & 0 & 0\\
b_{21}(\omega) & b_{22}(\omega) & b_{23}(\omega) & b_{24}(\omega) & b_{25}(\omega) & b_{26}(\omega) & 0 & 0 & 0 & 0 & 0 & 0\\
b_{31}(\omega) & b_{32}(\omega) & b_{33}(\omega) & b_{34}(\omega) & b_{35}(\omega) & b_{36}(\omega) & 0 & 0 & 0 & 0 & 0 & 0\\
b_{41}(\omega) & b_{42}(\omega) & b_{43}(\omega) & b_{44}(\omega) & b_{45}(\omega) & b_{46}(\omega) & 0 & 0 & 0 & 0 & 0 & 0\\
b_{51}(\omega) & b_{52}(\omega) & b_{53}(\omega) & b_{54}(\omega) & b_{55}(\omega) & b_{56}(\omega) & 0 & 0 & 0 & 0 & 0 & 0\\
b_{61}(\omega) & b_{62}(\omega) & b_{63}(\omega) & b_{64}(\omega) & b_{65}(\omega) & b_{66}(\omega) & 0 & 0 & 0 & 0 & 0 & 0\\
\cdots & \cdots & \cdots & \cdots & \cdots & \cdots & \cdots & \cdots & \cdots & \cdots & \cdots & \cdots\\
\cdots & \cdots & \cdots & \cdots & \cdots & \cdots & \cdots & \cdots & \cdots & \cdots & \cdots & \cdots\\
\cdots & \cdots & \cdots & \cdots & \cdots & \cdots & \cdots & \cdots & \cdots & \cdots & \cdots & \cdots\\
\cdots & \cdots & \cdots & \cdots & \cdots & \cdots & \cdots & \cdots & \cdots & \cdots & \cdots & \cdots\\
\cdots & \cdots & \cdots & \cdots & \cdots & \cdots & \cdots & \cdots & \cdots & \cdots & \cdots & \cdots\\
\cdots & \cdots & \cdots & \cdots & \cdots & \cdots & \cdots & \cdots & \cdots & \cdots & \cdots & \cdots
\end{bmatrix} \tag{6-15}$$

$$[\mathbf{C}]=\begin{bmatrix}
c_{11} & c_{12} & c_{13} & c_{14} & c_{15} & c_{16} & 0 & 0 & 0 & 0 & 0 & 0\\
c_{21} & c_{22} & c_{23} & c_{24} & c_{25} & c_{26} & 0 & 0 & 0 & 0 & 0 & 0\\
c_{31} & c_{32} & c_{33} & c_{34} & c_{35} & c_{36} & 0 & 0 & 0 & 0 & 0 & 0\\
c_{41} & -m_2g+c_{42} & c_{43} & c_{44} & c_{45} & c_{46} & 0 & m_2g & 0 & 0 & 0 & 0\\
m_2g+c_{51} & c_{52} & c_{53} & c_{54} & c_{55} & c_{56} & -m_2g & 0 & 0 & 0 & 0 & 0\\
c_{61} & c_{62} & c_{63} & c_{64} & c_{65} & c_{66} & 0 & 0 & 0 & 0 & 0 & 0\\
\cdots & \cdots & \cdots & \cdots & \cdots & \cdots & \cdots & \cdots & \cdots & \cdots & \cdots & \cdots\\
\cdots & \cdots & \cdots & \cdots & \cdots & \cdots & \cdots & \cdots & \cdots & \cdots & \cdots & \cdots\\
\cdots & \cdots & \cdots & \cdots & \cdots & \cdots & \cdots & \cdots & \cdots & \cdots & \cdots & \cdots\\
\cdots & \cdots & \cdots & \cdots & \cdots & \cdots & \cdots & \cdots & \cdots & \cdots & \cdots & \cdots\\
\cdots & \cdots & \cdots & \cdots & \cdots & \cdots & \cdots & \cdots & \cdots & \cdots & \cdots & \cdots\\
\cdots & \cdots & \cdots & \cdots & \cdots & \cdots & \cdots & \cdots & \cdots & \cdots & \cdots & \cdots
\end{bmatrix} \tag{6-16}$$

The results for each control system, No compensation, Perfect compensation and Filter compensation are shown in Appendix E, section E-3.

6-5 12 DOF model include translation of Ampelmann location

In this section the 12 DOF coupled vessel-Ampelmann model is determined, it includes the translation of the Ampelmann location. The model consists of linearised frequency domain expressions and only first order motions apply. Due to linearisation this analysis is only valid for small motions. It is assumed that a multiplication of two small first order motions is small enough to neglect. This limits the amount of coupling mechanism involved in the coupled vessel-Ampelmann system. Table 6-1 summarizes all first order, static and dynamic mechanical coupling terms.

Table 6-1: First order mechanical coupling terms for the coupled vessel-Ampelmann system

	x_1, surge V	y_1, sway V	z_1, heave V	ϕ_1, roll V	θ_1, pitch V	ψ_1, yaw V
x_2, surge TD	1				L_a, L_z, $M_{\theta,x}$	L_y
y_2, sway TD		1		L_a, L_z, $M_{\phi,y}$		L_x
z_2, heave TD			1	L_y	L_x	
ϕ_2, roll TD				1		
θ_2, pitch TD					1	
ψ_2, yaw TD						1

The table should be read as follows:

- A dynamic contribution due to a TD surge acceleration causes a reaction force in surge to the vessel, this is independent of an Ampelmann translation L_x, L_y or L_z. Furthermore it excites the vessel in pitch and yaw. These depend on L_a and L_z and for yaw on L_y.
- A static contribution due to a relative surge displacement of the TD and the vessel causes a pitch moment $M_{\theta,x}$.

An empty cell indicates no mechanical coupling. See Appendix D how this table is verified and applies to the models derived or determined earlier.

From Table 6-1 vessel yaw is excited by three dynamic mechanisms: TD surge (depending on L_y), TD sway (depending on L_x) and TD yaw. The first two are illustrated in Figure 6-8. Translating the Ampelmann in x and y creates a lever arm for the reaction forces due to TD surge and TD sway acceleration.

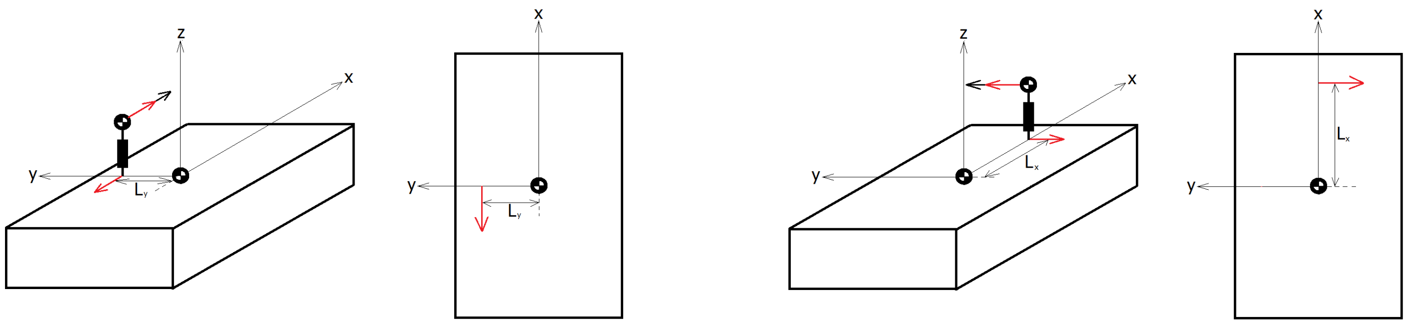

Figure 6-8: Reaction forces due to the TD surge and sway, exciting vessel yaw

Hence the 12 DOF EOM is written in the following form with $[\mathbf{M}+\mathbf{A}(\omega)]$, $[\mathbf{B}(\omega)]$ and $[\mathbf{C}]$. The lower 6 rows are to be filled in by the implicit relations relating vessel and TD motions, which depend on the control system.

$$\left(-\omega^2[\mathbf{M}+\mathbf{A}(\omega)]+i\omega[\mathbf{B}(\omega)]+[\mathbf{C}]\right)\begin{bmatrix}\hat{X}_1\\ \hat{Y}_1\\ \hat{Z}_1\\ \hat{\Phi}_1\\ \hat{\Theta}_1\\ \hat{\Psi}_1\\ \hat{X}_2\\ \hat{Y}_2\\ \hat{Z}_2\\ \hat{\Phi}_2\\ \hat{\Theta}_2\\ \hat{\Psi}_2\end{bmatrix}=\begin{bmatrix}\hat{F}_1\\ \hat{F}_2\\ \hat{F}_3\\ \hat{M}_4\\ \hat{M}_5\\ \hat{M}_6\\ 0\\ 0\\ 0\\ 0\\ 0\\ 0\end{bmatrix} \tag{6-17}$$

$$[\mathbf{M}+\mathbf{A}(\omega)]=$$
$$\begin{bmatrix}
m_1+a_{11}(\omega) & a_{12}(\omega) & a_{13}(\omega) & a_{14}(\omega) & a_{15}(\omega) & a_{16}(\omega) & m_2 & 0 & 0 & 0 & 0 & 0\\
a_{21}(\omega) & m_1+a_{22}(\omega) & a_{23}(\omega) & a_{24}(\omega) & a_{25}(\omega) & a_{26}(\omega) & 0 & m_2 & 0 & 0 & 0 & 0\\
a_{31}(\omega) & a_{32}(\omega) & m_1+a_{33}(\omega) & a_{34}(\omega) & a_{35}(\omega) & a_{36}(\omega) & 0 & 0 & m_2 & 0 & 0 & 0\\
a_{41}(\omega) & a_{42}(\omega) & a_{43}(\omega) & I_{xx1}+a_{44}(\omega) & a_{45}(\omega) & a_{46}(\omega) & 0 & -(L_z+L_a)m_2 & L_y m_2 & I_{xx2} & 0 & 0\\
a_{51}(\omega) & a_{52}(\omega) & a_{53}(\omega) & a_{54}(\omega) & I_{yy1}+a_{55}(\omega) & a_{56}(\omega) & (L_z+L_a)m_2 & 0 & -L_x m_2 & 0 & I_{yy2} & 0\\
a_{61}(\omega) & a_{62}(\omega) & a_{63}(\omega) & a_{64}(\omega) & a_{65}(\omega) & I_{zz1}+a_{66}(\omega) & -m_2 L_y & L_x m_2 & 0 & 0 & 0 & I_{zz2}\\
\cdots & \cdots & \cdots & \cdots & \cdots & \cdots & \cdots & \cdots & \cdots & \cdots & \cdots & \cdots\\
\cdots & \cdots & \cdots & \cdots & \cdots & \cdots & \cdots & \cdots & \cdots & \cdots & \cdots & \cdots\\
\cdots & \cdots & \cdots & \cdots & \cdots & \cdots & \cdots & \cdots & \cdots & \cdots & \cdots & \cdots\\
\cdots & \cdots & \cdots & \cdots & \cdots & \cdots & \cdots & \cdots & \cdots & \cdots & \cdots & \cdots\\
\cdots & \cdots & \cdots & \cdots & \cdots & \cdots & \cdots & \cdots & \cdots & \cdots & \cdots & \cdots\\
\cdots & \cdots & \cdots & \cdots & \cdots & \cdots & \cdots & \cdots & \cdots & \cdots & \cdots & \cdots
\end{bmatrix} \tag{6-18}$$

$$[\mathbf{B}(\omega)]=\begin{bmatrix}
b_{11}(\omega) & b_{12}(\omega) & b_{13}(\omega) & b_{14}(\omega) & b_{15}(\omega) & b_{16}(\omega) & 0 & 0 & 0 & 0 & 0 & 0\\
b_{21}(\omega) & b_{22}(\omega) & b_{23}(\omega) & b_{24}(\omega) & b_{25}(\omega) & b_{26}(\omega) & 0 & 0 & 0 & 0 & 0 & 0\\
b_{31}(\omega) & b_{32}(\omega) & b_{33}(\omega) & b_{34}(\omega) & b_{35}(\omega) & b_{36}(\omega) & 0 & 0 & 0 & 0 & 0 & 0\\
b_{41}(\omega) & b_{42}(\omega) & b_{43}(\omega) & b_{44}(\omega) & b_{45}(\omega) & b_{46}(\omega) & 0 & 0 & 0 & 0 & 0 & 0\\
b_{51}(\omega) & b_{52}(\omega) & b_{53}(\omega) & b_{54}(\omega) & b_{55}(\omega) & b_{56}(\omega) & 0 & 0 & 0 & 0 & 0 & 0\\
b_{61}(\omega) & b_{62}(\omega) & b_{63}(\omega) & b_{64}(\omega) & b_{65}(\omega) & b_{66}(\omega) & 0 & 0 & 0 & 0 & 0 & 0\\
\cdots & \cdots & \cdots & \cdots & \cdots & \cdots & \cdots & \cdots & \cdots & \cdots & \cdots & \cdots\\
\cdots & \cdots & \cdots & \cdots & \cdots & \cdots & \cdots & \cdots & \cdots & \cdots & \cdots & \cdots\\
\cdots & \cdots & \cdots & \cdots & \cdots & \cdots & \cdots & \cdots & \cdots & \cdots & \cdots & \cdots\\
\cdots & \cdots & \cdots & \cdots & \cdots & \cdots & \cdots & \cdots & \cdots & \cdots & \cdots & \cdots\\
\cdots & \cdots & \cdots & \cdots & \cdots & \cdots & \cdots & \cdots & \cdots & \cdots & \cdots & \cdots\\
\cdots & \cdots & \cdots & \cdots & \cdots & \cdots & \cdots & \cdots & \cdots & \cdots & \cdots & \cdots
\end{bmatrix} \tag{6-19}$$

$$[\mathbf{C}]=\begin{bmatrix}
c_{11} & c_{12} & c_{13} & c_{14} & c_{15} & c_{16} & 0 & 0 & 0 & 0 & 0 & 0\\
c_{21} & c_{22} & c_{23} & c_{24} & c_{25} & c_{26} & 0 & 0 & 0 & 0 & 0 & 0\\
c_{31} & c_{32} & c_{33} & c_{34} & c_{35} & c_{36} & 0 & 0 & 0 & 0 & 0 & 0\\
c_{41} & -m_2g+c_{42} & c_{43} & c_{44} & c_{45} & c_{46} & 0 & m_2g & 0 & 0 & 0 & 0\\
m_2g+c_{51} & c_{52} & c_{53} & c_{54} & c_{55} & c_{56} & -m_2g & 0 & 0 & 0 & 0 & 0\\
c_{61} & c_{62} & c_{63} & c_{64} & c_{65} & c_{66} & 0 & 0 & 0 & 0 & 0 & 0\\
\cdots & \cdots & \cdots & \cdots & \cdots & \cdots & \cdots & \cdots & \cdots & \cdots & \cdots & \cdots\\
\cdots & \cdots & \cdots & \cdots & \cdots & \cdots & \cdots & \cdots & \cdots & \cdots & \cdots & \cdots\\
\cdots & \cdots & \cdots & \cdots & \cdots & \cdots & \cdots & \cdots & \cdots & \cdots & \cdots & \cdots\\
\cdots & \cdots & \cdots & \cdots & \cdots & \cdots & \cdots & \cdots & \cdots & \cdots & \cdots & \cdots\\
\cdots & \cdots & \cdots & \cdots & \cdots & \cdots & \cdots & \cdots & \cdots & \cdots & \cdots & \cdots\\
\cdots & \cdots & \cdots & \cdots & \cdots & \cdots & \cdots & \cdots & \cdots & \cdots & \cdots & \cdots
\end{bmatrix} \tag{6-20}$$

The results for each control system, No compensation, Perfect compensation and Filter compensation are shown in Appendix E, section E-4. Here depending on the control system the empty entries from Equation 6-17 are substituted. In addition to the 12 DOF model, L_x, L_y and L_z are included. L_z adds to L_a and L_x and L_y introduce coupling of translational TD motions to rotational vessel motions.

6-6 Results

In this chapter three models are discussed, each model is solved by MATLAB. Depending on the input variables different results are obtained. The results in this chapter are given for scaled vessel parameters, $\lambda = 0.65[-]$. The purpose of scaling vessel parameters is discussed in section 5-5 and Appendix B. The model input variables for $\lambda = 0.65[-]$ are repeated below in Table 6-2. The values for L_x, L_y and L_z as for the wave incident angle are stated per set of results.

Table 6-2: Input values for couple vessel-Ampelmann model

Input variable	Input value, $\lambda = 0.65[-]$
m_1	$3.197 \cdot 10^5[kg]$
I_{xx1}	$2.135 \cdot 10^6[kgm^2]$
m_2	$2 \cdot 10^4[kg]$
I_{xx2}	$1 \cdot 10^5[kgm^2]$
L_a	$3.8[m]$

6-6-1 Results horizontal Ampelmann translation

The 6 DOF model including translation of the Ampelmann location is solved for a wave incident angle of $90[deg]$. Three results are given, each for a different combination of L_y and L_z. See Table 6-3.

Table 6-3: Input values for couple vessel-Ampelmann model

Result	Value L_y	Value L_z
1	$L_y = 0[m]$	$L_z = 0[m]$
2	$L_y = 2[m]$	$L_z = 0[m]$
3	$L_y = 4[m]$	$L_z = 0[m]$

Figures 6-9, 6-10 and 6-11 show the results for each case. For larger L_y values, the roll natural frequency for No compensation decreases to a lower frequency. This is also observed from the roll phase graph where the $90[deg]$ phase shift for No compensation occurs at a lower frequency for larger values of L_y. For Filter compensation the amplitude of the roll natural frequency peak decreases for larger values of L_y. For Perfect compensation all results are identical and independent of L_y. For both Perfect compensation and Filter compensation the

natural frequency is independent of L_y and remains constant for each L_y value.

Sway RAO show discrepancies at the roll natural frequency, this discrepancy moves with the natural frequency peak. Furthermore the sway frequency characteristics are not affected due to the changing value of L_y.

The Heave RAO shows a small increment at approximately the roll natural frequency for No compensation for larger values of L_y. Furthermore the graphs show similar results independent of L_y.

In addition to the results, Figures F-9, F-11 and F-12 Appendix F show the results per control system for different values of L_y plotted in one graph. These results confirm that when the Ampelmann is compensating the roll RAO for the entire frequency range increases but this increase is independent of L_y. Also the results are computed for a larger vessel $\lambda = 1[-]$ there the changing dynamic vessel behaviour becomes less significant.

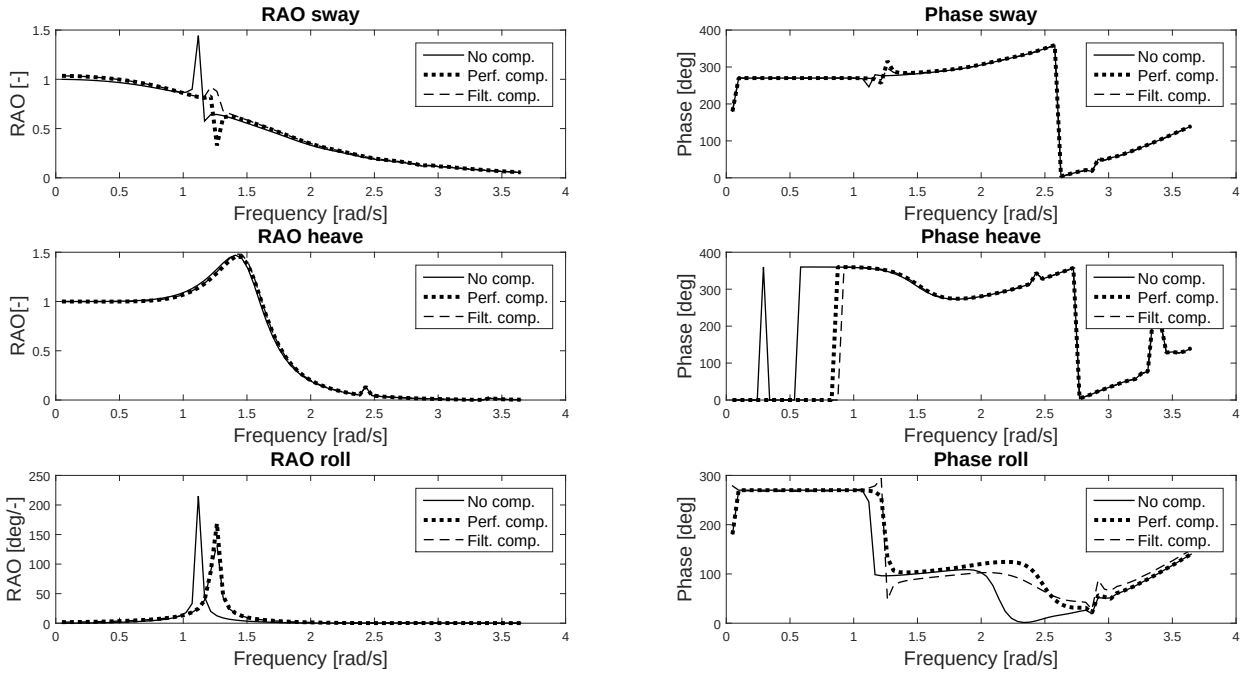

Figure 6-9: Vessel frequency characteristics: $\lambda = 0.65[-]$, $L_y = 0[m]$ and $L_z = 0[m]$

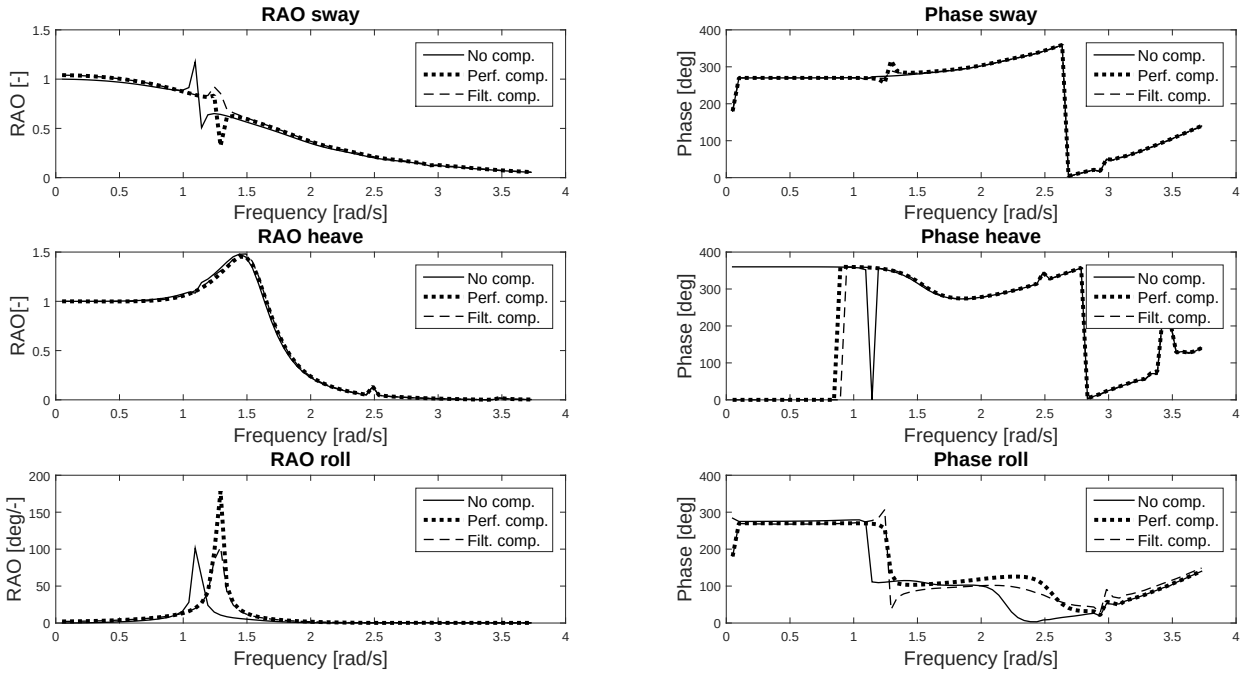

Figure 6-10: Vessel frequency characteristics: $\lambda = 0.65[-]$, $L_y = 2[m]$ and $L_z = 0[m]$

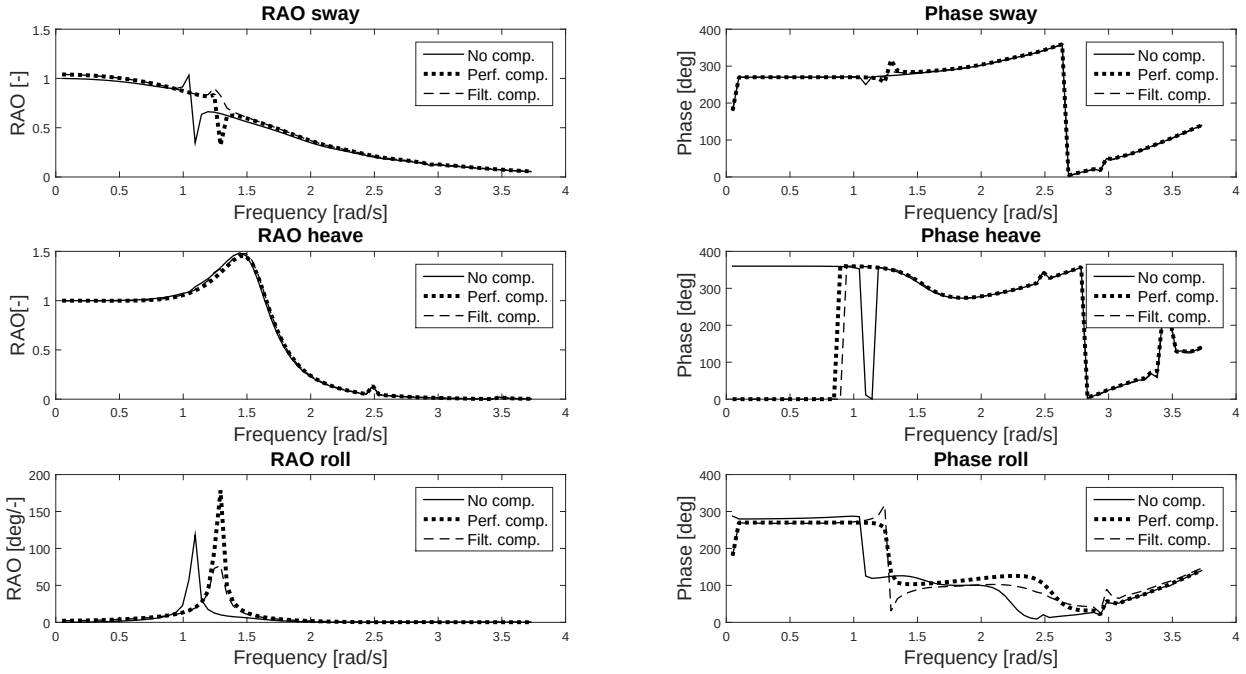

Figure 6-11: Vessel frequency characteristics: $\lambda = 0.65[-]$, $L_y = 4[m]$ and $L_z = 0[m]$

6-6-2 Results vertical Ampelmann translation

The 6 DOF model including translation of the Ampelmann location is solved for a wave incident angle of 90$[deg]$. Three results are given, each for different combinations of L_y and L_z. See Table 6-4.

Table 6-4: Input values for couple vessel-Ampelmann model

Result	Value L_y	Value L_z
1	$L_y = 0[m]$	$L_z = 0[m]$
2	$L_y = 0[m]$	$L_z = 4[m]$
3	$L_y = 0[m]$	$L_z = 8[m]$

Figures 6-9, 6-12 and 6-13 show the results for each case. In the EOM for No compensation, Perfect compensation and Filter compensation the vertical translation of the Ampelmann system L_z always adds to $L_a \rightarrow (L_z + L_a)$. The roll natural frequency peak for No compensation shifts to a lower frequency for an increasing L_z. The results also show that for larger values of L_z the natural frequency amplitude for No compensation reduces. An explanation is that for an increasing L_z the mass moment of inertia of the combined vessel-Ampelmann system increases. Because the mass moment of inertia increases and the wave forces and moments remain unchanged, the motion amplitudes decrease. This observation is not further argued since the model is a linear frequency domain model and the roll amplitudes at the natural frequency go beyond the linear limits. Furthermore in Perfect compensation the results are identical and independent of L_z.

The frequency characteristics for all cases are derived with respect to the CoG of the vessel. The mass moment of inertia of the vessel in No compensation is.

$$I_{xx1} + I_{xx2} + m_2(L_a + L_z)^2 + m_2 L_y^2 \tag{6-21}$$

When comparing roll natural frequency shift from Figure 6-11 ($L_y = 4[m]$ and $L_z = 0[m]$) with the roll natural frequency shift from Figure 6-12 ($L_y = 0[m]$ and $L_z = 4[m]$) it is seen that the natural frequency shift for $L_z = 4$ causes a larger shift. This is because L_z adds to L_a first and is then squared before multiplying with m_2 and adding to the total.

As with a horizontal translation L_y, the sway RAO show discrepancies at the roll natural frequency peak, this is due to coupling. Furthermore the sway frequency characteristics show similar results.

The heave frequency characteristics show similar results independent of L_z.

In addition to the results, Figures F-13, F-15 and F-16 in Appendix F show the results per control system for different values of L_z plotted in one graph. These results confirm that when the Ampelmann is compensating the roll RAO for the entire frequency range increases but this increase is independent of L_z. Also the results are computed for a larger vessel, $\lambda = 1[-]$, there the changing dynamic vessel behaviour becomes less significant.

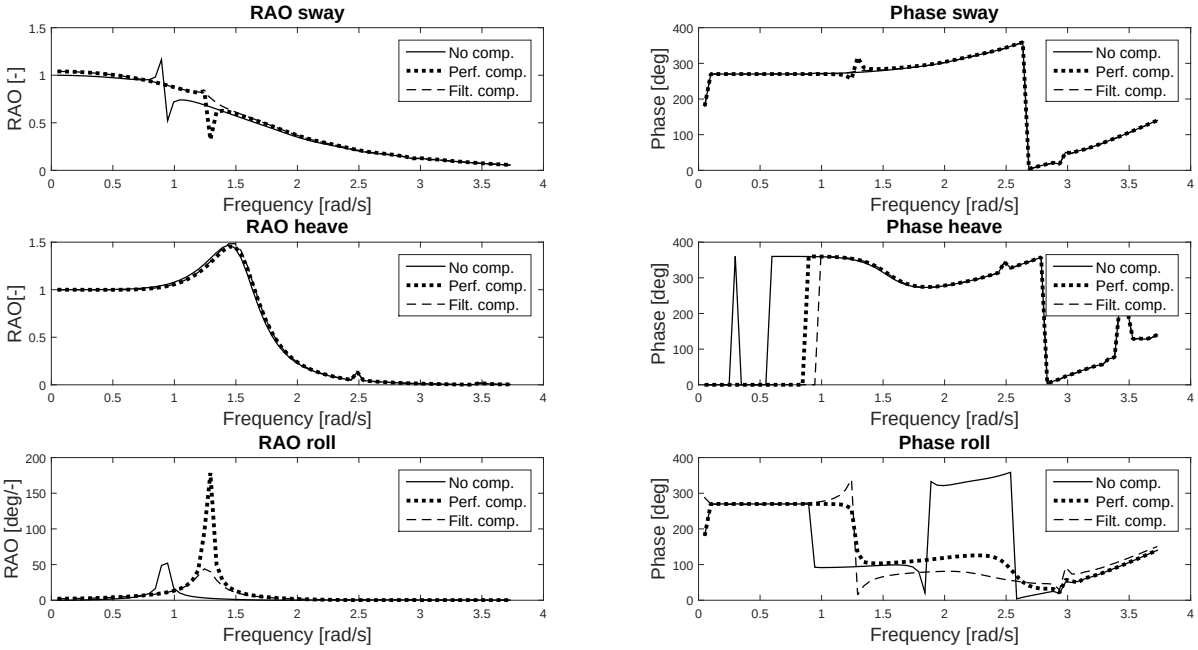

Figure 6-12: Vessel frequency characteristics: $\lambda = 0.65[-]$, $L_y = 0[m]$ and $L_z = 4[m]$

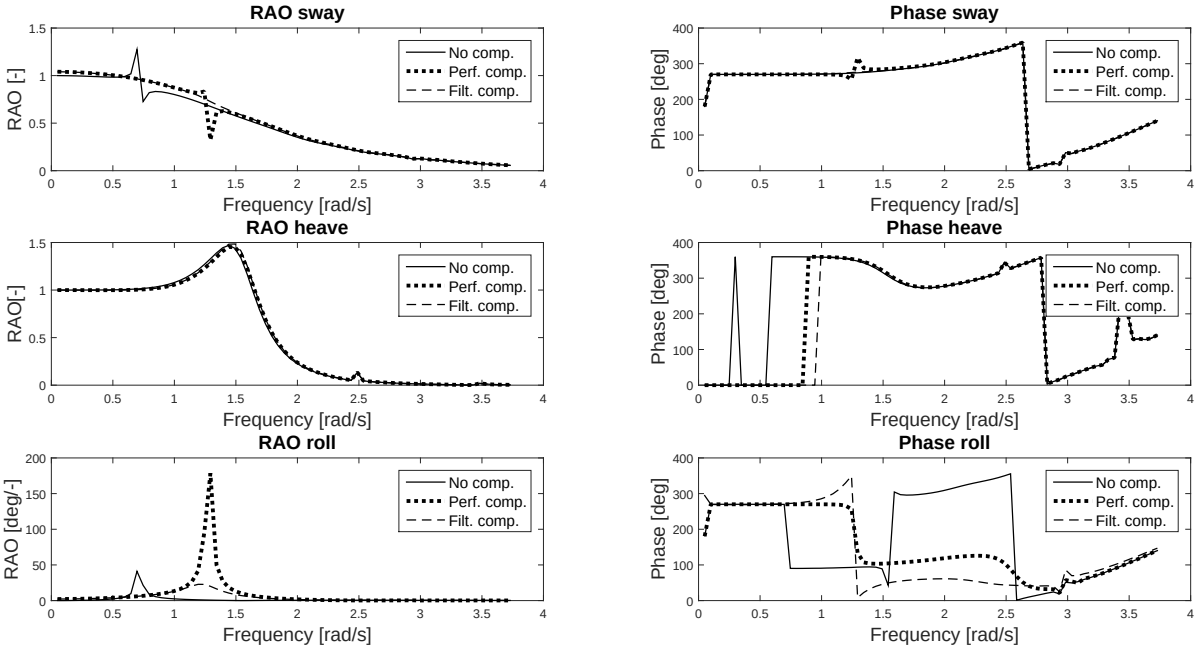

Figure 6-13: Vessel frequency characteristics: $\lambda = 0.65[-]$, $L_y = 0[m]$ and $L_z = 8[m]$

6-6-3 Results 12 DOF model

The 12 DOF model is solved for a wave incident angle of 15[deg]. The Ampelmann is positioned at the CoG of the vessel. The results are shown in Figure 6-14 and 6-15.

The results show an increased sway and surge motion for Perfect compensation and Filter compensation. Perfect compensation and Filter compensation show similar results. The sway RAO shows a discrepancy at the roll natural frequency. The roll graph shows a significant change between No compensation and compensation. The roll RAO increases and the natural frequency shifts to a lower frequency. Despite the small wave incident angle it is expected that the pitch RAO is affected due to a compensating Ampelmann. This is not the case, only roll is excited for lower frequencies. See Figure 6-16 where the roll and pitch frequency characteristics are zoomed in.

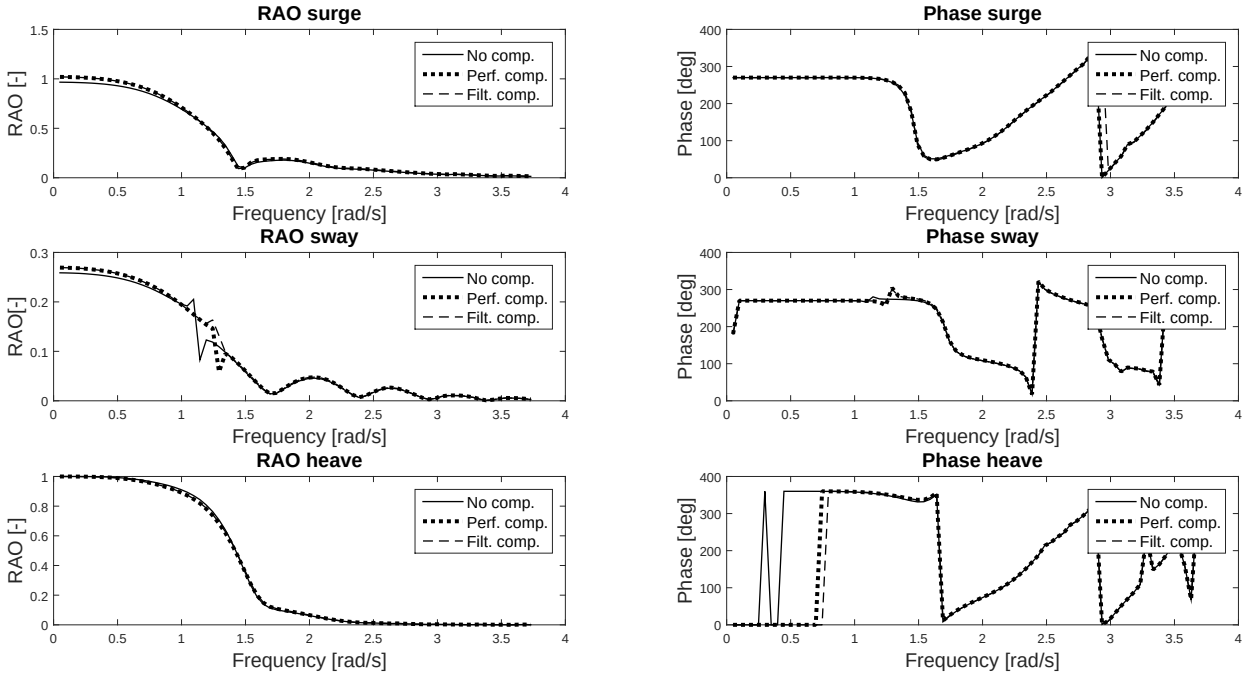

Figure 6-14: Vessel translation frequency characteristics, Ampelmann at CoG of vessel. $\lambda = 0.65[-]$, wave incident angle: $15[deg]$

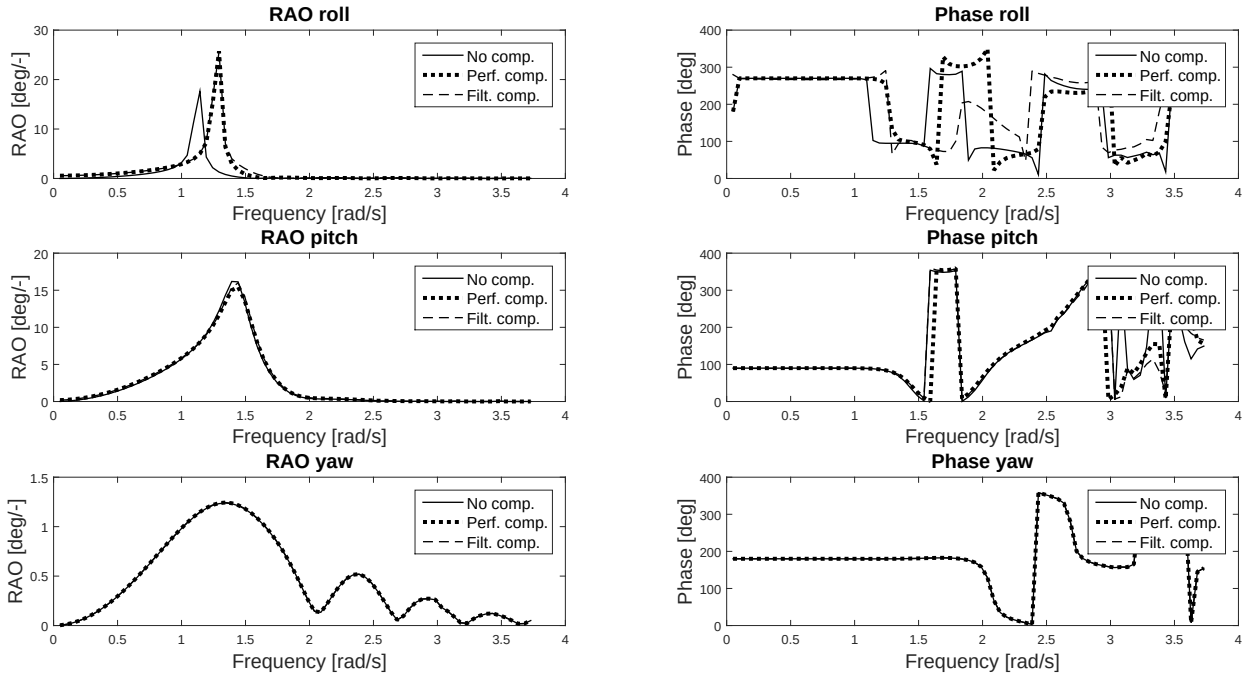

Figure 6-15: Vessel rotation frequency characteristics, Ampelmann at CoG of vessel. $\lambda = 0.65[-]$, wave incident angle: $15[deg]$

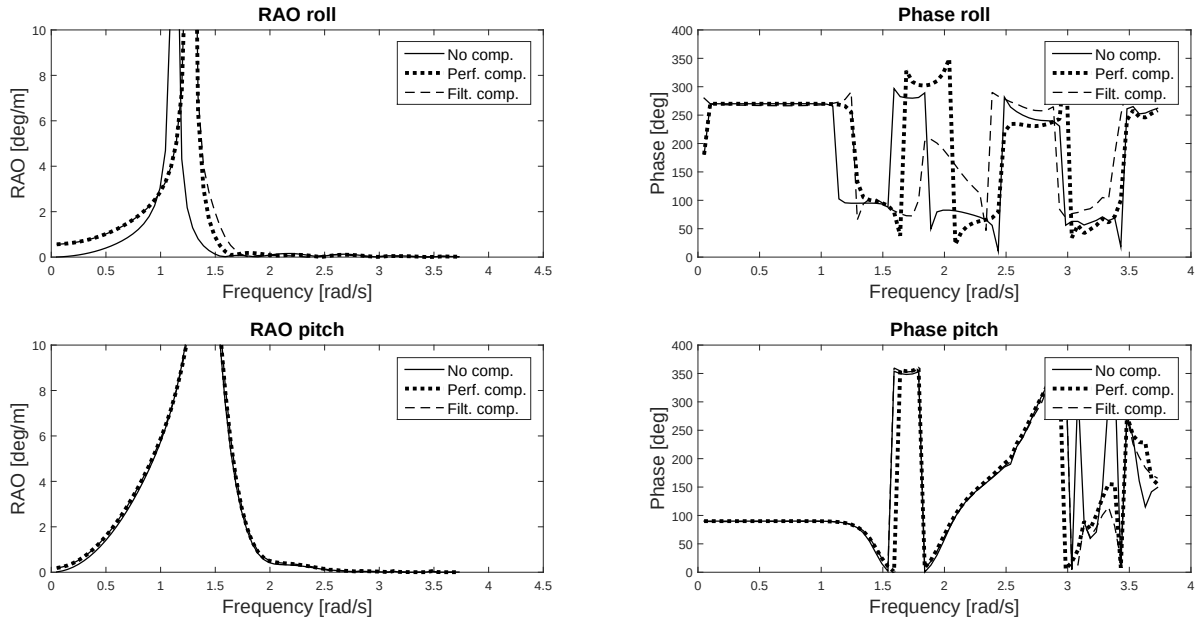

Figure 6-16: Zoomed vessel frequency characteristics roll and pitch, Ampelmann at CoG of vessel. $\lambda = 0.65[-]$, wave incident angle $15[deg]$.

6-6-4 Results 12 DOF model include translation of Ampelmann location

The 12 DOF model including the translation of the Ampelmann location is solved for a wave incident angle of $45[deg]$, in addition to No compensation, Perfect compensation and Filter compensation, also No sway/surge compensation is added to the results. This is done by setting $\hat{X}_2 = \hat{X}_1$ and $\hat{Y}_2 = \hat{Y}_1$. Furthermore the location of the Ampelmann is set to: $L_x = 5[m]$, $L_y = 3[m]$ and $L_z = 4[m]$. The results are shown in Figure 6-17 and 6-18.

For surge, sway and roll NSC shows reduced motion amplitudes compared to Perfect compensation and Filter compensation.

The surge frequency characteristics for Perfect compensation and Filter compensation are higher than for No compensation. Only for a frequency of approximately $1.4[rad/s]$ this is not the case. This is due to the coupling with pitch, the natural frequency for pitch is at approximately $1.4[rad/s]$. The surge phase shows similar results for each control system.

The sway frequency characteristics show an increased sway for Perfect compensation and Filter compensation compared to No compensation. Discrepancies occur at the roll natural frequency, this is due to coupling with roll. The sway phase shows similar results for each control system

The heave frequency characteristics show similar results for each control system, only at the pitch natural frequency there is a slight discrepancy. The heave phase show similar results for each control system.

The roll frequency characteristics show that the roll natural frequency increases for Perfect compensation and Filter compensation, also the roll amplitudes are increased. At the natural frequencies for each control system the roll phase shows a phase shift of $90[deg]$.

The pitch frequency characteristics show that the pitch natural frequency for Perfect compensation and Filter compensation are shifted to a higher frequency compared to No compensation. Filter compensation shows a higher pitch amplitude at the pitch natural frequency compared to Perfect compensation.

The yaw frequency characteristics show discrepancies at the roll natural frequency for No compensation and Filter compensation. No compensation also show a discrepancy at the pitch natural frequency.

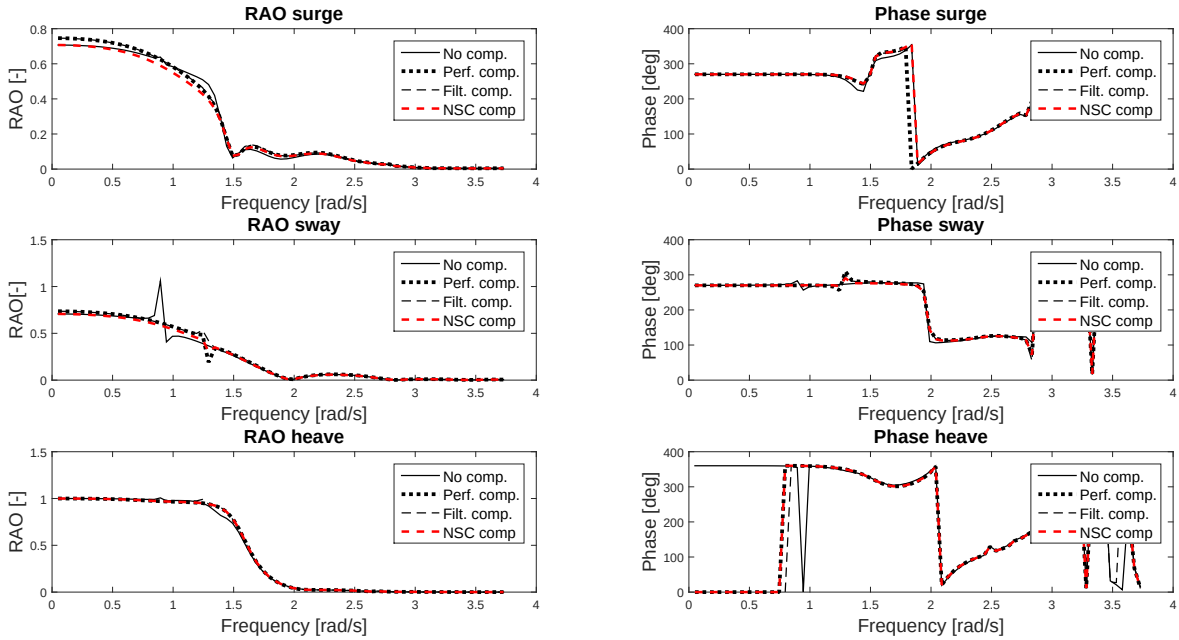

Figure 6-17: Vessel translation frequency characteristics. Wave incident angle $45[deg]$. Location Ampelmann $L_x = 5[m]$, $L_y = 3[m]$, $L_z = 4[m]$. $\lambda = 0.65[-]$.

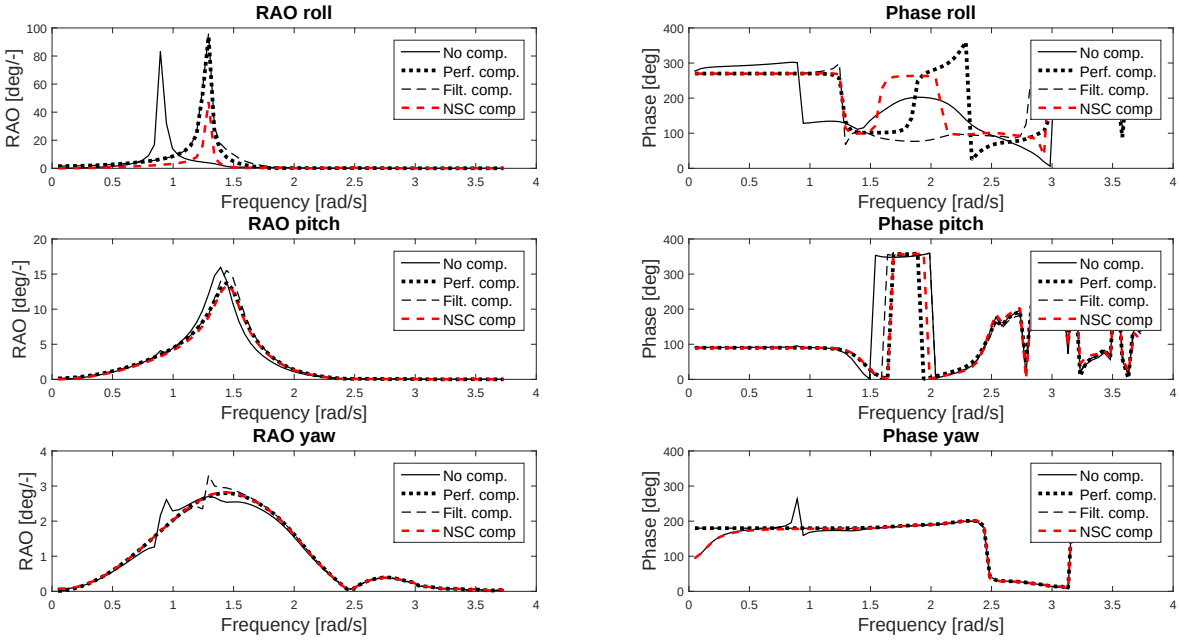

Figure 6-18: Vessel rotation frequency characteristics. Wave incident angle $45[deg]$. Location Ampelmann $L_x = 5[m]$, $L_y = 3[m]$, $L_z = 4[m]$. $\lambda = 0.65[-]$.

6-7 Model validation and verification

The results of the No compensation 12 DOF model are compared to the DELFRAC results. Then the TD motions for Perfect compensation are compared to a time trance of the TD motions based on the modelled Ampelmann control system [7]. It is assumed that the DELFRAC results and the time trace of the TD motions are a representation of reality. The differences between the No compensation, the Perfect compensation, Filter compensation and DELFRAC results are verified and explained. Ultimately to confirm the validity of the models practical tests shall be performed, this is beyond the scope of this thesis.

6-7-1 Validation of No compensation and Perfect compensation

Validation of the No compensation model is performed by comparing the results to the DELFRAC results. This comparison is performed for a chosen wave incident angle of 45[deg] and for the Ampelmann positioned at the CoG of the vessel. Figure 6-19 and 6-20 show the results for No compensation and the DELFRAC results.

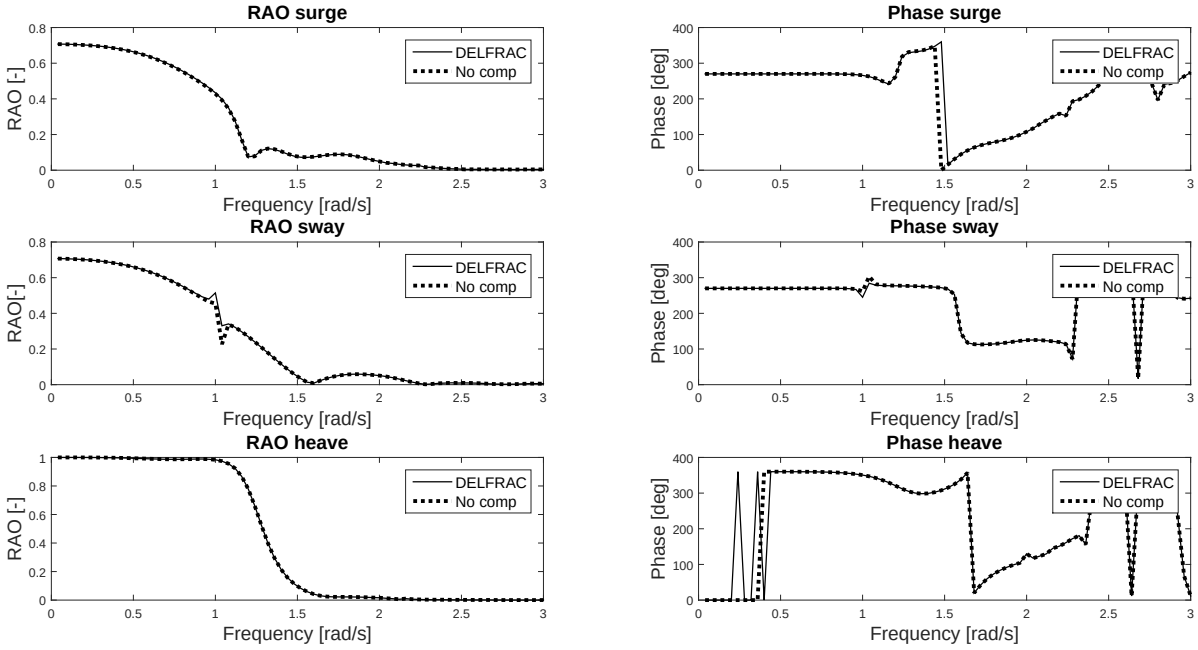

Figure 6-19: Frequency characteristics vessel translations No compensation and DELFRAC results. $\lambda = 1[-]$, wave incident angle $45[deg]$

The results are not identical. The difference is explained, it is expected that the natural roll frequency for No compensation shifts to a lower frequency because the mass moment of inertia with respect to the vessel's CoG has increased to:

$$I_{xx1} \rightarrow I_{xx1} + I_{xx2} + m_2 L_a^2 \tag{6-22}$$

Sway and heave are unaffected because the total mass $m_1 + m_2 = m_v$ does not change.

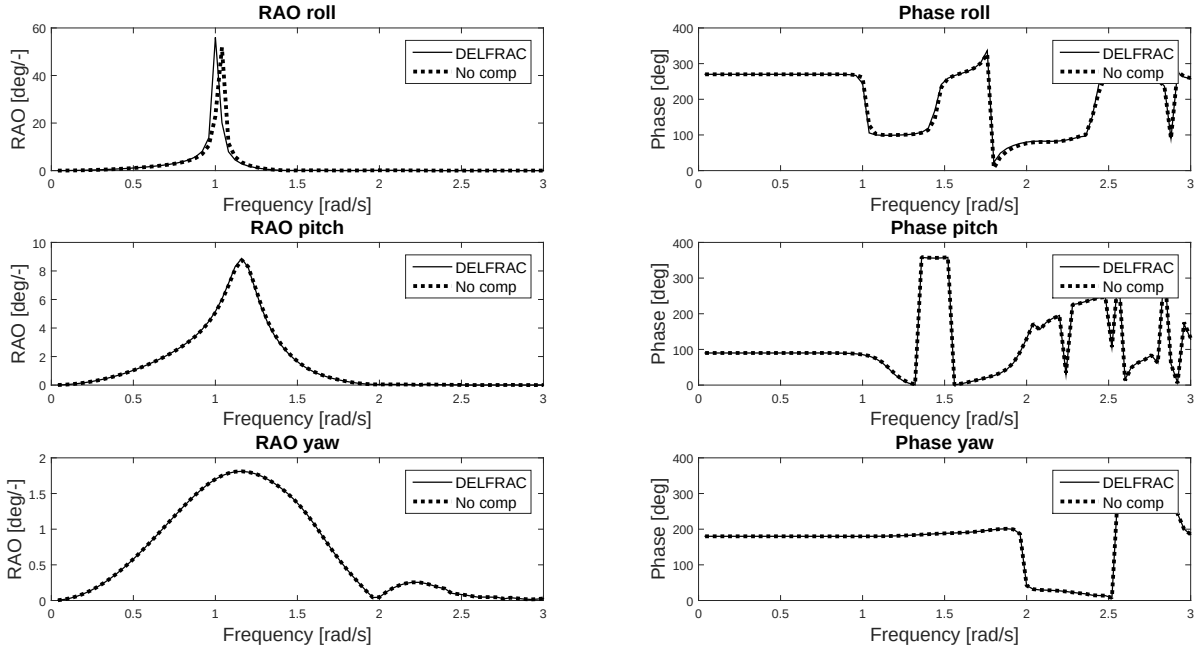

Figure 6-20: Frequency characteristics vessel rotations No compensation and DELFRAC results. $\lambda = 1[-]$, wave incident angle $45[deg]$

Furthermore the TD frequency characteristics are compared to a time trance of the TD motions. This time trace is shown in Figure C-5 in Appendix C. The TD of a compensating Ampelmann system that has no mechanical limitations is kept motionless. The TD frequency characteristics for Perfect compensation are shown in Figure 6-22 and 6-21, all RAO for Perfect compensation are zero. In absence of mechanical limitations of the Ampelmann system the results coincide confirming the validity of the Perfect compensation model.

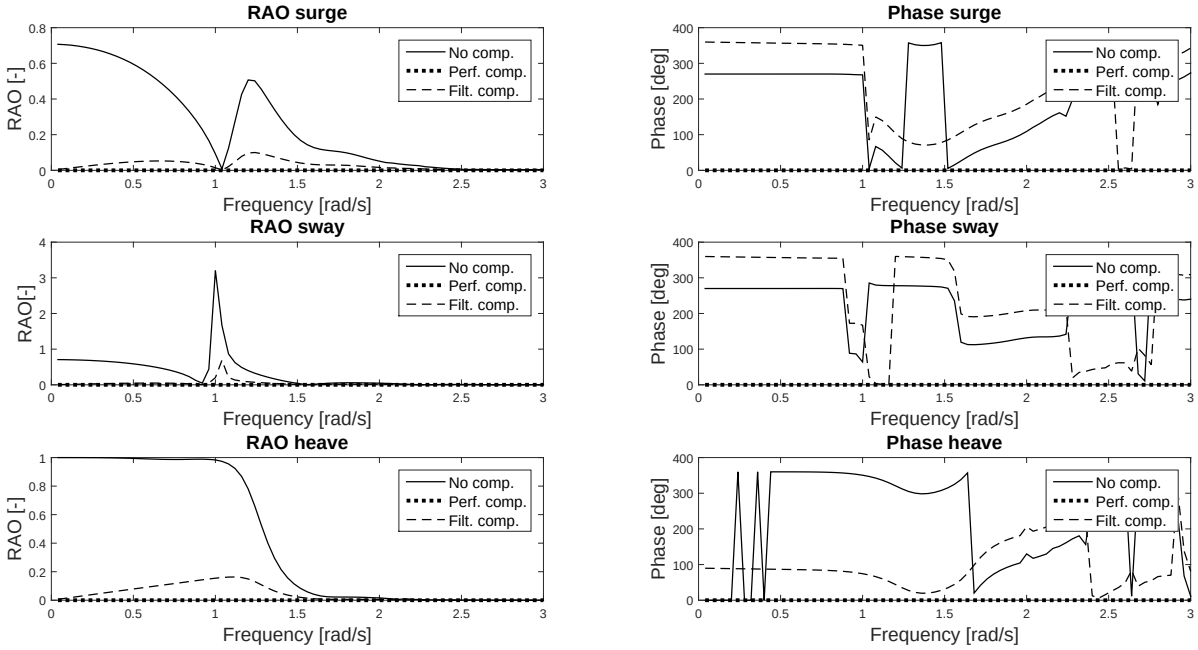

Figure 6-21: TD Frequency characteristics translations. $\lambda = 1[-]$, wave incident angle $45[deg]$.

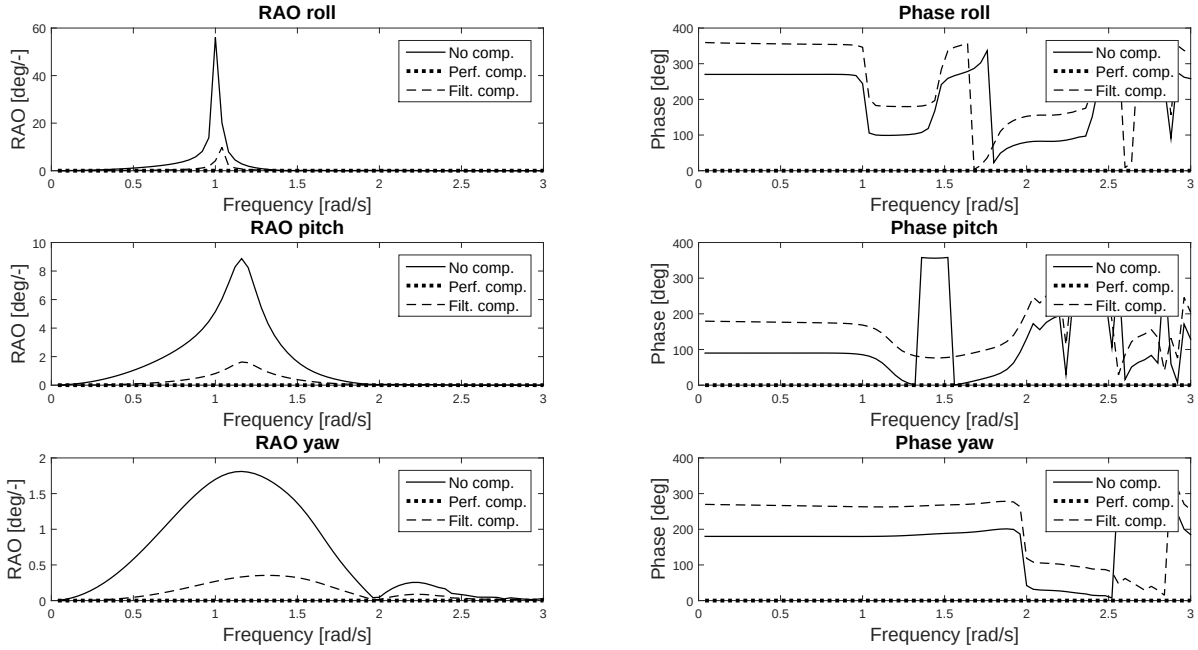

Figure 6-22: TD Frequency characteristics rotations. $\lambda = 1[-]$, wave incident angle $45[deg]$.

6-7-2 6 DOF model verification

The major concepts are discussed in section 5-6 of the previous chapter. The 6 DOF model is extended with the variable L_y and L_y. This section verifies only roll natural frequency shift. For increasing values of L_y and L_z it is observed that the difference in roll natural frequency increases between No compensation and compensation. For increasing values of L_y and L_z the roll natural frequency decreases for No compensation. The natural frequency for Perfect compensation and Filter compensation are both independent of L_y and L_z. Comparing No compensation with compensation, the natural frequency shift increases for larger values of L_y and L_z. The natural frequency shift is verified. Equation 5-34 is extended where L_z is in addition to L_a and L_y adds to the mass moment of inertia of the combined system.

$$\sqrt{\mu_I \mu_c} = \frac{\omega_{n4,comp}}{\omega_{n4,nocomp}} = \sqrt{\frac{c_{44}}{c_{44} - (L_a + L_z)m_2 g} \cdot \frac{I_{xx1} + I_{xx2} + (L_a^2 + L_y^2 + L_z^2)m_2}{I_{xx1}}} \tag{6-23}$$

For $\lambda = 0.65[-]$, $\sqrt{\mu_I \mu_c} = 1.44[-]$. By multiplying the frequency range of the No compensation frequency characteristics with $\sqrt{\mu_I \mu_c}$ and plotting the results in one graph, the natural frequencies for both No compensation and compensation show similar results. This is confirmed by the phase graph where the 90[deg] phase shift for each control system matches. See Figure 6-23. It is confirmed that the natural frequency shift mainly depends on the changing stiffness and mass moment of inertia. Hence Equation 5-35 is applicable.

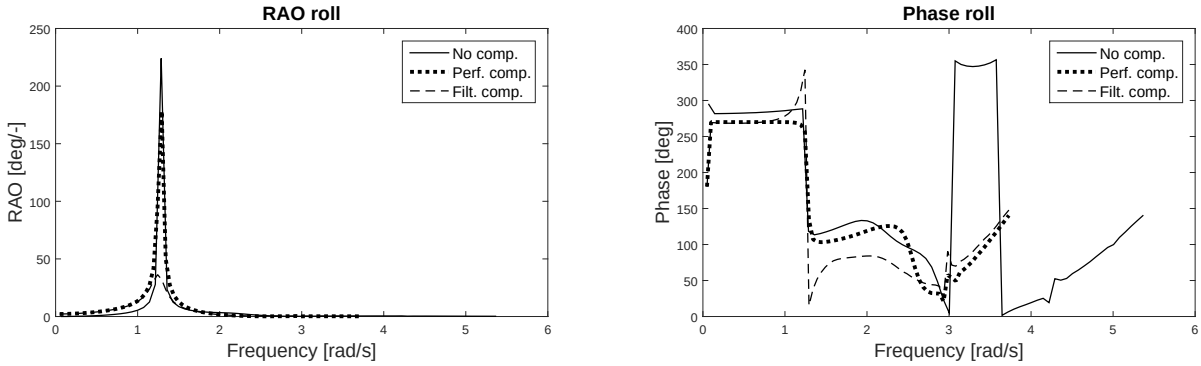

Figure 6-23: Vessel roll frequency characteristics, multiply the frequency of No compensation with $\sqrt{\mu_I} = 1.44[-]$ for $\lambda = 0.65[-]$, $L_y = 4[m]$ and $L_z = 4[m]$.

6-7-3 12 DOF model verification

Verification of the 12 DOF model is performed. The results for No compensation, Perfect compensation, Filter compensation and DELFRAC results are compared. By setting the model input values $m_2 = 0[m]$, $I_{xx2} = 0[kgm^2]$, $I_{yy2} = 0[kgm^2]$, $I_{zz2} = 0[kgm^2]$ for any chosen wave incident angle and $\lambda = 1[-]$ the results are identical. The results are shown in Appendix F, Figure F-17 and F-18.

6-8 Conclusion

Three coupled vessel-Ampelmann models are made. The first model is a 2D 6 DOF model and allows to position the Ampelmann relative to the CoG of the vessel. When translating the Ampelmann horizontally it is assumed that it does not cause a static trim angle to the vessel. Based on the results it is concluded that the dynamic behaviour of the vessel is independent of the location of the Ampelmann system on the vessel. When the Ampelmann is passive and moves with the vessel the dynamic behaviour of the vessel does depend on the position of the Ampelmann system on the vessel. The Ampelmann system may be translated horizontally and/or vertically. A vertical translation of the Ampelmann location causes the largest natural frequency shift when comparing the results between No compensation and compensation. Then the roll natural frequency shift between No compensation and compensation increases. When the Ampelmann is activated on a vessel where the Ampelmann is translated a large distance from the vessel's CoG, the change in dynamic behaviour is greater than when the Ampelman is not translated.

From the results of the 12 DOF models it is concluded that an active Ampelmann system causes vessel surge, sway and roll RAO to increase and it causes the vessels roll natural frequency to shift to a higher frequency. The 12 DOF model including the translation of the Ampelmann location is the final result of this thesis. For a chosen vessel and a specified location of the Ampelmann system on the vessel, it allows to determine the coupled vessel frequency characteristics for a given wave incident angle.

The concept of No sway compensation shows that the vessel motion amplitudes in each DOF are below or equal to the vessel motion amplitudes for Perfect or Filter compensation. The vessel motion amplitudes are selectively reduced by selectively allowing TD motions. It is concluded that the dynamic behaviour of the vessel is positively affected by application of No sway compensation compared to a fully compensated transfer deck.

Chapter 7

Workability study

7-1 Introduction

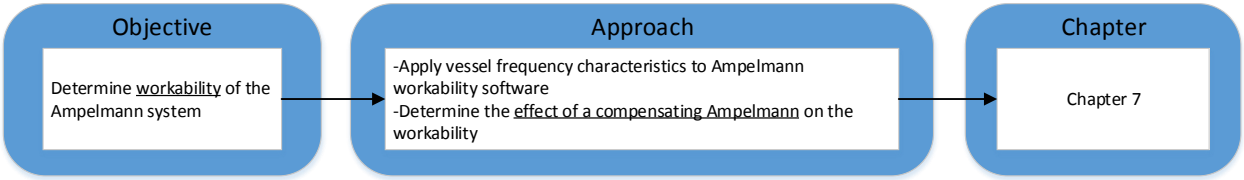

Figure 7-1: Flow chart of the objective and approach of this chapter

This chapters objective is to determine the workability of the Ampelmann system and show the effect of the dynamic interaction between the vessel and the Ampelmann system to the workability. For each control system the frequency characteristics are determined. The vessel frequency characteristics for No compensation represent the frequency characteristics that do not take into account the dynamic interaction between the vessel and the Ampelmann. Normally Ampelmann Operations B.V. performs it workability studies based on frequency characteristics which do not take into account the dynamic interaction between the vessel and the Ampelmann system. The frequency characteristics resulting from Perfect compensation and Filter compensation do take into account the dynamic vessel-Ampelmann interaction. The frequency characteristics for each control system are applied to Ampelmann's workability software G. The results are compared and illustrate how the calculated workability changes when the dynamic interaction between the vessel and the Ampelmann system is taken into account.

The workability calculated for NSC is compared to the workability results of the other three control system. Section 7-2 discusses Ampelmann's workability software. Then in section 7-3 a case study is defined, for which the workability is calculated. Then in section 7-4 for the same case the workability for NSC is calculated and in section 7-5 the results are discussed.

7-2 Ampelmann workability software

Ampelmann Operations B.V. has developed in-house software to calculate the workability of an Ampelmann system on a vessel. Based on the vessel frequency characteristics, a time trace is made of the vessel motions. In assessing the workability it is assumed that the TD is fixed in space. The required corresponding cylinder lengths are calculated. When the maximum cylinder length is exceeded for more than 3% of the time, the situation is marked as not workable. Appendix G, elaborates further on the Ampelmann workability software tool [9] [10] [1].

Vessel motions are a result of the sea state. A sea state is characterised by two parameters. The significant wave height H_s and the zero crossing period T_z. These parameters define the wave spectrum. The shape of a wave spectrum depends on the location on earth. For the north sea a JONSWAP spectrum is applicable, for fully developed seas a Pierson-Moskowitz spectrum [11]. A wave spectrum is a statistical representation for a sea state. The wave spectrum combined with the vessel frequency characteristics gives the vessel response spectrum [3]. A time trace of the vessel motions is made, then the required cylinder lengths are calculated. For each specific H_s, T_z combination the situation is judged to be workable. This calculation is performed for a large set of combinations for H_s and T_z. H_s ranges from 0 up to 8.5 [m] with a chosen step size and T_z ranges from 0 up to 26 [s] with a chosen step size. A typical workability output is shown in Figure 7-2.

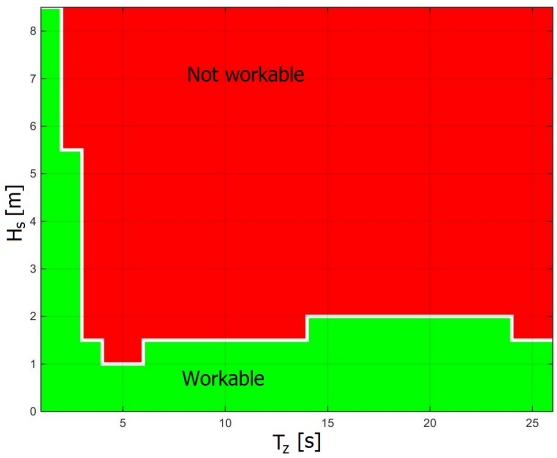

Figure 7-2: Typical output of the workability calculation

The output is applied to a wave scatter diagram. Then the workability is expressed as a percentage. Ampelmann's workability software requires the following input:

- The vessel frequency characteristics for each incoming wave direction
- The location of the Ampelmann on the vessel
- The wave scatter diagram

7-3 Workability results

Workability calculations are based on the frequency characteristics of the vessel. Because of the changing dynamic behaviour of the vessel due to a compensating Ampelmann, the practical workability is lower than the calculated workability. The frequency characteristics, which where put into the workability software, do not take into account the dynamic interaction between the vessel and the Ampelmann system. Therefore vessel frequency characteristics are computed that do take into account the dynamic interaction between the vessel and Ampelmann: Perfect compensation and Filter compensation. The workability results are compared to those of No compensation: the reference case that does not take into account the dynamic interaction between the vessel and the Ampelmann.

The workability results presented in this section are computed for the frequency characteristics of $\lambda = 1[-]$ of the case study. The Ampelmann system is positioned at the CoG of the vessel and a wave incident angle is $90[deg]$. Figure 7-3 shows the workability assessment. The workable area for No compensation is larger than for Perfect compensation and Filter compensation. Figure 7-4 shows the application of the workability assessment to annual wave scatter data from the German Bight. The white line shows the separation line between what is workable and not workable. The back ground colours indicate the probability of occurrence of a certain sea state characterized by a H_s, T_z combination. Lighter colors have a large probability of occurrence the dark color does not occur. The workability is calculated. The frequency characteristics for No compensation result in a workability of 59%. This is higher than the workability resulting from the frequency characteristics of Perfect and Filter compensation: 47% and 49%. Ampelmann Operation B.V. would have calculated a workability of 59%, the practical workability is thus approximately overestimated with 10%.

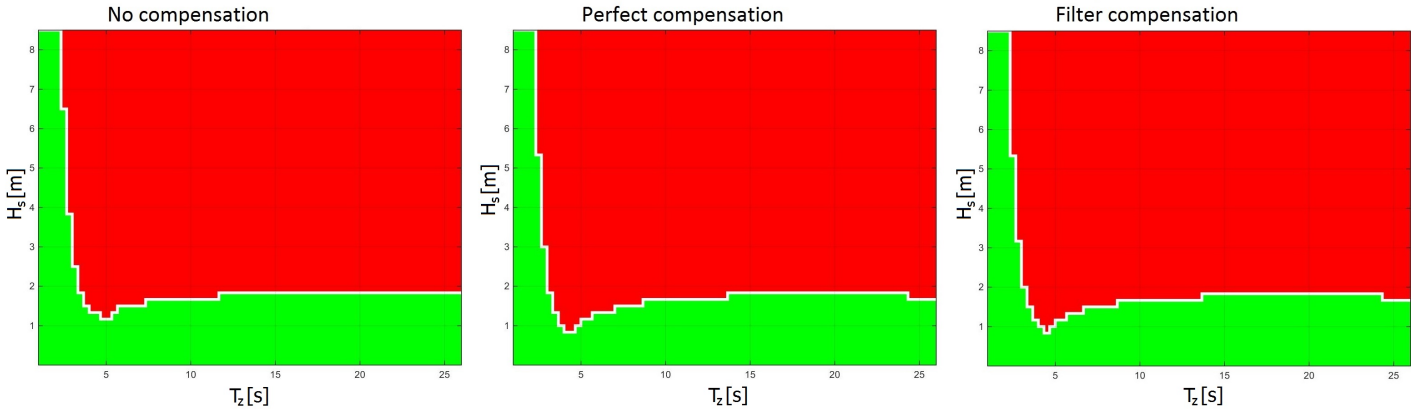

Figure 7-3: Workability JONSWAP spectrum: No compensation, Perfect compensation and Filter compensation

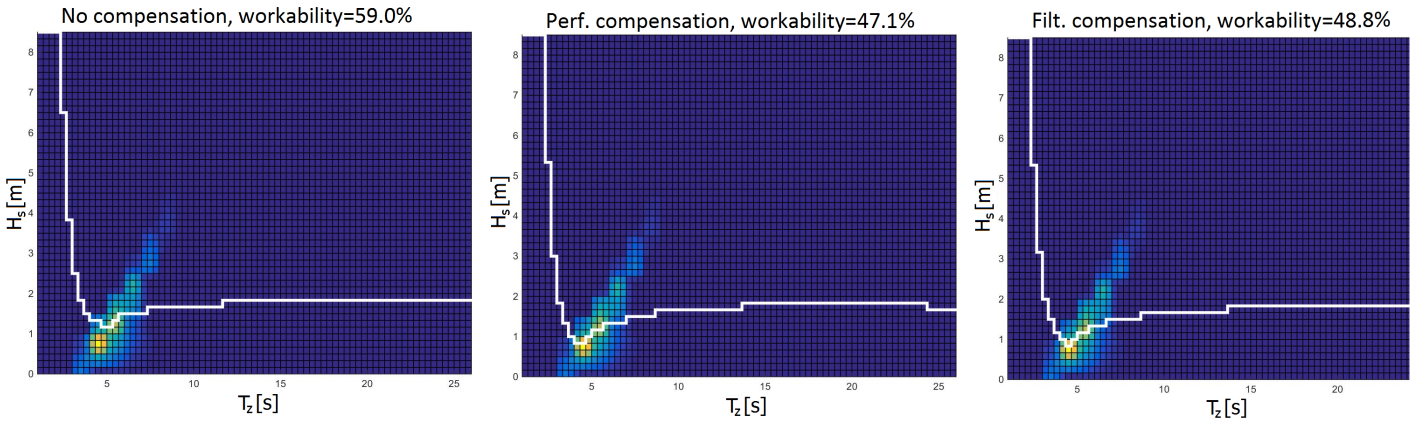

Figure 7-4: Annual workability for the German Bight

7-4 Workability for No sway compensation

Ampelmann workability software calculates vessel motions based on the frequency characteristics of the vessel, then it calculates the required cylinder length for a motionless TD. In NSC this is not the case, the TD is not fixed in space but moves with the vessel in sway, $\hat{Y}_1 = \hat{Y}_2$. Because there is no relative sway, the vessel sway RAO are set to zero for the workability analysis. Sway is not to be compensated, hence no cylinder length is required to compensate sway.

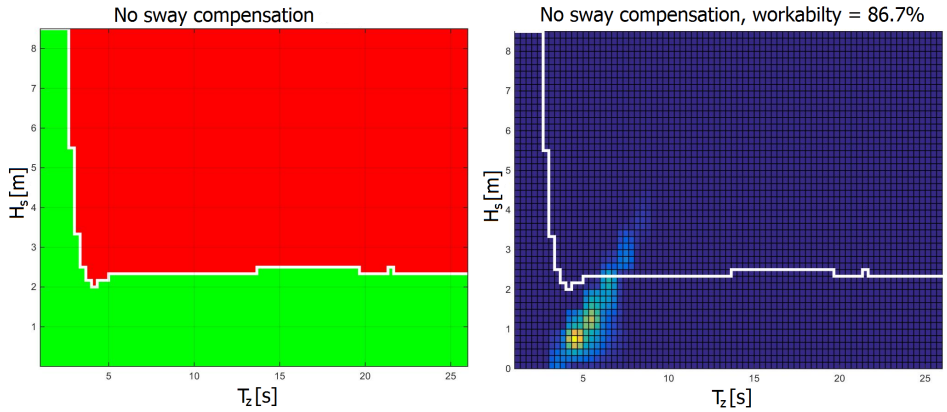

Figure 7-5: NCS annual workability for the German Bight

Figure 7-5 shows the annual workability results for the German Bight. For the whole range of T_z the maximum workable wave height H_s has increased compared to both No compensation and Perfect compensation. The workability is 87%. This result is evaluated in the next section.

7-5 Evaluation of results

By allowing the TD to sway with the vessel: NSC. The calculated workability has significantly increased compared to Perfect and Filter compensation where all 6 DOF are compensated by the Stewart platform. It is concluded that by allowing TD motions, in this case sway, their is more cylinder stroke length available to compensate for other DOF. However NSC is based on the assumption that all residual motions can be compensated by slewing, luffing and telescoping. See Figure 7-6. These capabilities have limitations and shall always stay within the limits stated in Table 7-1. The specified ranges ensure a safe operation.

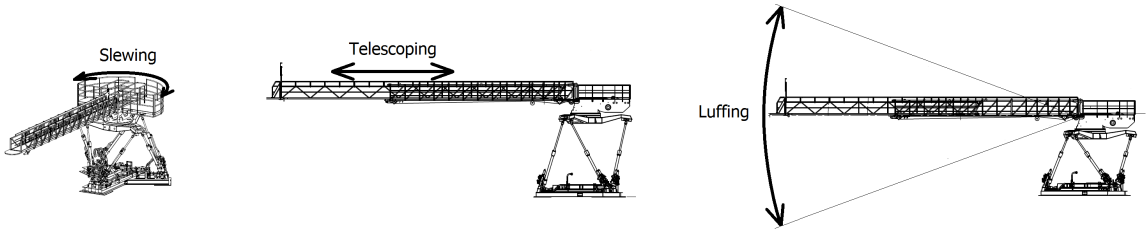

Figure 7-6: DOF of the telescoping access bridge (TAB). Slewing, telescoping and luffing

Table 7-1: Limitations to TAB [12]

	Acceleration	Velocity	Displacement
Slewing	Not available	Not available	± 360 $[deg]$
Telescoping	$\pm$ 0.5 $[m/s^2]$	$\pm$ 0.5 $[m/s]$	17-24 $[m]$
Luffing	$\pm$ 3.7 $[deg/s^2]$	$\pm$ 3.7 $[deg/s]$	$\pm$ 20 $[deg]$

In operation the tip of the gangway is a virtual pivot point, around which the Ampelmann system operates. During crew transfer at all times the tip shall remain at the target position. When introducing TD motions the TAB shall be capable of compensating for these motions. Table 7-2 states the required TAB capabilities that are required in order to compensated for the induced TD motions for any given landing direction.

Table 7-2: Required DOF for the TAB to compensate for induced TD motions, TD roll and pitch can not be compensated by the TAB

	DOF TAB		
TD motion	Slewing	Telescoping	Luffing
Surge	x	x	x
Sway	x	x	x
Heave		x	x
Roll			
Pitch			
Yaw	x		

Roll and pitch can not be taken care of by the three TAB functionalities. A TD yaw motion requires slewing, heave requires telescoping and luffing. Both translations in the horizontal

plane, surge and sway require all 3 TAB functionalities. So when allowing residual TD motions it shall be ensured the TAB is able to compensate these motions.

For the workability calculation of NSC the vessel sway RAO is set to zero because the relative sway displacement between the vessel and the Ampelmann is zero. It is assumed that the TAB takes care of the induced TD sway motions. As an example assume this same concept can be applied to all other TD motions, then the workability is 100% because there is no relative displacement between the vessel and the TD, all RAO are set to zero. The TD moves with the vessel and it is assumed that the TAB takes care of all induced TD motions. Off course this is not a realistic assumption, from a practical point of view the TAB is not designed to compensate for 6 DOF vessel motions. Furthermore all functionalities of the 6 hydraulic cylinder are taken away. The point here is, is that by selectively introducing TD motions and making use of the TAB capabilities a higher workability can be obtained. Hereby to Stewart platform and the TAB shall work together to ensure a safe operation. This is illustrated in Figure 7-7. Now an Ampelmann system compensates for all vessel motions and the TD is motionless.

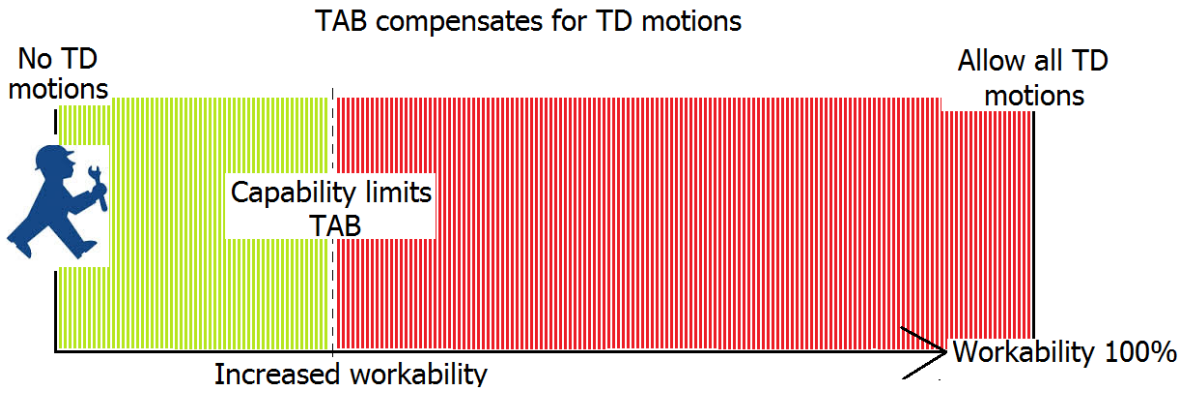

Figure 7-7: The workability of the Ampelmann can be increased by making use of TAB capabilities

7-5-1 Effect of telescoping in No sway compensation

The concept of NSC is based on the assumption that all residual motions are compensated by the TAB, therein the TAB does not cause any induced forces and moments. In case the gangway is pointing in sway direction, the gangway requires to telescope in and out to keep contact with the target platform. See figure 7-8 both full sway compensation and NSC are illustrated, in NSC the gangway slides in and out to compensate sway. With sway compensation the moment working on the TD due to the gangway is constant since the gangway length does not vary. In NSC the moment working on the TD due to gangway varies due to the telescoping of the gangway.

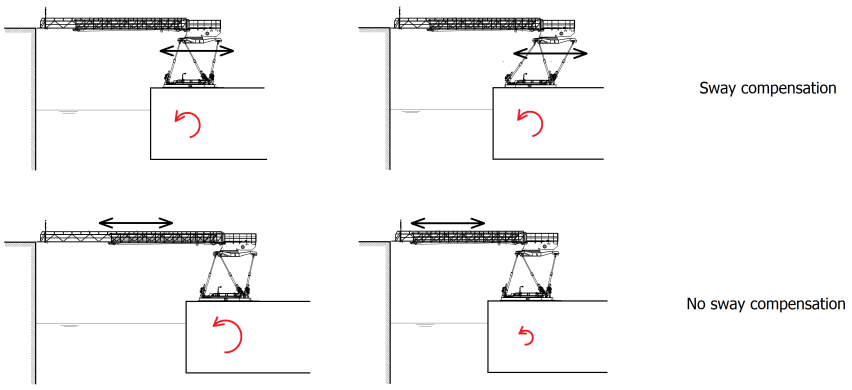

Figure 7-8: Telescoping of gangway during NSC.

During operation the T-boom, the gangway part which slides in and out, is fixed in space. It stays connected to its target position. From the basis of design of an Ampelmann A-type with gangway XL [6], the T-boom is 10% of the weight of the total TD assembly. The total mass that moves with the vessel in NSC is reduces with 10% of the total TD mass. In future analysis this effect shall be taken into account, in this thesis this effect is neglected.

7-6 Conclusion

The frequency characteristics are determined for three control systems, No compensation, Perfect compensation and Filter compensation. The frequency characteristics show amplified vessel motions when the Ampelmann is compensating. It is concluded that a compensating Amplemann system reduces the workability.

Ampelmann's compensation philosophy is based on a motionless TD, from which crew transfers take place. However, a fully compensated TD causes vessel motions to amplify reducing the workability of the system. By allowing selective TD motions, which shall be compensated by the TAB, the workability is significantly increased. The concept of No sway compensation is introduced. More favourable vessel motions are accomplished and more cylinder stroke length is available to compensate other DOF.

Chapter 8

Conclusion

This chapter concludes this thesis, first the conclusions for this thesis are discussed in section 8-1. Then in section 8-2 recommendations are made for improvements to the model and future research topics are stated.

8-1 Conclusions

The dynamic behaviour of a coupled vessel-Ampelmann system is applied to workability studies, the research objective for this thesis is achieved. A linear frequency domain model of a coupled vessel-Ampelmann system is made. Vessel frequency characteristics are calculated that take into account the dynamic interaction between the vessel and the Ampelmann system. The model requires four input variables, these are: The hydromechanic properties for a chosen vessel, the vessel and the Ampelmann mass properties, the location of the Ampelmann on the vessel and the control system. Based on these input variables the coupled vessel frequency characteristics are calculated. The frequency characteristics are input to the workability analysis. The workability results show that the calculated workability based on vessel frequency characteristics that take into account the dynamic interaction is lower than when not taking into account the dynamic interaction. It is concluded that due to the dynamic interaction between the vessel and the Ampelmann system the workability is reduced.

The model confirms the observation, vessel motions amplify and the vessel's roll natural frequency changes when the Ampelmann system is activated. It is concluded that an active Ampelmann causes amplified surge, sway and roll motions and causes a vessels roll natural frequency shift to a higher frequency. The vessel dynamics for an active Ampelmann system are independent of the location of the Ampelmann on the vessel. However, the dynamic vessel behaviour for a passive Ampelmann system does depend on the location of the Ampelmann on the vessel. For a larger translations of the Ampelmann location with respect to the vessel's CoG, the change in dynamic behaviour increases when the Ampelmann is activated.

The dynamic behaviour of the vessel is determined by the control system that controls the motions of the transfer deck relative to the vessel. Three control systems are applied to the model: 1) No compensation, representing a passive Ampelmann on a vessel. 2) Perfect compensation, an active Ampelmann system where the transfer deck is kept motionless. 3) Filter compensation, an active Ampelmann system where residual motions are introduced to the transfer deck. For an Ampelmann system positioned at the CoG of the vessel Perfect compensation and Filter compensation show similar results, it is concluded that residual motions resulting from the application of a second order low pass filter to the control signal are not the source for amplified vessel motions in a frequency domain analysis. The major factor causing amplified roll motions is due to the static weight of the transfer deck that causes a roll moment to the vessel as a result of a relative sway displacement of the vessel. Surge and sway motions are amplified because in compensation the transfer deck mass is excluded from surge and sway motions. then only the vessel mass is excited and the wave forces remain unchanged.

No sway compensation is new proposed compensation method. A fully compensated transfer deck causes vessel motions to amplify reducing the workability of the system. By selectively allowing TD motions, which shall be compensated by the TAB the workability is significantly increased. Vessel motions are not amplified and more cylinder stroke length of the Stewart platform is available to compensate for other DOF. This is achieved by making active use of the TAB capabilities in combination with the Stewart platform.

8-2 Recommendations

Ampelmannn Operations B.V. performs its workability studies based on the vessel frequency characteristics. These frequency characteristics do not take into account the dynamic interaction between the vessel and the Ampelmann system. In this thesis a method is presented to calculate the vessel frequency characteristics that takes into account the dynamic interaction between the vessel and the Ampelmann system. Based on these calculated coupled frequency characteristics a better estimation is made of the practical workability. A 12 DOF model is made that gives insight into the dynamic interaction between the vessel and the Ampelmann system. In this section recommendations are made for possible model improvements and a number of future research topics are proposed that follow from this thesis.

For the practical application of the coupled vessel-Ampelmann model, Ampelmann Operations B.V. should ask its clients for hydromechanic vessel properties of the vessel in addition to the frequency characteristics on which normally the workability study is based. Only then the coupled frequency characteristics are calculated.

8-2-1 Model improvements

Below three items are stated for improvements to the coupled vessel-Ampelmann model:

- *Viscous damping*: The vessel hydromechanic properties are determined based on potential theory, this does not take into account viscosity. When including viscosity damping

is added. For vessel motions with large velocity amplitudes viscous effect play a significant role.

- *First order motions*: The models discussed in this thesis are based on linear theory, only first order motions are included. Second order motions and non-linearities in the control system are excluded. To include discontinuities to the control system a time domain model is required, this is discussed in section 8-2-2.

- *External loads to the coupled vessel-Ampelmann system*: The external loading to the coupled vessel-Ampelmann model is limited to the wave forces only and it is assumed that the mass of the transfer deck is centred on the Stewart platform. To make a better reality representative model other external forces should also be included.

8-2-2 Future research

The motivation for this research is based on observations. Preferably to confirm the validity of the models, practical data should be obtained and compared to the model results. Practical data gives a qualitative understanding of how the dynamic behaviour of the vessel changes when the Ampelmann is activated. Insight is gained into what factors are determining for exceeding the workability limits of the Ampelmann system. Logging vessel motions may be performed by the Octans motions sensor of the Ampelmann system. This section states all future research topic that follow from this thesis.

- *Obtain hydromechanic vessel properties*: Ampelmann Operation B.V. performs a workability analysis for its clients. This analysis is based on the vessel's frequency characteristics. These should be supplied by the client. In some cases these are not available and Ampelmann Operations B.V. is still asked to estimate the workability. The hydromechanic properties or the frequency characteristics shall be determined. Two methods are proposed:

  1. By applying scaling laws as discussed in Appendix B, the unknown vessel parameter for a certain vessel can be determined from a vessel for which these are known. The two vessel shall fulfil the condition of geometric similitude. Theoretically this method is completely correct. For applications of scaling in practice, one should take care that it is likely to use this method for vessel which do not fulfil the condition of geometric similitude but look similar. The limitations shall be known concerning the validity of applying scaling laws to vessels which do not apply to the conditions of geometric similitude. It shall be investigated how the hydromechanic properties change depending on the hull shape.
  2. Ampelmann Operation B.V. should invest in hydromechanic software to determine the hydromechanic properties for a specified hull shape.

- *Time domain model*: A time domain analysis allows to incorporate the complete Ampelmann control system to the coupled vessel-Ampelmann system. Then the EOM shall be extended with the retardation function, which includes all fluid memory effects of the water surrounding the vessel. A time domain model allows to study:

1. The effect of mechanical limitations, non-linearities and discontinuities of the Ampelmann system to the dynamic behaviour of the vessel.
2. The dynamic behaviour of the coupled vessel-Ampelmann system for non-harmonic loading conditions.
3. Define a stability criteria for when the coupled vessel-Ampelmann system becomes self exciting as witnessed during the first scaled model tests as discussed in section 1-2.

- *Rules of thumb for changing dynamic vessel behaviour*: In this thesis it is verified how the sway and surge motion amplitudes increase based on the relative mass of the vessel and the TD. It is also verified and how the roll natural frequency shift depends on the relative mass moment of inertia and the vessel roll stiffness. It shall be investigated if these rules of thumb can be generalized for the application to different vessels.

- *Reduce TD mass*: The changing dynamic behaviour of the vessel largely depends on the mass of TD. Reducing the TD mass, the mass which suspended by the 6 hydraulic cylinders of the Stewart platform, reduces the dynamic interaction between the vessel and the Ampelmann system. Especially for the application of Ampelmann system on smaller vessel this becomes advantageous.

- *Implementation of No sway compensation*: In order to make a significant increase to the workability, it is argued that by selectively introducing TD motions in sway direction, the working range of the Stewart platform is extended and vessel sway and roll motions do not amplify. The introduced residual TD motions shall be compensated by the TAB. The implementation of the concept of No sway compensation shall be tested in practice. Then the control system should be designed such that the Stewart platform and the TAB work together in order to optimize for the workability. At all times crew safety shall be taken into account.

  The concept of NSC is contrary to the trade mark of Ampelmann Operations B.V., which is a 6 DOF motion compensated transfer deck. From a commercial point of view Ampelmann systems are the business standard for safe and easy crew transfers, but with the growing market for offshore compensating systems the competition is also growing. The patent of Ampelmann Operations B.V. [1] limits the competitors to design offshore access systems that compensate 6 DOF by use of 6 hydraulic cylinders. Competitors design systems that partially compensate vessel motions and allow transfer deck motions. This thesis shows that partial compensation is advantageous in terms of workability and vessel motions. From the perspective of Ampelmann Operations B.V. it is important to know what the capabilities of the Ampelmann systems are and how these can be optimized to future market demands.

Appendix A

Ampelmann terminology

This appendix contains the Terminology used within Ampelmann Operations: See page 90.

Ampelmann Terms
L-Type A-Type E-Type
AMPELMANN
Add-ons
Ship to ship
V-Shape
KIB
Slideway
Butler
T-Boom
Telescoping part of gangway
Main Boom
Part of boom attached to transfer deck, holds T-Boom
Transfer deck
Waiting area for transferring crew
Luffing cylinder
Provides vertical movement of gangway
Operator 1
Makes sure people transfer safely
Base frame
Connects slewing ring to transfer deck, holds drives and provides counter weight
Slewing ring
Provides rotating movement
Hydraulic cylinders
Compensate vessel movements
Mercedes frame
Connects hydraulic cylinders to slewing ring
Nitrogen set + PTA
Back up system to maintain oil pressure in case of double HPU failure
Control cabinets
Encloses electronics to perform motion compensation
Scoop
Presses against platform or other vessel
Boom tip
End of gangway, provides step to other platform
Operator 2
Oversees operations and operates HPU
Bottom frame
Connects Ampelmann to vessel
Gimbals
Pivot point for cylinders
37 m
10,8 m
6,6 m
3,8 m
CTS
L-type
A-Type + Gangway XL
E-Type + Gangway XL
E-Type + CTS
Gangway
Hexapod

Appendix B

Vessel parameters

This Appendix discusses how an DELFRAC input file is obtained and elaborates on the chosen barge from chapter 3. It validates, 1. the calculation method to get from vessel parameters to frequency characteristics. And 2. the scaling laws for scaling vessel parameters.

B-1 DELFRAC input

The DELFRAC input file requires the mass matrix of the vessel. From the underwater hull geometry a panel model is made. Section B-1-1 calculates the mass matrix for the chosen barge. Section B-1-2 discusses how a DELFRAC input file is made.

B-1-1 Mass matrix

The simplified hull shape representing a small vessel is chosen. A barge with:

- Length: L=34[m]
- Beam: B=12[m]
- Depth: D=6[m]
- Draft: T=3[m]

The mass matrix is determined as if it is a homogeneous solid body with the CoG centred. The mass matrix includes the mass of the vessel and the static mass of the TD.

$$\begin{bmatrix} m_v & 0 & 0 & 0 & 0 & 0 \\ 0 & m_v & 0 & 0 & 0 & 0 \\ 0 & 0 & m_v & 0 & 0 & 0 \\ 0 & 0 & 0 & I_{xx1} & 0 & 0 \\ 0 & 0 & 0 & 0 & I_{yy1} & 0 \\ 0 & 0 & 0 & 0 & 0 & I_{zz1} \end{bmatrix} = 10^6 \begin{bmatrix} 1.254 & 0 & 0 & 0 & 0 & 0 \\ 0 & 1.254 & 0 & 0 & 0 & 0 \\ 0 & 0 & 1.254 & 0 & 0 & 0 \\ 0 & 0 & 0 & 18.82 & 0 & 0 \\ 0 & 0 & 0 & 0 & 124.6 & 0 \\ 0 & 0 & 0 & 0 & 0 & 135.9 \end{bmatrix} \tag{B-1}$$

With:

$$\nabla = L * B * T = 1224[m^3] \tag{B-2}$$

$$\rho = 1025[m^3] \tag{B-3}$$

$$m = \nabla\rho = 1.255 \cdot 10^6[kg] \tag{B-4}$$

$$I_{xx} = \frac{1}{12}m_v(B^2 + D^2) = 18.82 \cdot 10^6[kgm^2] \tag{B-5}$$

$$I_{yy} = \frac{1}{12}m_v(L^2 + D^2) = 124.6 \cdot 10^6[kgm^2] \tag{B-6}$$

$$I_{zz} = \frac{1}{12}m_v(L^2 + B^2) = 135.9 \cdot 10^6[kgm^2] \tag{B-7}$$

B-1-2 DELFRAC input files

DELFRAC requires a specific input file format. A .DAT file shall be made in the format shown below on next page. Also a matching example is given.

Input file structure for DELFRAC

TITLE 1	
XORIG, YORIG, HEAD	*#dummy values*
INV, INF, ISW, PANFAC	*#number of points, number of panels, symmetry code, integration code*
INOM	*#number of frequencies*
(OMEGA(I), I = 1,INOM **)**	*#frequencies*
IDIR	*#number of wave directions*
(WDIR(I), I = 1,IDIR)	*#wave directions*
WD	*#waterdepth [m], -1 = infinite*
ZG	*#z co-ordinate COG*
RHO, GRAV	*#water density, gravity acceleration*
LENGTH	*#dummy*
DO I=1,6	
(**KXX(J),** J=1,6)	*#mass moment of inertia radii*
END DO	
DO I=1,INV	
I, (**X(I,J),** J=1,3)	*#point number, x-co-ordinate, y-co-ordinate, z-co-ordinate*
END DO	
DO I=1,INF	
I, (**IFAC(I,J),** J=1,4)	*#panel number, no. of first, second, third and fourth corner point*
END DO	
INW, INE, LENFAC	*#nr of waterline vertices, nr of waterline elements, panel integration number (for non-linear drift force calculations)*
DO I=1,INW	
I, XW(I,1), XW(I,2)	*#no. of waterline vertice, x-co-ordinate, y-co-ordinate*
END DO	
DO I=1,INE	
I, ILEN(I,1), ILEN(I,2)	*#no. of waterline element, first w.l. point, second w.l. point*
END DO	
IRP	*#nr. of reference points*
DO I=1,IRP	
I, (**XRP(I,J),** J=1,3)	*#no. of reference point, x-co-ordinate, y-co-ordinate, z-co-ordinate*
END DO	
NPRP	*#nr. of panels for pressure output*
(PRP(I), I=1,NPRP)	*#panel numbers for pressure output.*

```
Thesis <student>: <title>
 0.0       0.0         0.0
1314    1336     4    4
50
 0.040 0.080 0.120 0.160 0.200 0.240 0.280 0.320 0.360 0.400 0.440 0.480 0.520 0.560 0.600 0.640 0.680 0.720 0.760 0.800 0.840
0.880 0.920 0.960 1.000 1.040 1.080 1.120 1.160 1.200 1.240 1.280 1.320 1.360 1.400 1.440 1.480 1.520 1.560 1.600 1.640 1.680
1.720 1.760 1.800 1.840 1.880 1.920 1.960 2.000
13
   0.00
  15.00
  30.00
  45.00
  60.00
  75.00
  90.00
 105.00
 120.00
 135.00
 150.00
 165.00
 180.00
500
2.62
1025.000    9.807
102.75
1.0   0.0   0.0   0.0   0.0   0.0
0.0   1.0   0.0   0.0   0.0   0.0
0.0   0.0   1.0   0.0   0.0   0.0
0.0   0.0   0.0  29.4   0.0   0.0
0.0   0.0   0.0   0.0  29.5   0.0
0.0   0.0   0.0   0.0   0.0  33.2
   1   34.700      31.896     -10.154
   2   34.700      32.848     -11.106
   3   34.700      34.433      -9.519
...
 1313   48.343      25.954      -8.250
 1314   49.859      25.954      -8.250
  1       1      2      3      3
  2       4      5      2      2
  3       3      2      5      5
...
1335      395    1314     449     393
1336      446     447    1311    1310
 40  40    4
  1      34.700     19.850
  2      34.700     21.340
...
 39      31.720     19.850
 40      33.210     19.850
  1     1      2
  2     2      3
  3     3      4
...
 39     39     40
 40     40      1
 0
 0
```

The mass matrix derived in section B-1-1 is put into the .DAT files as the normalized mass matrix. The mass is normalized to, 1 [-]. The mass moments of inertia are put in as the inertia radius normalized according to:

$$m_1 r^2 = 1 \tag{B-8}$$

Where m_v is the mass of the vessel and r the inertia radius.

B-2 Validation for calculating frequency characteristics

DELFRAC output comprises, the vessel parameters and the frequency characteristics. This section shows that the method used to calculated frequency characteristics from the vessel parameters is correct. This is done by taking the vessel parameters, substituting these into the EOM. And solving the EOM. DELFRAC data is obtained for wave incident angles ranging from 0[deg] to 180[deg] with steps of 15[deg]. For all wave incident angles the results match, only the results are given for a wave incident angle of μ =45[deg]. The results are shown in Figure B-1 and B-2 on page 95 and 96. Each plot show two data ranges: the first are the black dots, which are the calculated RAOs. The second is the solid line: the data generated by DELFRAC.

Figure B-1: RAOs and phase for all translations, wave incident angle μ=45[deg]

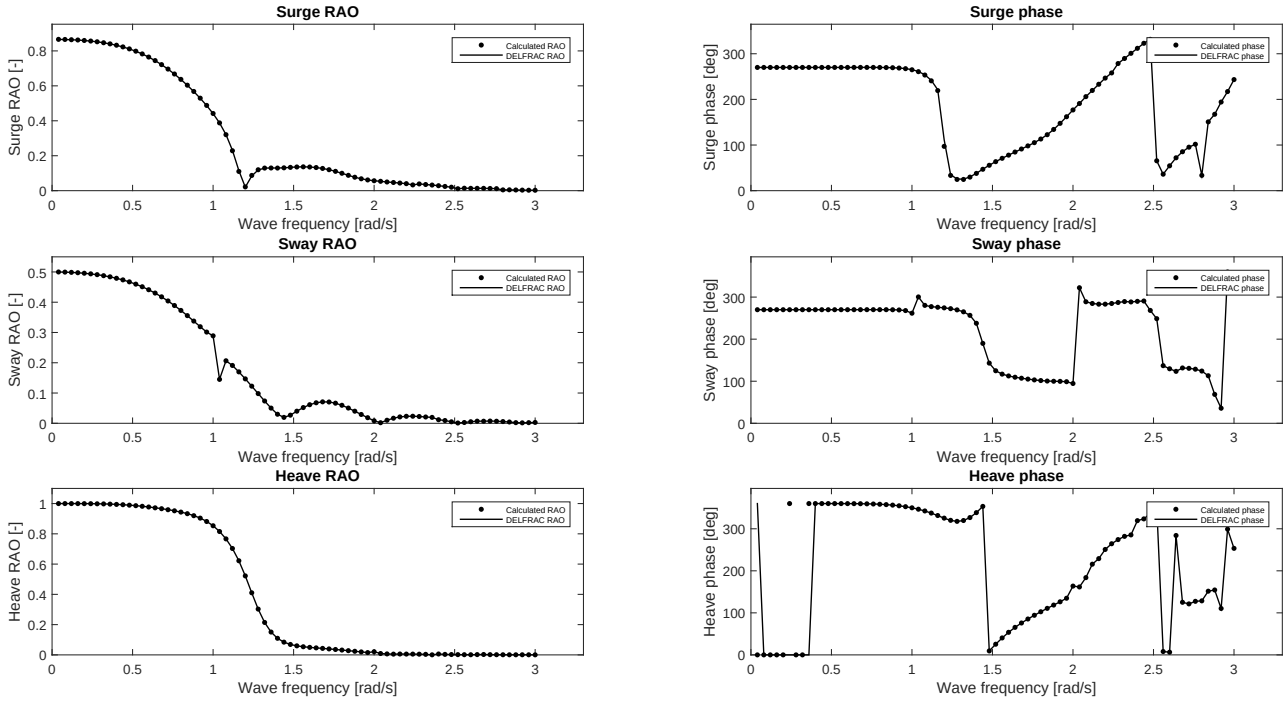

Figure B-2: RAOs and phase for all rotations, wave incident angle μ=45[deg]

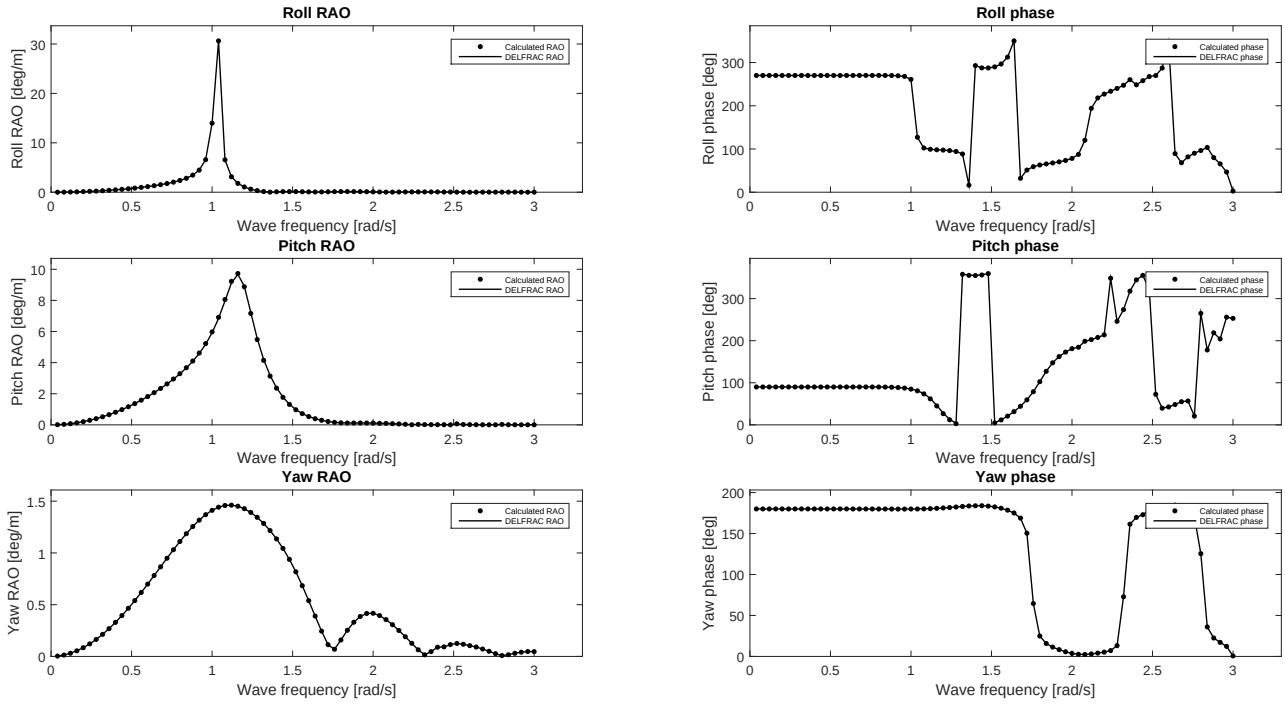

It can be seen that all calculated RAOs and phases coincide with the by DELFRAC generated RAOs and phases. This confirms the calculation method used to generate RAOs. Note that in the heave phase plot there are a few points that do not coincide: a phase of 0[deg] equals a phase of 360[deg] this still confirms the results. Two remarks on the results:

- The roll RAO goes up to approximately 50[deg/m] this is an unrealistically high value, this can by explained by the significance of viscous damping, only potential damping is taken into account. [3].
- When RAOs tends to zero, the phases tend to get a random character.

Figure B-1 and B-2 are computed for a wave incident angle of μ=45[deg], for all wave incident angles the results match. This confirms the calculation method for calculating frequency characteristics from vessel parameters.

B-3 Scaling vessel parameters

Calculating frequency characteristics, RAOs and phases, of a vessel requires hydromechanic data. Obtaining hydromechanic data is a time consuming process. When for a certain vessel class the hydromechanic properties are known, this data can be scaled with scaling laws. Scaling vessel data allows to analyse the dynamic behaviour of a smaller or larger vessel of the same class. The scaled version of the original vessel requires geometric similitude, only then linear hydromechanic properties may be scaled. This chapter discusses the scaling laws required to scale hydromechanic data. First the scaling laws as result of geometric similitude are discussed. Second the scaling laws are applied to the hydromechanic data.

B-3-1 Scaling laws

Hydromechanic data is obtained for a chosen vessel. Wave forces are determined for waves of 1 [m] amplitude. With the EOM of the vessel the vessel frequency characteristics are calculated. Geometric scaling is usually applied in model testing. Here all units including the vessel dimensions, the wave amplitude and time are scaled. In this case it is desired to only scale vessel parameters and hydromechanic properties. But to keep the wave amplitude, the water density and the gravitational acceleration constant. Dimensions scale with scaling factor λ. All dimensions in meter change as such: $m \rightarrow \lambda m$. A meter, m, becomes λm . Gravity scales with 1, this can only be compromised when time, s, scales as: $s \rightarrow \sqrt{\lambda}s$. A unity check confirms this scaling law: $\frac{m}{s^2} \rightarrow \frac{\lambda m}{(\sqrt{\lambda}s)^2} = \frac{m}{s^2}$. Table B-1 on page 97, summarizes the scaling factors for geometric similitude for constant gravity and water density.

Table B-1: Scaling factors

	Units	Scaling factor
Length	m	λ
Velocity	m/s	$\sqrt{\lambda}$
Acceleration	m/s^2	1
Time	s	$\sqrt{\lambda}$
Density	$\frac{kg}{m^3}$	1
Mass	kg	λ^3
Force	$\frac{kgm}{s^2}$	λ^3
Moment	$\frac{kgm^2}{s^2}$	λ^4

B-3-2 Scaling hydromechanic data

Scaling hydromechanic data allows us to scale a vessel. And in the same time keep the sea state unchanged. All terms in the EOM change due to scaling. The 6 DOF equation of motion contains 7 terms: the frequency, the mass term, the added mass term, the damping term, the restoring term, the complex vessel motions and the complex wave force. The EOM of the vessel is written in Equation B-9.

$$\{-\omega^2[\mathbf{M}+\mathbf{A}(\omega)]+[i\omega\mathbf{B}(\omega)]+[\mathbf{C}]\}\hat{X}_a=\hat{F}_a \tag{B-9}$$

Depending on the unit of each term, each term is scaled according to the scaling laws discussed previous. Frequency scales with time:

$$\omega \rightarrow \frac{1}{\sqrt{\lambda}}\omega \tag{B-10}$$

The vessel mass matrix scales as:

$$\mathbf{M} \rightarrow \begin{bmatrix} \lambda^3 m & 0 & 0 & 0 & 0 & 0 \\ 0 & \lambda^3 m & 0 & 0 & 0 & 0 \\ 0 & 0 & \lambda^3 m & 0 & 0 & 0 \\ 0 & 0 & 0 & \lambda^4 I_{xx} & 0 & 0 \\ 0 & 0 & 0 & 0 & \lambda^4 I_{yy} & 0 \\ 0 & 0 & 0 & 0 & 0 & \lambda^4 I_{zz} \end{bmatrix} \tag{B-11}$$

Added mass $\mathbf{A}(\omega)$ depends on the scaled frequency. And is independent of wave incident angle:

$$\mathbf{A}(\omega) \rightarrow \begin{bmatrix} \lambda^3 a_{11} & \lambda^3 a_{12} & \lambda^3 a_{13} & \lambda^4 a_{14} & \lambda^4 a_{15} & \lambda^4 a_{16} \\ \lambda^3 a_{21} & \lambda^3 a_{22} & \lambda^3 a_{23} & \lambda^4 a_{24} & \lambda^4 a_{25} & \lambda^4 a_{26} \\ \lambda^3 a_{31} & \lambda^3 a_{32} & \lambda^3 a_{33} & \lambda^4 a_{34} & \lambda^4 a_{35} & \lambda^4 a_{36} \\ \lambda^4 a_{41} & \lambda^4 a_{42} & \lambda^4 a_{43} & \lambda^5 a_{44} & \lambda^5 a_{45} & \lambda^5 a_{46} \\ \lambda^4 a_{51} & \lambda^4 a_{52} & \lambda^4 a_{53} & \lambda^5 a_{54} & \lambda^5 a_{55} & \lambda^5 a_{56} \\ \lambda^4 a_{61} & \lambda^4 a_{62} & \lambda^4 a_{63} & \lambda^5 a_{64} & \lambda^5 a_{65} & \lambda^5 a_{66} \end{bmatrix}(\omega) \tag{B-12}$$

Damping depends on the scaled frequency. And is independent of the wave incident angle:

$$\mathbf{B}(\omega) \rightarrow \begin{bmatrix} \frac{\lambda^3}{\sqrt{\lambda}} b_{11} & \frac{\lambda^3}{\sqrt{\lambda}} b_{12} & \frac{\lambda^3}{\sqrt{\lambda}} b_{13} & \frac{\lambda^4}{\sqrt{\lambda}} b_{14} & \frac{\lambda^4}{\sqrt{\lambda}} b_{15} & \frac{\lambda^4}{\sqrt{\lambda}} b_{16} \\ \frac{\lambda^3}{\sqrt{\lambda}} b_{21} & \frac{\lambda^3}{\sqrt{\lambda}} b_{22} & \frac{\lambda^3}{\sqrt{\lambda}} b_{23} & \frac{\lambda^4}{\sqrt{\lambda}} b_{24} & \frac{\lambda^4}{\sqrt{\lambda}} b_{25} & \frac{\lambda^4}{\sqrt{\lambda}} b_{26} \\ \frac{\lambda^3}{\sqrt{\lambda}} b_{31} & \frac{\lambda^3}{\sqrt{\lambda}} b_{32} & \frac{\lambda^3}{\sqrt{\lambda}} b_{33} & \frac{\lambda^4}{\sqrt{\lambda}} b_{34} & \frac{\lambda^4}{\sqrt{\lambda}} b_{35} & \frac{\lambda^4}{\sqrt{\lambda}} b_{36} \\ \frac{\lambda^4}{\sqrt{\lambda}} b_{41} & \frac{\lambda^4}{\sqrt{\lambda}} b_{42} & \frac{\lambda^4}{\sqrt{\lambda}} b_{43} & \frac{\lambda^5}{\sqrt{\lambda}} b_{44} & \frac{\lambda^5}{\sqrt{\lambda}} b_{45} & \frac{\lambda^5}{\sqrt{\lambda}} b_{46} \\ \frac{\lambda^4}{\sqrt{\lambda}} b_{51} & \frac{\lambda^4}{\sqrt{\lambda}} b_{52} & \frac{\lambda^4}{\sqrt{\lambda}} b_{53} & \frac{\lambda^5}{\sqrt{\lambda}} b_{54} & \frac{\lambda^5}{\sqrt{\lambda}} b_{55} & \frac{\lambda^5}{\sqrt{\lambda}} b_{56} \\ \frac{\lambda^4}{\sqrt{\lambda}} b_{61} & \frac{\lambda^4}{\sqrt{\lambda}} b_{62} & \frac{\lambda^4}{\sqrt{\lambda}} b_{63} & \frac{\lambda^5}{\sqrt{\lambda}} b_{64} & \frac{\lambda^5}{\sqrt{\lambda}} b_{65} & \frac{\lambda^5}{\sqrt{\lambda}} b_{66} \end{bmatrix}(\omega) \tag{B-13}$$

The restoring force is independent of frequency. And independent of wave incident angle:

$$\mathbf{C} \rightarrow \begin{bmatrix} \lambda^2 c_{11} & \lambda^2 c_{12} & \lambda^2 c_{13} & \lambda^3 c_{14} & \lambda^3 c_{15} & \lambda^3 c_{16} \\ \lambda^2 c_{21} & \lambda^2 c_{22} & \lambda^2 c_{23} & \lambda^3 c_{24} & \lambda^3 c_{25} & \lambda^3 c_{26} \\ \lambda^2 c_{31} & \lambda^2 c_{32} & \lambda^2 c_{33} & \lambda^3 c_{34} & \lambda^3 c_{35} & \lambda^3 c_{36} \\ \lambda^3 c_{41} & \lambda^3 c_{42} & \lambda^3 c_{43} & \lambda^4 c_{44} & \lambda^4 c_{45} & \lambda^4 c_{46} \\ \lambda^3 c_{51} & \lambda^3 c_{52} & \lambda^3 c_{53} & \lambda^4 c_{54} & \lambda^4 c_{55} & \lambda^4 c_{56} \\ \lambda^3 c_{61} & \lambda^3 c_{62} & \lambda^3 c_{63} & \lambda^4 c_{64} & \lambda^4 c_{65} & \lambda^4 c_{66} \end{bmatrix} \tag{B-14}$$

Note that each, mass, added mass, damping and restoring matrix contains different units these are divided in equal quadrants. Each quadrant contains 3*3 terms.

The wave force depends on scaled frequency and the wave incident angle. The wave force is

computed for a wave amplitude of 1 [m]: The wave force per meter wave. With the wave force per meter wave, the vessel response per meter wave is calculated. The wave force scales with N/m and the wave moment with Nm/m, the wave height shall not be scaled:

$$F_a \rightarrow \begin{bmatrix} \lambda^2 F_x \\ \lambda^2 F_y \\ \lambda^2 F_z \\ \lambda^3 M_x \\ \lambda^3 M_y \\ \lambda^3 M_z \end{bmatrix} \tag{B-15}$$

The wave phase depends on the scaled frequency and depends on the wave incident angle. This dimensionless parameter does not scale. With all scaled terms the vessel response $\hat{X}_a$ is calculated for a wave elevation of 1 meter amplitude. Validation of this scaling law is discussed in Appendix B.

B-3-3 Applying the Ampelmann system to a scaled vessel

This thesis analyses the dynamic interaction between the vessel and the Ampelmann system. When an Ampelmann system is mounted on the deck of the vessel the draft of the vessel increases. Weight is added to the vessel. Before performing the hydromechanic analysis this increase in weight shall be taken into account. For smaller vessels of geometric similitude the absolute change in draft is larger than for larger vessels. This is illustrated in Figure B-3.

Figure B-3: Scaling vessel with geometric similitude and applying the Ampelmann system.

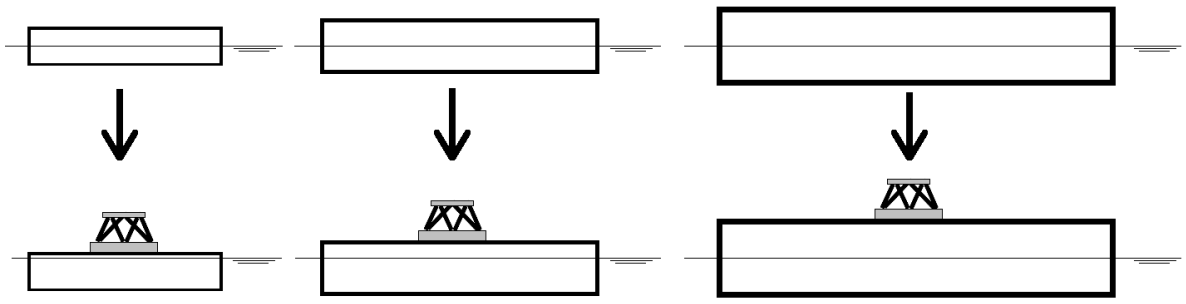

The Ampelmann does not scale when the vessel is scaled. This causes the draft of a scaled vessel to change, when only vessel parameter are scaled. Geometric similitude does not hold any more for the under water hull geometry. This effect is larger for smaller vessels. As such hydromechanic properties may not be scaled since the underwater hull geometry is different. The hydromechanic properties depend on the under water hull geometry. This problem may be overcome in two ways. Either the vessel mass is not scaled according to the scaling law or the hydromechanic properties are determined for different drafts. The first option requires the vessel mass of the scaled vessel to be adapted to ensure that the wetter hull surface has geometric similitude. This is illustrated in Figure B-4. Think of de-ballasting the vessel when scaled down.

Figure B-4: Scaling vessel with geometric similitude with the Ampelmann system. Vessel mass does not scale according to scaling law.

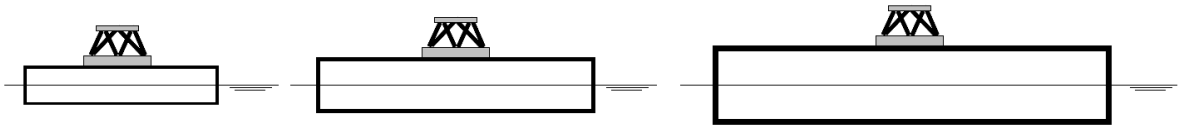

For the second option by forehand it is anticipated how the vessel draft of the scaled vessel changes when the Ampelmann is mounted. The hydromechanic properties are determined for multiple vessel drafts. In this way all conditions are met: the Ampelmann mass remains constant and all scaling laws apply. This is illustrated in Figure B-5. For the remainder of this thesis the first option is taken. When scaling, the vessel mass is adopted such that the under water hull geometry has geometric similitude.

Figure B-5: Scaling vessel with geometric similitude with the Ampelmann system. Perform hydromechanic analysis for multiple drafts.

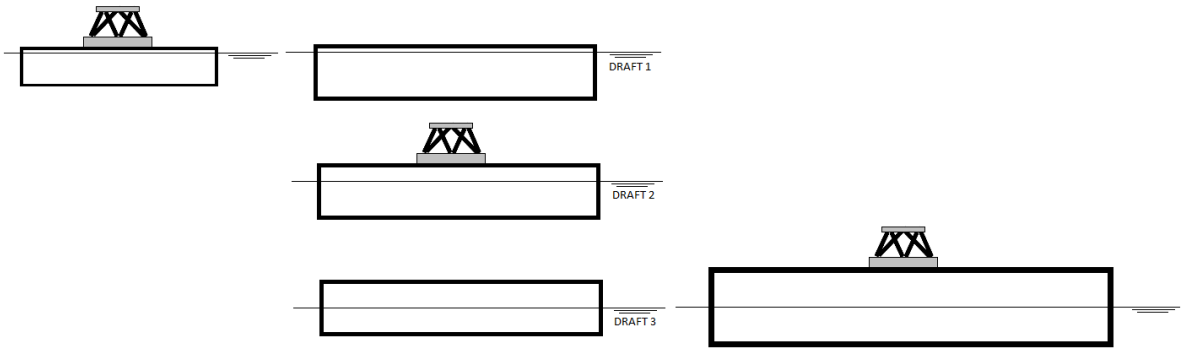

Five steps are listed below that are performed to determined the hydro mechanic properties for the vessel of the coupled vessel-Ampelmann system

1. Choose a vessel with a certain hull geometry.

2. Determine the CoG of the vessel.

3. Take into account the additional weight of the Ampelmann to the vessel. Then determine the underwater hull geometry. The sum of the weight of the vessel and the Ampelmann determine the draft of the vessel.

4. Perform the hydromechanic analysis with respect to the CoG of the vessel. The masses in the mass matrix shall be the sum of the vessel mass and the Ampelmann mass: m_v.

5. Now that the hydromechanic parameters are known. Add the Ampelmann as and external load to the vessel. This is done in chapter 5, the vessel mass reduces to $m_v \rightarrow m_1$.

B-4 Validation of scaling vessel parameters

This Appendix validates the scaling laws discussed previous. The validation is performed for the chosen hull shape. The Barge from chapter 3 is taken. As discussed, scaling a vessel requires geometric similitude. The hydromechanic properties and frequency characteristics for three vessels with geometric similitude are obtained by DELFRAC. The validation is performed as shown in Figure B-6. For a chosen vessel the vessel parameters and the frequency

Figure B-6: Validation of scaling laws

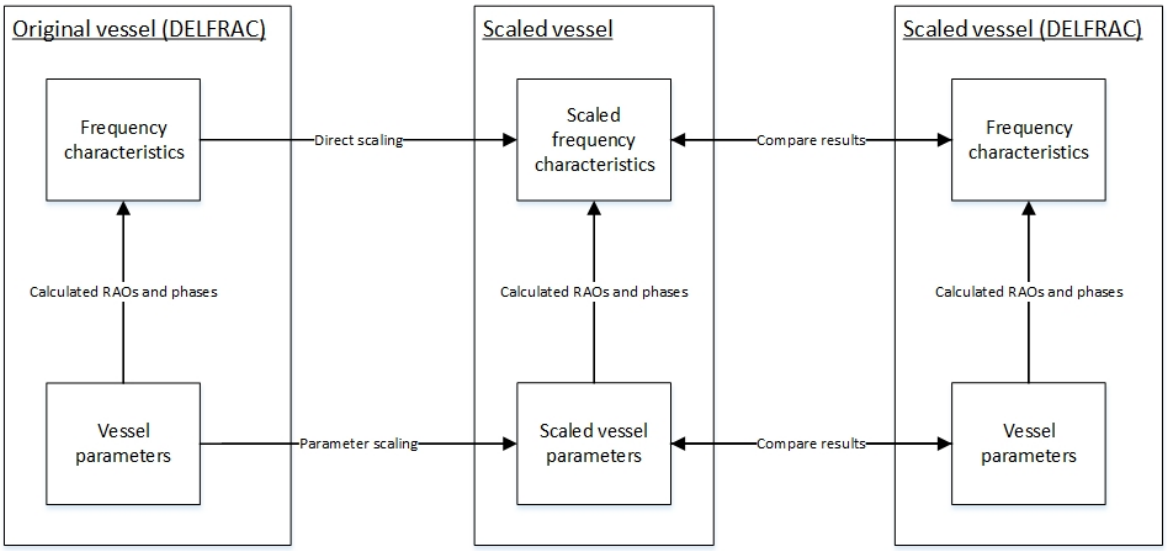

characteristics are obtained, left hand side. For a scaled vessel with geometric similitude the vessel parameters and frequency characteristics are obtained, right hand side. In the center box the scaled vessel parameters en frequency characteristics are calculated from the original vessel. These results are compared to the scaled vessel (DELFRAC), right hand side. Validating the scaling laws is performed in three steps:

- *Direct scaling*: The frequency characteristics are scaled according to the axis units. The scaled frequency characteristics are obtained, Figure B-6 center top. These are compared to the scaled vessel (DELFRAC) frequency characteristics, right hand side top.

- *Parameter scaling*: The vessel parameters, the mass, the added mass, the damping, the restoring term, the frequency, the wave force and wave phase are scaled. The scaled vessel parameters, center bottom. Are compared to the vessel parameters of the scaled vessel (DELFRAC), right hand side top.

- *Scaled frequency characteristics from scaled vessel parameters*: From the scaled vessel parameters, center bottom. The scaled frequency characteristics are calculated, center top. The results are compared to the frequency characteristics of the scaled vessel (DELFRAC), right hand side top.

This validation procedure is applied to three barges of geometric similitude. Barge 1 is taken as the original. Barge 2 is scaled with $\lambda = 0.7[-]$ and Barge 3 with $\lambda = 0.49[-]$. The following dimensions hold.

- Barge 1: 34 [m]* 12 [m]* 3 [m]
- Barge 2: 23.8 [m]* 8.4 [m]* 2.1 [m]
- Barge 3: 16.7 [m]* 5.9 [m]* 1.5 [m]

Figure B-7 and B-8 on page 102 and 103 show the results. Four data sets are identified for each plot: Barge 1, Barge 2, Barge 3 and scaled Barge 1 to Barge 3. Scaled Barge 1 to Barge 3 coincides with Barge 3. Each validation step is discussed in the following sections all confirm the correctness of the scaling laws.

Figure B-7: Translational frequency characteristics for hull shapes of different sizes with geometric similitude

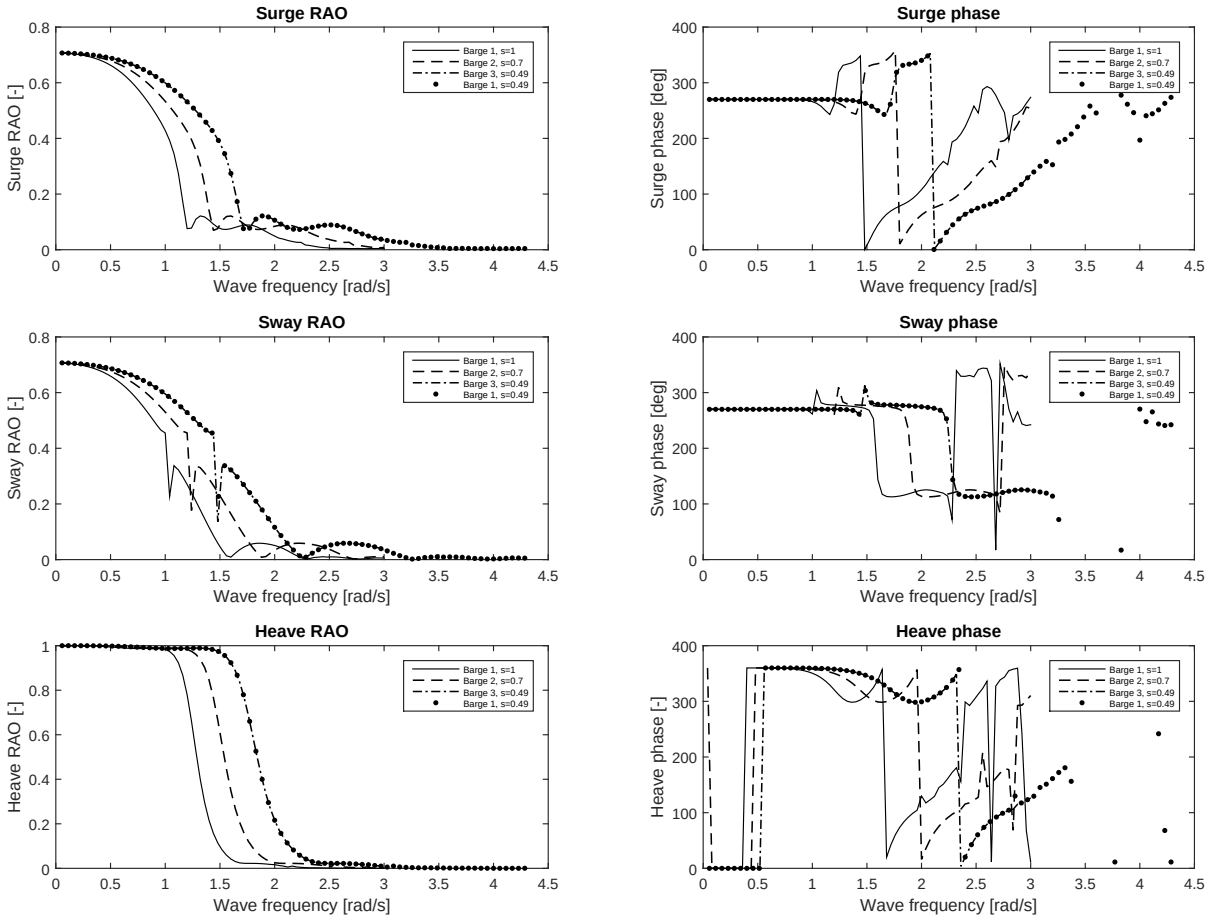

Figure B-8: Rotational frequency characteristics for hull shapes of different sizes with geometric similitude

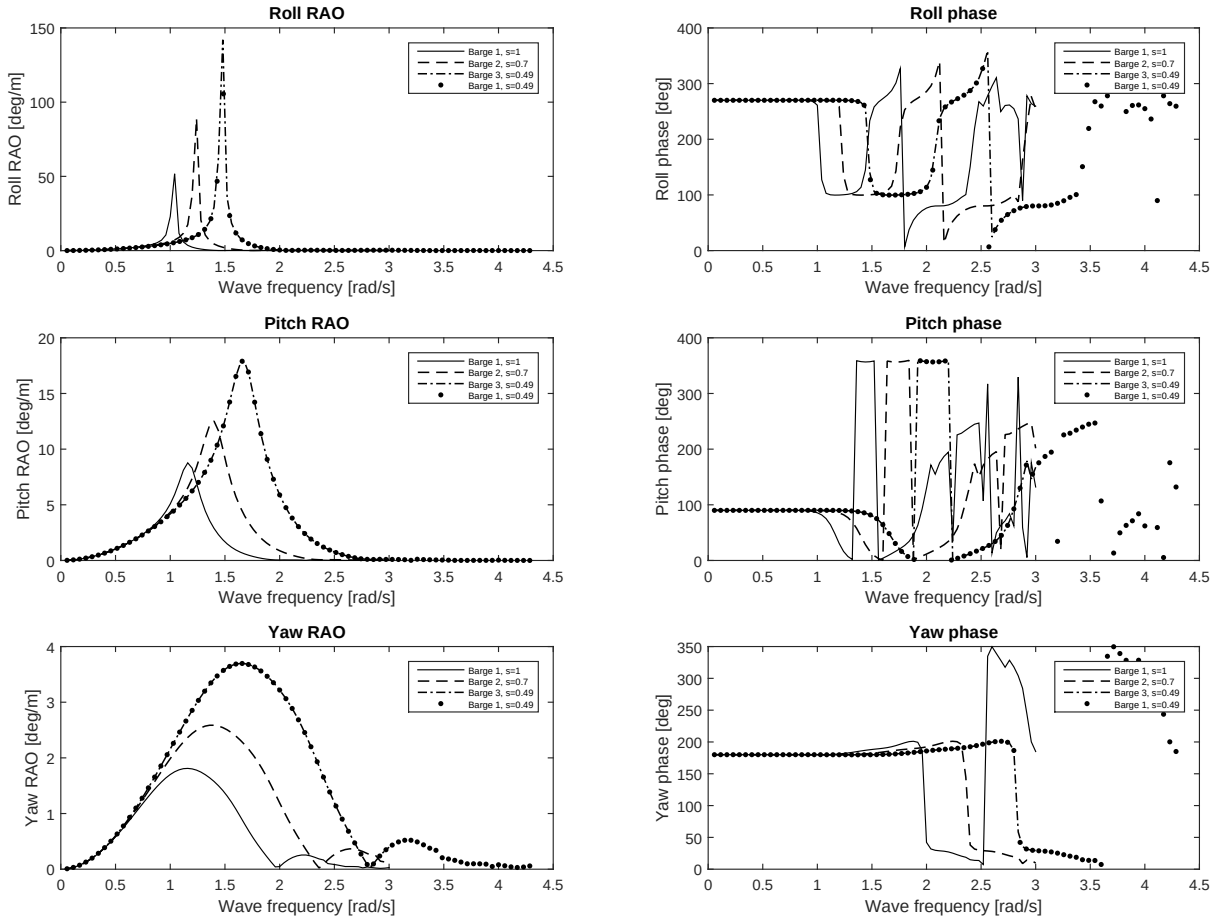

B-4-1 Direct scaling of frequency characteristics

Frequency characteristics for vessels with geometric similitude are scaled directly. The scaling laws are applied to the axis units. This causes the graph depending on the scaling factor to compress or stretch along its reference axis. Translational RAOs and phases do not scale, these are dimensionless. The frequency axis scales with: $\omega \rightarrow \frac{1}{\sqrt{\lambda}}\omega$. Scaling factors smaller than 1 [-] cause the RAO and phase graph to stretch horizontally. The frequency range for the RAO and phases are increased. Scaling factors larger than 1 [-] cause the RAO and phase graph to compress horizontally. The frequency range for the RAO and phase decrease. Figure B-7 and B-8 confirm the correctness of direct scaling. Scaled Barge 1, $\lambda = 0.49[-]$, coincides with Barge 3. Note however that the data range for scaled Barge 1 is defined for a larger frequency range than Barge 3. This is due to the scaling of the frequency. For $\lambda > 1[-]$ the frequency band will narrow. As such scaling Barge 3 to Barge 1 will narrow the frequency band of scaled Barge 3.

Figure B-9: Scaling vessel parameters, added mass and damping in sway due to sway

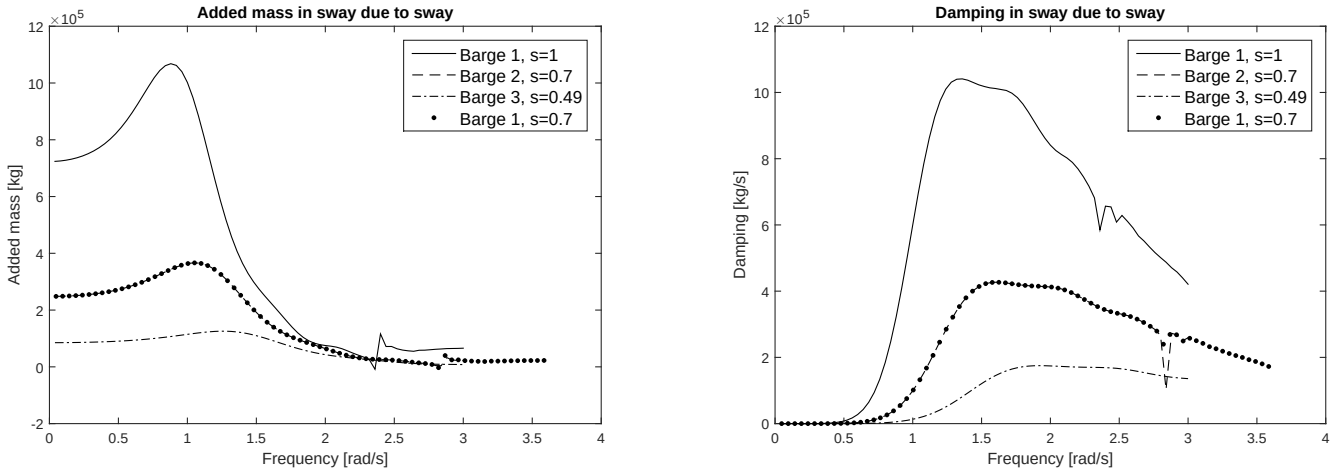

B-4-2 Scaling vessel parameters

Each term in the EOM of motion is scaled according to the scaling laws of geometric similitude. Samples of each parameter of scaled vessel and sceled vessel (DELFRAC) are taken and compared. All samples coincide and show similar values. As illustration this is shown for added mass and damping in Figure B-9. Here Barge 1 is scaled with $\lambda = 0.7[-]$.

B-4-3 Scaled frequency characteristics from scaled vessel parameters

From the scaled vessel parameters the frequency characteristics are calculated. As with direct scaling the results are compared. Because the results are similar to those of direct scaling reference is made to Figure B-7 and B-8.

B-4-4 Concluding remarks

Based on the three validation steps it is concluded that the scaling laws are correct. Each step in the process to get from origional vessel parameters to scaled frequency characteristics is checked.

Appendix C

Ampelmann control system

This Appendix discusses the control system of the Ampelmann system. It shows that the Ampelmann control system perfectly compensates small vessel motion that are within the mechanical limitations of the Ampelmann system. For larger vessel motions residual motions occur. Two frequency domain control system are identified, which are applied to the models discussed in this thesis. In the first control system the TD is perfectly compensated and in the second control system a low pass filter is applied which causes a time lag and gain to the control signal. The final section of this Appendix gives a mathematical description of how a filter causes residual motions.

C-1 The motion control loop

The Ampelmann control systems consists of 5 items, these form the motion control loop and are all shown in Figure C-1 on page 106. The task of the motion control loop is to keep the transfer deck motionless. At the left side the motion sensor gives the input to the Programmable Logic Controller (PLC). This measured input signal contains all 6 DOF ship motions: x, y, z, φ, θ, ψ. The PLC is responsible for controlling the complete system, first the reference generator calculates six cylinder reference positions: $r_{1....,6}$. Then the hydraulic actuators are controlled to their reference positions by control input $u_{1....,6}$ and the actuator positions are measured by the position transducer $l_{1....,6}$, which creates a feed back loop to the controller.

C-1-1 Motion sensor

An Octans motion sensor is used to measure the ship motions. It makes use of three Fibre Optic Gyroscopes (FOG), three accelerometers and a real-time Digital Signal Processing computer (DSP). The FOGs measure the three rotational velocities: $\dot{\varphi}$, $\dot{\theta}$, $\dot{\psi}$. By integrating once the motion angles φ, θ, ψ are obtained. The combination of the three accelerometers and the DSP measures the translational accelerations $\ddot{x}$, $\ddot{y}$, $\ddot{z}$. By integrating twice, the translations x, y and z are determined.

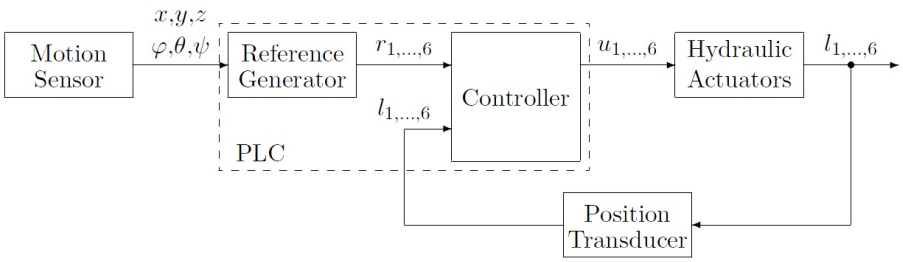

Figure C-1: Block diagram of the Ampelmann motion control loop [7]

C-1-2 Reference generator

The reference generator calculates the required length for each hydraulic cylinder to create a motionless transfer deck. This is performed as shown in the Figure C-2.

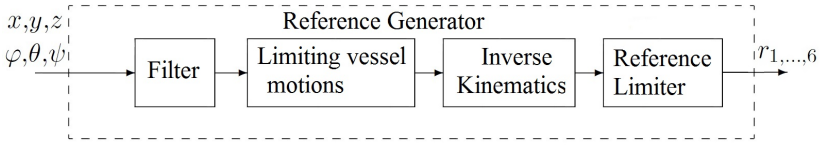

Figure C-2: Block diagram of the reference generator [7]

- The signal is filtered with both a low and high pass filter
- The measured ship motions are limited to avoid large platform motions, each DOF is limited towards a maximum value by using an asymptote function.
- By inverse kinematics the six actuator lengths are determined
- The required actuator lengths are limited where required to make sure these do not exceed the maximum available stroke length and actuator velocity.

The determined cylinder reference lengths are fed to the controller.

C-1-3 Controller

The controller combines the signals from the Position Transducer, $l_{1,...,6}$ and the Reference Generator. The Positions transducer measures the cylinder length. See Figure C-3. The control input for the hydraulic actuators is calculated with a velocity Feed Forward (FF) and a proportional Feed Back (FB) control. Because the characteristics of the actuator is non linear, the valve position is determined by a look up table. Finally the actuator signal is filtered.

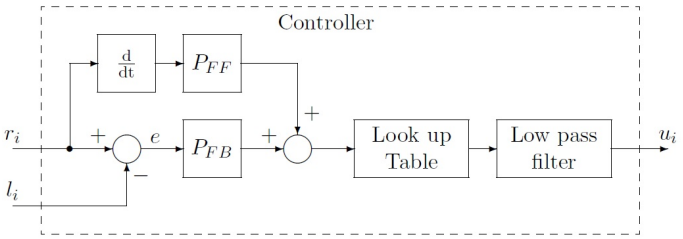

Figure C-3: Block diagram of a single actuator controller [7]

C-2 Residual TD motions

This section shows four plots, these illustrate the source of residual motions. Two motions cases are shows for which both the vessel and TD motions in 6 DOF are shown. The first motion cases shows relative small vessel motions. No residual TD motion result. See Figure C-4 and C-5. For larger vessel motions, the control system causes residual motions to the TD due to mechanical limitations of the Ampelmann system. This is shown in Figure C-6 and C-7. As shown in the figures the source for residual TD motions is due to the mechanical limitations of the system. For small vessel motions it shows that the TD is motionless.

From previous research a time lag in the control system also causes residual motions, which affects vessel dynamics. In this thesis three models are made, one for a passive Ampelmann system and two for an active Ampelmann system. Here the TD is compensated. The first compensating system compensate perfectly as illustrated in Figure C-5 no residual motions exist. The second control system is chosen, it cause residual TD motions due to a time lag in the control system. The motion control loop consists of multiple filters, filters introduce a time lag and gain to the control signal. Filters are applicable for a frequency domain analysis. Therefore for the second compensating model a second order low pass filter is applied as used in the Ampelmann control system. The goal of this last control system is to show what the effect is of residual motions to the coupled vessel-Ampelmann system. A filter only is a continuous source of residual motions and is applicable to a frequency domain analysis. The next section shows the effect of the application of the second order low pass filter to the control signal.

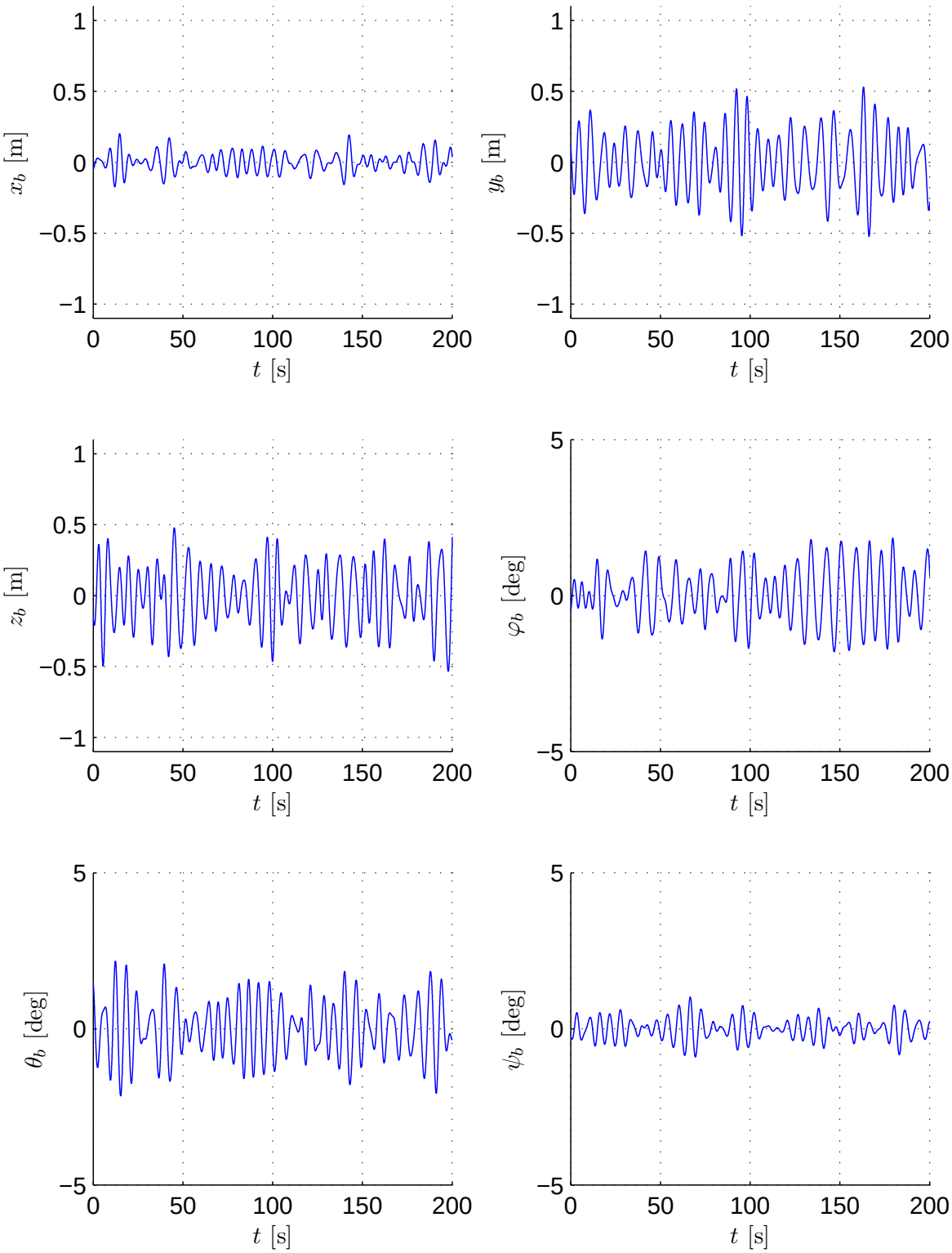

Figure C-4: Shipmotions in six DOF, motion case 1 [7]

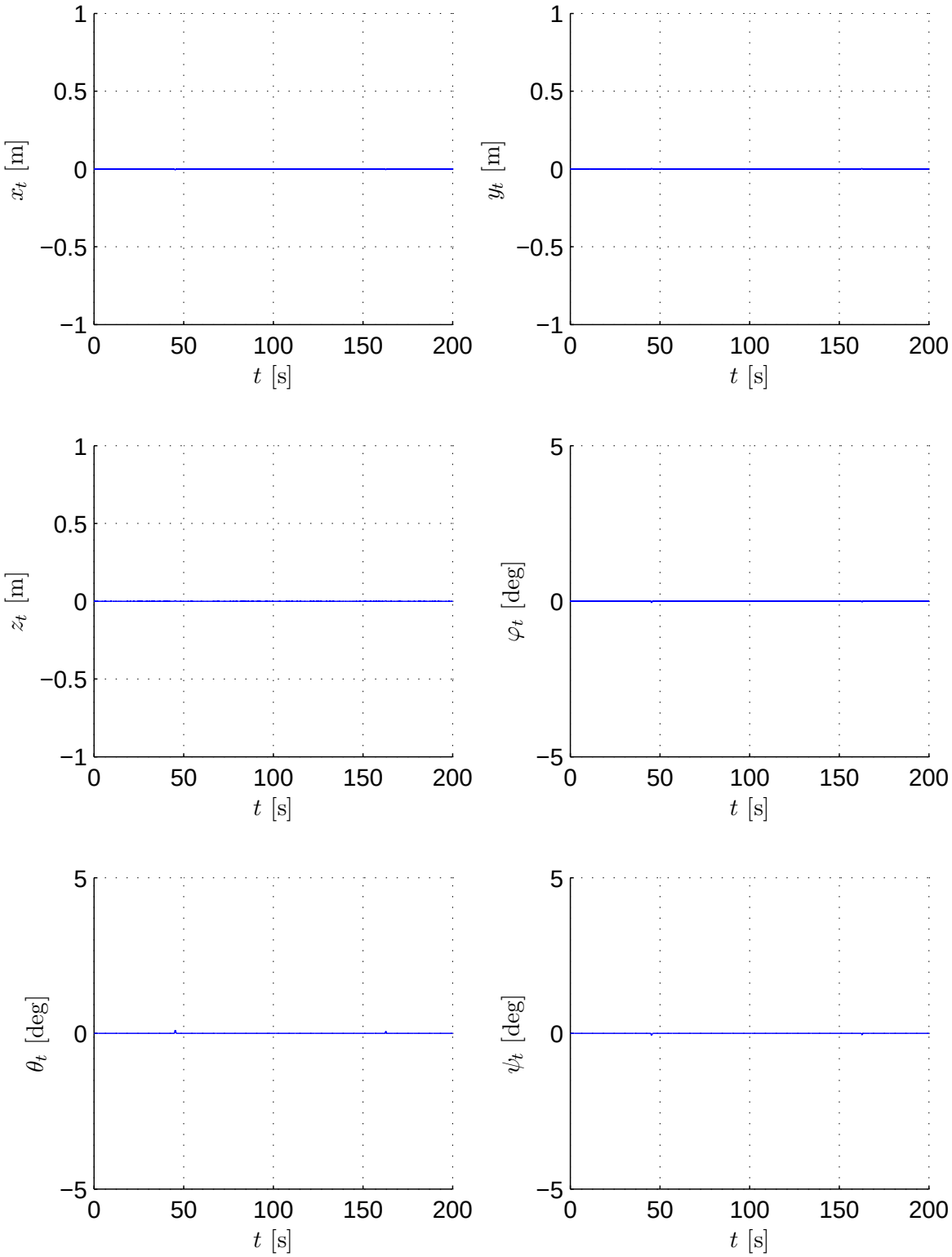

Figure C-5: Transfer deck motions in six DOF, motion case 1 [7]

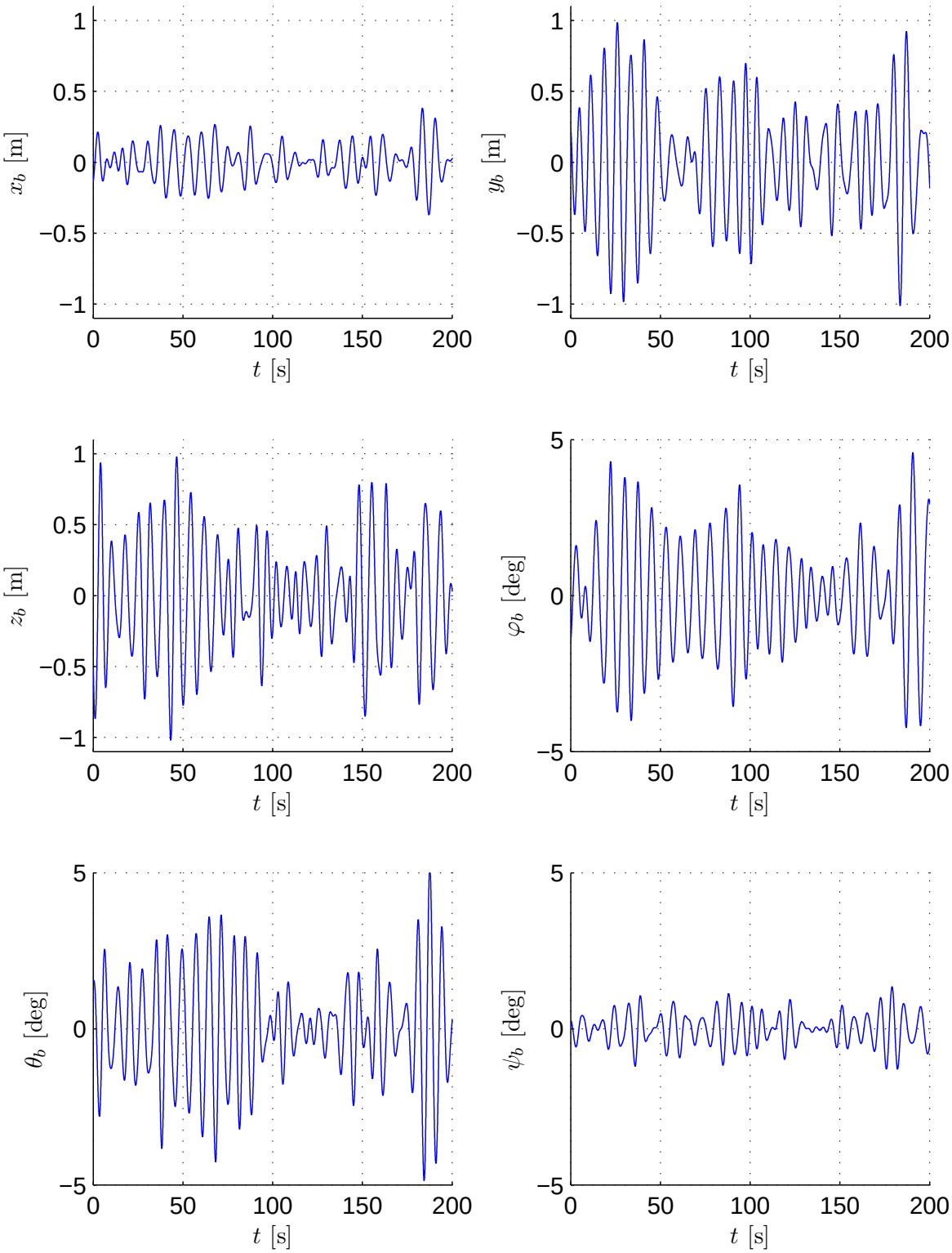

Figure C-6: Shipmotions in six DOF, motion case 2 [7]

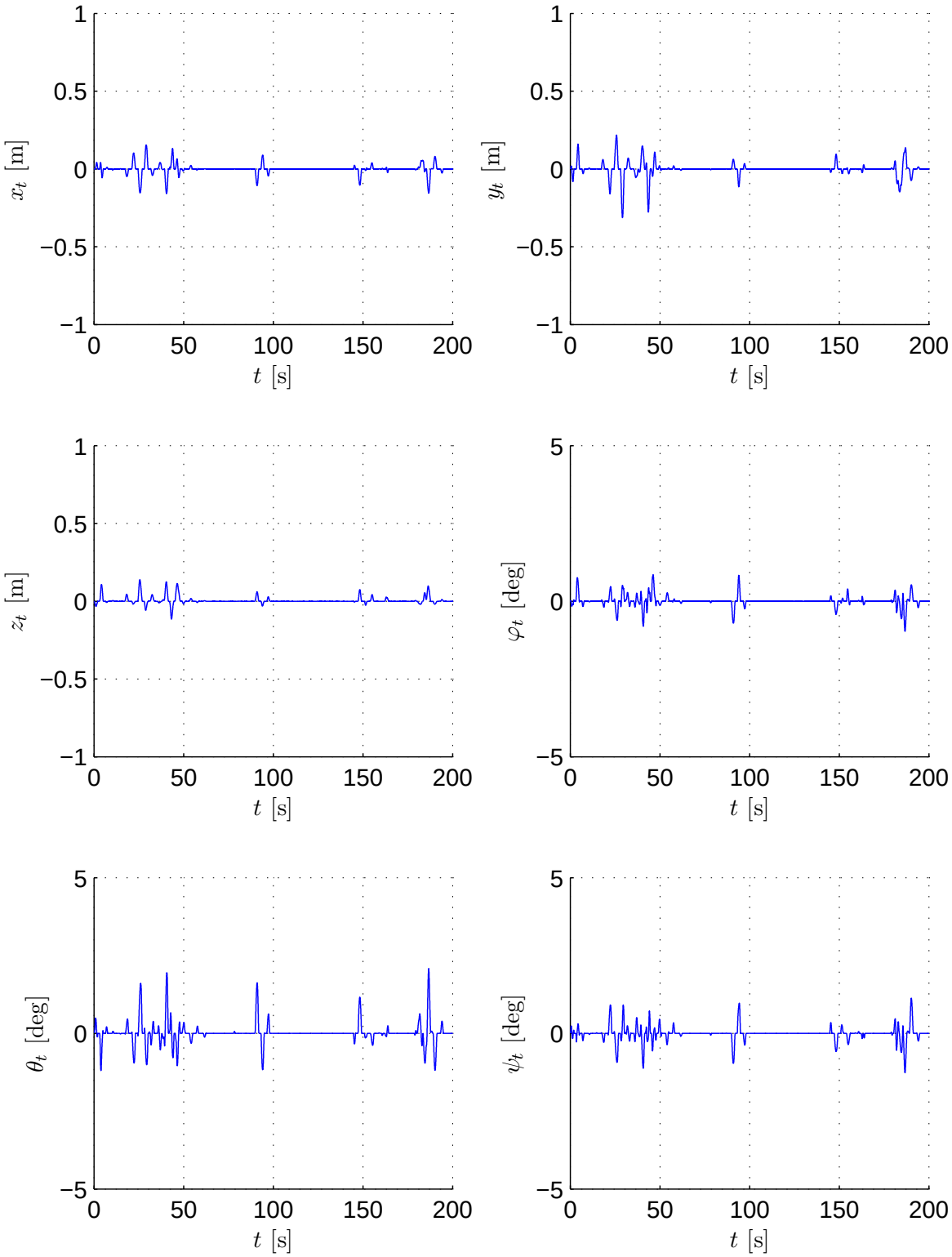

Figure C-7: Transfer deck motions in six DOF, motion case 2 [7]

C-3 Time lag and gain due to filtering the control signal

For the dynamic vessel-Ampelmann model one second order low pass filter is applied as control system, the goal of this section is to mathematically show what happens to a signal when the second order low pass filter is applied. A harmonic signal is fed tot the filter, an output signal results:

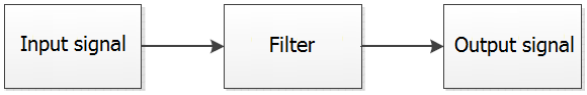

Figure C-8: A filter causes a time lag to the motion control signal

Suppose we have an harmonic input signal with unit amplitude $Z_1 = 1$ and a given frequency ω:

$$z_1(\omega) = Z_1 e^{i\omega t} \tag{C-1}$$

The output signal is of a similar form with the same frequency ω:

$$z_2(\omega) = Z_2 e^{i\omega t} \tag{C-2}$$

The second order low pass filter used for the dynamic model and used to filter the vessel motions has a cut off frequency of f_c=2[Hz]:

$$w_c = 2\pi f_c \tag{C-3}$$

$$H(s) = \frac{\omega_c^2}{s^2 + 2s\omega_c + \omega_c^2} \tag{C-4}$$

The second order low pass filter $H(s)$ is expressed in the frequency domain where $i\omega$=s. The process described in Figure C-8 is mathematically described as:

$$Z_2 = Z_1 H(s) \tag{C-5}$$

$$H(s) = \frac{\omega_c^2}{s^2 + 2s\omega_c + \omega_c^2} \rightarrow H(\omega) = \frac{\omega_c^2}{-\omega^2 + 2i\omega\omega_c + \omega_c^2} \tag{C-6}$$

The latter has an imaginary number in the denominator, it is desired to write the expression in the following form: $a + ib$, where all imaginary terms appear in the numerator:

$$H(\omega) = \frac{\omega_c^2}{-\omega^2 + 2i\omega\omega_c + \omega_c^2} = \frac{(\omega_c^2 - \omega^2\omega_c^2)}{(\omega_c^2 - \omega^2)^2 + 4\omega^2\omega_c^2} + i\frac{-2\omega\omega_c^3}{(\omega_c^2 - \omega^2)^2 + 4\omega^2\omega_c^2} = a + ib \tag{C-7}$$

With:

$$a = \frac{(\omega_c^2 - \omega^2\omega_c^2)}{(\omega_c^2 - \omega^2)^2 + 4\omega^2\omega_c^2} \tag{C-8}$$

$$b = \frac{-2\omega\omega_c^3}{(\omega_c^2 - \omega^2)^2 + 4\omega^2\omega_c^2} \tag{C-9}$$

Applying Equation C-5: From calculus any complex number Z can be written in the form:

$$Z = r(cos\theta + isin\theta) = re^{i\theta} \tag{C-10}$$

Where:

$$r = \sqrt{a^2 + b^2} \tag{C-11}$$

$$\theta = tan^{-1}(b/a) \tag{C-12}$$

Applying this to the previous result obtained for Z_2 yields:

$$Z_2 = \sqrt{a^2 + b^2} \cdot e^{i\theta} \tag{C-13}$$

$$z_2(\omega) = Z_2 e^{i\omega t} = \sqrt{a^2 + b^2} \cdot e^{i\theta} e^{i\omega t} = \sqrt{a^2 + b^2} \cdot e^{i(\omega t + \theta)} \tag{C-14}$$

The latter expression shows that a phase lag θ is introduced to the output signal, $z_2(\omega)$. The bode plot of the second order low pass filter with f_c=2[Hz] is visualized in Figure C-9. It can be seen that with an increasing frequency the gain reduces for 1 and the phase negatively increases from 0.

Figure C-9: Bode plot of a second order low pass filter

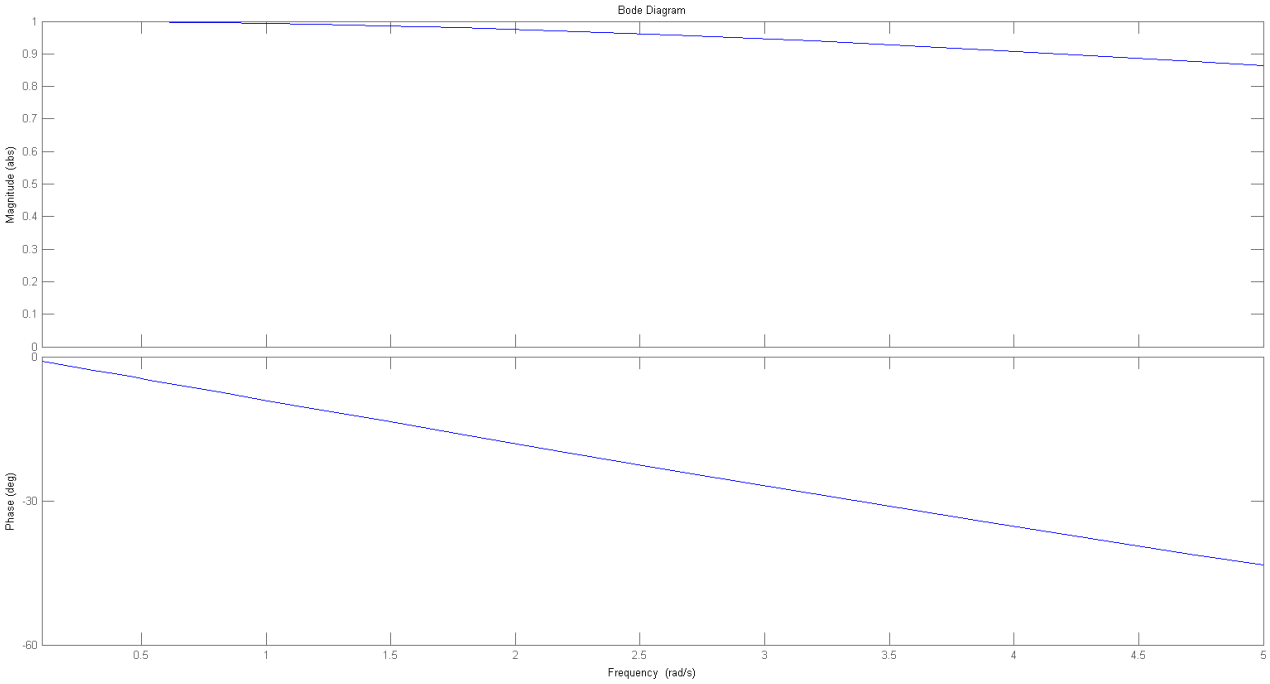

Appendix D

Determination 12 DOF model include translation of Ampelmann location

This appendix shows how table D-1 summarizes all first order mechanical coupling mechanism and shows that it applies to all models discussed in this thesis.

Table D-1: First order mechanical coupling mechanisms of coupled vessel-Ampelmann system

	x_1, surge V	y_1, sway V	z_1, heave V	ϕ_1, roll V	θ_1, pitch	ψ_1, yaw
x_2, surge TD	1				L_a, L_z, $M_{\theta,x}$	L_y
y_2, sway TD		1		L_a, L_z, $M_{\phi,y}$		L_x
z_2, heave TD			1	L_y	L_x	
ϕ_2, roll TD				1		
θ_2, pitch TD					1	
ψ_2, yaw TD						1

D-1 6 DOF model, with and without translation of Ampelmann location

Below the 6DOF EOM is written. Sway, heave and roll apply. From Table D-1 the applicable coupling mechanics are coloured. These can directly be found in the EOM. All dynamic terms are included in the mass and added mass matrix in the last three column of the first three rows: m_2, m_2, I_{xx2}, $-(L_a + L_z)m_2$ and $L_y m_2$. These are the forces and moments of the Ampelman working on the vessel. All static terms in the stiffness matrix indicated by: $-m_2 g$ and $m_2 g$. A relative displacement causes a static moment to the vessel. For $L_y = 0$ and $L_z = 0$.

Table D-2: First order mechanical coupling mechanisms of coupled vessel-Ampelmann system for 6 DOF, sway, heave roll model

	x_1, surge V	y_1, sway V	z_1, heave V	ϕ_1, roll V	θ_1, pitch	ψ_1, yaw
x_2, surge TD	1				L_a, L_z, $M_{\theta,x}$	L_y
y_2, sway TD		1		L_a, L_z, $M_{\phi,y}$		L_x
z_2, heave TD			1	L_y	L_x	
ϕ_2, roll TD				1		
θ_2, pitch TD					1	
ψ_2, yaw TD						1

$$\left(-\omega^2[\mathbf{M}+\mathbf{A}(\omega)]+i\omega[\mathbf{B}(\omega)]+[\mathbf{C}]\right)\begin{bmatrix}\hat{Y}_1\\ \hat{Z}_1\\ \hat{\Phi}_1\\ \hat{Y}_2\\ \hat{Z}_2\\ \hat{\Phi}_2\end{bmatrix}=\begin{bmatrix}\hat{F}_2\\ \hat{F}_3\\ \hat{M}_4\\ 0\\ 0\\ 0\end{bmatrix} \tag{D-1}$$

$$[\mathbf{M}+\mathbf{A}(\omega)]=\begin{bmatrix}m_1+a_{22}(\omega) & a_{23}(\omega) & a_{24}(\omega) & m_2 & 0 & 0\\ a_{32}(\omega) & m_1+a_{33}(\omega) & a_{34}(\omega) & 0 & m2 & 0\\ a_{42}(\omega) & a_{43}(\omega) & I_{xx1}+a_{44}(\omega) & -(L_a+L_z)m_2 & L_y m_2 & I_{xx2}\\ 0 & 0 & 0 & 0 & 0 & 0\\ 0 & 0 & 0 & 0 & 0 & 0\\ 0 & 0 & 0 & 0 & 0 & 0\end{bmatrix} \tag{D-2}$$

$$[\mathbf{B}(\omega)]=\begin{bmatrix}b_{22}(\omega) & b_{23}(\omega) & b_{24}(\omega) & 0 & 0 & 0\\ b_{32}(\omega) & b_{33}(\omega) & b_{34}(\omega) & 0 & 0 & 0\\ b_{42}(\omega) & b_{43}(\omega) & b_{44}(\omega) & 0 & 0 & 0\\ 0 & 0 & 0 & 0 & 0 & 0\\ 0 & 0 & 0 & 0 & 0 & 0\\ 0 & 0 & 0 & 0 & 0 & 0\end{bmatrix} \tag{D-3}$$

$$[\mathbf{C}]=\begin{bmatrix}c_{22} & c_{23} & c_{24} & 0 & 0 & 0\\ c_{32} & c_{33} & c_{34} & 0 & 0 & 0\\ -m_2 g+c_{42} & c_{43} & c_{44} & m_2 g & 0 & 0\\ 0 & 0 & 0 & 0 & 0 & 0\\ 0 & 0 & 0 & 0 & 0 & 0\\ 0 & 0 & 0 & 0 & 0 & 0\end{bmatrix} \tag{D-4}$$

D-2 12 DOF model Ampelmann at CoG of vessel

The EOM is repeated below. All terms from Table D-1 are included except for $L_x = 0$, $L_y = 0$ and $L_z = 0$. The results are confirmed by the EOM derived in chapter 6:

$$\left(-\omega^2[\mathbf{M}+\mathbf{A}(\omega)] + i\omega[\mathbf{B}(\omega)] + [\mathbf{C}]\right) \begin{bmatrix} \hat{X}_1 \\ \hat{Y}_1 \\ \hat{Z}_1 \\ \hat{\Phi}_1 \\ \hat{\Theta}_1 \\ \hat{\Psi}_1 \\ \hat{X}_2 \\ \hat{Y}_2 \\ \hat{Z}_2 \\ \hat{\Phi}_2 \\ \hat{\Theta}_2 \\ \hat{\Psi}_2 \end{bmatrix} = \begin{bmatrix} \hat{F}_1 \\ \hat{F}_2 \\ \hat{F}_3 \\ \hat{M}_4 \\ \hat{M}_5 \\ \hat{M}_6 \\ 0 \\ 0 \\ 0 \\ 0 \\ 0 \\ 0 \end{bmatrix} \tag{D-5}$$

$$[\mathbf{M}+\mathbf{A}(\omega)] = \begin{bmatrix} m_1 + a_{11}(\omega) & a_{12}(\omega) & a_{13}(\omega) & a_{14}(\omega) & a_{15}(\omega) & a_{16}(\omega) & m_2 & 0 & 0 & 0 & 0 & 0 \\ a_{21}(\omega) & m_1 + a_{22}(\omega) & a_{23}(\omega) & a_{24}(\omega) & a_{25}(\omega) & a_{26}(\omega) & 0 & m_2 & 0 & 0 & 0 & 0 \\ a_{31}(\omega) & a_{32}(\omega) & m_1 + a_{33}(\omega) & a_{34}(\omega) & a_{35}(\omega) & a_{36}(\omega) & 0 & 0 & m_2 & 0 & 0 & 0 \\ a_{41}(\omega) & a_{42}(\omega) & a_{43}(\omega) & I_{xx1} + a_{44}(\omega) & a_{45}(\omega) & a_{46}(\omega) & 0 & -L_a m_2 & 0 & I_{xx2} & 0 & 0 \\ a_{51}(\omega) & a_{52}(\omega) & a_{53}(\omega) & a_{54}(\omega) & I_{yy1} + a_{55}(\omega) & a_{56}(\omega) & L_a m_2 & 0 & 0 & 0 & I_{yy2} & 0 \\ a_{61}(\omega) & a_{62}(\omega) & a_{63}(\omega) & a_{64}(\omega) & a_{65}(\omega) & I_{zz1} + a_{66}(\omega) & 0 & 0 & 0 & 0 & 0 & I_{zz2} \\ 0 & 0 & 0 & 0 & 0 & 0 & 0 & 0 & 0 & 0 & 0 & 0 \\ 0 & 0 & 0 & 0 & 0 & 0 & 0 & 0 & 0 & 0 & 0 & 0 \\ 0 & 0 & 0 & 0 & 0 & 0 & 0 & 0 & 0 & 0 & 0 & 0 \\ 0 & 0 & 0 & 0 & 0 & 0 & 0 & 0 & 0 & 0 & 0 & 0 \\ 0 & 0 & 0 & 0 & 0 & 0 & 0 & 0 & 0 & 0 & 0 & 0 \\ 0 & 0 & 0 & 0 & 0 & 0 & 0 & 0 & 0 & 0 & 0 & 0 \end{bmatrix} \tag{D-6}$$

$$[\mathbf{B}(\omega)] = \begin{bmatrix} b_{11}(\omega) & b_{12}(\omega) & b_{13}(\omega) & b_{14}(\omega) & b_{15}(\omega) & b_{16}(\omega) & 0 & 0 & 0 & 0 & 0 & 0 \\ b_{21}(\omega) & b_{22}(\omega) & b_{23}(\omega) & b_{24}(\omega) & b_{25}(\omega) & b_{26}(\omega) & 0 & 0 & 0 & 0 & 0 & 0 \\ b_{31}(\omega) & b_{32}(\omega) & b_{33}(\omega) & b_{34}(\omega) & b_{35}(\omega) & b_{36}(\omega) & 0 & 0 & 0 & 0 & 0 & 0 \\ b_{41}(\omega) & b_{42}(\omega) & b_{43}(\omega) & b_{44}(\omega) & b_{45}(\omega) & b_{46}(\omega) & 0 & 0 & 0 & 0 & 0 & 0 \\ b_{51}(\omega) & b_{52}(\omega) & b_{53}(\omega) & b_{54}(\omega) & b_{55}(\omega) & b_{56}(\omega) & 0 & 0 & 0 & 0 & 0 & 0 \\ b_{61}(\omega) & b_{62}(\omega) & b_{63}(\omega) & b_{64}(\omega) & b_{65}(\omega) & b_{66}(\omega) & 0 & 0 & 0 & 0 & 0 & 0 \\ 0 & 0 & 0 & 0 & 0 & 0 & 0 & 0 & 0 & 0 & 0 & 0 \\ 0 & 0 & 0 & 0 & 0 & 0 & 0 & 0 & 0 & 0 & 0 & 0 \\ 0 & 0 & 0 & 0 & 0 & 0 & 0 & 0 & 0 & 0 & 0 & 0 \\ 0 & 0 & 0 & 0 & 0 & 0 & 0 & 0 & 0 & 0 & 0 & 0 \\ 0 & 0 & 0 & 0 & 0 & 0 & 0 & 0 & 0 & 0 & 0 & 0 \\ 0 & 0 & 0 & 0 & 0 & 0 & 0 & 0 & 0 & 0 & 0 & 0 \end{bmatrix} \tag{D-7}$$

$$[\mathbf{C}] = \begin{bmatrix} c_{11} & c_{12} & c_{13} & c_{14} & c_{15} & c_{16} & 0 & 0 & 0 & 0 & 0 & 0 \\ c_{21} & c_{22} & c_{23} & c_{24} & c_{25} & c_{26} & 0 & 0 & 0 & 0 & 0 & 0 \\ c_{31} & c_{32} & c_{33} & c_{34} & c_{35} & c_{36} & 0 & 0 & 0 & 0 & 0 & 0 \\ c_{41} & -m_2 g + c_{42} & c_{43} & c_{44} & c_{45} & c_{46} & 0 & m_2 g & 0 & 0 & 0 & 0 \\ m_2 g + c_{51} & c_{52} & c_{53} & c_{54} & c_{55} & c_{56} & -m_2 g & 0 & 0 & 0 & 0 & 0 \\ c_{61} & c_{62} & c_{63} & c_{64} & c_{65} & c_{66} & 0 & 0 & 0 & 0 & 0 & 0 \\ 0 & 0 & 0 & 0 & 0 & 0 & 0 & 0 & 0 & 0 & 0 & 0 \\ 0 & 0 & 0 & 0 & 0 & 0 & 0 & 0 & 0 & 0 & 0 & 0 \\ 0 & 0 & 0 & 0 & 0 & 0 & 0 & 0 & 0 & 0 & 0 & 0 \\ 0 & 0 & 0 & 0 & 0 & 0 & 0 & 0 & 0 & 0 & 0 & 0 \\ 0 & 0 & 0 & 0 & 0 & 0 & 0 & 0 & 0 & 0 & 0 & 0 \\ 0 & 0 & 0 & 0 & 0 & 0 & 0 & 0 & 0 & 0 & 0 & 0 \end{bmatrix} \tag{D-8}$$

Appendix E

Results EOM

This Appendix shows the results for the EOM for the 6 DOF model and the 12 DOF models.

E-1 6 DOF model

For each control system the EOM for the 6 DOF models are given.

$$\left(-\omega^2[\mathbf{M}+\mathbf{A}(\omega)]+i\omega[\mathbf{B}(\omega)]+[\mathbf{C}]\right)\begin{bmatrix}\hat{Y}_1\\ \hat{Z}_1\\ \hat{\Phi}_1\\ \hat{Y}_2\\ \hat{Z}_2\\ \hat{\Phi}_2\end{bmatrix}=\begin{bmatrix}\hat{F}_2\\ \hat{F}_3\\ \hat{M}_4\\ 0\\ 0\\ 0\end{bmatrix} \tag{E-1}$$

E-1-1 No compensation

A passive Ampelmann system has a fixed cylinder length. $\hat{Y}_1$, $\hat{Z}_1$, $\hat{\Phi}_1$, $\hat{Y}_2$, $\hat{Z}_2$ and $\hat{\Phi}_2$ are related by Equation 4-8. Substitution to Equation 5-14 yields the following expressions for $[\mathbf{M}+\mathbf{A}(\omega)]$, $[\mathbf{B}(\omega)]$ and $[\mathbf{C}]$.

$$[\mathbf{M}+\mathbf{A}(\omega)]=\begin{bmatrix}m_1+a_{22}(\omega) & a_{23}(\omega) & a_{24}(\omega) & m_2 & 0 & 0\\ a_{32}(\omega) & m_1+a_{33}(\omega) & a_{34}(\omega) & 0 & m_2 & 0\\ a_{42}(\omega) & a_{43}(\omega) & I_{xx1}+a_{44}(\omega) & -L_a m_2 & 0 & I_{xx2}\\ 0 & 0 & 0 & 0 & 0 & 0\\ 0 & 0 & 0 & 0 & 0 & 0\\ 0 & 0 & 0 & 0 & 0 & 0\end{bmatrix} \tag{E-2}$$

$$[\mathbf{B}(\omega)] = \begin{bmatrix} b_{22}(\omega) & b_{23}(\omega) & b_{24}(\omega) & 0 & 0 & 0 \\ b_{32}(\omega) & b_{33}(\omega) & b_{34}(\omega) & 0 & 0 & 0 \\ b_{42}(\omega) & b_{43}(\omega) & b_{44}(\omega) & 0 & 0 & 0 \\ 0 & 0 & 0 & 0 & 0 & 0 \\ 0 & 0 & 0 & 0 & 0 & 0 \\ 0 & 0 & 0 & 0 & 0 & 0 \end{bmatrix} \tag{E-3}$$

$$[\mathbf{C}] = \begin{bmatrix} c_{22} & c_{23} & c_{24} & 0 & 0 & 0 \\ c_{32} & c_{33} & c_{34} & 0 & 0 & 0 \\ -m_2 g + c_{42} & c_{43} & c_{44} & m_2 g & 0 & 0 \\ 1 & 0 & -L_a & -1 & 0 & 0 \\ 0 & 1 & 0 & 0 & 0-1 & 0 \\ 0 & 0 & 1 & 0 & 0 & -1 \end{bmatrix} \tag{E-4}$$

E-1-2 Perfect compensation

The TD is motionless. $\hat{Y}_2$, $\hat{Z}_2$ and $\hat{\Phi}_2$ are described by Equation 4-9. Substitution to Equation 5-14 yields the following expressions for $[\mathbf{M} + \mathbf{A}(\omega)]$, $[\mathbf{B}(\omega)]$ and $[\mathbf{C}]$.

$$[\mathbf{M} + \mathbf{A}(\omega)] = \begin{bmatrix} m_1 + a_{22}(\omega) & a_{23}(\omega) & a_{24}(\omega) & m_2 & 0 & 0 \\ a_{32}(\omega) & m_1 + a_{33}(\omega) & a_{34}(\omega) & 0 & m_2 & 0 \\ a_{42}(\omega) & a_{43}(\omega) & I_{xx1} + a_{44}(\omega) & -L_a m_2 & 0 & I_{xx2} \\ 0 & 0 & 0 & 0 & 0 & 0 \\ 0 & 0 & 0 & 0 & 0 & 0 \\ 0 & 0 & 0 & 0 & 0 & 0 \end{bmatrix} \tag{E-5}$$

$$[\mathbf{B}(\omega)] = \begin{bmatrix} b_{22}(\omega) & b_{23}(\omega) & b_{24}(\omega) & 0 & 0 & 0 \\ b_{32}(\omega) & b_{33}(\omega) & b_{34}(\omega) & 0 & 0 & 0 \\ b_{42}(\omega) & b_{43}(\omega) & b_{44}(\omega) & 0 & 0 & 0 \\ 0 & 0 & 0 & 0 & 0 & 0 \\ 0 & 0 & 0 & 0 & 0 & 0 \\ 0 & 0 & 0 & 0 & 0 & 0 \end{bmatrix} \tag{E-6}$$

$$[\mathbf{C}] = \begin{bmatrix} c_{22} & c_{23} & c_{24} & 0 & 0 & 0 \\ c_{32} & c_{33} & c_{34} & 0 & 0 & 0 \\ -m_2 g + c_{42} & c_{43} & c_{44} & m_2 g & 0 & 0 \\ 0 & 0 & 0 & 1 & 0 & 0 \\ 0 & 0 & 0 & 0 & 1 & 0 \\ 0 & 0 & 0 & 0 & 0 & 1 \end{bmatrix} \tag{E-7}$$

E-1-3 Filter compensation

In Filter compensation the TD motions are a results of the vessel motions and the negative of the filtered vessel motions. $\hat{Y}_1$, $\hat{Z}_1$, $\hat{\Phi}_1$, $\hat{Y}_2$, $\hat{Z}_2$ and $\hat{\Phi}_2$ are related by Equation 4-15. Substitution to Equation 5-14 yields the following expressions for $[\mathbf{M} + \mathbf{A}(\omega)]$, $[\mathbf{B}(\omega)]$ and $[\mathbf{C}]$.

$$[\mathbf{M}+\mathbf{A}(\omega)] = \begin{bmatrix} m_1+a_{22}(\omega) & a_{23}(\omega) & a_{24}(\omega) & m_2 & 0 & 0 \\ a_{32}(\omega) & m_1+a_{33}(\omega) & a_{34}(\omega) & 0 & m_2 & 0 \\ a_{42}(\omega) & a_{43}(\omega) & I_{xx1}+a_{44}(\omega) & -L_a m_2 & 0 & I_{xx2} \\ -1 & 0 & L_a & 1 & 0 & 0 \\ 0 & -1 & 0 & 0 & 1 & 0 \\ 0 & 0 & -1 & 0 & 0 & 1 \end{bmatrix} \tag{E-8}$$

$$[\mathbf{B}(\omega)] = \begin{bmatrix} b_{22}(\omega) & b_{23}(\omega) & b_{24}(\omega) & 0 & 0 & 0 \\ b_{32}(\omega) & b_{33}(\omega) & b_{34}(\omega) & 0 & 0 & 0 \\ b_{42}(\omega) & b_{43}(\omega) & b_{44}(\omega) & 0 & 0 & 0 \\ -2\omega_c & 0 & 2\omega_c L_a & 2\omega_c & 0 & 0 \\ 0 & -2\omega_c & 0 & 0 & 2\omega_c & 0 \\ 0 & 0 & -2\omega_c & 0 & 0 & 2\omega_c \end{bmatrix} \tag{E-9}$$

$$[\mathbf{C}] = \begin{bmatrix} c_{22} & c_{23} & c_{24} & 0 & 0 & 0 \\ c_{32} & c_{33} & c_{34} & 0 & 0 & 0 \\ -m_2 g + c_{42} & c_{43} & c_{44} & m_2 g & 0 & 0 \\ 0 & 0 & 0 & \omega_c^2 & 0 & 0 \\ 0 & 0 & 0 & 0 & \omega_c^2 & 0 \\ 0 & 0 & 0 & 0 & 0 & \omega_c^2 \end{bmatrix} \tag{E-10}$$

E-2 6 DOF model, include translation of Ampelmann location

For each control system the final expressions for $[\mathbf{M}+\mathbf{A}(\omega)]$, $[\mathbf{B}(\omega)]$ and $[\mathbf{C}]$ are given.

E-2-1 No compensation

A passive Ampelmann system has a fixed cylinder length. $\hat{Y}_1$, $\hat{Z}_1$, $\hat{\Phi}_1$, $\hat{Y}_2$, $\hat{Z}_2$ and $\hat{\Phi}_2$ are related by Equation 4-8. Substitution to Equation 6-5 yields the following expression for $[\mathbf{M}+\mathbf{A}(\omega)]$, $[\mathbf{B}(\omega)]$ and $[\mathbf{C}]$.

$$[\mathbf{M}+\mathbf{A}(\omega)] = \begin{bmatrix} m_1+a_{22}(\omega) & a_{23}(\omega) & a_{24}(\omega) & m_2 & 0 & 0 \\ a_{32}(\omega) & m_1+a_{33}(\omega) & a_{34}(\omega) & 0 & m2 & 0 \\ a_{42}(\omega) & a_{43}(\omega) & I_{xx1}+a_{44}(\omega) & -(L_a+L_z)m_2 & L_y m_2 & I_{xx2} \\ 0 & 0 & 0 & 0 & 0 & 0 \\ 0 & 0 & 0 & 0 & 0 & 0 \\ 0 & 0 & 0 & 0 & 0 & 0 \end{bmatrix} \tag{E-11}$$

$$[\mathbf{B}(\omega)] = \begin{bmatrix} b_{22}(\omega) & b_{23}(\omega) & b_{24}(\omega) & 0 & 0 & 0 \\ b_{32}(\omega) & b_{33}(\omega) & b_{34}(\omega) & 0 & 0 & 0 \\ b_{42}(\omega) & b_{43}(\omega) & b_{44}(\omega) & 0 & 0 & 0 \\ 0 & 0 & 0 & 0 & 0 & 0 \\ 0 & 0 & 0 & 0 & 0 & 0 \\ 0 & 0 & 0 & 0 & 0 & 0 \end{bmatrix} \tag{E-12}$$

$$[\mathbf{C}] = \begin{bmatrix} c_{22} & c_{23} & c_{24} & 0 & 0 & 0 \\ c_{32} & c_{33} & c_{34} & 0 & 0 & 0 \\ -m_2g + c_{42} & c_{43} & c_{44} & m_2g & 0 & 0 \\ 1 & 0 & -(L_a + L_z) & -1 & 0 & 0 \\ 0 & 1 & L_y & 0 & -1 & 0 \\ 0 & 0 & 1 & 0 & 0 & -1 \end{bmatrix} \tag{E-13}$$

E-2-2 Perfect compensation

The TD is motionless. $\hat{Y}_2$, $\hat{Z}_2$ and $\hat{\Phi}_2$ are described by Equation 4-9. Substitution to Equation 6-5 yields the following expression for $[\mathbf{M} + \mathbf{A}(\omega)]$, $[\mathbf{B}(\omega)]$ and $[\mathbf{C}]$.

$$[\mathbf{M} + \mathbf{A}(\omega)] = \begin{bmatrix} m_1 + a_{22}(\omega) & a_{23}(\omega) & a_{24}(\omega) & m_2 & 0 & 0 \\ a_{32}(\omega) & m_1 + a_{33}(\omega) & a_{34}(\omega) & 0 & m2 & 0 \\ a_{42}(\omega) & a_{43}(\omega) & I_{xx1} + a_{44}(\omega) & -(L_a + L_z)m_2 & L_y m_2 & I_{xx2} \\ 0 & 0 & 0 & 0 & 0 & 0 \\ 0 & 0 & 0 & 0 & 0 & 0 \\ 0 & 0 & 0 & 0 & 0 & 0 \end{bmatrix} \tag{E-14}$$

$$[\mathbf{B}(\omega)] = \begin{bmatrix} b_{22}(\omega) & b_{23}(\omega) & b_{24}(\omega) & 0 & 0 & 0 \\ b_{32}(\omega) & b_{33}(\omega) & b_{34}(\omega) & 0 & 0 & 0 \\ b_{42}(\omega) & b_{43}(\omega) & b_{44}(\omega) & 0 & 0 & 0 \\ 0 & 0 & 0 & 0 & 0 & 0 \\ 0 & 0 & 0 & 0 & 0 & 0 \\ 0 & 0 & 0 & 0 & 0 & 0 \end{bmatrix} \tag{E-15}$$

$$[\mathbf{C}] = \begin{bmatrix} c_{22} & c_{23} & c_{24} & 0 & 0 & 0 \\ c_{32} & c_{33} & c_{34} & 0 & 0 & 0 \\ -m_2g + c_{42} & c_{43} & c_{44} & m_2g & 0 & 0 \\ 0 & 0 & 0 & 1 & 0 & 0 \\ 0 & 0 & 0 & 0 & 1 & 0 \\ 0 & 0 & 0 & 0 & 0 & 1 \end{bmatrix} \tag{E-16}$$

E-2-3 Filter compensation

In Filter compensation the TD motions are a result of the vessel motions and the negative of the filtered vessel motions. $\hat{Y}_1$, $\hat{Z}_1$, $\hat{\Phi}_1$, $\hat{Y}_2$, $\hat{Z}_2$ and $\hat{\Phi}_2$ are related by Equation 4-15. Substitution to Equation 6-5 yields the following expression for $[\mathbf{M} + \mathbf{A}(\omega)]$, $[\mathbf{B}(\omega)]$ and $[\mathbf{C}]$.

$$[\mathbf{M} + \mathbf{A}(\omega)] = \begin{bmatrix} m_1 + a_{22}(\omega) & a_{23}(\omega) & a_{24}(\omega) & m_2 & 0 & 0 \\ a_{32}(\omega) & m_1 + a_{33}(\omega) & a_{34}(\omega) & 0 & m2 & 0 \\ a_{42}(\omega) & a_{43}(\omega) & I_{xx1} + a_{44}(\omega) & -(L_a + L_z)m_2 & L_y m_2 & I_{xx2} \\ 1 & 0 & -(L_z + L_a) & -1 & 0 & 0 \\ 0 & 1 & L_y & 0 & -1 & 0 \\ 0 & 0 & 1 & 0 & 0 & -1 \end{bmatrix} \tag{E-17}$$

$$[\mathbf{B}(\omega)] = \begin{bmatrix} b_{22}(\omega) & b_{23}(\omega) & b_{24}(\omega) & 0 & 0 & 0 \\ b_{32}(\omega) & b_{33}(\omega) & b_{34}(\omega) & 0 & 0 & 0 \\ b_{42}(\omega) & b_{43}(\omega) & b_{44}(\omega) & 0 & 0 & 0 \\ 2\omega_c & 0 & -2\omega_c(L_a + L_z) & -2\omega_c & 0 & 0 \\ 0 & 2\omega_c & 2\omega_c L_y & 0 & -2\omega_c & 0 \\ 0 & 0 & 2\omega_c & 0 & 0 & -2\omega_c \end{bmatrix} \tag{E-18}$$

$$[\mathbf{C}] = \begin{bmatrix} c_{22} & c_{23} & c_{24} & 0 & 0 & 0 \\ c_{32} & c_{33} & c_{34} & 0 & 0 & 0 \\ -m_2 g + c_{42} & c_{43} & c_{44} & m_2 g & 0 & 0 \\ 0 & 0 & 0 & -\omega_c^2 & 0 & 0 \\ 0 & 0 & 0 & 0 & -\omega_c^2 & 0 \\ 0 & 0 & 0 & 0 & 0 & -\omega_c^2 \end{bmatrix} \tag{E-19}$$

E-3 12 DOF model

E-3-1 No compensation

A passive Ampelmann system has a fixed cylinder length. $\hat{X}_1$, $\hat{Y}_1$, $\hat{Z}_1$, $\hat{\Phi}_1$, $\hat{\Theta}_1$, $\hat{\Psi}_1$, $\hat{X}_2$, $\hat{Y}_2$, $\hat{Z}_2$, $\hat{\Phi}_2$, $\hat{\Theta}_2$ and $\hat{\Psi}_2$ are related by Equation 4-8. Substitution to Equation 6-13 yields the expression for $[\mathbf{M} + \mathbf{A}(\omega)]$, $[\mathbf{B}(\omega)]$ and $[\mathbf{C}]$.

$$[\mathbf{M} + \mathbf{A}(\omega)] = \begin{bmatrix} m_1 + a_{11}(\omega) & a_{12}(\omega) & a_{13}(\omega) & a_{14}(\omega) & a_{15}(\omega) & a_{16}(\omega) & m_2 & 0 & 0 & 0 & 0 & 0 \\ a_{21}(\omega) & m_1 + a_{22}(\omega) & a_{23}(\omega) & a_{24}(\omega) & a_{25}(\omega) & a_{26}(\omega) & 0 & m_2 & 0 & 0 & 0 & 0 \\ a_{31}(\omega) & a_{32}(\omega) & m_1 + a_{33}(\omega) & a_{34}(\omega) & a_{35}(\omega) & a_{36}(\omega) & 0 & 0 & m_2 & 0 & 0 & 0 \\ a_{41}(\omega) & a_{42}(\omega) & a_{43}(\omega) & I_{xx1} + a_{44}(\omega) & a_{45}(\omega) & a_{46}(\omega) & 0 & -L_a m_2 & 0 & I_{xx2} & 0 & 0 \\ a_{51}(\omega) & a_{52}(\omega) & a_{53}(\omega) & a_{54}(\omega) & I_{yy1} + a_{55}(\omega) & a_{56}(\omega) & L_a m_2 & 0 & 0 & 0 & I_{yy2} & 0 \\ a_{61}(\omega) & a_{62}(\omega) & a_{63}(\omega) & a_{64}(\omega) & a_{65}(\omega) & I_{zz1} + a_{66}(\omega) & 0 & 0 & 0 & 0 & 0 & I_{zz2} \\ 0 & 0 & 0 & 0 & 0 & 0 & 0 & 0 & 0 & 0 & 0 & 0 \\ 0 & 0 & 0 & 0 & 0 & 0 & 0 & 0 & 0 & 0 & 0 & 0 \\ 0 & 0 & 0 & 0 & 0 & 0 & 0 & 0 & 0 & 0 & 0 & 0 \\ 0 & 0 & 0 & 0 & 0 & 0 & 0 & 0 & 0 & 0 & 0 & 0 \\ 0 & 0 & 0 & 0 & 0 & 0 & 0 & 0 & 0 & 0 & 0 & 0 \\ 0 & 0 & 0 & 0 & 0 & 0 & 0 & 0 & 0 & 0 & 0 & 0 \end{bmatrix} \tag{E-20}$$

$$[\mathbf{B}(\omega)] = \begin{bmatrix} b_{11}(\omega) & b_{12}(\omega) & b_{13}(\omega) & b_{14}(\omega) & b_{15}(\omega) & b_{16}(\omega) & 0 & 0 & 0 & 0 & 0 & 0 \\ b_{21}(\omega) & b_{22}(\omega) & b_{23}(\omega) & b_{24}(\omega) & b_{25}(\omega) & b_{26}(\omega) & 0 & 0 & 0 & 0 & 0 & 0 \\ b_{31}(\omega) & b_{32}(\omega) & b_{33}(\omega) & b_{34}(\omega) & b_{35}(\omega) & b_{36}(\omega) & 0 & 0 & 0 & 0 & 0 & 0 \\ b_{41}(\omega) & b_{42}(\omega) & b_{43}(\omega) & b_{44}(\omega) & b_{45}(\omega) & b_{46}(\omega) & 0 & 0 & 0 & 0 & 0 & 0 \\ b_{51}(\omega) & b_{52}(\omega) & b_{53}(\omega) & b_{54}(\omega) & b_{55}(\omega) & b_{56}(\omega) & 0 & 0 & 0 & 0 & 0 & 0 \\ b_{61}(\omega) & b_{62}(\omega) & b_{63}(\omega) & b_{64}(\omega) & b_{65}(\omega) & b_{66}(\omega) & 0 & 0 & 0 & 0 & 0 & 0 \\ 0 & 0 & 0 & 0 & 0 & 0 & 0 & 0 & 0 & 0 & 0 & 0 \\ 0 & 0 & 0 & 0 & 0 & 0 & 0 & 0 & 0 & 0 & 0 & 0 \\ 0 & 0 & 0 & 0 & 0 & 0 & 0 & 0 & 0 & 0 & 0 & 0 \\ 0 & 0 & 0 & 0 & 0 & 0 & 0 & 0 & 0 & 0 & 0 & 0 \\ 0 & 0 & 0 & 0 & 0 & 0 & 0 & 0 & 0 & 0 & 0 & 0 \\ 0 & 0 & 0 & 0 & 0 & 0 & 0 & 0 & 0 & 0 & 0 & 0 \end{bmatrix} \tag{E-21}$$

$$[\mathbf{C}] = \begin{bmatrix} c_{11} & c_{12} & c_{13} & c_{14} & c_{15} & c_{16} & 0 & 0 & 0 & 0 & 0 & 0 \\ c_{21} & c_{22} & c_{23} & c_{24} & c_{25} & c_{26} & 0 & 0 & 0 & 0 & 0 & 0 \\ c_{31} & c_{32} & c_{33} & c_{34} & c_{35} & c_{36} & 0 & 0 & 0 & 0 & 0 & 0 \\ c_{41} & -m_2 g + c_{42} & c_{43} & c_{44} & c_{45} & c_{46} & 0 & m_2 g & 0 & 0 & 0 & 0 \\ m_2 g + c_{51} & c_{52} & c_{53} & c_{54} & c_{55} & c_{56} & -m_2 g & 0 & 0 & 0 & 0 & 0 \\ c_{61} & c_{62} & c_{63} & c_{64} & c_{65} & c_{66} & 0 & 0 & 0 & 0 & 0 & 0 \\ 1 & 0 & 0 & 0 & L_a & 0 & -1 & 0 & 0 & 0 & 0 & 0 \\ 0 & 1 & 0 & -L_a & 0 & 0 & 0 & -1 & 0 & 0 & 0 & 0 \\ 0 & 0 & 1 & 0 & 0 & 0 & 0 & 0 & -1 & 0 & 0 & 0 \\ 0 & 0 & 0 & 1 & 0 & 0 & 0 & 0 & 0 & -1 & 0 & 0 \\ 0 & 0 & 0 & 0 & 1 & 0 & 0 & 0 & 0 & 0 & -1 & 0 \\ 0 & 0 & 0 & 0 & 0 & 1 & 0 & 0 & 0 & 0 & 0 & -1 \end{bmatrix} \tag{E-22}$$

E-3-2 Perfect compensation

The TD is motionless. $\hat{X}_2$, $\hat{Y}_2$, $\hat{Z}_2$, $\hat{\Phi}_2$, $\hat{\Theta}_2$ and $\hat{\Psi}_2$ are related by Equation 4-9. Substitution to Equation 6-13 yields the expression for $[\mathbf{M}+\mathbf{A}(\omega)]$, $[\mathbf{B}(\omega)]$ and $[\mathbf{C}]$.

$$[\mathbf{M}+\mathbf{A}(\omega)] =$$

$$\begin{bmatrix}
m_1+a_{11}(\omega) & a_{12}(\omega) & a_{13}(\omega) & a_{14}(\omega) & a_{15}(\omega) & a_{16}(\omega) & m_2 & 0 & 0 & 0 & 0 & 0 \\
a_{21}(\omega) & m_1+a_{22}(\omega) & a_{23}(\omega) & a_{24}(\omega) & a_{25}(\omega) & a_{26}(\omega) & 0 & m_2 & 0 & 0 & 0 & 0 \\
a_{31}(\omega) & a_{32}(\omega) & m_1+a_{33}(\omega) & a_{34}(\omega) & a_{35}(\omega) & a_{36}(\omega) & 0 & 0 & m_2 & 0 & 0 & 0 \\
a_{41}(\omega) & a_{42}(\omega) & a_{43}(\omega) & I_{xx1}+a_{44}(\omega) & a_{45}(\omega) & a_{46}(\omega) & 0 & -L_a m_2 & 0 & I_{xx2} & 0 & 0 \\
a_{51}(\omega) & a_{52}(\omega) & a_{53}(\omega) & a_{54}(\omega) & I_{yy1}+a_{55}(\omega) & a_{56}(\omega) & L_a m_2 & 0 & 0 & 0 & I_{yy2} & 0 \\
a_{61}(\omega) & a_{62}(\omega) & a_{63}(\omega) & a_{64}(\omega) & a_{65}(\omega) & I_{zz1}+a_{66}(\omega) & 0 & 0 & 0 & 0 & 0 & I_{zz2} \\
0 & 0 & 0 & 0 & 0 & 0 & 0 & 0 & 0 & 0 & 0 & 0 \\
0 & 0 & 0 & 0 & 0 & 0 & 0 & 0 & 0 & 0 & 0 & 0 \\
0 & 0 & 0 & 0 & 0 & 0 & 0 & 0 & 0 & 0 & 0 & 0 \\
0 & 0 & 0 & 0 & 0 & 0 & 0 & 0 & 0 & 0 & 0 & 0 \\
0 & 0 & 0 & 0 & 0 & 0 & 0 & 0 & 0 & 0 & 0 & 0 \\
0 & 0 & 0 & 0 & 0 & 0 & 0 & 0 & 0 & 0 & 0 & 0
\end{bmatrix} \tag{E-23}$$

$$[\mathbf{B}(\omega)] = \begin{bmatrix}
b_{11}(\omega) & b_{12}(\omega) & b_{13}(\omega) & b_{14}(\omega) & b_{15}(\omega) & b_{16}(\omega) & 0 & 0 & 0 & 0 & 0 & 0 \\
b_{21}(\omega) & b_{22}(\omega) & b_{23}(\omega) & b_{24}(\omega) & b_{25}(\omega) & b_{26}(\omega) & 0 & 0 & 0 & 0 & 0 & 0 \\
b_{31}(\omega) & b_{32}(\omega) & b_{33}(\omega) & b_{34}(\omega) & b_{35}(\omega) & b_{36}(\omega) & 0 & 0 & 0 & 0 & 0 & 0 \\
b_{41}(\omega) & b_{42}(\omega) & b_{43}(\omega) & b_{44}(\omega) & b_{45}(\omega) & b_{46}(\omega) & 0 & 0 & 0 & 0 & 0 & 0 \\
b_{51}(\omega) & b_{52}(\omega) & b_{53}(\omega) & b_{54}(\omega) & b_{55}(\omega) & b_{56}(\omega) & 0 & 0 & 0 & 0 & 0 & 0 \\
b_{61}(\omega) & b_{62}(\omega) & b_{63}(\omega) & b_{64}(\omega) & b_{65}(\omega) & b_{66}(\omega) & 0 & 0 & 0 & 0 & 0 & 0 \\
0 & 0 & 0 & 0 & 0 & 0 & 0 & 0 & 0 & 0 & 0 & 0 \\
0 & 0 & 0 & 0 & 0 & 0 & 0 & 0 & 0 & 0 & 0 & 0 \\
0 & 0 & 0 & 0 & 0 & 0 & 0 & 0 & 0 & 0 & 0 & 0 \\
0 & 0 & 0 & 0 & 0 & 0 & 0 & 0 & 0 & 0 & 0 & 0 \\
0 & 0 & 0 & 0 & 0 & 0 & 0 & 0 & 0 & 0 & 0 & 0 \\
0 & 0 & 0 & 0 & 0 & 0 & 0 & 0 & 0 & 0 & 0 & 0
\end{bmatrix} \tag{E-24}$$

$$[\mathbf{C}] = \begin{bmatrix}
c_{11} & c_{12} & c_{13} & c_{14} & c_{15} & c_{16} & 0 & 0 & 0 & 0 & 0 & 0 \\
c_{21} & c_{22} & c_{23} & c_{24} & c_{25} & c_{26} & 0 & 0 & 0 & 0 & 0 & 0 \\
c_{31} & c_{32} & c_{33} & c_{34} & c_{35} & c_{36} & 0 & 0 & 0 & 0 & 0 & 0 \\
c_{41} & -m_2 g + c_{42} & c_{43} & c_{44} & c_{45} & c_{46} & 0 & m_2 g & 0 & 0 & 0 & 0 \\
m_2 g + c_{51} & c_{52} & c_{53} & c_{54} & c_{55} & c_{56} & -m_2 g & 0 & 0 & 0 & 0 & 0 \\
c_{61} & c_{62} & c_{63} & c_{64} & c_{65} & c_{66} & 0 & 0 & 0 & 0 & 0 & 0 \\
0 & 0 & 0 & 0 & 0 & 0 & 1 & 0 & 0 & 0 & 0 & 0 \\
0 & 0 & 0 & 0 & 0 & 0 & 0 & 1 & 0 & 0 & 0 & 0 \\
0 & 0 & 0 & 0 & 0 & 0 & 0 & 0 & 1 & 0 & 0 & 0 \\
0 & 0 & 0 & 0 & 0 & 0 & 0 & 0 & 0 & 1 & 0 & 0 \\
0 & 0 & 0 & 0 & 0 & 0 & 0 & 0 & 0 & 0 & 1 & 0 \\
0 & 0 & 0 & 0 & 0 & 0 & 0 & 0 & 0 & 0 & 0 & 1
\end{bmatrix} \tag{E-25}$$

E-3-3 Filter compensation

In Filter compensation the TD motions are a results of vessel motions and the negative of the filtered vessel motions. $\hat{X}_1$, $\hat{Y}_1$, $\hat{Z}_1$, $\hat{\Phi}_1$, $\hat{\Theta}_1$, $\hat{\Psi}_1$, $\hat{X}_2$, $\hat{Y}_2$, $\hat{Z}_2$, $\hat{\Phi}_2$, $\hat{\Theta}_2$ and $\hat{\Psi}_2$ are related by Equation 4-8. Substitution to Equation 6-13 yields the expression for $[\mathbf{M}+\mathbf{A}(\omega)]$, $[\mathbf{B}(\omega)]$ and $[\mathbf{C}]$.

$$[\mathbf{M}+\mathbf{A}(\omega)] =$$

$$\begin{bmatrix}
m_1+a_{11}(\omega) & a_{12}(\omega) & a_{13}(\omega) & a_{14}(\omega) & a_{15}(\omega) & a_{16}(\omega) & m_2 & 0 & 0 & 0 & 0 & 0 \\
a_{21}(\omega) & m_1+a_{22}(\omega) & a_{23}(\omega) & a_{24}(\omega) & a_{25}(\omega) & a_{26}(\omega) & 0 & m_2 & 0 & 0 & 0 & 0 \\
a_{31}(\omega) & a_{32}(\omega) & m_1+a_{33}(\omega) & a_{34}(\omega) & a_{35}(\omega) & a_{36}(\omega) & 0 & 0 & m_2 & 0 & 0 & 0 \\
a_{41}(\omega) & a_{42}(\omega) & a_{43}(\omega) & I_{xx1}+a_{44}(\omega) & a_{45}(\omega) & a_{46}(\omega) & 0 & -L_a m_2 & 0 & I_{xx2} & 0 & 0 \\
a_{51}(\omega) & a_{52}(\omega) & a_{53}(\omega) & a_{54}(\omega) & I_{yy1}+a_{55}(\omega) & a_{56}(\omega) & L_a m_2 & 0 & 0 & 0 & I_{yy2} & 0 \\
a_{61}(\omega) & a_{62}(\omega) & a_{63}(\omega) & a_{64}(\omega) & a_{65}(\omega) & I_{zz1}+a_{66}(\omega) & 0 & 0 & 0 & 0 & 0 & I_{zz2} \\
1 & 0 & 0 & 0 & L_a & 0 & -1 & 0 & 0 & 0 & 0 & 0 \\
0 & 1 & 0 & -L_a & 0 & 0 & 0 & -1 & 0 & 0 & 0 & 0 \\
0 & 0 & 1 & 0 & 0 & 0 & 0 & 0 & -1 & 0 & 0 & 0 \\
0 & 0 & 0 & 1 & 0 & 0 & 0 & 0 & 0 & -1 & 0 & 0 \\
0 & 0 & 0 & 0 & 1 & 0 & 0 & 0 & 0 & 0 & -1 & 0 \\
0 & 0 & 0 & 0 & 0 & 1 & 0 & 0 & 0 & 0 & 0 & -1
\end{bmatrix} \tag{E-26}$$

$$[\mathbf{B}(\omega)] = \begin{bmatrix}
b_{11}(\omega) & b_{12}(\omega) & b_{13}(\omega) & b_{14}(\omega) & b_{15}(\omega) & b_{16}(\omega) & 0 & 0 & 0 & 0 & 0 & 0 \\
b_{21}(\omega) & b_{22}(\omega) & b_{23}(\omega) & b_{24}(\omega) & b_{25}(\omega) & b_{26}(\omega) & 0 & 0 & 0 & 0 & 0 & 0 \\
b_{31}(\omega) & b_{32}(\omega) & b_{33}(\omega) & b_{34}(\omega) & b_{35}(\omega) & b_{36}(\omega) & 0 & 0 & 0 & 0 & 0 & 0 \\
b_{41}(\omega) & b_{42}(\omega) & b_{43}(\omega) & b_{44}(\omega) & b_{45}(\omega) & b_{46}(\omega) & 0 & 0 & 0 & 0 & 0 & 0 \\
b_{51}(\omega) & b_{52}(\omega) & b_{53}(\omega) & b_{54}(\omega) & b_{55}(\omega) & b_{56}(\omega) & 0 & 0 & 0 & 0 & 0 & 0 \\
b_{61}(\omega) & b_{62}(\omega) & b_{63}(\omega) & b_{64}(\omega) & b_{65}(\omega) & b_{66}(\omega) & 0 & 0 & 0 & 0 & 0 & 0 \\
2\omega_c & 0 & 0 & 0 & 2\omega_c L_a & 0 & -2\omega_c & 0 & 0 & 0 & 0 & 0 \\
0 & 2\omega_c & 0 & -2\omega_c L_a & 0 & 0 & 0 & -2\omega_c & 0 & 0 & 0 & 0 \\
0 & 0 & 2\omega_c & 0 & 0 & 0 & 0 & 0 & -2\omega_c & 0 & 0 & 0 \\
0 & 0 & 0 & 2\omega_c & 0 & 0 & 0 & 0 & 0 & -2\omega_c & 0 & 0 \\
0 & 0 & 0 & 0 & 2\omega_c & 0 & 0 & 0 & 0 & 0 & -2\omega_c & 0 \\
0 & 0 & 0 & 0 & 0 & 2\omega_c & 0 & 0 & 0 & 0 & 0 & -2\omega_c
\end{bmatrix} \tag{E-27}$$

$$
[\mathbf{C}] = \begin{bmatrix}
c_{11} & c_{12} & c_{13} & c_{14} & c_{15} & c_{16} & 0 & 0 & 0 & 0 & 0 & 0 \\
c_{21} & c_{22} & c_{23} & c_{24} & c_{25} & c_{26} & 0 & 0 & 0 & 0 & 0 & 0 \\
c_{31} & c_{32} & c_{33} & c_{34} & c_{35} & c_{36} & 0 & 0 & 0 & 0 & 0 & 0 \\
c_{41} & -m_2 g + c_{42} & c_{43} & c_{44} & c_{45} & c_{46} & 0 & m_2 g & 0 & 0 & 0 & 0 \\
m_2 g + c_{51} & c_{52} & c_{53} & c_{54} & c_{55} & c_{56} & -m_2 g & 0 & 0 & 0 & 0 & 0 \\
c_{61} & c_{62} & c_{63} & c_{64} & c_{65} & c_{66} & 0 & 0 & 0 & 0 & 0 & 0 \\
0 & 0 & 0 & 0 & 0 & 0 & -\omega_c^2 & 0 & 0 & 0 & 0 & 0 \\
0 & 0 & 0 & 0 & 0 & 0 & 0 & -\omega_c^2 & 0 & 0 & 0 & 0 \\
0 & 0 & 0 & 0 & 0 & 0 & 0 & 0 & -\omega_c^2 & 0 & 0 & 0 \\
0 & 0 & 0 & 0 & 0 & 0 & 0 & 0 & 0 & -\omega_c^2 & 0 & 0 \\
0 & 0 & 0 & 0 & 0 & 0 & 0 & 0 & 0 & 0 & -\omega_c^2 & 0 \\
0 & 0 & 0 & 0 & 0 & 0 & 0 & 0 & 0 & 0 & 0 & -\omega_c^2
\end{bmatrix} \tag{E-28}
$$

E-4 12 DOF model, include translation of Ampelmann location

For each control system the final expressions for $[\mathbf{M}+\mathbf{A}(\omega)]$, $[\mathbf{B}(\omega)]$ and $[\mathbf{C}]$ are given.

E-4-1 No compensation

A passive Ampelmann system has a fixed cylinder length. $\hat{X}_1$, $\hat{Y}_1$, $\hat{Z}_1$, $\hat{\Phi}_1$, $\hat{\Theta}_1$, $\hat{\Psi}_1$, $\hat{X}_2$, $\hat{Y}_2$, $\hat{Z}_2$, $\hat{\Phi}_2$, $\hat{\Theta}_2$ and $\hat{\Psi}_2$ are related by Equation 4-8. Substitution to Equation 6-17 yields the expression for $[\mathbf{M}+\mathbf{A}(\omega)]$, $[\mathbf{B}(\omega)]$ and $[\mathbf{C}]$.

$$
[\mathbf{M}+\mathbf{A}(\omega)] = \begin{bmatrix}
m_1 + a_{11}(\omega) & a_{12}(\omega) & a_{13}(\omega) & a_{14}(\omega) & a_{15}(\omega) & a_{16}(\omega) & m_2 & 0 & 0 & 0 & 0 & 0 \\
a_{21}(\omega) & m_1 + a_{22}(\omega) & a_{23}(\omega) & a_{24}(\omega) & a_{25}(\omega) & a_{26}(\omega) & 0 & m_2 & 0 & 0 & 0 & 0 \\
a_{31}(\omega) & a_{32}(\omega) & m_1 + a_{33}(\omega) & a_{34}(\omega) & a_{35}(\omega) & a_{36}(\omega) & 0 & 0 & m_2 & 0 & 0 & 0 \\
a_{41}(\omega) & a_{42}(\omega) & a_{43}(\omega) & I_{xx1} + a_{44}(\omega) & a_{45}(\omega) & a_{46}(\omega) & 0 & -(L_z + L_a)m_2 & L_y m_2 & I_{xx2} & 0 & 0 \\
a_{51}(\omega) & a_{52}(\omega) & a_{53}(\omega) & a_{54}(\omega) & I_{yy1} + a_{55}(\omega) & a_{56}(\omega) & (L_z + L_a)m_2 & 0 & -L_x m_2 & 0 & I_{yy2} & 0 \\
a_{61}(\omega) & a_{62}(\omega) & a_{63}(\omega) & a_{64}(\omega) & a_{65}(\omega) & I_{zz1} + a_{66}(\omega) & -m_2 L_y & L_x m_2 & 0 & 0 & 0 & I_{zz2} \\
0 & 0 & 0 & 0 & 0 & 0 & 0 & 0 & 0 & 0 & 0 & 0 \\
0 & 0 & 0 & 0 & 0 & 0 & 0 & 0 & 0 & 0 & 0 & 0 \\
0 & 0 & 0 & 0 & 0 & 0 & 0 & 0 & 0 & 0 & 0 & 0 \\
0 & 0 & 0 & 0 & 0 & 0 & 0 & 0 & 0 & 0 & 0 & 0 \\
0 & 0 & 0 & 0 & 0 & 0 & 0 & 0 & 0 & 0 & 0 & 0 \\
0 & 0 & 0 & 0 & 0 & 0 & 0 & 0 & 0 & 0 & 0 & 0
\end{bmatrix} \tag{E-29}
$$

$$
[\mathbf{B}(\omega)] = \begin{bmatrix}
b_{11}(\omega) & b_{12}(\omega) & b_{13}(\omega) & b_{14}(\omega) & b_{15}(\omega) & b_{16}(\omega) & 0 & 0 & 0 & 0 & 0 & 0 \\
b_{21}(\omega) & b_{22}(\omega) & b_{23}(\omega) & b_{24}(\omega) & b_{25}(\omega) & b_{26}(\omega) & 0 & 0 & 0 & 0 & 0 & 0 \\
b_{31}(\omega) & b_{32}(\omega) & b_{33}(\omega) & b_{34}(\omega) & b_{35}(\omega) & b_{36}(\omega) & 0 & 0 & 0 & 0 & 0 & 0 \\
b_{41}(\omega) & b_{42}(\omega) & b_{43}(\omega) & b_{44}(\omega) & b_{45}(\omega) & b_{46}(\omega) & 0 & 0 & 0 & 0 & 0 & 0 \\
b_{51}(\omega) & b_{52}(\omega) & b_{53}(\omega) & b_{54}(\omega) & b_{55}(\omega) & b_{56}(\omega) & 0 & 0 & 0 & 0 & 0 & 0 \\
b_{61}(\omega) & b_{62}(\omega) & b_{63}(\omega) & b_{64}(\omega) & b_{65}(\omega) & b_{66}(\omega) & 0 & 0 & 0 & 0 & 0 & 0 \\
0 & 0 & 0 & 0 & 0 & 0 & 0 & 0 & 0 & 0 & 0 & 0 \\
0 & 0 & 0 & 0 & 0 & 0 & 0 & 0 & 0 & 0 & 0 & 0 \\
0 & 0 & 0 & 0 & 0 & 0 & 0 & 0 & 0 & 0 & 0 & 0 \\
0 & 0 & 0 & 0 & 0 & 0 & 0 & 0 & 0 & 0 & 0 & 0 \\
0 & 0 & 0 & 0 & 0 & 0 & 0 & 0 & 0 & 0 & 0 & 0 \\
0 & 0 & 0 & 0 & 0 & 0 & 0 & 0 & 0 & 0 & 0 & 0
\end{bmatrix} \tag{E-30}
$$

$$
[\mathbf{C}] = \begin{bmatrix}
c_{11} & c_{12} & c_{13} & c_{14} & c_{15} & c_{16} & 0 & 0 & 0 & 0 & 0 & 0 \\
c_{21} & c_{22} & c_{23} & c_{24} & c_{25} & c_{26} & 0 & 0 & 0 & 0 & 0 & 0 \\
c_{31} & c_{32} & c_{33} & c_{34} & c_{35} & c_{36} & 0 & 0 & 0 & 0 & 0 & 0 \\
c_{41} & -m_2 g + c_{42} & c_{43} & c_{44} & c_{45} & c_{46} & 0 & m_2 g & 0 & 0 & 0 & 0 \\
m_2 g + c_{51} & c_{52} & c_{53} & c_{54} & c_{55} & c_{56} & -m_2 g & 0 & 0 & 0 & 0 & 0 \\
c_{61} & c_{62} & c_{63} & c_{64} & c_{65} & c_{66} & 0 & 0 & 0 & 0 & 0 & 0 \\
1 & 0 & 0 & 0 & (Lz + La) & -Ly & -1 & 0 & 0 & 0 & 0 & 0 \\
0 & 1 & 0 & -(Lz + La) & 0 & Lx & 0 & -1 & 0 & 0 & 0 & 0 \\
0 & 0 & 1 & Ly & -Lx & 0 & 0 & 0 & -1 & 0 & 0 & 0 \\
0 & 0 & 0 & 1 & 0 & 0 & 0 & 0 & 0 & -1 & 0 & 0 \\
0 & 0 & 0 & 0 & 1 & 0 & 0 & 0 & 0 & 0 & -1 & 0 \\
0 & 0 & 0 & 0 & 0 & 1 & 0 & 0 & 0 & 0 & 0 & -1
\end{bmatrix} \tag{E-31}
$$

E-4-2 Perfect compensation

The TD is motionless. $\hat{X}_2$, $\hat{Y}_2$, $\hat{Z}_2$, $\hat{\Phi}_2$, $\hat{\Theta}_2$ and $\hat{\Psi}_2$ are related by Equation 4-9. Substitution to Equation 6-17 yield the expression for $[\mathbf{M}+\mathbf{A}(\omega)]$, $[\mathbf{B}(\omega)]$ and $[\mathbf{C}]$.

$$[\mathbf{M}+\mathbf{A}(\omega)] = \begin{bmatrix} m_1+a_{11}(\omega) & a_{12}(\omega) & a_{13}(\omega) & a_{14}(\omega) & a_{15}(\omega) & a_{16}(\omega) & m_2 & 0 & 0 & 0 & 0 & 0 \\ a_{21}(\omega) & m_1+a_{22}(\omega) & a_{23}(\omega) & a_{24}(\omega) & a_{25}(\omega) & a_{26}(\omega) & 0 & m_2 & 0 & 0 & 0 & 0 \\ a_{31}(\omega) & a_{32}(\omega) & m_1+a_{33}(\omega) & a_{34}(\omega) & a_{35}(\omega) & a_{36}(\omega) & 0 & 0 & m_2 & 0 & 0 & 0 \\ a_{41}(\omega) & a_{42}(\omega) & a_{43}(\omega) & I_{xx1}+a_{44}(\omega) & a_{45}(\omega) & a_{46}(\omega) & 0 & -(L_z+L_a)m_2 & L_y m_2 & I_{xx2} & 0 & 0 \\ a_{51}(\omega) & a_{52}(\omega) & a_{53}(\omega) & a_{54}(\omega) & I_{yy1}+a_{55}(\omega) & a_{56}(\omega) & (L_z+L_a)m_2 & 0 & -L_x m_2 & 0 & I_{yy2} & 0 \\ a_{61}(\omega) & a_{62}(\omega) & a_{63}(\omega) & a_{64}(\omega) & a_{65}(\omega) & I_{zz1}+a_{66}(\omega) & -m_2 L_y & L_x m_2 & 0 & 0 & 0 & I_{zz2} \\ 0 & 0 & 0 & 0 & 0 & 0 & 0 & 0 & 0 & 0 & 0 & 0 \\ 0 & 0 & 0 & 0 & 0 & 0 & 0 & 0 & 0 & 0 & 0 & 0 \\ 0 & 0 & 0 & 0 & 0 & 0 & 0 & 0 & 0 & 0 & 0 & 0 \\ 0 & 0 & 0 & 0 & 0 & 0 & 0 & 0 & 0 & 0 & 0 & 0 \\ 0 & 0 & 0 & 0 & 0 & 0 & 0 & 0 & 0 & 0 & 0 & 0 \\ 0 & 0 & 0 & 0 & 0 & 0 & 0 & 0 & 0 & 0 & 0 & 0 \end{bmatrix} \tag{E-32}$$

$$[\mathbf{B}(\omega)] = \begin{bmatrix} b_{11}(\omega) & b_{12}(\omega) & b_{13}(\omega) & b_{14}(\omega) & b_{15}(\omega) & b_{16}(\omega) & 0 & 0 & 0 & 0 & 0 & 0 \\ b_{21}(\omega) & b_{22}(\omega) & b_{23}(\omega) & b_{24}(\omega) & b_{25}(\omega) & b_{26}(\omega) & 0 & 0 & 0 & 0 & 0 & 0 \\ b_{31}(\omega) & b_{32}(\omega) & b_{33}(\omega) & b_{34}(\omega) & b_{35}(\omega) & b_{36}(\omega) & 0 & 0 & 0 & 0 & 0 & 0 \\ b_{41}(\omega) & b_{42}(\omega) & b_{43}(\omega) & b_{44}(\omega) & b_{45}(\omega) & b_{46}(\omega) & 0 & 0 & 0 & 0 & 0 & 0 \\ b_{51}(\omega) & b_{52}(\omega) & b_{53}(\omega) & b_{54}(\omega) & b_{55}(\omega) & b_{56}(\omega) & 0 & 0 & 0 & 0 & 0 & 0 \\ b_{61}(\omega) & b_{62}(\omega) & b_{63}(\omega) & b_{64}(\omega) & b_{65}(\omega) & b_{66}(\omega) & 0 & 0 & 0 & 0 & 0 & 0 \\ 0 & 0 & 0 & 0 & 0 & 0 & 0 & 0 & 0 & 0 & 0 & 0 \\ 0 & 0 & 0 & 0 & 0 & 0 & 0 & 0 & 0 & 0 & 0 & 0 \\ 0 & 0 & 0 & 0 & 0 & 0 & 0 & 0 & 0 & 0 & 0 & 0 \\ 0 & 0 & 0 & 0 & 0 & 0 & 0 & 0 & 0 & 0 & 0 & 0 \\ 0 & 0 & 0 & 0 & 0 & 0 & 0 & 0 & 0 & 0 & 0 & 0 \\ 0 & 0 & 0 & 0 & 0 & 0 & 0 & 0 & 0 & 0 & 0 & 0 \end{bmatrix} \tag{E-33}$$

$$[\mathbf{C}] = \begin{bmatrix} c_{11} & c_{12} & c_{13} & c_{14} & c_{15} & c_{16} & 0 & 0 & 0 & 0 & 0 & 0 \\ c_{21} & c_{22} & c_{23} & c_{24} & c_{25} & c_{26} & 0 & 0 & 0 & 0 & 0 & 0 \\ c_{31} & c_{32} & c_{33} & c_{34} & c_{35} & c_{36} & 0 & 0 & 0 & 0 & 0 & 0 \\ c_{41} & -m_2 g + c_{42} & c_{43} & c_{44} & c_{45} & c_{46} & 0 & m_2 g & 0 & 0 & 0 & 0 \\ m_2 g + c_{51} & c_{52} & c_{53} & c_{54} & c_{55} & c_{56} & -m_2 g & 0 & 0 & 0 & 0 & 0 \\ c_{61} & c_{62} & c_{63} & c_{64} & c_{65} & c_{66} & 0 & 0 & 0 & 0 & 0 & 0 \\ 0 & 0 & 0 & 0 & 0 & 0 & 1 & 0 & 0 & 0 & 0 & 0 \\ 0 & 0 & 0 & 0 & 0 & 0 & 0 & 1 & 0 & 0 & 0 & 0 \\ 0 & 0 & 0 & 0 & 0 & 0 & 0 & 0 & 1 & 0 & 0 & 0 \\ 0 & 0 & 0 & 0 & 0 & 0 & 0 & 0 & 0 & 1 & 0 & 0 \\ 0 & 0 & 0 & 0 & 0 & 0 & 0 & 0 & 0 & 0 & 1 & 0 \\ 0 & 0 & 0 & 0 & 0 & 0 & 0 & 0 & 0 & 0 & 0 & 1 \end{bmatrix} \tag{E-34}$$

E-4-3 Filter compensation

In Filter compensation the TD motions are a results of vessel motions and the negative of the filtered vessel motions. $\hat{X}_1$, $\hat{Y}_1$, $\hat{Z}_1$, $\hat{\Phi}_1$, $\hat{\Theta}_1$, $\hat{\Psi}_1$, $\hat{X}_2$, $\hat{Y}_2$, $\hat{Z}_2$, $\hat{\Phi}_2$, $\hat{\Theta}_2$ and $\hat{\Psi}_2$ are related by Equation 4-8. Substitution to Equation 6-17 yields the expression for $[\mathbf{M}+\mathbf{A}(\omega)]$, $[\mathbf{B}(\omega)]$ and $[\mathbf{C}]$.

$$[\mathbf{M}+\mathbf{A}(\omega)] = \begin{bmatrix} m_1+a_{11}(\omega) & a_{12}(\omega) & a_{13}(\omega) & a_{14}(\omega) & a_{15}(\omega) & a_{16}(\omega) & m_2 & 0 & 0 & 0 & 0 & 0 \\ a_{21}(\omega) & m_1+a_{22}(\omega) & a_{23}(\omega) & a_{24}(\omega) & a_{25}(\omega) & a_{26}(\omega) & 0 & m_2 & 0 & 0 & 0 & 0 \\ a_{31}(\omega) & a_{32}(\omega) & m_1+a_{33}(\omega) & a_{34}(\omega) & a_{35}(\omega) & a_{36}(\omega) & 0 & 0 & m_2 & 0 & 0 & 0 \\ a_{41}(\omega) & a_{42}(\omega) & a_{43}(\omega) & I_{xx1}+a_{44}(\omega) & a_{45}(\omega) & a_{46}(\omega) & 0 & -(L_z+L_a)m_2 & L_y m_2 & I_{xx2} & 0 & 0 \\ a_{51}(\omega) & a_{52}(\omega) & a_{53}(\omega) & a_{54}(\omega) & I_{yy1}+a_{55}(\omega) & a_{56}(\omega) & (L_z+L_a)m_2 & 0 & -L_x m_2 & 0 & I_{yy2} & 0 \\ a_{61}(\omega) & a_{62}(\omega) & a_{63}(\omega) & a_{64}(\omega) & a_{65}(\omega) & I_{zz1}+a_{66}(\omega) & -m_2 L_y & L_x m_2 & 0 & 0 & 0 & I_{zz2} \\ 1 & 0 & 0 & 0 & (L_z+L_a) & -L_y & -1 & 0 & 0 & 0 & 0 & 0 \\ 0 & 1 & 0 & -(L_z+L_a) & 0 & L_x & 0 & -1 & 0 & 0 & 0 & 0 \\ 0 & 0 & 1 & L_y & -L_x & 0 & 0 & 0 & -1 & 0 & 0 & 0 \\ 0 & 0 & 0 & 1 & 0 & 0 & 0 & 0 & 0 & -1 & 0 & 0 \\ 0 & 0 & 0 & 0 & 1 & 0 & 0 & 0 & 0 & 0 & -1 & 0 \\ 0 & 0 & 0 & 0 & 0 & 1 & 0 & 0 & 0 & 0 & 0 & -1 \end{bmatrix} \tag{E-35}$$

$$[\mathbf{B}(\omega)] = \begin{bmatrix} b_{11}(\omega) & b_{12}(\omega) & b_{13}(\omega) & b_{14}(\omega) & b_{15}(\omega) & b_{16}(\omega) & 0 & 0 & 0 & 0 & 0 & 0 \\ b_{21}(\omega) & b_{22}(\omega) & b_{23}(\omega) & b_{24}(\omega) & b_{25}(\omega) & b_{26}(\omega) & 0 & 0 & 0 & 0 & 0 & 0 \\ b_{31}(\omega) & b_{32}(\omega) & b_{33}(\omega) & b_{34}(\omega) & b_{35}(\omega) & b_{36}(\omega) & 0 & 0 & 0 & 0 & 0 & 0 \\ b_{41}(\omega) & b_{42}(\omega) & b_{43}(\omega) & b_{44}(\omega) & b_{45}(\omega) & b_{46}(\omega) & 0 & 0 & 0 & 0 & 0 & 0 \\ b_{51}(\omega) & b_{52}(\omega) & b_{53}(\omega) & b_{54}(\omega) & b_{55}(\omega) & b_{56}(\omega) & 0 & 0 & 0 & 0 & 0 & 0 \\ b_{61}(\omega) & b_{62}(\omega) & b_{63}(\omega) & b_{64}(\omega) & b_{65}(\omega) & b_{66}(\omega) & 0 & 0 & 0 & 0 & 0 & 0 \\ 2\omega_c & 0 & 0 & 0 & 2\omega_c(L_z+L_a) & -2\omega_c L_y & -2\omega_c & 0 & 0 & 0 & 0 & 0 \\ 0 & 2\omega_c & 0 & -2\omega_c(L_z+L_a) & 0 & 2\omega_c L_x & 0 & -2\omega_c & 0 & 0 & 0 & 0 \\ 0 & 0 & 2\omega_c & 2\omega_c L_y & -2\omega_c L_x & 0 & 0 & 0 & -2\omega_c & 0 & 0 & 0 \\ 0 & 0 & 0 & 2\omega_c & 0 & 0 & 0 & 0 & 0 & -2\omega_c & 0 & 0 \\ 0 & 0 & 0 & 0 & 2\omega_c & 0 & 0 & 0 & 0 & 0 & -2\omega_c & 0 \\ 0 & 0 & 0 & 0 & 0 & 2\omega_c & 0 & 0 & 0 & 0 & 0 & -2\omega_c \end{bmatrix} \tag{E-36}$$

$$[\mathbf{C}] = \begin{bmatrix} c_{11} & c_{12} & c_{13} & c_{14} & c_{15} & c_{16} & 0 & 0 & 0 & 0 & 0 & 0 \\ c_{21} & c_{22} & c_{23} & c_{24} & c_{25} & c_{26} & 0 & 0 & 0 & 0 & 0 & 0 \\ c_{31} & c_{32} & c_{33} & c_{34} & c_{35} & c_{36} & 0 & 0 & 0 & 0 & 0 & 0 \\ c_{41} & -m_2 g + c_{42} & c_{43} & c_{44} & c_{45} & c_{46} & 0 & m_2 g & 0 & 0 & 0 & 0 \\ m_2 g + c_{51} & c_{52} & c_{53} & c_{54} & c_{55} & c_{56} & -m_2 g & 0 & 0 & 0 & 0 & 0 \\ c_{61} & c_{62} & c_{63} & c_{64} & c_{65} & c_{66} & 0 & 0 & 0 & 0 & 0 & 0 \\ 0 & 0 & 0 & 0 & 0 & 0 & -\omega_c^2 & 0 & 0 & 0 & 0 & 0 \\ 0 & 0 & 0 & 0 & 0 & 0 & 0 & -\omega_c^2 & 0 & 0 & 0 & 0 \\ 0 & 0 & 0 & 0 & 0 & 0 & 0 & 0 & -\omega_c^2 & 0 & 0 & 0 \\ 0 & 0 & 0 & 0 & 0 & 0 & 0 & 0 & 0 & -\omega_c^2 & 0 & 0 \\ 0 & 0 & 0 & 0 & 0 & 0 & 0 & 0 & 0 & 0 & -\omega_c^2 & 0 \\ 0 & 0 & 0 & 0 & 0 & 0 & 0 & 0 & 0 & 0 & 0 & -\omega_c^2 \end{bmatrix} \tag{E-37}$$

Appendix F

Result appendix, validation

This appendix contains plots that illustrate the validation of the models presented in chapter 5 and 6.

F-1 DELFRAC results for wave incident angle 90 [deg]

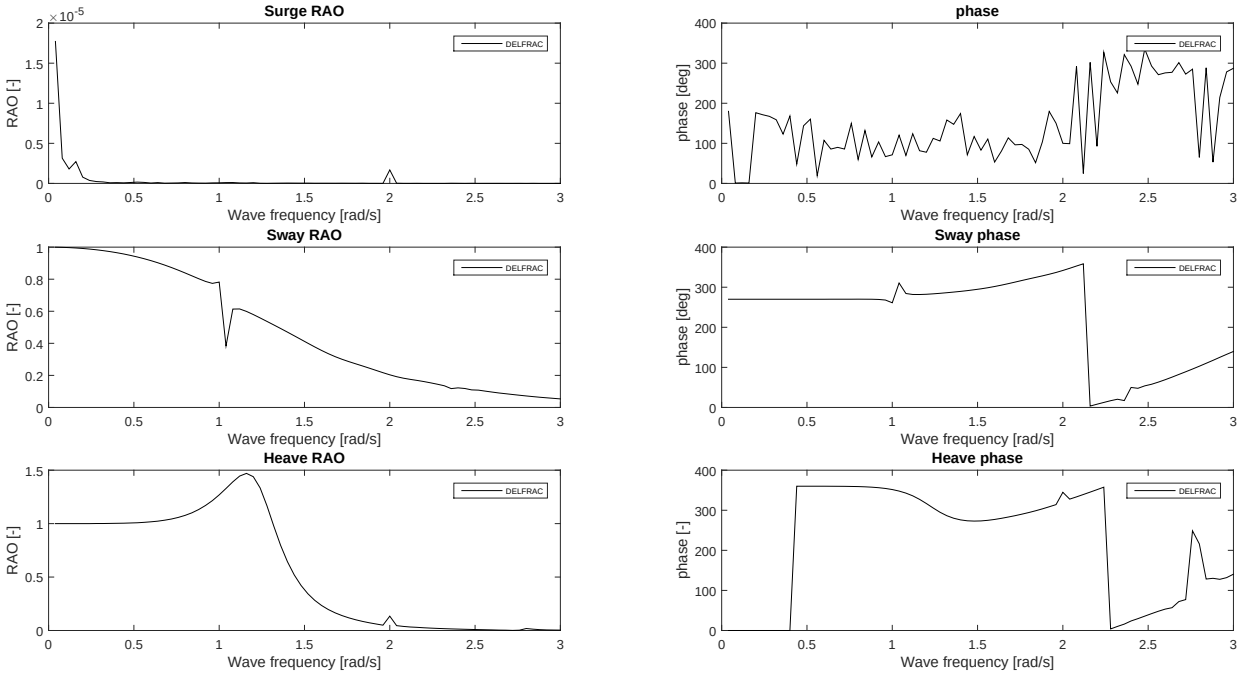

Figure F-1: DELFRAC results translation. $\lambda = 1[-]$, wave incident angle $90[deg]$

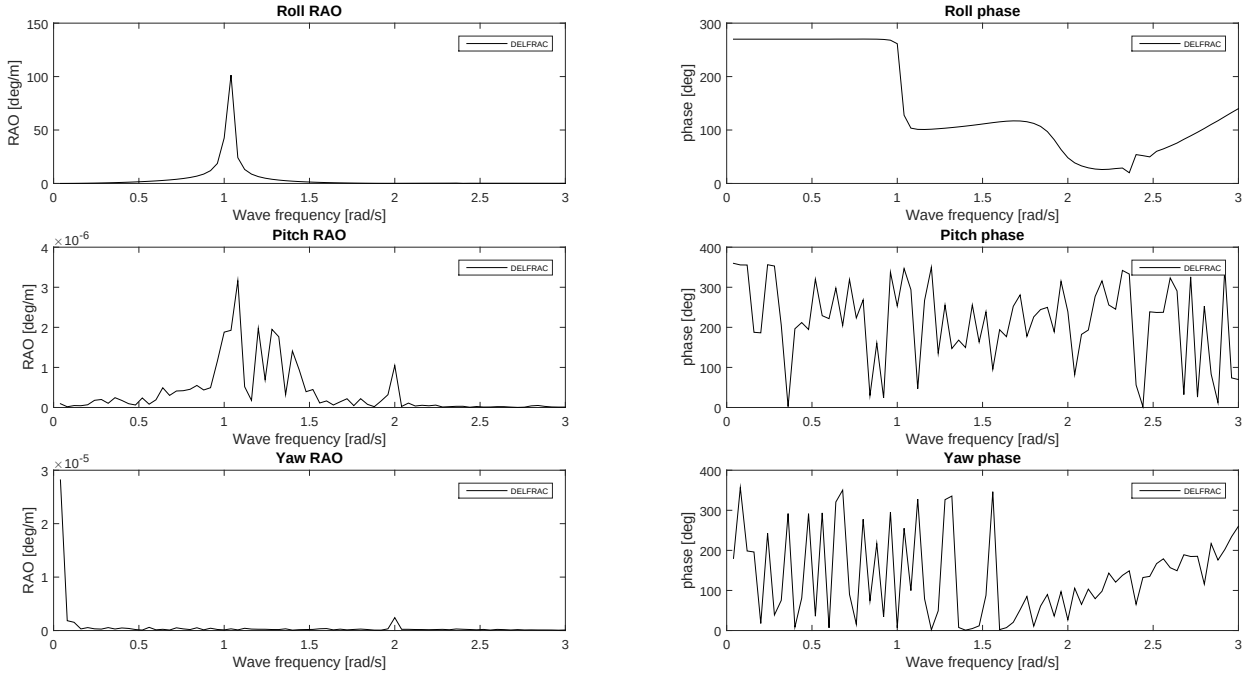

Figure F-2: DELFRAC results rotations. $\lambda = 1[-]$, wave incident angle $90[deg]$

F-2 DELFRAC results compared to coupled vessel Ampelmann model. $\lambda = 1[-]$

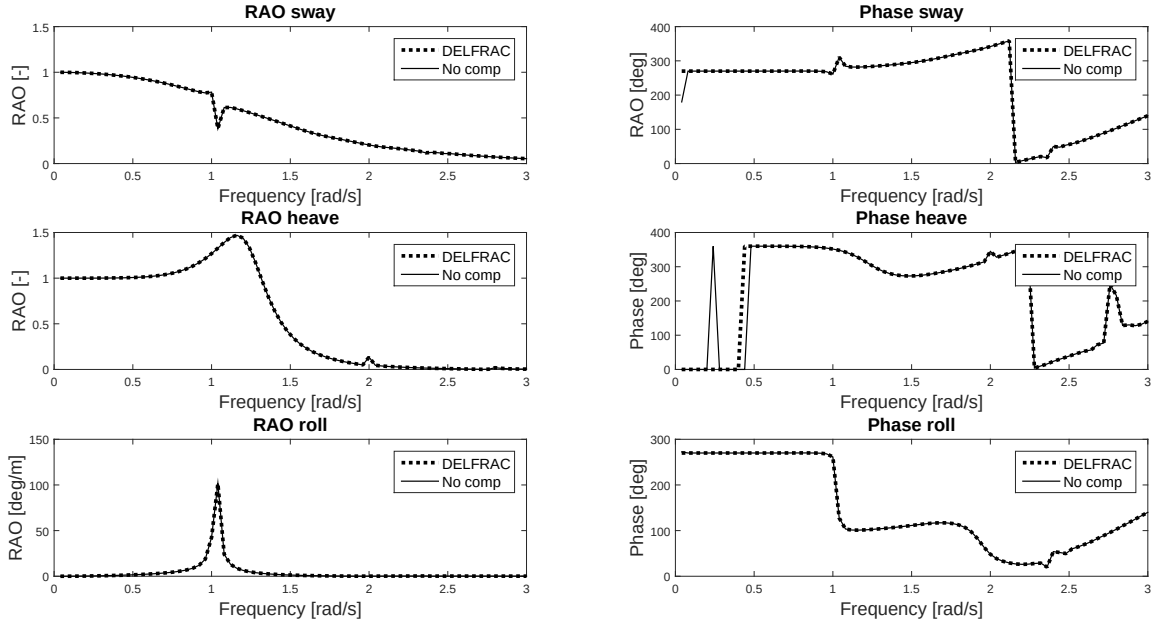

Figure F-3: DELFRAC results compared to No compensation model 6 DOF model, wave incident angle $90[deg]$, $\lambda = 1[-]$, $m_2 = 0[kg]$ and $I_{xx2} = 0[kgm^2]$

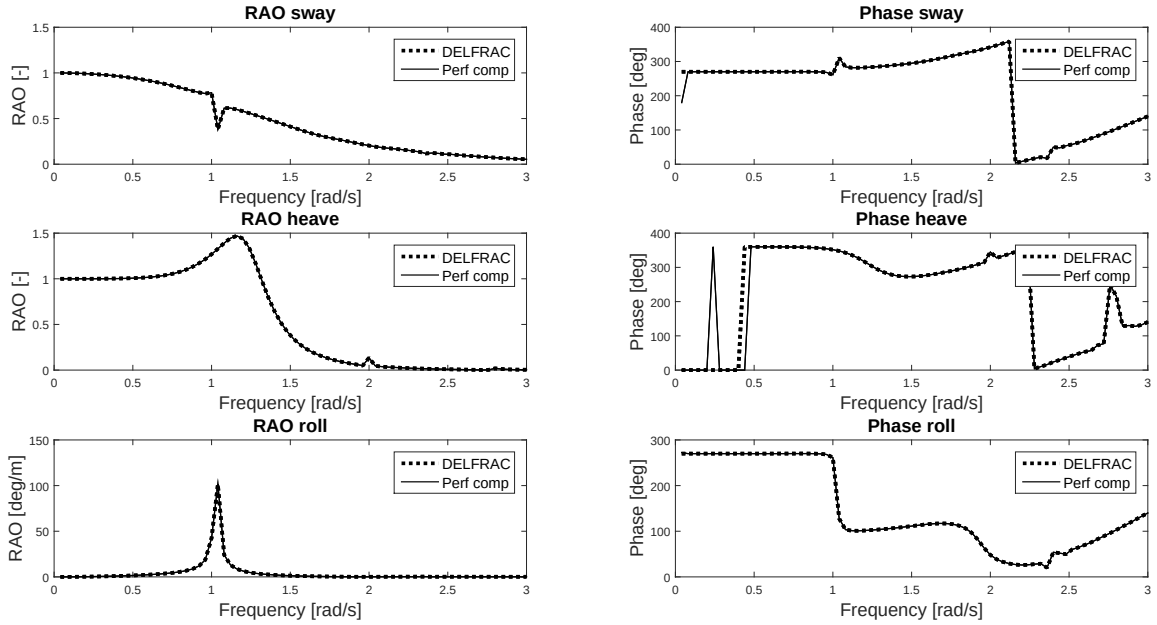

Figure F-4: DELFRAC results compared to Perfect compensation model 6 DOF model, wave incident angle $90[deg]$, $\lambda = 1[-]$, $m_2 = 0[kg]$ and $I_{xx2} = 0[kgm^2]$

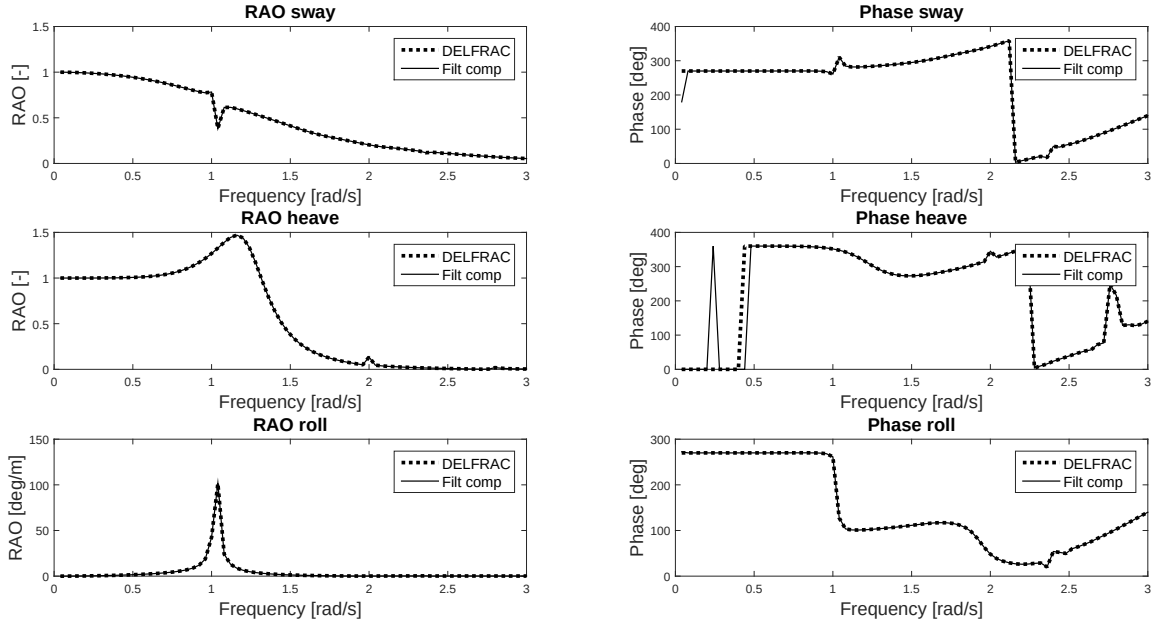

Figure F-5: DELFRAC results compared to Filter compensation model 6 DOF model, wave incident angle $90[deg]$, $\lambda = 1[-]$, $m_2 = 0[kg]$ and $I_{xx2} = 0[kgm^2]$

F-3 Results horizontal translation L_y, $\lambda = 1[-]$

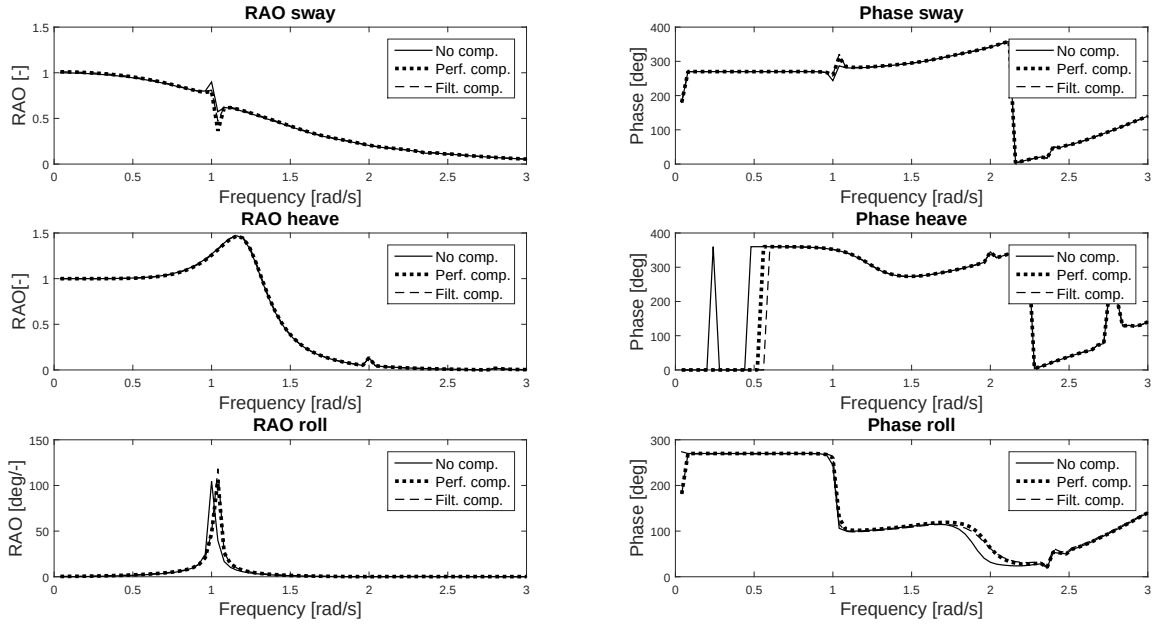

Figure F-6: Vessel frequency characteristics 6DOF model: wave incident angle $90[deg]$, $\lambda = 1[-]$, $L_y = 0[m]$

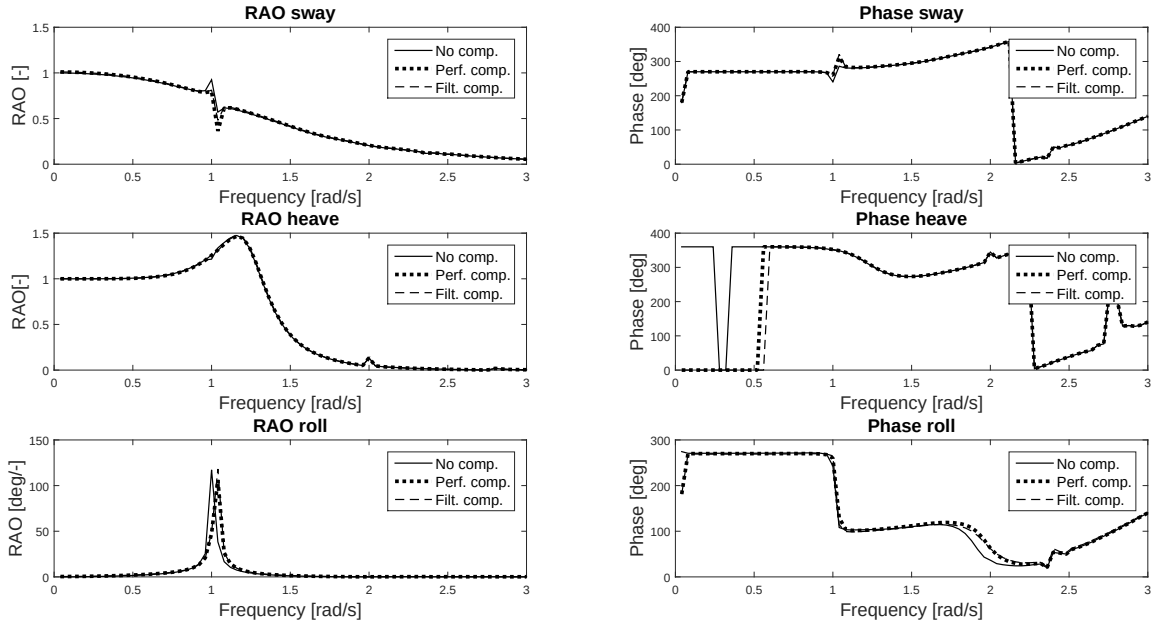

Figure F-7: Vessel frequency characteristics 6DOF model: wave incident angle $90[deg]$, $\lambda = 1[-]$, $L_y = 2[m]$

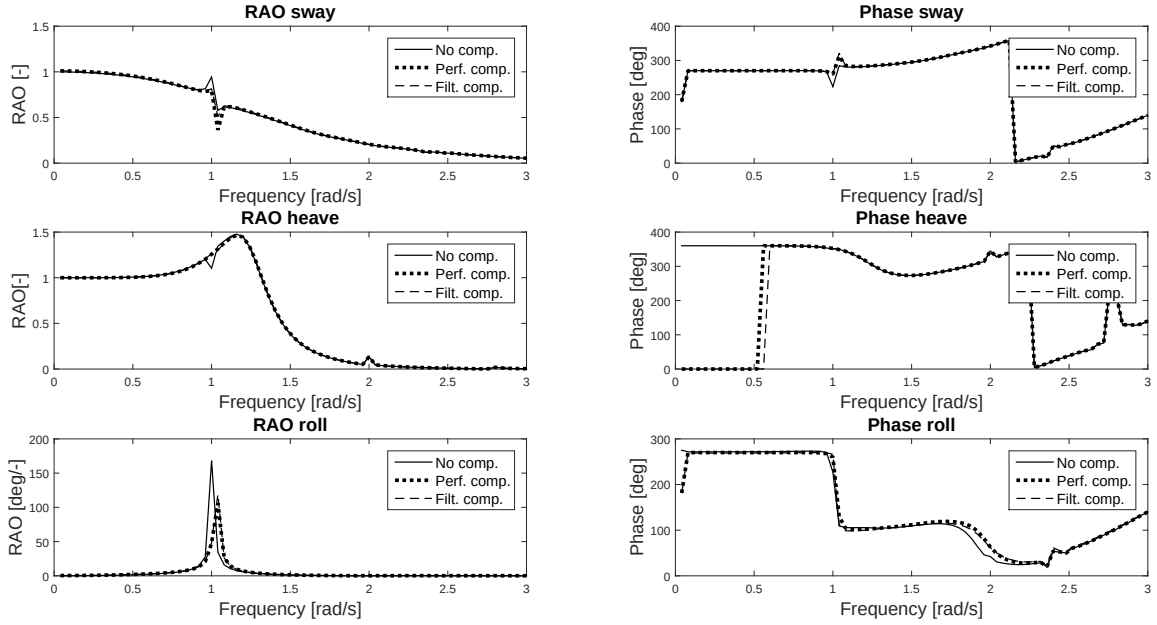

Figure F-8: Vessel frequency characteristics 6DOF model: wave incident angle $90[deg]$, $\lambda = 1[-]$, $L_y = 4[m]$

F-4 Results No compensation variable L_y, $\lambda = 0.65[-]$ and $\lambda = 1[-]$

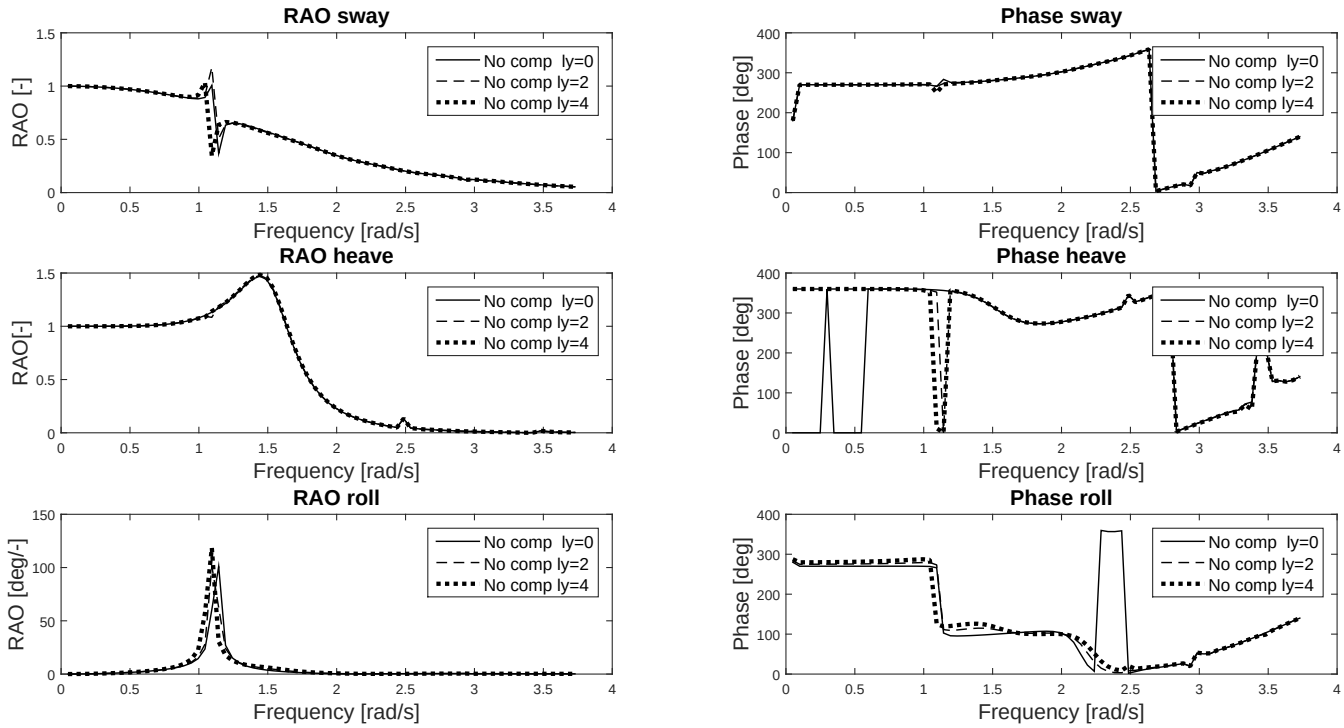

Figure F-9: Vessel frequency characteristics No compensation: wave incident angle $90[deg]$, $\lambda = 0.65[-]$, $L_y = 0[m]$, $L_y = 2[m]$ and $L_y = 4[m]$

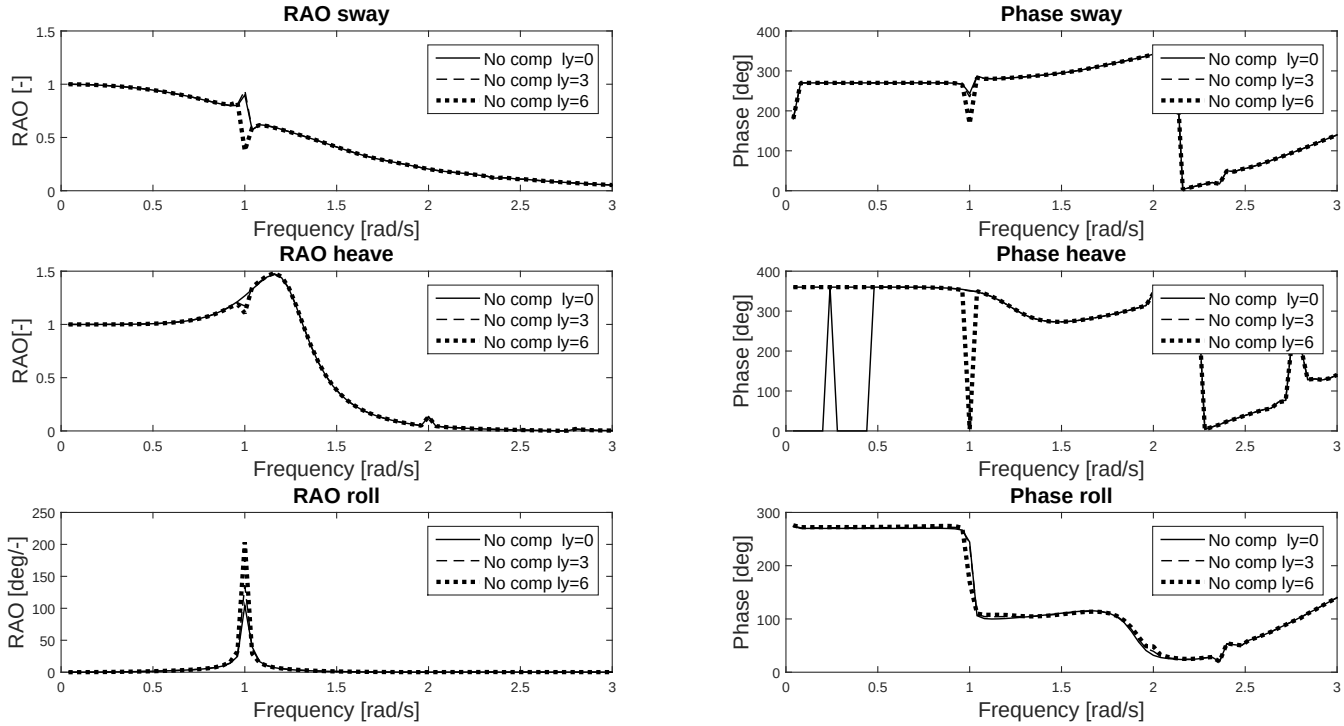

Figure F-10: Vessel frequency characteristics No compensation: wave incident angle $90[deg]$, $\lambda = 1[-]$, $L_y = 0[m]$, $L_y = 3[m]$ and $L_y = 6[m]$

F-5 Results Perfect compensation variable L_y, $\lambda = 0.65[-]$

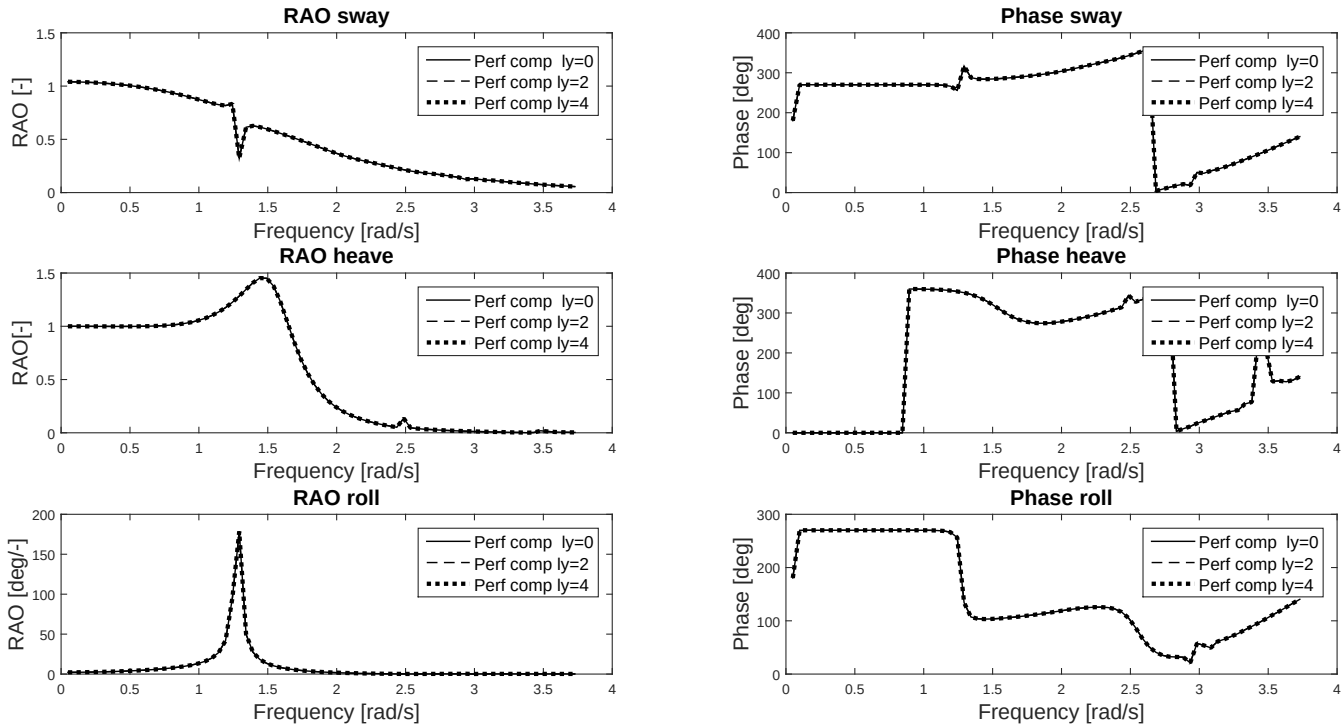

Figure F-11: Vessel frequency characteristics Perfect compensation: wave incident angle $90[deg]$, $\lambda = 0.65[-]$, $L_y = 0[m]$, $L_y = 2[m]$ and $L_y = 4[m]$

F-6 Results Filter compensation variable L_y, $\lambda = 0.65[-]$

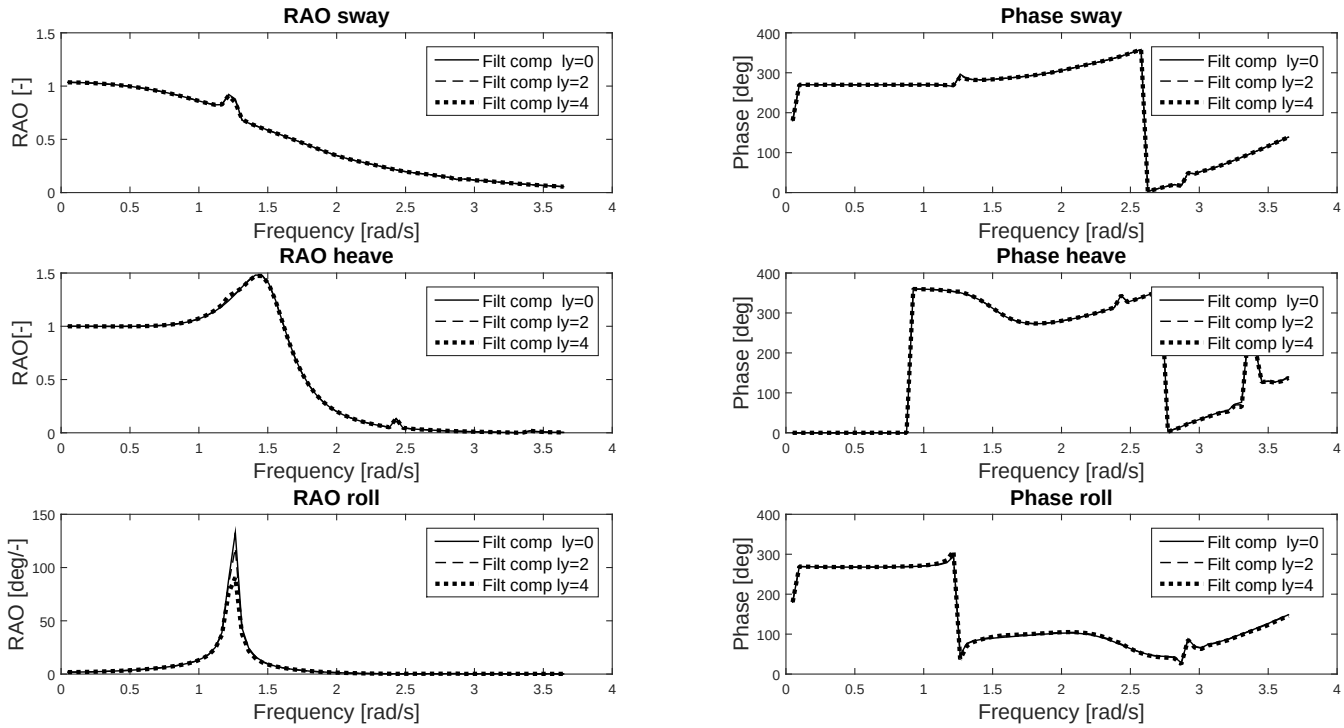

Figure F-12: Vessel frequency characteristics Filter compensation: wave incident angle $90[deg]$, $\lambda = 0.65[-]$, $L_y = 0[m]$, $L_y = 2[m]$ and $L_y = 4[m]$

F-7 Results No compensation variable L_z, $\lambda = 0.65[-]$ and $\lambda = 1[-]$

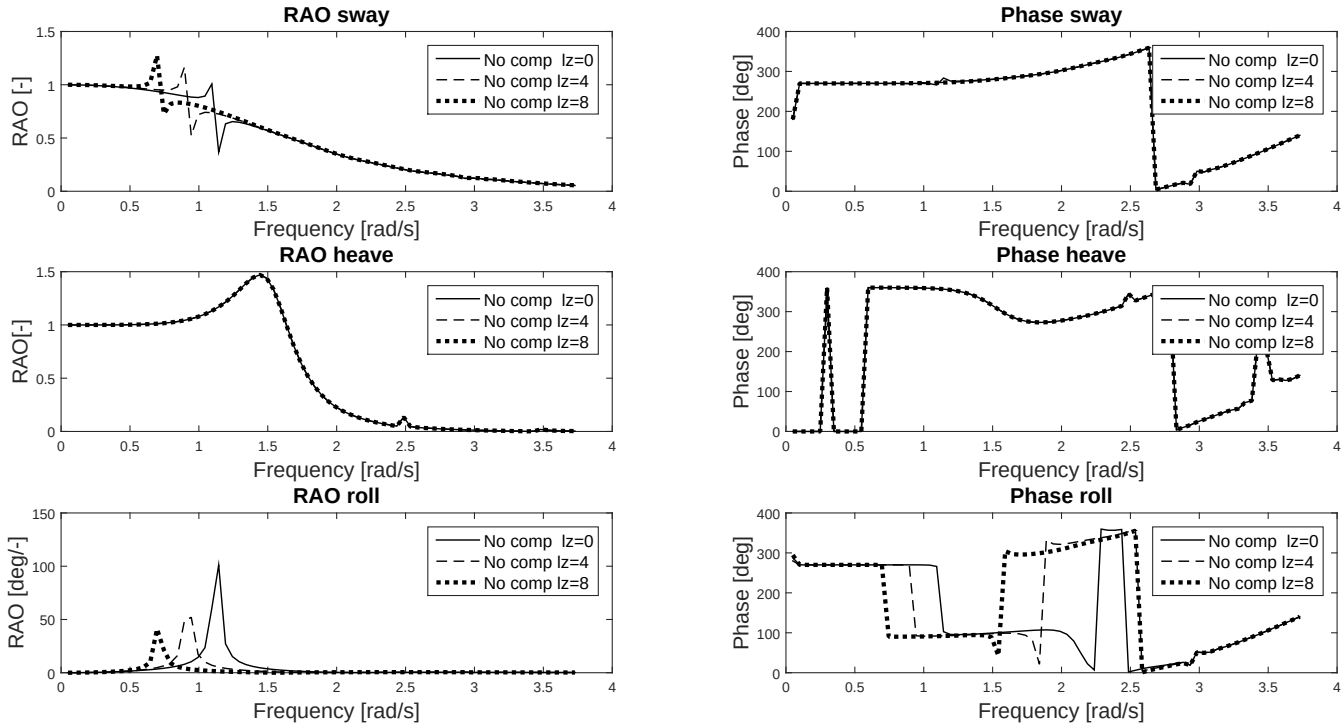

Figure F-13: Vessel frequency characteristics Perfect compensation: wave incident angle $90[deg]$, $\lambda = 0.65[-]$, $L_z = 0[m]$, $L_z = 4[m]$ and $L_z = 8[m]$

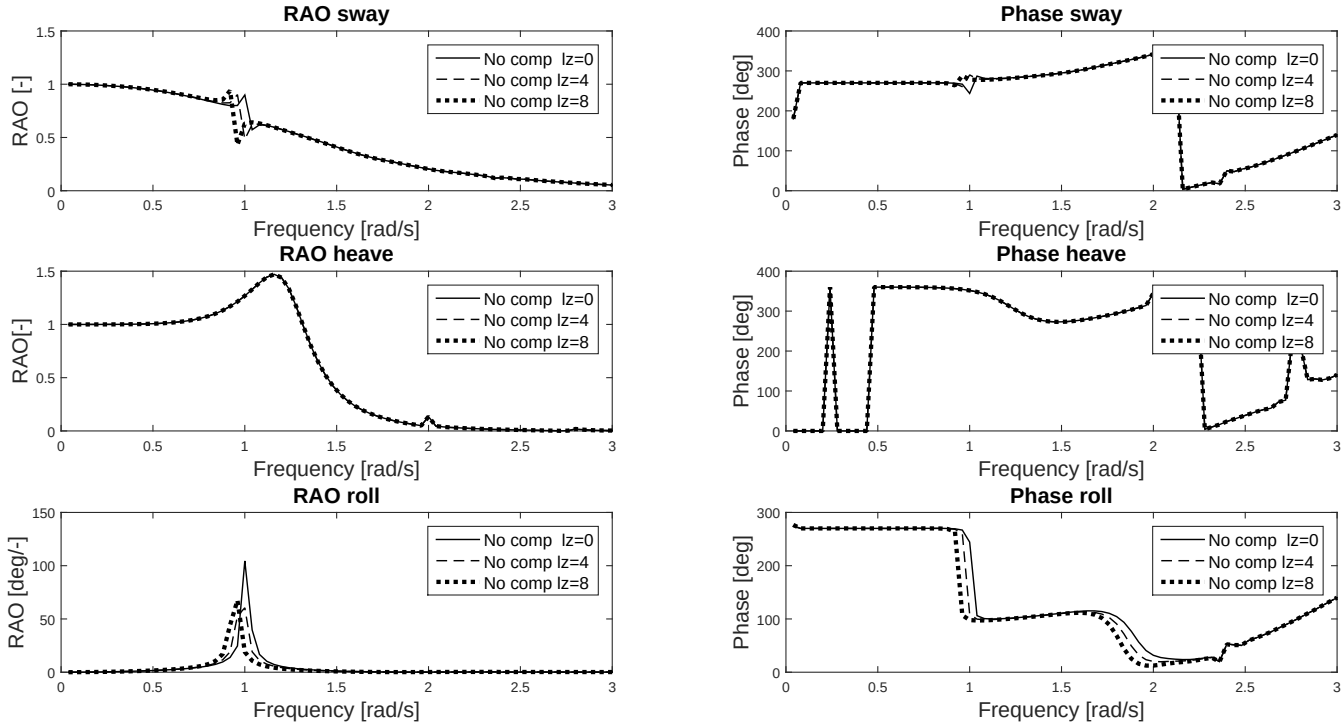

Figure F-14: Vessel frequency characteristics No compensation: $\lambda = 1[-]$, $L_z = 0$, $L_z = 4$ and $L_z = 8$

F-8 Results Perfect compensation variable L_z, $\lambda = 0.65[-]$

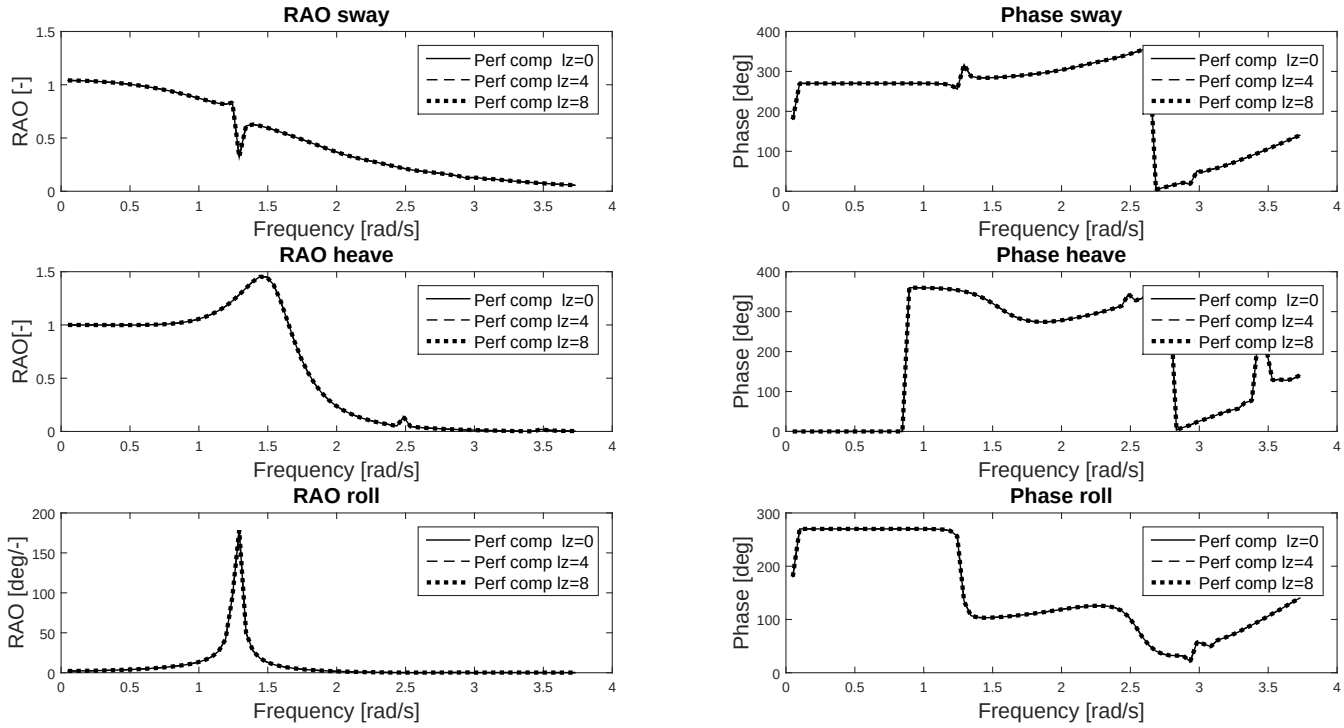

Figure F-15: Vessel frequency characteristics Perfect compensation: wave incident angle $90[deg]$, $\lambda = 0.65[-]$, $L_z = 0[m]$, $L_z = 4[m]$ and $L_z = 8[m]$

F-9 Results Filter compensation variable L_z, $\lambda = 0.65[-]$

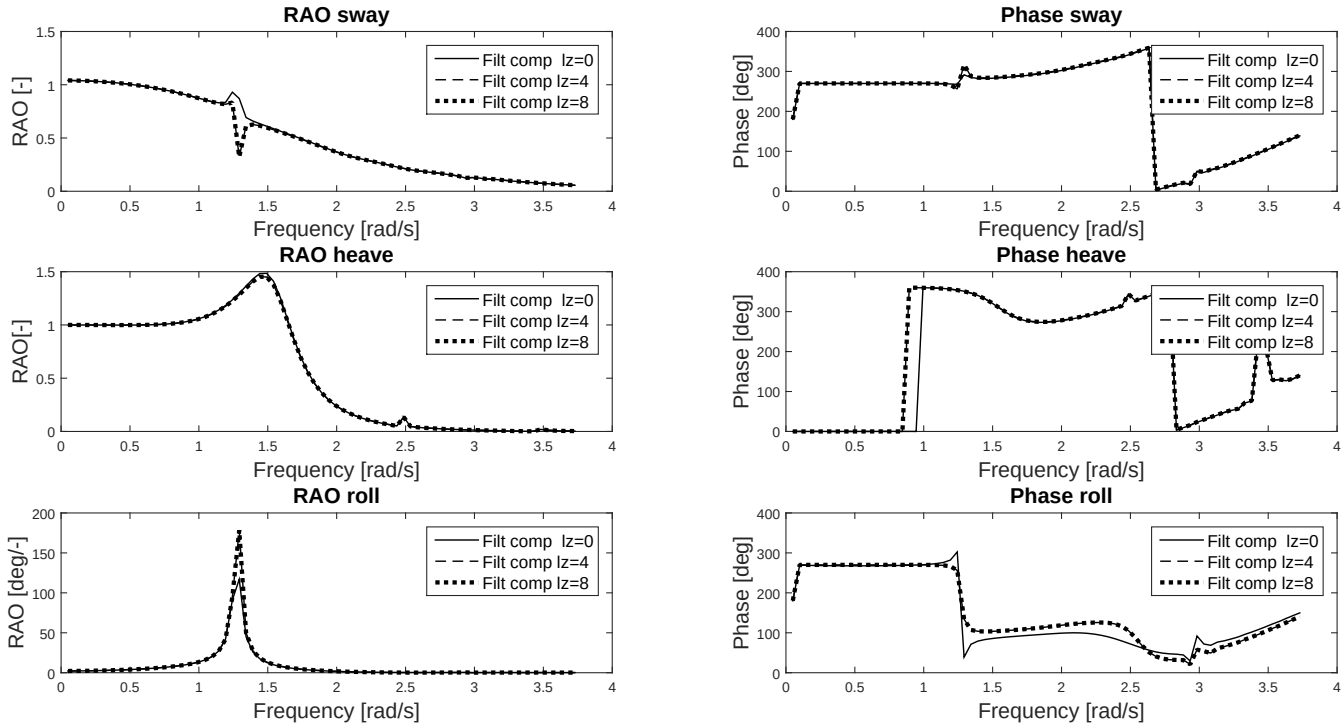

Figure F-16: Vessel frequency characteristics Filter compensation: wave incident angle $90[deg]$, $\lambda = 0.65[-]$, $L_z = 0[m]$, $L_z = 4[m]$ and $L_z = 8[m]$

F-10 Validation 12 DOF model

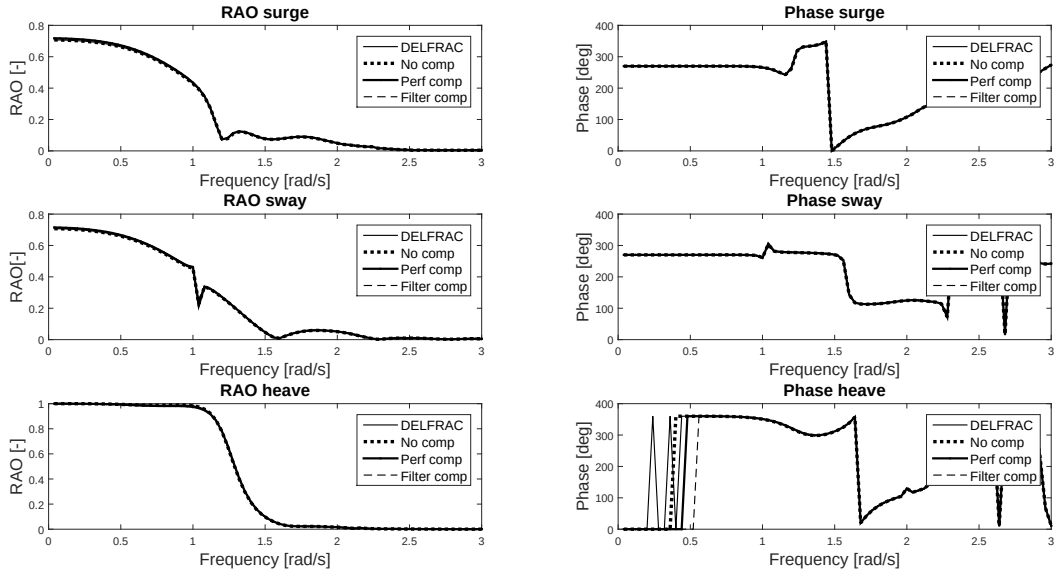

Figure F-17: Vessel translation frequency characteristics No compensation, Perfect compensation, Filter compensation and DELFRAC results. $\lambda = 1[-]$, $m_2 = 0[m]$, $I_{xx2} = 0[kgm^2]$, $I_{yy2} = 0[kgm^2]$, $I_{zz2} = 0[kgm^2]$, wave incident angle $45[deg]$

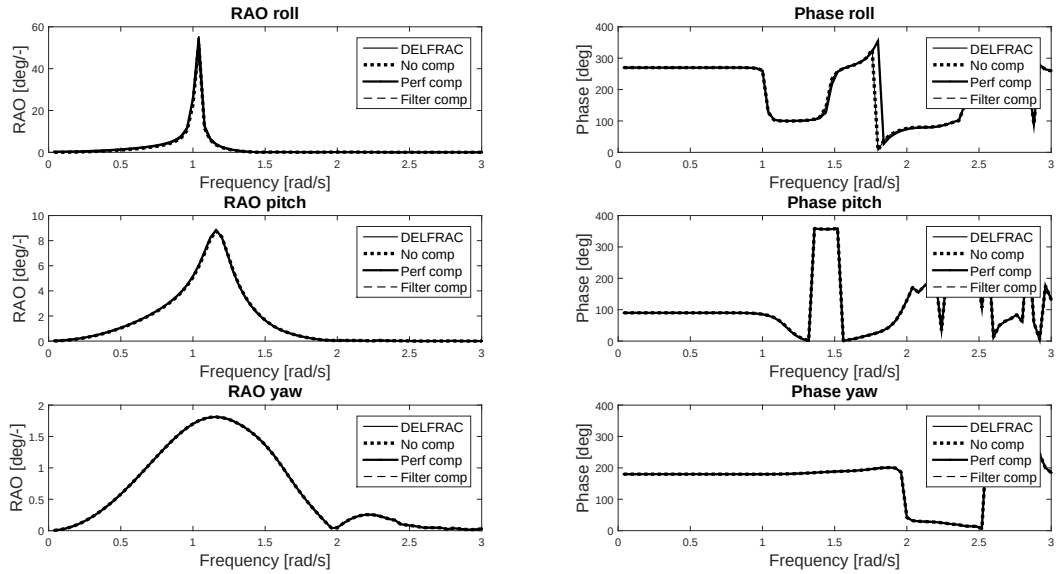

Figure F-18: Vessel rotation frequency characteristics No compensation, Perfect compensation, Filter compensation and DELFRAC results. $\lambda = 1[-]$, $m_2 = 0[m]$, $I_{xx2} = 0[kgm^2]$, $I_{yy2} = 0[kgm^2]$, $I_{zz2} = 0[kgm^2]$, wave incident angle $45[deg]$

Appendix G

Ampelmann workability software

Ampelmann Operations B.V. has developed software [10], which assesses the vessel at sea. With the vessel motions the required cylinder lengths are calculated to keep the TD motionless. The repose spectrum of the vessel is calculated from the vessel frequency characteristics and the wave spectrum. Although response spectra provide fast insight into the vessel motions, the geometry of a Stewart platform does not allow for straight forward derivation of the required cylinder lengths in the frequency domain [9]. Time series do provide insight to the cylinder lengths. It is found that the statistical properties of these time series are constant when a time length of 20 hours is used [1]. A time series is made and the required cylinders length are calculated to keep the TD motionless. Then when 97% of that time series the cylinder lengths stay within its working range the situation is marked as workable.

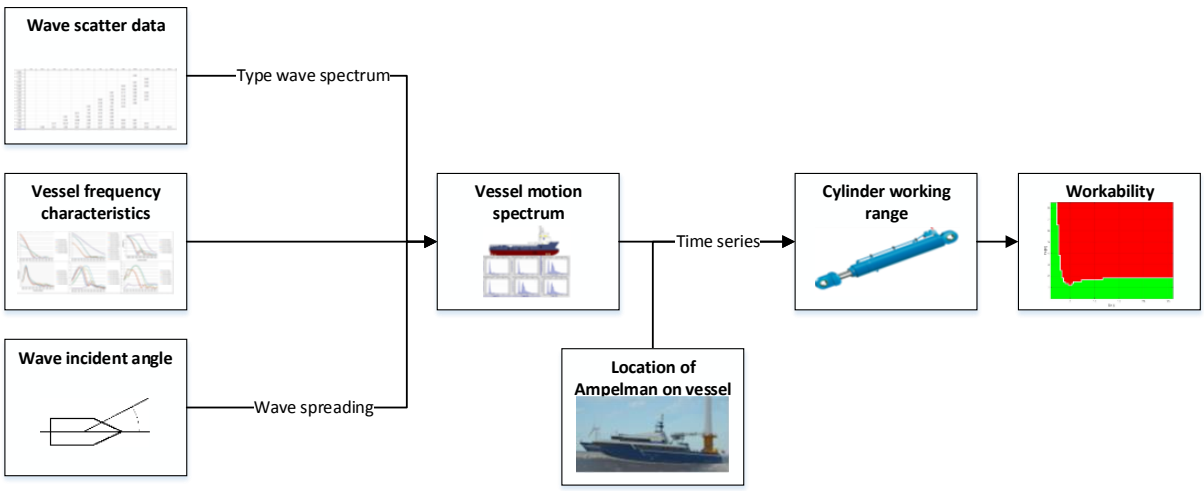

Figure G-1: Calculation procedure workability

The workability calculation procedure is shown in Figure G-1. From the wave scatter data, the vessel frequency characteristics and the wave incident angle the vessel motion spectrum is determined. Then a time series of the vessel motions is made. Based on the location of the Ampelmann on the vessel the required cylinder lengths are calculated. The input parameters to the workability software are:

- *Vessel-Ampelmann properties*
  - Vessel frequency characteristics
  - Location of the Ampelmann on the vessel
  - The cylinder working range, type of Ampelmann system
- *Environmental properties*
  - Wave scatter data with significant wave height and mean zero crossing period
  - The type of wave spectrum for the wave scatter data
  - Wave incident and directional wave spreading

Bibliography

[1] D. C. Salzmann, *Ampelmann Development of the Access System for Offshore Wind Turbines*. David Cerda Salzmann, Offshore Engineering and DUWIND, Technical University Delft, 2010.

[2] J. Journeé and W. Massie, *OFFSHORE HYDROMECHANICS*. Delft University of Technology, 2001.

[3] P. Naaijen, *OFFSHORE HYDROMECHANICS OE4630 D2 2012-2013*. Delft University of Technology, 2012.

[4] P. de Jong, *OFFSHORE HYDROMECHANICS OE4630 D1 2012-2013*. Delft University of Technology, 2012.

[5] H. de Koning Gans, *Manual for experiments of Numerical Methods in Ship Hydromechanics*. Delft University of Technology, 2012.

[6] K. van valkenhoef, "Basis of design fix 2 ampelmann gxl v2/v3," tech. rep., Ampelmann Operations B.V., 2014.

[7] A. van Leer, "Motion control enhancements for the ampelmann system," Master's thesis, Delft University of Technology, 2012.

[8] A. van Leer. MCM engineer at Ampelmann Operations B.V. Limitations for TAB motions.

[9] A. G Master's thesis.

[10] "Ampelmann software tool, workability analysis," tech. rep., Ampelmann Operations B.V., 2014.

[11] L. Holthuijsen, *Waves in oceanic and coastal waters*. Camebridge University, 2007.

[12] A. Ronse. C&C engineer at Ampelmann Operations B.V. Maximum allowable tranferdeck velocities and accelerations.

Glossary

List of Acronyms

AWESOME	Ampelmann Workability Evaluation Ship Oriented Motions and cylinder Excitations
CoG	Center of Gravity
CTS2	Cargo transfer system version 2
DOF	Degree(s) of freedom
DSP	Digital signal processing
EOM	Equation(s) of motion
FB	Feed back
FF	Feed forward
FOG	Fibre optic gyroscope(s)
NSC	No sway compensation
PLC	Programmable logic controller
RAO	Response amplitude operator(s)
TAB	Telescoping access bridge
TD	Transfer deck
2D	2 dimensional
3D	3 dimensional

List of Symbols

ϵ	Phase angle	$[rad]$
ζ	Wave elevation	$[m]$
θ	Pitch motion vessel	$[rad]$
Θ	Pitch motion amplitude	$[rad]$
$\hat{\Theta}$	Complex pitch motion amplitude	$[rad]$
λ	Geometric scaling factor	$[-]$
μ	Wave incident angle	$[deg]$
μ_m	Relative mass ratio	$[-]$
μ_I	Relative mass moment of inertia ratio	$[-]$

ρ	Water density	$[kg/m^3]$
ϕ	Roll motion vessel	$[rad]$
Φ	Roll motion amplitude	$[rad]$
$\hat{\Phi}$	Complex roll motion amplitude	$[rad]$
ψ	Yaw motion vessel	$[rad]$
Ψ	Yaw motion amplitude	$[rad]$
$\hat{\Psi}$	Complex yaw motion amplitude	$[rad]$
ω	Angular frequency	$[rad/s]$
ω_c	Cut off frequency	$[rad/s]$
∇	Submerged volume	$[m^3]$
a_{12}	Added mass term, see List of Subscripts: 12	$[kg], [kgm], [kgm^2]$
$[\mathbf{A}]$	Added mass matrix depending on ω	na
b_{12}	Damping term, see List of Subscripts: 12	$[kgm/s], [kgm^2/s], [kgm^3/s]$
B	Location of Ampelmann with respect to vessel's CoG	na
B	Beam/width vessel	$[m]$
B	Point indicating buoyancy point of the vessel	na
$[\mathbf{B}]$	Damping matrix depending on ω	na
c_{12}	Stiffness term	$[kg/s^2], [kgm/s^2], [kgm^2/s^2]$
$\mathbf{[C]}$	Stiffness mass matrix, see List of Subscripts: 12	na
D	Depth vessel	$[m]$
f_c	Cut off frequency	$[Hz]$
F	Wave force	$[N]$
$\hat{F}$	Complex wave force	$[N]$
F_{mg}	Force due to weight TD	$[N]$
g	Gravitational acceleration	$[m/s^2]$
G	Point indicating CoG of the vessel	na
$H(\omega)$	Second order low pass filter	$[-]$
H_s	Significant wave height	$[m]$
I	Mass moment of inertia	$[kgm^2]$
I_t	Area moment of inertia of water plane area	$[m^4]$
K	Point indicating keel of the vessel	na
$l_{1...6}$	Actuator position	na
L	Barge length	$[m]$
L_x	Translation of Ampelmann location in x-direction	$[m]$
L_y	Translation of Ampelmann location in y-direction	$[m]$
L_z	Translation of Ampelmann location in z-direction	$[m]$
L_a	Actuator length	$[m]$
L_2	Distance from upper actuator pivot point to CoG TD	$[m]$
M	Wave moment	$[Nm]$
M	Point indicating metacenter of the vessel	na
$\hat{M}$	Complex wave moment	$[Nm]$
M_a	Actuator moment	$N[m]$
M_g	Moment due to static weigh Ampelmann	$[Nm]$
M_v	Vessel mass	$[kg]$

M_1	Vessel mass in coupled system	$[kg]$
M_2	TD mass in coupled system	$[kg]$
$[\mathbf{M}]$	Mass matrix	na
r	Radius	$[m]$
$r_{1...6}$	Reference position	na
t	Time	$[s]$
T	Draft vessel	$[m]$
T_z	Zero crossing wave period	$[s]$
$u_{1...6}$	Reference position	na
x	Surge motion vessel	$[m]$
X	Surge motion amplitude	$[m]$
$\hat{X}$	Complex surge motion amplitude	$[m]$
y	Sway motion vessel	$[m]$
Y	Sway motion amplitude	$[m]$
$\hat{Y}$	Complex sway motion amplitude	$[m]$
z	Heave motion vessel	$[m]$
Z	Heave motion amplitude	$[m]$
$\hat{Z}$	Complex heave motion amplitude	$[m]$

List of Subscripts

θ	θ-direction
$\theta\zeta$	θ-motion with respect to wave elevation
θ, x	Pitch due to relative displacement in x-direction
ϕ	ϕ-direction
$\phi\zeta$	ϕ-motion with respect to wave elevation
ϕ, x	Roll due to relative displacement in x-direction
$\psi\zeta$	ψ-motion with respect to wave elevation
a	Amplitude
a, h	Horizontal actuator
a, v	Vertical actuator
$a1$	Due to sway acceleration
$a2$	Due to sway acceleration
c	Stiffness
$comp$	Compensating
$filt$	Filter compensation
$F_x\zeta$	wave force in x-direction with respect to wave elevation
$F_y\zeta$	wave force in y-direction with respect to wave elevation
$F_z\zeta$	wave force in z-direction with respect to wave elevation
$g1$	Due to static weight TD
$g2$	Due to static weight TD
$M_\phi\zeta$	wave moment in ϕ-direction with respect to wave elevation
$M_\theta\zeta$	wave moment in θ-direction with respect to wave elevation

$M_\psi\zeta$	wave moment in ψ-direction with respect to wave elevation
n	Natural frequency
$Nocomp$	Not compensating
$r1$	Due to TD roll acceleration
$r1$	Due to TD roll acceleration
$s1$	due to TD sway acceleration
$s2$	due to TD sway acceleration
x	x-direction
$xx1$	Around vessel's x-axis
$xx2$	Around TD's x-axis
$x\zeta$	x-motion with respect to wave elevation
y	y-direction
$yy1$	Around vessel's y-axis
$yy2$	Around TD's y-axis
$y\zeta$	y-motion with respect to wave elevation
z	z-direction
$zz1$	Around vessel's z-axis
$zz2$	Around TD's z-axis
$z\zeta$	z-motion with respect to wave elevation
1	-F_1: Wave force in surge -Terms related to the vessel
2	-F_2: Wave force in sway -Terms related to the TD
3	In in heave direction
4	In roll direction
5	In pitch direction
6	In yaw direction
12	Refers to vessel motions: "in direction 1 due to direction 2"